GE Hitachi Nuclear Energy

NEDO-33922-A
Revision 3
June 2022

Non-Proprietary Information

Licensing Topical Report

BWRX-300 Containment Evaluation Method

ONTARIO POWER GENERATION	
OPG Document Number	
NK054-REP-03555-00001	
OPG Security Classification	
Confidential	
ACCEPTED	
ACCEPTED AS NOTED	x
REVISE AND RESUBMIT	
Bala	March 14, 2024
Signature	**Date**
Name: Balraj Jassar, Manager	
Dept: Nuclear Safety, Projects, DNNP	
This acceptance does not relieve the contractor from responsibility for errors or omissions or from any obligations or liability under this contract.	
Notes: Refer to the adjacent notes	

ACCEPTED AS NOTED:
This document was produced in accordance with GEH approved procedure CP-03-100, "Design Control" and reviewed by OPG as applicable per NK054-PLAN-01210-00035, "DNNP Engineering Oversight Plan". As indicated in Section 3.4 of DNNP Engineering Oversight Plan, OPG acceptance of applicable Design and Safety Analysis Deliverables is to be conducted in Baselines 2 and 3. Accordingly, at this stage of design, OPG has not conducted formal acceptance of individual design and safety analysis deliverables. Acceptance of this document indicates OPG's concurrence for formal submission to CNSC staff for the purposes documented in the associated correspondence.

INFORMATION NOTICE

This is a non-proprietary version of the GE Hitachi Nuclear Energy (GEH) document NEDC-33922P-A Revision 3, which has the proprietary information removed. Portions of the document that have been removed are indicated by an open and closed bracket as shown here [[ ]].

IMPORTANT NOTICE REGARDING CONTENTS OF THIS REPORT

Please Read Carefully

The design, engineering, and other information contained in this document is furnished for the purpose of obtaining Nuclear Regulatory Commission (NRC) review and determination of acceptability for use for the BWRX-300 design and licensing basis information contained herein. The only undertakings of GEH with respect to information in this document are contained in the contracts between GEH and its customers or participating utilities, and nothing contained in this document shall be construed as changing those contracts. The use of this information by anyone for any purpose other than that for which it is intended is not authorized; and with respect to any unauthorized use, GEH makes no representation or warranty, and assumes no liability as to the completeness, accuracy, or usefulness of the information contained in this document.

UNITED STATES
NUCLEAR REGULATORY COMMISSION
WASHINGTON, D.C. 20555-0001

April 27, 2022

Ms. Michelle Catts
Senior Vice President, Nuclear Programs
GE-Hitachi Nuclear Energy Americas, LLC
P.O. Box 780, M/C A-18
Wilmington, NC 28402

SUBJECT: FINAL SAFETY EVALUATION FOR GE-HITACHI LICENSING TOPICAL REPORT NEDC-33922P, REVISION 2, "BWRX-300 CONTAINMENT EVALUATION METHOD" (DOCKET NO. 99900003)

Dear Ms. Catts:

By letter dated September 25, 2021, GE-Hitachi Nuclear Energy Americas, LLC (GEH), submitted Licensing Topical Report (LTR) NEDO-33922, "BWRX-300 Containment Evaluation Method," Revision 0 (Agencywide Documents Access and Management System (ADAMS) Accession No. ML20269A469), to the U.S. Nuclear Regulatory Commission (NRC) staff for review and approval in support of a future licensing application for the GEH small modular reactor (SMR) under Title 10 of the *Code of Federal Regulations* (10 CFR) Part 50, "Domestic Licensing of Production and Utilization Facilities," or Part 52, "Licenses, Certifications, and Approvals for Nuclear Power Plants." Subsequently, during the staff review, GEH submitted Revision 1, By letter dated November 19, 2021 (ADAMS Accession No. ML21323A008), and then on December 17, 2021 (ADAMS Accession No. ML21351A168), GEH submitted Revision 2 of the LTR.

The NRC staff has found GEH LTR NEDC-33922, Revision 2, to be acceptable for referencing in licensing applications for the GEH SMR design to the extent specified in the enclosed final safety evaluation (SE) that defines the basis for acceptance. In addition, on April 21, 2022 (ADAMS Accession No. ML22101A298), the Advisory Committee on Reactor Safeguards concluded that the staff's SE for LTR NEDC-33922, Revision 2, with the limitations and conditions imposed, is appropriate and should be issued. Therefore the staff did not make any changes to the staff Advanced Final Safety Evaluation submitted to you on March 09, 2022 (ADAMS Accession No. ML22004A080 - Non-Public and ML22040A004 - Public).

In accordance with the guidance provided on the NRC's LTR Web site (http://www.nrc.gov/about-nrc/regulatory/licensing/topical-reports.html), the NRC requests that GEH publish an accepted version of this LTR within three months of receipt of this letter. The accepted version shall incorporate this letter and the enclosed SE after the title page. Also, it must contain in its appendices historical review information, such as requests for additional information, accepted responses, and the actual revised pages (showing revision bars) that were included as part of LTR NEDC-33922, Revision 2. The accepted version shall include an "-A" (designated accepted) following the report identification symbol.

If the NRC's criteria or regulations change so that its conclusion in this letter (that the LTR is acceptable) is invalidated, GEH and/or an applicant referencing the LTR will be expected to revise and resubmit its respective documentation or submit justification for the continued applicability of the LTR without revision of the respective documentation.

If you have any questions or comments concerning this matter, I can be reached via e-mail at James.Shea@nrc.gov.

Sincerely,

/RA/

James J. Shea, Senior Project Manager
New Reactor Licensing Branch
Division of New and Renewed Licenses
Office of Nuclear Reactor Regulation

Docket No.: 99900003

Enclosure:
Safety Evaluation

cc: GEH BWRX-300 NEDO-33922P ListServ

SUBJECT: FINAL SAFETY EVALUATION FOR GE-HITACHI LICENSING TOPICAL REPORT NEDC-33922P, REVISION 2, "BWRX-300 CONTAINMENT EVALUATION METHOD" (DOCKET NO. 99900003)
DATED: APRIL 27, 2022

DISTRIBUTION (w/o/ safety evaluation):
PUBLIC
NRLB R/F
MDudek, NRR
BSmith, NRR
RPatton, NRR
SKrepel, NRR
SHaider, NRR
JShea, NRR
ASchiller, NRR
SGreen, NRR
RidsNrrOd
RidsNrrDnrl
RidsNrrDnrlNrlb
RidsOgcMailCenter
RidsAcrsMailCenter
RidsNrrLACSmith Resource

ADAMS Accession Nos.:
PKG: ML22110A007
LTR: ML22110A008
SE: ML22040A004 (Public)
SE: ML22004A080(Non-Public) ***via e-mail** **NRR-106**

OFFICE	DNRL/NRLB:PM	DNRL/NRLB:LA	DNRL/NRLB: BC	DNRL/NRLB:PM
NAME	JShea	SGreen	MDudek	JShea
DATE	04/19/2022	04/20/2022	04/27/2022	04/27/2022

OFFICIAL RECORD COPY

SAFETY EVALUATION BY THE OFFICE OF NUCLEAR REACTOR REGULATION

LICENSING TOPICAL REPORT NEDC-33922P, REVISION 2

BWRX-300 CONTAINMENT EVALUATION METHOD

GE-HITACHI NUCLEAR ENERGY AMERICAS, LLC

DOCKET NO. 99900003

1.0 INTRODUCTION

The purpose of GE-Hitachi Nuclear Energy Americas, LLC (GEH), Licensing Topical Report (LTR) NEDC-33922P, Revision 0, "BWRX-300 Containment Evaluation Method," dated September 25, 2020 (Agencywide Documents Access and Management System (ADAMS) Accession No. ML20269A469), supplemented November 19, 2021 (ADAMS Accession No. ML21323A008) and updated in Revision 2, dated December 17, 2021 (ADAMS Accession No. ML21351A168), is to present an acceptable analysis method for BWRX-300 containment thermal-hydraulic performance to demonstrate that the containment design satisfies the acceptance criteria documented in the approved LTR NEDC-33911P-A, Revision 3, "BWRX-300 Containment Performance," dated January 7, 2022 (ADAMS Accession No. ML22007A021). Specifically, Section 3.0 of NEDC-33911P-A, Revision 3, outlines the scope of the acceptance criteria for the containment analysis method for the BWRX-300 design-basis events (DBEs) to show that the containment performance analysis meets the acceptance criteria for the following:

- anticipated operational occurrences (AOOs)
- station blackout as required by Title 10 of the *Code of Federal Regulations* (10 CFR) 50.63, "Loss of all alternating current power"
- anticipated transients without scram (ATWS) as required by 10 CFR 50.62, "Requirements for reduction of risk from anticipated transients without scram (ATWS) events for light-water-cooled nuclear power plants"
- large-break loss-of-coolant accident (LBLOCA) inside containment
- small-break loss-of-coolant accident (SBLOCA) inside containment

In this safety evaluation (SE), the U.S. Nuclear Regulatory Commission (NRC) staff describes its review and the acceptability of the BWRX-300 containment evaluation method (CEM) proposed for the BWRX-300 small modular reactor (SMR) using the Transient Reactor Analysis Code General Electric (TRACG) code for the reactor pressure vessel (RPV) model and the Generation of Thermal-Hydraulic Information for Containments (GOTHIC) code used separately for the containment model as described in LTR NEDC-33911-A, Revision 2, Section 3.3 and Section 3.4. This review included NRC staff requests for additional information (RAIs) that GEH responded to in letters dated May 19, 2021 (ADAMS Accession No. ML21139A110); September 17, 2021 (ADAMS Accession No. ML21260A010); October 8, 2021 (ADAMS Accession No. ML21281A081); October 29, 2021 (ADAMS Accession No. ML21302A080); and December 17, 2021 (ADAMS Accession No. ML21351A168). Additionally, the staff conducted a regulatory audit from January 5, 2021 to December 8, 2021 (ADAMS Accession No. ML20363A025). The

staff detailed audit activities and review can be found in the audit report (ADAMS Accession No. ML21343A194).

The NRC staff will evaluate the compliance of the final BWRX-300 SMR design including the containment and the final CEM during future licensing activities in accordance with 10 CFR Part 50, "Domestic Licensing of Production and Utilization Facilities," or 10 CFR Part 52, "Licenses, Certifications, and Approvals for Nuclear Power Plants," as applicable.

The staff evaluated the applicable regulations and guidance for the BWRX-300 CEM in Section 3.1 of the staff SE as part of the approved LTR NEDC-33911P-A, Revision 3. The staff views this SE as a continuation of LTR NEDC-33911P-A, Revision 3 and, as such, the same regulatory evaluation applies herein. However, for ease of reference, regulations related to CEM are as follows:

- 10 CFR Part 50 Appendix A, "General Design Criteria for Nuclear Power Plants," General Design Criterion 50, "Containment design basis." (GDC 50), as it relates to the containment design basis, requires that the reactor containment structure, including access openings, penetrations, and the containment heat removal system, be designed so that the containment structure and its internal compartments can accommodate, without exceeding the design leakage rate and with sufficient margin, the calculated pressure and temperature conditions resulting from any loss-of-coolant-accident (LOCA). This margin shall reflect consideration of (1) the effects of potential energy sources that have not been included in the determination of the peak conditions, such as energy in steam generators and as required by 10 CFR 50.44, "Combustible gas control for nuclear power reactors," energy from metal-water and other chemical reactions that may result from degradation but not total failure of emergency core cooling functioning, (2) the limited experience and experimental data available for defining accident phenomena and containment responses, and (3) the conservatism of the calculational model and input parameters.

- 10 CFR Part 50, Appendix K, "ECCS Evaluation Models," as it relates to sources of energy during the LOCA, provides requirements to assure that all the energy sources have been considered.

- 10 CFR 50.44, "Conditions of License," as it relates to boiling-water reactors (BWRs) and pressurized-water reactors (PWRs) being designed to accommodate hydrogen generation equivalent to a 100-percent fuel clad-coolant reaction; to limit containment hydrogen concentration to no greater than 10 percent; to have a capability for ensuring a mixed atmosphere during design-basis and significant beyond-design-basis (BDB) accidents (a significant beyond-design-basis accident (BDBA) being an accident comparable to a degraded core accident at an operating (as of October 16, 2003) light-water reactor in which a metal-water reaction occurs involving 100 percent of the fuel cladding surrounding the active fuel region (excluding the cladding surrounding the plenum volume)); and to provide containment-wide hydrogen control (such as igniters or inerting), if necessary, for certain severe accidents, noting that post-accident conditions should be such that an uncontrolled hydrogen/oxygen recombination would not take place in the containment, or the plant should withstand the consequences of uncontrolled hydrogen/oxygen recombination without loss of safety function or containment structural integrity.

- 10 CFR 50.46, "Acceptance criteria for emergency core cooling systems for light-water nuclear power reactors," as it relates to requirements for long-term cooling, including

adequate net positive suction head margin in the presence of LOCA-generated and latent debris

2.0 OVERVIEW OF THE BWRX-300 REACTOR PRESSURE VESSEL AND CONTAINMENT FEATURES PERTINENT TO THE APPLICATION METHOD

LTR Section 2.0 provides high-level information about the BWRX-300 CEM. Previously approved LTRs NEDC-33910P-A, Revision 2, "BWRX-300 Reactor Pressure Vessel Isolation and Overpressure Protection," June 2021 (ADAMS Accession No. ML21183A259) and NEDC-33911P-A, Revision 3, describe the BWRX-300 RPV isolation and overpressure protection and BWRX-300 containment performance, respectively.

The following containment design features are relevant to the purposes of the LTR:

- The containment is a dry enclosure, near atmospheric pressure during normal operation.
- The containment design pressure and temperature are within the experience base of conventional boiling-water reactors (BWRs).
- The containment is inerted with nitrogen during normal operation.
- There are no subcompartments containing large bore high energy lines.
- The subcompartments have sufficiently large openings such that the boundaries of the subcompartments do not experience large pressure differentials resulting from pipe breaks outside the subcompartments.
- The passive containment cooling system (PCCS) is a [[

]].

3.0 LOSS-OF-COOLANT ACCIDENT SCENARIOS AND LIMITING PIPE BREAKS

LTR Section 3.0, describes DBEs of pipe breaks inside containment and break scenarios to establish the limiting pipe breaks for the containment performance evaluation. The postulated breaks include large breaks of main steam pipes, feedwater pipes, isolation condenser system (ICS) steam supply and condensate return pipes, reactor water cleanup (RWCU) pipes, and shutdown cooling (SDC) pipes, and all unisolated small steam and liquid pipe breaks. All the large breaks listed above have RPV isolation valves, which limit the amount of mass and energy (M&E) release from the RPV to the containment.

For the CEM described in the LTR, the outboard containment isolation valves are assumed to remain open for a main steam pipe break, but the turbine stop valve is closed instantaneously, concurrent with the break. Because the two steam pipes are connected to a common header upstream of the turbine stop and control, the intact loop also contributes to the break flow rate before the RPV isolation valves are closed. Using this set of assumptions maximizes the discharge of steam to containment.

As described in the LTR, the feedwater pipes have a check valve outside containment. As a result, the intact feedwater loop does not feed backward to the break. The feedwater pump trips on a pipe break. The hot water in the feedwater piping may flash and contribute to break flow. The isolation condenser (IC) steam supply pipe flow area is smaller than the main steam pipe flow limiter flow area. The IC condensate return pipe flow area is much smaller than the feedwater pipe; therefore, a break in the condensate return piping in an IC train is bounded by the feedwater pipe breaks. Further, pipe inventory in the main steam piping is much larger than the inventory in an IC train and its attached piping. Considering the pipe size, configuration, and isolation signal timing assumed in the analysis, a break in the ICS piping is bounded by a break in the main steam and/or feedwater pipe as analyzed.

The LTR states that, because the RWCU and SDC pipes are smaller in diameter than the feedwater pipes, and the isolation valve closure timing is the same for all pipes, breaks in these pipes are also bounded by feedwater pipe breaks.

The applicant stated in the LTR that from the spectrum of breaks the limiting large breaks are:

- main steam pipe
- and the feedwater pipe

The limiting small breaks are unisolated instrument line breaks, either in the steam or liquid space. The inside diameters of the instrument lines are [[
]].

LTR NEDC-33911P-A, Revision 3, Section 3.1, states that the containment design will be based on consideration of a full spectrum of DBEs that would result in the release of reactor coolant to pressurize the containment. These containment DBEs include liquid and steam breaks and will be evaluated using the TRACG code as a boundary condition to the GOTHIC code to calculate the containment response.

The NRC staff finds that the description in LTR Section 3.0 is consistent with the scope of the evaluation model as described in LTR NEDC-33911P-A, Revision 3, and addresses the full spectrum of DBEs being included to determine the limiting breaks for the containment analyses. When the BWRX-300 CEM is applied to the final design, the spectrum of breaks will be used in the containment analyses to determine M&E and the resulting containment pressure and temperature.

4.0 OVERVIEW OF THE EVALUATION MODEL

The BWRX-300 CEM is based on using TRACG code to evaluate the M&E from the RPV, and the GOTHIC, code to evaluate the resulting containment response. The M&E calculated by the TRACG RPV model is used as a boundary condition in the GOTHIC containment model used to calculate the containment pressure and temperature response. The M&E model for the BWRX-300 containment response uses the applicable parts of NEDC-33083P-A, Revision 1, “TRACG Application for ESBWR,” issued October 2010 (ADAMS Accession No. ML102800567), which is incorporated in the approved Economic Simplified Boiling-Water Reactor (ESBWR) design certification (DC), certified by the NRC in 2014 (10 CFR Part 52, Appendix E, "Design Certification Rule for the Economic Simplified Boiling-Water Reactor.") Section 5.0 of this SE discusses the acceptability of this application of the ESBWR TRACG method to the BWRX-300 for calculation of the M&E to containment.

The LTR presents the standalone GOTHIC containment model developed for the BWRX-300. GOTHIC is a commercially available computer code that has been developed consistent with regulatory requirements in 10 CFR Part 50, Appendix B, and meets the GEH software quality requirements. The containment analyses in this LTR are performed using the latest GOTHIC version 8.3. The LTR states that, "Future BWRX-300 containment analyses may be performed using newer versions of the GOTHIC code provided the newer versions meet the same 10 CFR Part 50, Appendix B quality requirements and changes in calculated results for [the] BWRX-300 containment application caused by any code changes can be successfully dispositioned." The final SE for GEH LTR NEDE-32906P-A, Supplement 3, "Migration to TRACG04/PANAC11 from TRACG02/PANAC10 for TRACG AOO and ATWS Overpressure Transients" dated April 16, 2010 (ADAMS Accession No. ML110970401) shows that the NRC staff had allowed similar usage of updated versions of the TRACG code maintained under the quality assurance criteria of 10 CFR Part 50, Appendix B. GEH also stated that they intend to use any future GOTHIC versions under 10 CFR 50.59 process. The staff evaluated GEH's position regarding the use of future versions of GOTHIC code and finds it to be acceptable and consistent with NRC requirements controlling changes made without requiring prior NRC review and approval.

The LTR states that the "BWRX-300 containment design is much simpler than the ESBWR containment, and many of the ESBWR containment phenomena do not apply to the BWRX-300 containment. Phenomena that are of secondary importance to the ESBWR containment response may become important to the BWRX-300 containment response." The staff has reviewed the information provided in LTR Sections 6.1, 6.2, and 6.4 about the GOTHIC phenomenon identification and ranking table (PIRT), the PIRT survey, and the knowledge level for the phenomena pertinent to containment analysis has been reviewed and the staff has documented its findings in the corresponding sections in this SE.

The LTR states that "the evaluation method for the BWRX-300 containment response to DBEs has been developed following the applicable elements of Regulatory Guide (RG) 1.203, "Transient and Accident Analysis Methods," issued December 2005 (ADAMS Accession No. ML053500170)." In Section 6.3 of this SE, the staff discusses the acceptability of the assessment basis for the BWRX-300 containment model using RG 1.203.

5.0 TRANSIENT REACTOR ANALYSIS CODE GENERAL ELECTRIC METHOD FOR MASS AND ENERGY RELEASE

5.1 Transient Reactor Analysis Code General Electric Code and Qualification

The TRACG code is the GEH proprietary version of the Transient Reactor Analysis Code (TRAC) used for best-estimate analysis of BWR transients ranging from AOOs to design-basis LOCAs and ATWS events. This code has been previously reviewed and found acceptable for applications of current operating BWRs, the Simplified Boiling-Water Reactor (SBWR), and the ESBWR, based on results of separate effects tests, component performance tests, integral effects tests, and full-scale plant data as described in the following qualification reports; (1) NEDC-32725P, Revision 1," General Electric Company TRACG Qualification for SBWR, Vol. 1 & 2, for Pre-Application Review of ESBWR, issued September 2002 (ADAMS Accession No. ML022560081); (2) NEDC-33080P, Revision 1, "TRACG Qualification for ESBWR," issued May 2005, (ADAMS Accession No. ML051600373); (3) NEDE-33005P-A, Revision 2, "Licensing Topical Report, TRACG Application for Emergency Core Cooling Systems / Loss-of-Coolant-Accident Analyses for BWR/2-6," issued May 2018 (ADAMS Accession No. ML18143A214);

and (4) NEDC-33083P-A, Revision 1. Therefore, the staff focused its review on changes made to the code and modeling methods that postdate the ESBWR DC, as well as the application of this method to the BWRX-300 design. As such, the staff determined that the M&E rate is a crucial component of the containment analysis where the focus is on conservatively biasing the M&E to determine the peak containment pressure (PCP) and temperature.

The applicant performed extensive qualification and application studies (NEDC-33080P and NEDC-33083P-A, Revision 1) for the ESBWR design due to higher power and other design differences as compared to the SBWR. The applicant, however, did not perform similar in-depth studies of the BWRX-300 since the applicant considers it to be a scaled down version of the ESBWR design. Upon review, the staff largely agrees with this conclusion (specifically with respect to the reactor vessel and its internal systems/components), however, the designs have several key differences in safety system components. The containment “dry” design and other redesigned supporting safety systems described in NEDC-33910P-A, Revision 2, for the BWRX-300 result in a significantly different transient progression and response compared to those evaluated for the ESBWR design. Therefore, the staff focused its review on these aspects where the PIRT consideration of application of the TRACG code to the ESBWR may not completely address the phenomenological progression of the LOCA event for the BWRX-300.

To determine whether using the M&E evaluation model described in the LTR results in an acceptable prediction of the M&E release, the NRC staff reviewed the various phenomena modeled in the LTR and considered whether they were modeled appropriately. These key phenomena are different for the large and small break assessments. For the large break, [[ ]] before the RPV isolation valves close, which prevents further M&E release to containment. Reactor cooldown is then managed by the ICS and [[ ]]. In this method, M&E from each side of the break, before RPV isolation, is summed as a source input for the GOTHIC analysis. In addition, M&E from the intact loop continues for a short time to drain steam and condensate remaining in the steam lines.

For small breaks [[ ]], there are no isolation valves, so the M&E releases [[ ]] throughout the 72-hour transient used for passive plant designs. Consequently, the RCS inventory loss during small breaks can result in reactor core water levels dropping below the top of active fuel (TAF), creating the potential for fuel cladding heat up.

The applicant conservatively assumed in the TRACG code analysis that back pressure from the containment will remain at atmospheric pressure to maximize the M&E release. The staff agrees that this decoupled method will result in higher break flow rates than if the analysis considered pressure increase in the containment. However, since the break flow remains mostly choked, the inclusion of containment back pressure would have minimal to no effect on total M&E from the RCS during the blowdown period.

The staff understands that for this design the LOCA blowdown is very different from that for typical large light-water reactors (LWRs). This is due to the much smaller pipe sizes and the number and extent of passive safety systems employed. As mentioned, GEH did not perform a specific PIRT for the BWRX-300 TRACG code M&E method in accordance with RG 1.203 but relied on previous ESBWR evaluations to determine the important phenomena and the appropriate uncertainties to be applied. The applicant details these differences with the

BWRX-300, which affect modeling inputs, in Section 5.2 of the LTR and concludes that they remain within the same qualification range of conditions as the ESBWR.

RG 1.203 indicates that fidelity in an evaluation model is related to the existence and completeness of validation efforts. Although the staff agrees that the preliminary BWRX-300 design described in the LTR shares many similarities with the ESBWR design, the applicant did not present a complete review of differences related to the new safety system functions in the LTR. However, the staff notes that such a review is not necessarily required for the limited scope of this LTR to determine the maximum M&E to containment from a postulated LOCA, which involves primarily a RPV blowdown, calculation of critical flow, and the longer-term RCS cooldown. Based on the limited scope of this LTR and expected similar behavior of the M&E release modeled in this LTR to the ESBWR qualification range, the staff evaluated the similarities/differences and determined that use of the TRACG code and the qualification basis performed for the ESBWR as shown in Section 3.3 of LTR NEDC-33911P-A, Revision 3, is acceptable for this use. The staff determination however, is limited to the extension of the PIRT application for the purpose of M&E for containment analysis only.

5.2 Application of the ESBWR TRACG Loss-of-Coolant Accident Method to BWRX-300 Mass and Energy Release Calculations

5.2.1 Transient Reactor Analysis Code General Electric Reactor Pressure Vessel Nodalization for BWRX-300

The GEH TRACG M&E RPV model for the BWRX-300 described in the LTR is a modification of the previously approved M&E model described in NEDC-33080P, Revision 1, developed for the much larger ESBWR. Since the vessels are similar in height, the axial nodalization is very similar to ESBWR. The radial nodalization is increased significantly in the core region, even though the core diameter is smaller, while one region is still used for the downcomer. The applicant indicated that this refinement allows the use of the same RPV model both in safety analysis transients and LOCA analyses; however, the staff only reviewed this model for its use for M&E analysis.

Related piping for main steam and feedwater systems are attached to the RPV and scaled from the ESBWR with RPV isolation valves added. The model includes the ICS noding, but the BWRX-300 ICS performs a different function than in the ESBWR design, since the ICS alone provides overpressure protection and emergency core cooling for the BWRX-300 design (as described in NEDC-33910P-A, Revision 2). The ICS has three loops, but only two of the three are modeled as one is assumed unavailable for the licensing-basis single failure criterion. The redesigned BWRX-300 PCCS is not modeled in TRACG and no other containment systems are modeled. For the ESBWR design, both RCS and containment wet well, suppression pool, and drywell systems were modeled within TRACG, but since the BWRX-300 design uses a dry containment, the applicant elected to use a standalone GOTHIC calculation to determine containment peak pressurization from the LOCA transients.

The model contains break noding for main steam and feedwater and small liquid and steam instrument line breaks as shown in LTR Figure 5-3. The ICS supply and return lines, steam box, tubing, water box, and return valves are modeled as shown in LTR Figure 5-4. Each ICS is contained [[ ]] of the reactor cooling pool (LTR Figure 2-2). The ICS noding is more detailed than that used for the ESBWR design. The applicant indicated this is, in part, the reason for code convergence issues related to deficiencies in modeling transport of radiolytic gases.

Main feedwater pumps, isolation valves and specific piping segments are used to model inlet piping at the elevation near the top of the chimney as shown in LTR Figure 5-2. [[

]]. The steam lines include the RPV isolation valves and piping modeled back to the turbine control valve.

Based on GEH's refinement of the modeling of the BWRX-300 in relation to the previously approved ESBWR as described in LTR Section 5.2.1 and appropriate modeling of the key design features of the plant, the staff determined that the TRACG RPV nodalization is acceptable for determining the M&E release.

5.2.2 Large and Small Pipe Breaks

The LTR states that the large steam line break modeling uses piping segments and break location nodes to simulate a double-ended guillotine break in piping just downstream of the RPV isolation valves, as shown in LTR Figure 5-3. [[

]].

For each of these large breaks, there are RPV isolation valves mounted directly to the vessel that [[

|]. In future licensing applications, the applicant would be expected to conservatively estimate the timing input for the drywell pressure signal for each break location.

The ICS valves for a minimum number of IC trains are also assumed to begin opening [[|] after the transient. One train is assumed for steam line break and two are assumed available for the feedwater line break cases. The applicant chose this additional conservatism to ensure that the main steam pipe break analysis is bounding as compared to an ICS steam pipe break, which would have fewer IC trains available for decay heat removal.

Reactor trip is assumed due to [[

]]. During the regulatory audit discussions, the staff sought clarification from the applicant as to whether reactor power will increase just after break initiation if there were a concurrent turbine trip. GEH indicated that the power was modeled conservatively to account for the potential increase in power by the [[ ]] is built into the decay heat curves. The staff agreed that

[[ ]] would reasonably bound the power surge resulting from a turbine trip pressure wave.

The small steam line break is modeled as a valve directly off the RPV to simulate the break opening, in a single sided configuration, discharging into a break node that is used to represent the containment. These are modeling unisolable RPV instrument taps, assumed [[ ]] in diameter, with the upper tap used for the steam break and the lower one for the liquid break. The small break transients each use two IC trains, with one unavailable due to single failure criteria. Consistent with the large-break modeling, the containment is assumed to remain at atmospheric pressure to maximize the break flow rate.

NUREG-0800, "Standard Review Plan for the Review of Safety Analysis Reports for Nuclear Power Plants: LWR Edition," the Standard Review Plan (SRP), Section 6.2.1.3, "Mass and Energy Release Analysis for Postulated Loss-of-Coolant Accidents (LOCAs)," Revision 3, issued March 2007 (ADAMS Accession No. ML053560191), provides guidance for the review of M&E release analysis from postulated LOCAs. The thermal-hydraulic modeling and nodalization used for the BWRX-300 must be adequate to predict all important phenomena in accordance with RG 1.203. Based on this limited scope of the LTR and the expected similar behavior of the M&E release modeled in the BWRX-300 to the ESBWR qualification range, the staff determined that the TRACG code modeling and assumptions used as shown in LTR Section 5.2.1 are acceptable.

5.2.3 Channel Grouping, Decay Heat and Power Shape

GEH states that the BWRX-300 core is modeled using a [[ ]]The outer [[ ]]. The core is modeled at 887.4 megawatts thermal (MWth) using a generic Global Nuclear Fuel (GNF) bundle type and standard-length core, similar to the ESBWR for the conservative cases. The core is modeled [[ ]]. The operating and decay heat [[ ]] by the applicant, consistent with NEDE-33005P-A, Revision 2. The staff found that the BWRX-300 core modeling was consistent with previously approved methods and therefore acceptable.

As identified in LTR Table 5-4, the applicant uses American Nuclear Society (ANS) 5.1-1979, "Decay Heat Power in Light Water Reactors," nominal as the decay heat curve to compute decay heat power for the base cases, and ANS 5.1-1979 plus 2 sigma for the conservative cases. SRP Section 6.2.1.3 provides guidance for the review of the M&E release analysis from postulated LOCAs and endorses ANS-5 1971, "Decay Energy Release Rates Following Shutdown of Uranium-Fueled Thermal Reactors," decay heat curve, to meet the requirements of 10 CFR Part 50, Appendix K, paragraph (I)(A) "Sources of heat during the LOCA," to calculate energy available for M&E releases. However, in response to RAI 06.02.01.03-01, dated May 19, 2021, GEH provided a description of the BWRX-300 M&E method's compliance with Appendix K (I)(A) and referenced consistency with ESBWR (NEDC-33083P-A, Revision 1) as justification for ANS 5-1 1979 decay heat method.

Based on staff's previous analysis in the ESBWR DC approval and recent review of Westinghouse containment method (WCAP-17721P-A, "Westinghouse Containment Analysis

Methodology," August 2015 (ADAMS Accession No. ML15221A008)), the staff agrees that the use of ANS 5.1 1979 with 2 sigma is appropriately conservative and acceptable for use in the TRACG code M&E method for the BWRX-300 design.

Additionally, the staff reviewed the other requirements of Appendix K, paragraph (I)(A) including (1) initial core power and RPV stored energy, (2) fission heat, (3) decay of actinides, (4) metal-water reaction rate, including the rate of energy release, hydrogen generation, and cladding oxidation from the metal/water reaction, and (5) reactor internals heat transfer. The staff found that the BWRX-300 design's modeling was consistent with these Appendix K requirements. It should be noted that although the TRACG code has the capability to compute energy from metal/water reactions, GEH has not considered the potential generation of hydrogen due to metal- water reactions. The staff agrees this is acceptable since the BWRX-300 LOCA acceptance criteria limits cladding temperatures (LTR Section 5.2.3) to those of normal operation such that the temperature threshold of the metal/water reaction would not be reached.

5.2.4 Isolation Condenser Modeling and Radiolytic Gases

The ICs are a similar design to those used for ESBWR; however, the function and connections to the reactor are quite different, as described in NEDC-33910P-A, Revision 2. LTR Figure 5-4 shows the modeling of the ICs. The system consists of [[

]].

In accordance with LTR Figure 2-3, [[

]].

The staff noted that In typical BWR reactor systems such as the BWRX-300, radiolytic gases (hydrogen (H_2) and oxygen (O_2)) are generated in the liquid water in the core and are then liberated during boiling. They become mixed in and carried with the steam into the IC tubing as the ICs begin operation. Then during the condensation process, these noncondensable gases (NCGs) would begin to accumulate in the lower drums and tubing. The accumulation and buildup of NCGs begins at the steam-water interface in the lower drum, and then continues to expand into the tube region, where the bulk of condensation is occurring. In its review, the staff considered that this buildup of NCG in the tubing can significantly degrade the ICs ability to condense steam, reducing its heat transfer capacity to cool the reactor. This buildup of NCG as related to IC performance degradation is critically important for SBLOCA cases where the break is unisolated [[
]]. The IC heat transfer performance must be adequate to cool and depressurize the reactor and to maintain a break flow low enough so that sufficient inventory remains within the reactor core region.

As such, the staff focused on the sufficiency of the method in accounting for the impact of the presence of NCGs. The IC model axial noding used for the BWRX-300 is more detailed than that used for the ESBWR, although physically the size of the component is the same. Its safety function is also expanded to include [[ ]] long-term cooling within a new dry containment system. [[
]]. For this LTR analysis, the large break cases assume the

high drywell pressure occurs at [[ ]] and the small break cases assume high drywell pressure at [[ ]]. The transport, intrusion, and buildup of NCG into the ICs is not explicitly modeled by GEH in the BWRX-300 model. During the staff's regulatory audit discussions, GEH stated [[

]].

The formulation used for generation of radiolytic gases per MWth was given in LTR Section 5.2.4 as a bounding value used generically for the BWR fleet. This volumetric rate was reviewed and approved by NRC staff in a previous submittal (NEDC-33004P-A, Revision 3, "Constant Pressure Power Uprate," dated March 2003 ADAMS Accession No. ML031190318), and thus judged suitable for application to the BWRX-300. The staff notes that this rate is based on post-trip off gas measurements and does not include or address hydrogen that could be generated from potential cladding oxidation, which is not expected to occur in the BWRX-300 based on the M&E LOCA criteria set forth in LTR NEDC-33911P-A, Revision 3.

The applicant then used a series of control block calculations in the BWRX-300 model to estimate radiolytic gas progression into the ICs for determining an overall percentage accumulation in the ICs. The standalone model included simulation of mechanistic transport of H_2 and O_2 within the code but with idealized boundary conditions used from the RPV steam supply and return line connections. [[

]]. The standalone model was run at a range of pressures and NCGs concentrations to develop degradation curve fits. These were then used in the BWRX-300 model to simulate IC tube heat transfer degradation via reduction of a PIRT multiplier based on the estimated accumulation of NCGs in the control blocks.

Because of the idealized boundary conditions used in the standalone model, the control block method will underpredict the accumulation of NCGs in the ICs and therefore the amount of IC heat transfer degradation. The applicant provided additional information in its response to RAI 06.02.01.03-01, dated May 19, 2021, on the conservatisms of the PIRT model used and further discussed degradation effects of the gradual accumulation of NCGs in ICs tube bundles, the associated uncertainties and the subsequent consequences for both the large break and small break limiting cases. The applicant acknowledged that [[

]].

The staff also reviewed the GEH response to RAI 06.02.01-01, dated May 19, 2021, regarding sensitivity analysis results performed by the applicant that demonstrated that [[

]].

The staff also considered the fact that the BWRX-300 design is not finalized, so the ultimate demonstration that [[

]]. Therefore, to enable the staff to reach the finding that the model

produces acceptably conservative results, the staff-imposed a Limitation and Condition (L&C) number (#) 1. documented in Section 7.0 of this SE, such that the total volumetric fraction of radiolytic gases in the IC lower drum be controlled to a sufficiently low level.

The staff noted that the IC return pipe layout for the BWRX-300 design is different from that used for the ESBWR design, and that [[
]]. During a SBLOCA, the chimney steam volume is at a higher pressure than the ICs and steam dome regions, so that at the discharge point, the ICs discharge pipe could face reverse steam flow toward the lower drum when the condensate flow rate is low and the system pressure is reduced. The staff identified that [[
]]. The applicant confirmed in its response to RAI 06.02.01-06 dated October 8, 2021, that the original ESBWR design's return line loop seal would be retained in the final design of the BWRX-300. The applicant acknowledged that large direction dependent form losses were added to the discharge into the chimney to represent the effect of a water loop seal. During the regulatory audit the staff confirmed that the periodic flushing through of steam that would still occur should not significantly degrade the IC performance since accumulation of NCGs are being controlled to a low concentration in the IC lower drums through L&C # 2. documented in Section 7.0 of this SE. [[

]].

The applicant confirmed in its RAI response to Question 06.02.01-01 dated May 17, 2021, that [[
]]. The staff also finds that the applicant's conclusion [[
]] is reasonable, and that it is not necessary to address these phenomena in the containment method. Therefore, the staff found that the method is adequate [[ ]].

5.2.5 Modeling Biases Phenomenon Identification and Ranking Tables

The TRACG code has built-in modeling bias parameters, called PIRTs (e.g., critical flow), that can be specified in code input to modify the results of code runs. TRACG PIRTs are placed strategically on important coefficients and correlations to add or remove biases. This is done with the objective of adding conservatisms or uncertainty locally, or globally, to internally calculated nominal code values. The PIRT ranges are developed from assessment comparisons between separate effects test data and TRACG calculations performed with the best-estimate version of the code and are related to probability density functions (NEDC-33083P-A, Revision 1).

These PIRT multipliers are related to but not the same as the PIRT process. In general, the PIRT process, per RG 1.203, is one of the key steps used to develop an evaluation methodology (EM) or a calculational framework for evaluating the behavior of a particular reactor system for postulated transient or design-basis accident (DBA) analysis. The applicant did not develop an EM specifically for the BWRX-300 design, but rather is depending on and refers to previous evaluations performed for the ESBWR as being directly applicable to this design.

The BWRX-300 is comparable in height to the ESBWR design, with the vessel radius, core flow area, quantity of fuel, and other internals scaled down from the ESBWRs 1,520 MWe to 300 MWe. With similar vertical internal features and apportionments, the staff agrees that internally the BWRX-300 is very similar to the ESBWR. However, outside of the reactor vessel, the safety systems and equipment, including the containment, are very different than the ESBWR design. Besides the new dry containment, the major safety equipment differences are related to using [[ ]] (NEDC-33910P-A, Revision 2). Therefore, the staff notes that the PIRT and modeling biases developed for the ESBWR are not all applicable to the BWRX-300 as is indicated, in part, by LTR Table 5-1. As such, the staff performed a sensitivity analysis of the relevant PIRT modeling parameters listed in LTR Table 5-1 and determined that there was negligible impact on the results and that they were conservatively applied for this M&E analysis application for the BWRX-300.

The PIRT multiplier used in the BWRX-300 TRACG LOCA M&E analysis [[ ]]. The staff also evaluated the critical flow modeling for consistency with

SRP Section 6.2.1.3 and 10 CFR Part 50, Appendix K, discussed in SE Section 5.3.2. In addition, the staff reviewed the conservatism in decay heat modeling that is based on ANS 5.1-1979 with 2 sigma uncertainty, consistent with ESBWR usage, and that evaluation was presented earlier in SE Section 5.2.3.

5.2.6 Initial Conditions for Base and Conservative Cases, Trips

The initial conditions used in the base and conservative cases are listed in LTR Table 5-2. These key initial conditions are considered important plant operating parameters describing steady-state nuclear and hydraulic conditions from which a transient is initiated. The reactor power is at 102 percent of the nominal 870 MWth and the steam and feedwater flow are increased commensurately. The steam dome pressure is increased by [[ ]] and the hot channel power profile is top peaked. The downcomer water level is modeled as [[ ]]. Since the RPV isolation valves close rapidly upon detection of a large break, the initial water level has very low significance for the large break cases. As such, the staff found that modeling of the initial RPV conditions and the valve closure timing inputs are acceptable.

Since this is a methodology LTR, the exact reactor trip signals are not modeled in the example cases provided, but reasonable times and events are assumed at transient initiation like loss of alternating current (AC) power at break initiation. The reactor scram delay is conservatively set at [[ ]] is built into the scram table. The high containment pressure trip, which actuates the ICs, is manually set at [[ ]] for the large break cases, and [[ ]] for the small break cases. Main feedwater coasts down to [[ ]] and postulated break opens instantly [[ ]]. High containment pressure or water level at Level 2 causes RPV isolation valves to close, isolating all connections [[ ]] or larger. For the LTR, it is assumed [[ ]]. The IC valves are actuated by [[ ]].

Due to single failure, generally only two of three ICs are assumed to be available for the M&E LOCA analyses. However, for the large steam break only one of three ICs is assumed available. The applicant added this conservatism to the large break steam case so that it remained limiting in comparison to an assumed IC supply line break case which would also

assume only one IC is available. Also, the containment backpressure for the TRACG M&E releases is conservatively assumed to remain at atmospheric pressure throughout the transient.

The staff reviewed these initial conditions for the base and conservative cases, particularly LTR Table 5-1, and determined they were correctly selected and biased, as necessary, to produce appropriately conservative results. The staff's own independent sensitivity studies that used the TRAC/RELAP Advanced Computational Engine (TRACE) best-estimate reactor systems code developed by the NRC for analyzing transient and steady-state thermal-hydraulic behavior in LWRs supports this finding. Therefore, the staff agrees that the initial conditions outlined in the LTR are acceptable for use.

5.3 Demonstration Cases for Large Breaks

5.3.1 Base Case for Large Feedwater and Steam Breaks

The main steam pipe breaks are analyzed conservatively to bound all other steam pipe breaks by assuming only one IC is available. The base cases use nominal initial conditions and nominal modeling parameters, (i.e., all the PIRT multipliers described in LTR Table 5-1 are set to 1.0). The staff reviewed the results of the base cases because they provide an indication of margin added to key figures of merit (FOM) by the conservative analysis.

The large steam break progresses as follows:

- Main steam pipe break occurs inside the containment concurrent with loss of offsite power.
- Feedwater pumps trip [[ ]].
- A reactor trip occurs [[ ]].
- Drywell high pressure is reached at [[ ]].
- [[ ]].
- The IC return valves for IC train A open at [[ ]].

The transient is run out to [[ ]], which allows the RPV to cooldown to near atmospheric pressure. The staff noted that [[ ]].

Main feedwater pipe breaks are modeled [[ ]]; otherwise, the assumptions used are the same as those for the large steam break. The progression of the feedwater line break have the following differences:

- The main feedwater pipe break occurs inside the containment.
- [[ ]].

The staff determined that the base cases are modeled appropriately, and that the overall conservatism of the conservative cases is sufficient. The staff reached this conclusion by reviewing the base cases, including information obtained during the regulatory audit, and confirming this conservatism with the staff's independent calculations using TRACE.

5.3.2 Conservative Case for Large Feedwater and Steam Breaks

The staff reviewed the LTR basis documents and calculations during the regulatory audit for the conservative cases of the large feedwater and steam breaks. These cases use initial power conditions with [[ ]] so main steam and feedwater flow are increased, and conservative modeling parameters, (i.e., the PIRT multipliers described in LTR Table 5-1, [[ ]]. The initial conditions are based on LTR Tables 5-2 and 5-4 inputs for conservative calculation cases. The applicant indicates in Section 5.2 of the LTR that the modeling inputs used for the BWRX-300 are within the qualification and assessment ranges performed for the ESBWR design, so that the PIRTs are directly applicable as previously indicated and reviewed in Section 5.2.5. [[

]]. Consequently, the conservative cases reach a worse outcome in terms of the FOM, so these are the cases the staff evaluated to determine acceptability of the method consistent with SRP Section 6.2.1.3 and 10 CFR Part 50, Appendix K.

The break mass flow for the conservative main steam line break case is shown in LTR Figure 5-13 and this case uses a [[ ]] on critical flow. [[

]]. The staff reviewed the mass flow generated by this input and found it to be reasonably conservative in comparison to results obtained by the staff calculations, using the Moody correlation (ADAMS Accession No. ML12142A162) extrapolations, and confirmatory TRACE code results. The staff therefore determined that the mass flow results are acceptable and consistent with meeting the requirements of 10 CFR Part 50, Appendix K, and Appendix A, GDC 50.

The staff also checked a sampling of the other PIRT settings to ensure they yielded conservative results in comparison to settings used in Table 5-1 of the LTR. The staff found that besides the PIRT multiplier for critical flow, [[

]]. The staff's analysis with TRACG code confirmed that the PIRT values have a very negligible effect on main steam break cases.

The staff also reviewed the main feedwater event results shown in LTR Figures 5-15 through 5-17 and determined that, the mass entering containment is slightly larger than the steam line break, but the energy released is significantly less, so it is not limiting for M&E releases. [[

]]. Both the large main feedwater and main steam transients retain adequate core inventories so that the core is never uncovered. The staff found that the modeling and results of the main steam and feedwater cases are reasonable and acceptable for determining M&E releases for the BWRX-300 design considering L&C # 1. as documented in Section 7.0 of this SE.

5.4 Demonstration Cases for Small Breaks

The staff reviewed the LTR and the basis documents and calculations during the staff regulatory audit regarding the small steam and liquid pipe breaks. The small steam and liquid pipe breaks are unisolated, so break flow continues throughout the 72-hour transient and the containment is conservatively assumed to remain at atmospheric pressure. [[

]].

The small breaks also include (1) base cases that use nominal initial conditions and nominal modeling parameters, (i.e., the PIRT multipliers set to 1.0) and (2) conservative cases that use increased initial power and increased main steam and feedwater flow, with conservative modeling parameter inputs, [[ ]]. The small breaks are modeled as single sided. Additionally, [[

]].

The staff noted that the small steam break progresses as follows:

- A small steam pipe break occurs inside the containment concurrent with a loss of offsite power.
- Feedwater pumps trip [[ ]].
- The reactor trips [[
  ]].
- Drywell high pressure is reached at [[ ]].
- [[
  ]].
- The IC return valves for IC trains A and B open [[
  ]].

The transient is run out to 72-hours, consistent with the analysis practice for passive emergency core cooling system (ECCS) plant applications that do not consider operator action or AC power to mitigate consequences for up to 3 days. The degradation of IC heat transfer performance is simulated by PIRT multipliers in the same manner as the large break cases.

The small liquid line pipe breaks are modeled similarly, also with two IC trains used. However, the liquid line break [[ ]].

LTR Figure 5-22 shows the break mass flow and enthalpy for the conservative case for the small steam line, and the conservative cases use the same PIRT multipliers as the large break

cases. The staff also reviewed the mass flow generated by the small break cases and found them conservative in comparison to calculation of Moody results by staff at various points of time throughout the small break transient. LTR Figure 5-20 shows the RPV downcomer level and indicates that core levels are trending toward the TAF.

LTR Figure 5-27 shows the break mass flow for the conservative case for the small liquid line. The staff reviewed the mass flow generated by these cases and also found them conservative in comparison to the calculation of the Moody results by the staff at various points of time throughout the transient. LTR Figure 5-25 shows the RPV downcomer level [[

]] (LTR Figure 5-26).

The GEH CEM acceptance criterion, approved by the staff in NEDC-33910P-A, Revision 2, maintains that clad temperatures remain below initial steady-state operating temperatures. Therefore, the uncertainty involved in the heat up calculations and the margin in the predicted core water level are important parameters calculated in the method. As such, the staff focused its review on these aspects. In addition to the uncertainty in the core heat up, the uncertainties related to RPV depressurization rates are strongly correlated to the effect of radiolytic gas on IC heat transfer performance, and the staff's review also focused on these effects. The applicant indicated a design change would be made to [[

]]. Therefore, the staff considers the existing method associated with the heat transfer multiplier for IC performance to be adequate considering L&C # 1, as documented in Section 7.0 of this SE.

Relative to heat up and the reactor core water level response, the staff noted that in the core modeling, the applicant [[

]]. The TRACG code uses NRC-approved critical heat flux (CHF) correlations that have been evaluated for (GNF2 fuel) in NEDC-33005P-A, Revision 2, for small break phenomena, which is similar to CHF occurring from small break cases for the BWRX-300 design. The staff notes that the modeling used for the BWRX-300 M&E release, although more detailed than the modeling used for ESBWR, is not to the level of detail previously approved by the staff (ADAMS Accession No. ML18143A221) for BWR/2-6 ECCS-LOCA application. The staff also notes that any uncertainties used for these TRACG ECCS-LOCA analysis methods for BWR/2-6 have not been applied here, although the applicant used some of the methods to develop channel grouping and core power shape. The staff notes that it did seek clarity on whether this methodology model has been adequately quantified for phenomena where the core is forty (40) percent uncovered (i.e., collapsed liquid level) with very low decay heat. However, since this method is strictly for M&E releases and it is not the limiting case for containment design, the staff concluded that this core modeling is acceptable for this LTR based on SRP Section 6.2.1.3 and requirements of Appendix K and GDC 50. In future licensing activities where an applicant seeks to demonstrate the criteria of 10 CFR 50.46 are met for SBLOCA analyses, the staff will evaluate the safety-significance of the core heat up response involving uncovery with very low decay heat that was not encountered for the ESBWR design.

The staff found that the modeling and results of the small break steam and liquid cases are reasonable and acceptable for determining M&E releases for the BWRX-300 design considering the implementation of L&C #'s 1, 2, 3, and 4, as documented in Section 7.0 of this SE.

5.5 Summary of the Application Method for Large and Small Break LOCA Analyses

The BWRX-300 TRACG model shown in LTR Figures 5-3 and 5-4 describes the nodalization and the modeling used to simulate the RPV and ICS functional behavior for large and SBLOCA transients. The modeling used and inputs chosen to rely heavily on previous assessments performed for the ESBWR design. Although the vessel geometry of the BWRX-300 design is scaled down from the ESBWR design, there are several important system differences and interfaces. Some of these have been adequately incorporated into the method while others, particularly the PIRTs, do not have as clear of a basis since a BWRX-300 specific PIRT was not performed, and as such the staff focused its review in these areas.

The staff noted in its review that the large break steam and feedwater events are isolated [[ ]] that these design differences between the BWRX-300 and the ESBWR will have very minimal impact on the results. The main steam case results in the maximum M&E and long-term cooling are ample since there is minimum core inventory loss as the reactor cools up to 72-hours. Since the small break steam and liquid cases remain unisolated (i.e., open and flowing) throughout the 72-hour transient, the consequences of the event are more complex and highly dependent on adequate cooling capacity by the ICs to depressurize the RPV and maintain core inventory. With the design change [[ ]] consistent with implementation of L&C # 1 as documented in Section 7.0 of this SE, the potential for IC heat transfer degradation due to buildup of radiolytic gases becomes negligible. [[ ]]. However, the implementation of L&C # 1, 2 and 3, in Section 7.0 of the SE, ensure the method is suitably conservative, since only a very low concentration of NCGs in the IC lower drums is permitted, which eliminates gas progression into the heat transfer tubes.

The staff finds the TRACG code M&E method acceptable based on the evaluation above and because it is consistent with the guidance in SRP Section 6.2.1.3. The staff also finds the method is appropriately conservative for determining the M&E release, subject to the implementation of the L&Cs in Section 7 of this SE.

6.0 CONTAINMENT ANALYSIS METHOD USING GOTHIC

Section 6.0 of the LTR describes the following aspects of the GOTHIC application method and the development of the BWRX-300 containment model:

- Identification of the relevant inputs and physical phenomena relevant to the BWRX-300 containment thermal-hydraulic response.
- Description of the GOTHIC input model for the BWRX-300 containment, including nominal inputs, assumptions, and correlations.
- Description of the base cases and results.
- Nodalization sensitivity studies for the containment and the PCCS.

- Identification of the key modeling uncertainties and biases used in the conservative GOTHIC input model for the BWRX-300 containment.

- Benchmark predictions of test data applicable to BWRX-300 containment design.

- Demonstration analyses to show the BWRX-300 containment response for various break sizes and locations using the conservative GOTHIC containment model.

- Demonstration of the capability of the PCCS to reduce the containment pressure in the long-term, recognizing the small unisolated liquid break as a potential limiting loss-of-coolant accident SBLOCA.

- Evaluation of the overall conservatism by comparison of the conservative and base case results.

- Description of the one-way coupling between the TRACG and GOTHIC calculations, and the use of atmospheric pressure as the break boundary condition used to calculate conservative TRACG M&E for input to the GOTHIC containment model.

6.1 Generation of Thermal-Hydraulic Information for Containments Phenomenon Identification and Ranking Table

LTR Section 6.1 discusses the references and bases for identifying the phenomena important to the analysis of the BWRX-300 containment response for DBEs. The identified DBE phenomena are listed and ranked in PIRT Table 6-2 of the LTR. The purpose of the table is to assess the ability and qualification of the evaluation model for calculating the effect of the identified phenomena on the containment pressure and temperature, and to determine any additional testing, scaling or analysis needed to qualify GOTHIC for analysis of the BWRX-300 containment response. The LTR states that the initial phenomena list relevant to the BWRX-300 containment analysis was obtained by reviewing the following sources:

- NEDC-33083P-A Revision 1, TRACG Application for ESBWR.

- NEA/CSNI/R3(2014), “Containment Code Validation Matrix,” issued May 2014 (ADAMS Accession No. ML15224B463).

- SMSAB-02-02, “An Assessment of CONTAIN 2.0: A Focus on Containment Thermal Hydraulics (Including Hydrogen Distributions),” issued July 2002 (ADAMS Accession No. ML022170122).

The LTR provides further details about the selection of the phenomena applicable to the BWRX-300 containment response analysis using the above references. The staff confirmed the referenced details about the phenomena and their significance in the cited references. The applicant considered the ESBWR phenomena for applicability to DBE evaluations of the BWRX-300 design, as well as the additional ones that might apply to the BWRX-300 but not to the ESBWR. The LTR does not include the phenomena related to fan and spray dynamics or M&E exchange, as they are not applicable to BWRX-300, and does not include non-DBE phenomena.

The staff found the applicant's use of the referenced information appropriate for the development of the GOTHIC PIRT for the BWRX-300. Since the BWRX-300 has a dry containment while ESBWR has a wet containment, the staff found it appropriate that many of the ESBWR containment phenomena would not apply to the BWRX-300 containment. However, the LTR stated "the information in Reference 7.10 was reviewed for phenomena that are applicable to the BWRX-300 containment pressure and temperature analysis, including phenomena that would have equivalent phenomena in BWRX-300, even if the component was of a different design (for example, the secondary side heat transfer to the ultimate sink pools was evaluated because the phenomena are equivalent for the [[

]]. The staff concludes that considering the critical role the PCCS plays in mitigating the long-term containment pressure during an unisolated SBLOCA as well as the potential for reverse flow from the containment back into the RPV, the applicant would need to justify the PCCS secondary-side heat transfer modeling for any alternate PCCS design. This is addressed in L&C # 4 in Section 7.0 of this SE.

6.2 Phenomenon Identification and Ranking Table Survey

Subject matter experts retained by the applicant reviewed the PIRT, and using the criteria identified in LTR Table 6-1, ranked the phenomena in importance to the GOTHIC BWRX-300 containment pressure and temperature analysis, and identified any missing significant phenomena. To facilitate the GOTHIC method qualification for large-break loss-of-coolant accident (LBLOCA) and SBLOCA, the phenomena rankings were evaluated separately for the short-term and long-term transient evolutions. As described, in the short-term, the momentum and inertial effects resulting from the break flow have a significant contribution to the flow circulation, stratification, and heat transfer in the containment. In the long-term, the momentum and inertial effects of the break flow are diminished, and buoyancy is the major contributor to the flow circulation, stratification and heat transfer. LTR Table 6-2 summarizes the rationale used by the experts to reach the tabulated short-term and long-term PIRT rankings for the phenomena applicable to the BWRX-300 containment and LOCA scenarios.

The staff reviewed the qualitative details of the BWRX-300 containment PIRT survey methodology and found it to be rigorous and consistent with the industry best practices. Sufficient interaction took place among the experts and the applicant for the consensus building on the PIRT rankings. The phenomena identification and rankings were finalized before performing the preliminary GOTHIC calculations, which the staff considers to be conservative. The staff also confirmed that the subsequent discussion of each phenomena is consistent with the information tabulated in in LTR Table 6-2.

6.3 Overview of the Development of Assessment Base

RG 1.203 describes a multistep process for developing and assessing evaluation models to analyze transient nuclear power plant responses during the postulated DBEs. RG 1.203 is used to establish an acceptable evaluation method based on a well-defined application and FOM. The LTR states that the development of the assessment base follows the applicable sections of RG 1.203 guidance. It also states that most of Elements 2 and 3 in RG 1.203 have been completed as part of the GOTHIC code development and documented in the GOTHIC technical and qualification reports. The following lists the remaining items of RG 1.203 Elements 2 and 3 covered in the LTR:

- determining uncertainty in the correlations relating to the phenomena ranked high and medium based upon the existing experimental base for these correlations

- establishing suitably conservative biases in the above correlations

- establishing suitably conservative input parameters

- benchmarking the method against the integral test's representative of the BWRX-300 containment to demonstrate the conservatism in the method

The staff reviewed the information in this LTR with respect to the remaining elements of RG 1.203 for a conservative BWRX-300 containment analysis method. The BWRX-300 CEM uses the code, scaling, applicability, and uncertainty described in NUREG/CR-5249, Revision 4, "Quantifying Reactor Safety Margins: Application of Code Scaling, Applicability, and Uncertainty Evaluation Methodology to a Large-Break, Loss-of-Coolant Accident," issued December 1989 (ADAMS Accession No. ML030380503), and RG 1.203, with containment pressure and structure temperature being the two FOM. The staff noted that LTR NEDC-33911P-A, Revision 3, describes the application of RG 1.203, Element 1 to the BWRX-300 evaluation model development, up to the GOTHIC PIRT development step. The identification of the FOM, systems, components, phases, geometries, fields, and processes for the purpose of modeling had been finished as a part of LTR NEDC-33911P-A, Revision 3. The staff determined that the LTR includes the remaining information needed to develop the assessment base for BWRX-300 for using GOTHIC code and qualifications, per Elements 2 and 3 in RG 1.203.

Sections 6.1 and 6.2 of this SE discuss the staff's evaluation of the GOTHIC PIRT development and justification for their rankings. The staff considered the information provided in the GOTHIC version 8.3 code qualification documentation and found it to be adequate to address most of the PIRT as applicable to the BWRX-300 thermal-hydraulic safety analyses. The staff concludes that that the applicant appropriately identified and has included the remaining information needed to address Elements 2 and 3 of RG 1.203 that is not part of the Gothic code qualifications in the LTR to be addressed as part of RG 1.203. The staff also agrees that the BWRX-300 CEM is consistent with RG 1.203 by using a conservative analysis utilizing mature computer codes with sufficient qualification base, and is therefore, acceptable. The staff evaluation of the remainder of the information provided to address Elements 2 and 3 of RG 1.203 that is not integral to the Gothic code is provided as follows in Sections 6.4 through 6.11 of this SE.

6.4 Knowledge Level for the Phenomena Pertinent to Containment Analysis

LTR Section 6.4 describes the assessment of the available knowledge for the important PIRT phenomena that were ranked High or Medium in LTR Table 6-2. LTR Table 6-3 summarizes the knowledge level for those phenomena, as decided by the expert panel that developed the PIRT in LTR Table 6-2. The knowledge level for each phenomenon is ranked from 1 (least confidence) to 4 (most confidence) in LTR Table 6-3, which also lists the consolidated rationale for the knowledge level. The staff reviewed the rationales provided for the development of knowledge levels and agrees with the elimination of the following three phenomena from LTR Table 6-3 due to their low PIRT rankings in LTR Table 6-2:

- [[

-
-]]

However, the staff does not agree with the elimination of a fourth “Potential system interactions” phenomenon, due to the potential in the BWRX-300 design for reverse break flow to occur during the long-term transient evolution, and subsequent nitrogen ingestion from the containment to the RPV. Section 6.10.2 of the SE discusses the possible interaction between the containment and RPV due to potential reverse break flow and nitrogen ingestion into the ICS during a SBLOCA. This specific phenomenon will be dispositioned at the licensing stage by addressing a limitation and condition to ensure that reverse break flow does not occur, or any reverse flow that occurs is not safety-significant.

In general, the staff notes that a PIRT phenomenon ranked high in LTR Table 6-2 for importance and low in LTR Table 6-3 for knowledge level would need further investigation. Therefore, the staff found it conservative to include all remaining LTR Table 6-2 PIRT phenomena in the base GOTHIC model calculations before evaluating their modeling uncertainties, even though some of the phenomena may not be applicable or their effect may be insignificant for this BWRX-300 DBE.

6.5 Generation of Thermal-Hydraulic Information for Containments Model

LTR Section 6.5 presents the salient geometrical and thermal-hydraulic features of the GOTHIC model used for the BWRX-300 containment analysis. LTR Figure 6-1 shows a schematic of the four components of the GOTHIC model, representing the main section of the containment, the containment dome region above the refueling bellows, the PCCS, and the reactor cavity pool (RCP). The LTR states that the containment dome is connected to the main containment section through two flowpaths, representing the manholes in the refueling bellows. The main cylindrical containment section and the hemispherical containment dome are nodalized in GOTHIC by using three-dimensional rectilinear sub-divided volumes, as shown in LTR Figure 6-2. [[

]].

Flowpaths are used to model the intake and exit openings of the [[ ]] connected to the RCP. These PCCS units are placed [[

]]. LTR Figures 6-2 and 6-3 show [[

]]. LTR Figure 6-3 shows [[

]]. The LTR describes how the [[

]]. LTR Figure 6-1 shows [[

]]. The LTR further describes [[

]].

The RPV is represented in the GOTHIC model by a blockage corresponding to the outer dimensions of the RPV insulation. Approximately [[ ]]of the remaining volume is assumed to be obstructed by various support structures, piping, catwalks, etc., which the staff found consistent with previous DCs. The properties of the thermal conductors that are distributed over the RPV surface cells are set to maximize the heat loads from the RPV and piping, which is conservative. The break mass flow rate and enthalpy, as obtained from the TRACG M&E calculations, are specified as a time-dependent boundary condition to the containment GOTHIC model. The fluid temperature in the piping is assumed to be the same as the RPV fluid temperature, which the staff finds to be conservative, and is specified as a function of time as obtained from the TRACG calculations. The thermal conductors for the RPV and piping are also coupled to the containment, which will account for the heat transfer from the RPV to the containment even after the break flow stops either due to the isolation valve closure or pressure equalization. The break flow path was modeled as being next to the containment shell with break flow directed toward the shell. The staff agrees that this is conservative for calculating the maximum shell temperature. The applicant submitted additional break location and flow orientation sensitivity studies to determine the limiting break location for the purpose of calculating PCP. [[

]] is conservative for calculating the PCP, as discussed in Section 6.10.1 of the SE.

The following is a list of the additional modeling parameters and assumptions used in the GOTHIC base cases.

- [[

]].

- The latent part of the heat transfer due to condensation is calculated using the Diffusion Layer Model (DLM) in GOTHIC (LTR Reference 7.16).

- [[

]].

- For the shell side heat transfer coefficient calculations, the characteristic length for forced convection is set to the [[

]].

- Wall friction is calculated from the Colebrook relationship for a smooth wall.
- The form loss coefficients in the PCCS are set to conservatively high values.
- Radiation heat transfer to the shell and the PCCS is conservatively ignored.

LTR Table 6-2 recognizes several thermal-hydraulic phenomena with medium to high PIRT rankings [[

]]. As presented in LTR Section 6.5, the BWRX-300 CEM uses a [[

]].

The LTR documents that the heat transfer coefficient inside the PCCS tubes is reduced by [[ ]] in all cases, which the staff found to be conservative. The applicant also compared the McAdams correlation form used for natural convection with the Churchill and Chu's correlation that is applicable to the entire range of Rayleigh (Ra) numbers. The applicant stated that "The Nusselt (Nu) number can be calculated as the higher of the Nu numbers in the laminar and turbulent natural convection regimes instead of determining whether the flow is in the laminar or turbulent flow regimes and calculating the Nu number from the respective correlation for natural convection." The selection of the higher Nu value would capture the correct flow regime, as the flow must be laminar at the very beginning that corresponds to a higher Nu, as demonstrated by $Ra \sim 10^{9}$. GEH provided additional information in its RAI response to RAI 06.02.01-08 dated October 8, 2021.

The staff concluded that [[

]]. Furthermore, the staff agrees that using the higher of the Nu numbers calculated for the laminar and turbulent flow in the BWRX-300 CEM for the PCCS design is also justified for both natural and forced convection regimes, as it appropriately captures the applicable convection regime.

The applicant provided an additional description in its response to RAI 06.02.01-08 dated October 8, 2021, of how the resulting density-driven single-phase flow recirculation gets established [[ ]]. The applicant provided a table showing the short-term and long-term snapshots for the PCCS parameters and nondimensional numbers (Re, Gr, Pr, Ra, and Ri) around the middle of PCCS Units #1 and #5. It also compared the small steam pipe break for PCCS Unit #1 (closest to the break) and PCCS Unit #5 (farthest from the break), for the flow velocity and temperatures of the containment space, outer and inner PCCS walls, and liquid between the inlet and middle of the PCCS. The staff determined that [[

]], as discussed in SE Sections 6.7.2 and 6.8.3. The NRC staff finds the overall GOTHIC modeling approach as discussed above to be acceptable for the BWRX-300 containment and PCCS design, based on the information provided in the LTR as well as additional information submitted in the applicant's RAI responses.

6.6 Base Cases and Results

LTR Sections 6.6.1 and 6.6.2 present the containment response to the M&E calculated in LTR Section 5.3.1 for large steam and feedwater pipe breaks using the base GOTHIC model, (i.e., without using conservative biases). LTR Table 6-4 in Section 6.6 lists the key containment inputs used in base cases, while a review of the containment nodalization and thermal-hydraulic modeling has been discussed in SE Section 6.5. As stated above, the calculations discussed in LTR Section 6.6 were performed using nominal initial conditions and nominal modeling parameters without any conservative biases and will be referred to as "base cases" that were performed using "base GOTHIC decks." The discussion in this SE will also reference "conservative cases" that were performed using "conservative GOTHIC decks," which are the same as the base GOTHIC decks except that, where appropriate, the input conditions and modeling parameters are biased in a conservative direction. The applicant submitted both base and conservative GOTHIC decks to facilitate the staff's review of the containment model dated December 17, 2020 (ADAMS Accession No. ML21028A471), then revised and updated on March 23, 2021 (ADAMS Accession No. ML21082A500) and December 14, 2021 (ADAMS Accession No. ML21348A073). The staff performed independent confirmatory analyses using the best-estimate reactor systems codes TRACE and MELCOR to analyze containment thermal hydraulic behavior in support of the staff's findings.

6.6.1 Containment Response to Large Steam Break, Base Case

LTR Section 6.6.1 presents information on the base case of a large steam pipe break. LTR Figure 6-4 shows the containment pressure response to a large steam line break inside the containment, with a PCP [[ ]] occurring at the time the RPV isolation valves fully close [[ ]]. The staff noted that after the closure of the RPV isolation valves, the BWRX-300 CEM appropriately accounts for the heat transfer to the containment due to convection from the RPV wall and hot pipe surfaces. With the break flow isolated, the containment pressure starts decreasing. [

]]. As such, the staff notes that a licensing-basis analyses would need to demonstrate that the pressure in the final BWRX-300 containment design is reduced to less than 50 percent of the peak accident pressure for the most limiting LOCA within 24 hours, in accordance with the third acceptance criterion identified in of LTR NEDC-33911P-A, Revision 3, Section 3.0.

LTR Figure 6-5 shows the airspace, containment shell, and PCCS exit temperature responses. The staff found that [[

]]. The figure shows the maximum and average of all nodal air temperatures in the containment. It also plots maximum shell temperatures for the inner and outer surfaces, as well as the PCCS exit temperature. LTR Section 6.6.1 appropriately describes various physical trends captured in LTR Figure 6-5. The temperature rise in the containment is attributed to both the expansion of steam from the RPV and to the compression of nitrogen in the containment. The PCCS exit temperature shows

[[
]].

LTR Figures 6-6 and 6-7 show the decay heat and heat removal by various mechanisms following the large main steam pipe break. The staff noted that the isolation condensers are the primary mechanism for removing decay heat from the isolated RPV, [[
]].
The staff performed confirmatory analyses that also showed that various trends depicted on Figures 6-6 and 6-7 are consistent with the event progression during the large main steam pipe break.

LTR Section 6.6.1 states “No credit is taken in these cases for the heat transfer from the containment shell to the concrete supporting structures.” Section 2.0 in the LTR states that “[[
]].” However, the LTR did not describe the thermal boundary condition for the containment outer surface, except for the PCCS pipes and the containment dome. To clarify the thermal boundary condition intended for the containment outer surface in the BWRX-300 CEM, the applicant described in its response to RAI 06.02.01-03, dated September 17, 2021, that the containment boundary includes a metal shell that would be free-standing (metal containment type), in loose contact with concrete (reinforced concrete containment vessel type), or in tight contact with concrete (steel concrete composite structure type). Regardless of the eventual containment type, no credit is taken for heat loss from the outer surface of the metal shell to air or concrete. This is not only an assumption used in the demonstration calculations but it is the boundary condition to be used in the application method. The applicant explained that there are also structures in the containment currently in development. The demonstration calculations did not credit the energy absorbed in these structures. The staff evaluated these conditions and agrees that neither the composition of the containment shell nor the modeling of internal structures is a limitation on the application method and finds the response to be acceptable.

LTR Section 6.6.1 also describes that the BWRX-300 containment subcompartments include the volume below the RPV, the space between the RPV and the biological shield, and the containment head area above the refueling bellows. The applicant identified the subcompartment in the containment head area above the refueling bellows as the limiting location with respect to differential pressures acting across subcompartment boundaries because of its relatively small flow area provided by the access manholes in the bellows. The other subcompartments inside the containment [[
]] have much larger openings. LTR Figure 6-8 shows the pressure differential across the refueling bellows, as calculated by the GOTHIC model using a high flow loss coefficient value [[ ]] across the manholes to maximize the differential pressure. Based on the lag between the sharp containment pressure rise closest and farthest from the break near the refueling bellows, the staff confirmed that the GOTHIC model realistically captures the pressure wave propagating through the containment immediately following the break. [[
]], which is [[ ]] of the PCP and is small for a subcompartment boundary. The staff agrees that the pressure drop across other subcompartment boundaries with larger flow area-to-volume ratios at farther locations from the break would be smaller, and that the GOTHIC model is an appropriate tool to analyze the break pressure waves and subcompartment pressurization. Determination of the jet

impingement loads acting on the containment structures is outside the scope of this LTR; therefore, an applicant or licensee will need to address the potential effect of pressure differentials on the structural integrity of the BWRX-300 containment subcompartment walls as part of future licensing actions.

6.6.2 Containment Response to Large Feedwater Pipe Break, Base Case

LTR Figure 6-9 shows the base case containment pressure response for a large feedwater pipe break. Similar to the large steam pipe break, the peak pressure [[ ]] is reached at the time the RPV isolation valves fully close [[ ]]. After the closure of the RPV isolation valves, the only heat input to the containment is from the RPV wall and hot pipes. [[

]]. This demonstrates that the PCP for the large feedwater pipe break is bounded by the PCP for a large steam pipe break.

LTR Figure 6-10 shows the airspace, containment shell, and PCCS exit temperature responses for the large feedwater pipe break base case. The figure shows the maximum and average of all nodal air temperatures in the containment. It also plots the maximum shell temperatures for the inner and outer surfaces, and the PCCS exit temperature. The staff determined that all physical trends in LTR Figure 6-10 are very similar to those of the large steam pipe break captured in LTR Figure 6-5. Therefore, all the discussion in SE Section 6.6.1 of large steam pipe break also applies to the containment response to feedwater pipe break. The staff also determined that all temperature responses depicted in LTR Figure 6-5 for the large steam pipe break bound the ones in LTR Figure 6-10 for the large feedwater pipe break; and are, therefore acceptable.

.

6.7 Nodalization Studies

6.7.1 Nodalization Study for Containment

The LTR presents a containment nodalization study, using the base case for the large steam pipe break (LBLOCA) event discussed in SE Section 6.6.1. LTR Figure 6-11 represents the following four main containment section nodalization study cases.

- base case [[ ]]
- coarser grid with twice the node size of the base case in each direction [[ ]]
- finer grid with half the node size in each direction in the horizonal plane as the base case and the same vertical node size [[ ]]
- finer grid with half the node size in the vertical direction as the base case and the same node size in the horizontal plane [[ ]]

LTR Figure 6-12 shows the effect of nodalization on the containment pressure for the large steam break base case for each of the four nodalization schemes. The applicant chose a default [[ ]] containment nodalization as the LBLOCA base case for the PCP calculation. LTR Figure 6-12 shows a difference of [[ ]] in the calculated PCP between the base case and finer nodalization cases, which indicates [[

]] compared to the [[ ]] conservatism demonstrated in LTR Figure 6-26. The LTR states that the placement of [[ ]] was accurately done [[

]] LTR Figures 6-12 and 6-13 show little difference in the containment pressure, air/steam mixture, and shell temperatures [[ ]], which suggests that [[ ]] is adequate to resolve the phenomena controlling the containment thermal-hydraulic response. The staff found the short/long-term temperature response differences to be consistent with the pressure trend differences shown in LTR Figure 6-12, as well as the DLM's flow field modeling discussed in SE Section 6.10.1. Therefore, the staff finds the [[ ]] to be acceptable for use in the CEM for evaluation of the BWRX-300 containment response during a LBLOCA. Since the modeling uncertainties are adequately addressed (see Section 6.11 of this SE) through conservative biases and input parameters, further conservatism via the choice of nodalization is unnecessary.

The SBLOCA and LBLOCA are different DBEs that involve different phenomenological concerns. As the break flow is not isolated in a SBLOCA while it is isolated in a LBLOCA, the steam/air movement inside the containment is expected to be different. [[

]]. LTR Figures 6-12 and 6-13 show some [[ ]]. These phenomena are equally applicable to SBLOCA. With the complex SBLOCA phenomenology involving the novel PCCS design and RCP heatup in the later stage of the transient, [[ ]]. The applicant provided a similar nodalization study for limiting SBLOCA including additional information in its RAI responses and revised response to Question 06.02.01-01, dated December 17, 2021, which confirm that the relevant thermal-hydraulic phenomena were adequately captured up to 72-hours in the [[ ]] containment nodalization for the SBLOCA analysis. Section 6.10.2 of this SE contains further discussion on SBLOCA phenomena and modeling.

6.7.2 Nodalization Study for Passive Containment Cooling System

LTR Sections 6.7.2 and 6.8.3 present a study on the effect of nodalization on the PCCS performance. The study was conducted on a single PCCS unit placed in a large containment volume that is kept at a specified temperature and steam concentration. The PCCS and containment nodalizations in the vertical direction used in this study are the same as that of the base case BWRX-300 containment model, as described in SE Section 6.5. Like the default base nodalization, the containment has [[

]].

As the objective is to study the sensitivity of the overall PCCS heat transfer to the PCCS nodalization, the second case used in the PCCS nodalization study doubles the number of nodes both in the PCCS [[ ]] and containment, and the third case doubles the number of nodes again [[ ]]The containment pressure is [[

]], and a [[ ]] reduction is applied to the heat transfer on the outer surface of the PCCS unit. LTR Figure 6-14 shows the effect of nodalization on the heat removal rate [[

]]. The staff also reviewed additional support calculations and analysis information during the regulatory audit regarding the GEH nodalization study and performed confirmatory analyses. The staff concluded that the applicant has demonstrated that the PCCS heat transfer performance is not sensitive to the finer nodalization beyond the base case and the differences are insignificant in the context of overall containment design conservatism. SE Section 6.8.3 contains further discussion of this study.

6.8 Model Uncertainties and Biases

LTR Section 6.2 identifies the source of uncertainties in the phenomena important to the containment pressure and temperature response, while LTR Table 6-3 in Section 6.4 summarizes the knowledge level for these phenomena. LTR Section 6.8 presents a grouping of the phenomena and their assessment based on the observations made from the base case containment analysis results as discussed in Section 6.6. LTR Section 6.8 identifies the conservative biases needed to cover the containment modeling uncertainties based on the relevance of the potential physical phenomenon and its available knowledge level. The LTR also identifies the phenomena in LTR Table 6-3 that are inapplicable to the BWRX-300 containment modeling. The following summarizes eight observations made in the LTR in this regard.

1. [[.
2. .
3. .
4.]].
5. The natural and forced circulation and stratification are affected by the friction factors, turbulence modeling, and the model nodalization for the containment and PCCS.
6. Bounding uncertainties in the convection and condensation heat transfer coefficients need to be accounted for.
7. The impact of bounding radiolytic hydrogen and oxygen generation in the RPV and release to the containment needs to be evaluated on the containment response.
8. Multi-component gas mixture properties need to be accounted for.

Observation 1 is physically realistic and is also reflected in various simulation results provided in the LTR. The staff accepts [[ ]] Observation 2 to be a bounding assumption. The staff finds [[ ]] Observation 3 to be conservative [[ ]]. The staff also accepts [[ ]] GOTHIC inputs, to address

several PIRT items. As Observations 1-4 are based on conservative assumptions, no quantification of their uncertainties is warranted.

Observation 5 pertains to the natural and forced circulation and stratification that would be driven by the friction factors and turbulence and could be sensitive to the model nodalization. LTR Section 6.8.1 presents a sensitivity study for the friction factors and turbulence modeling that shows [[ ]], while LTR Section 6.7 presents a nodalization study for the containment and PCCS. LTR Section 6.8.3 presents a sensitivity study for the PCCS performance closely tied to Observation 5 [[ ]]. LTR Section 6.8.2 adequately develops bounding values of uncertainties in the convection and condensation heat transfer coefficients, to address Observation 6. Observation 7 is addressed via L&C #1 documented in Section 7.0 of this SE, by limiting the amount of radiolytic gases to avoid ICS performance deterioration and hydrogen deflagration. The staff confirmed that the multi-component gas mixture properties in Observation 8 are calculated within GOTHIC as described in GOTHIC Thermal Analysis Package Technical Manual, Version 8.3(QA), issued in 2019 by the Electric Power Research Institute.

6.8.1 Effect of the Friction Factors and Turbulence Parameters on the Containment Response

LTR Section 6.8.1 presents a sensitivity study of the effect of friction factor and turbulence parameters on the containment pressure and temperature response. The study started from the nominal cases that use Colebrook's friction factor for a smooth surface, [[ ]]. A relative roughness of [[ ]] was used to study the sensitivity of the containment pressure and temperatures to the friction factor, which corresponds to a very high absolute value of surface roughness due the large containment hydraulic diameter. The LTR presents a case [[ ]] ("High Cf" case). Likewise, two cases of [[ ]] (high C_μ) and [[ ]] (low C_μ) [[ ]].

LTR Figures 6-15 through 6-17 compare the results obtained by the above sensitivity cases for the containment pressure/temperature responses and steam stratification for the large steam pipe break. The pressure and temperature plots for the sensitivity and nominal cases in LTR Figures 6-15 and 6-16 [[ ]]. During the regulatory audit, the staff reviewed details of the sensitivity studies and confirmed that they were appropriate to demonstrate [[ ]]. The staff did not explore the sensitivity for the SBLOCA, because the uncertainties quantified in condensation and convection heat transfer modeling, as discussed in Section 6.8.2 of this SE, are expected to bound any uncertainties in modeling turbulence and friction characteristics for the containment model. Therefore, the staff determined [[ ]]. A similar sensitivity study was performed for the PCCS separately, and is discussed in Section 6.8.3 and of this SE.

6.8.2 Uncertainties in the Convection and Condensation Heat Transfer Coefficient and the Bounding Values

Section 6.9 of this SE presents the staff evaluation of the benchmarking of the GOTHIC code containment simulation against the Carolinas Virginia Tube Reactor (CVTR) integral test data, which justified use of the conservative DLM condensation option without the film enhancement feature, as built into GOTHIC, for the BWRX-300 containment analysis. The additional biases included to the DLM model to bound the experimental uncertainties in the convection and condensation heat transfer correlations used in the BWRX-300 containment GOTHIC model are further discussed below.

The DLM condensation option used by the applicant is a mechanistic model which represents the underlying phenomena with a heat and mass transfer analogy. The total heat transfer to a condensing surface has two parts, the convection heat transfer from the bulk gas to the condensing liquid film and the heat transfer across the film thickness. The LTR presents a benchmarking of the similar Heat and Mass Transfer Analogy Method (HMTAM) against the CONdensation with Aerosols and Non-condensable gases (CONAN and COPAIN facility) test data to quantify the uncertainties in the convection and condensation correlations. The LTR also presents information to show that the DLM method used in the BWRX-300 CEM is more conservative than the HMTAM, which justifies use of the experimental uncertainties determined using the HMTAM in the BWRX-300 GOTHIC model.

LTR Figure 6-18 compares the forced and natural convection correlations to the COPAIN test data. The figure shows the ratios of the measured Nu number to the NU numbers calculated by using the Schlichting forced convection correlation and the McAdams natural convection correlation, for the entire range of the test data. By predicting each measured data point with both the forced and natural convection correlations, the applicant identified the applicable Richardson number ($Ri = Gr/Re^2$) ranges for the forced, natural, and mixed-convection regimes. The Richardson number represents the significance of the buoyancy forces with respect to inertial forces. LTR Figure 6-18 identifies the respective Richardson number regimes:
[[

]]. LTR Figure 6-18 clearly links the transition region with the maximum nonconservatism in heat transfer predictions, (i.e., where the forced and natural convection correlations overpredict the measured Nu number the most, thus, leading to the highest uncertainty in the test data). The LTR also accounts for the “relaminarization” of flow near the wall that would reduce the heat transfer by suppressing the turbulence in the natural convection flow near the wall until the free stream velocity is large enough to overcome the buoyancy forces. On the vertical containment walls at temperatures lower than that of the containment airspace, relaminarization would take place only when the bulk circulation flow is downward. LTR Figure 6-18 shows that this occurs in the transition region between natural and forced convection [[ ]].

For condensation, the correlation forms and coefficients for forced and natural convection remain the same as those used for convection, but the Prandtl (Pr) number is replaced by the Schmidt (Sc) number, and the Nu number is replaced by the Sherwood (Sh) number, and all the above discussion is equally applicable. LTR Figure 6-20 shows that
]]. Based on these considerations, LTR Section 6.8.2 proposed the following convection and condensation

correlation biases used in the GOTHIC model of the BWRX-300 containment to ensure that the heat transfer coefficients are appropriately reduced to bound the test data:

- convection correlation bias:

  1. [[

  2.]]

- condensation correlation bias:

  1. [[

  2.]]

The LTR clarifies that [[

]].

In order to disposition the possibility that GOTHIC may incorrectly predict the flow-direction or convection-mode and nonconservatively apply lower biases to the heat transfer coefficient, the applicant provided information on GOTHIC's qualifications to accurately predict the flow field (magnitude and direction) in the near wall region. The applicant also provided a summary of several GOTHIC validations against measured velocity data for situations that involve multidimensional flows where buoyancy forces are significant.

To quantitatively assess the use of the flow-direction/convection-mode dependent conservatisms used in the BWRX-300 CEM, the applicant performed a 180 degree break flow orientation sensitivity study in its response to RAI 06.02.01-03 dated September 17, 2021, and further clarified in RAI response to Question 06.02.01-01,dated October 29, 2021. This study modeled the break flow as being directed upward, downward, and sideways toward the containment shell. It was performed for the most limiting break location with respect to PCP, (i.e., [[

]], the applicant did not perform a small break orientation sensitivity study, citing that a small break case would show [[

]]. The staff reviewed the details of the sensitivity study as part of an audit and confirmed that the conclusions would be applicable to the range of conditions expected for potential applications of the CEM.

The staff also recognizes that benchmarking of the test data discussed above for the HMTAM model of condensation uses the Schlichting correlation for forced convection, while the BWRX-300 containment model uses [[

]]. LTR Figure 6-21 shows [[

]].

Based on the above evaluation, the staff concludes that the applicant has demonstrated GOTHIC's capability to calculate the velocity field in a vessel resulting from jets and buoyancy, and that the applicant has justified the use of the specified flow-direction/convection-mode dependent biases in the condensation/convection correlations. Therefore, the applicant's use of the conservative DLM condensation option [[ ]], as described in the LTR, is acceptable for the BWRX-300 containment analysis.

6.8.3 Sensitivity Analyses for PCCS Performance

LTR Section 6.8.3 presents a sensitivity study of the effect of the following parameters on the PCCS performance.

- PCCS loss coefficients
- PCCS liquid-side heat transfer coefficient
- fouling

The study was conducted on a single PCCS unit placed in a large containment volume that is kept at the specified containment pressure, temperature and steam volume fraction values, while each of the sensitivity parameters was individually varied to determine its effect on the PCCS performance. The base case PCCS and containment nodalizations in the vertical direction are the same as that used in the BWRX-300 containment model described in LTR Section 6.5, with the exception of using one node in the horizontal direction. The base case has no fouling or paint. The staff found using a single node in the horizontal direction appropriate, as the objective of this standalone PCCS study was to understand the sensitivity of the steady-state PCCS heat removal rate to specific parameters beyond the condensation heat transfer coefficient discussed in Section 6.8.2 of this SE. The applicant conducted the sensitivity study for each of the following conditions.

- containment pressure: [[ ]]
- containment airspace temperature: [[ ]]
- steam volume fraction: [[ ]]
- PCCS inlet temperature: [[ ]]
- PCCS total loss coefficient: [[ ]]

Reviewing LTR Section 6.7.2, the staff determined that the above conditions are steady-state snapshots of the containment at different times during the analyzed DBE. LTR Table 6-5 summarizes the results of the PCCS sensitivity cases. [[

]]. The LTR

documents the thermal conductivities of the paint and crud on the outer and inner surfaces of the PCCS, respectively.

The staff in its regulatory audit reviewed the supporting GOTHIC decks and detailed PCCS modeling information and performed confirmatory calculations. The applicant explained that [[

]]. The confirmatory calculations performed by the staff confirmed that [[

]]. Furthermore, the confirmatory calculation results verify the applicant's characterization [[

]].

The staff also notes that use of the CEM was demonstrated for the BWRX-300 design with the specific [[ ]] configuration and channel placement described in this LTR. The BWRX-300 safety analyses as presented in the LTR, and the additional sensitivity studies, are based on the premise that [[

]]. For example, the applicant did not perform an azimuthal study of the break location as a part of the CEM [[ ]]. However, the LTR mentions that the PCCS design has not been finalized, which means that the PCCS design submitted at the licensing stage may not have the same [[ ]]. An alternate PCCS design may involve additional phenomena not reviewed as a part of BWRX-300 method. The applicant did not provide sufficient information to generically extend the results from the GOTHIC sensitivity studies and justifications for the applicability of the CEM to other proposed PCCS designs. Therefore, the staff has imposed a L&C #4 as documented in Section 7.0 of this SE, to ensure that the BWRX-300 CEM is evaluated for its capability to accurately analyze any proposed alternative PCCS design configuration and layout at the licensing stage.

6.9 Benchmarking to the Carolinas Virginia Tube Reactor Integral Tests

LTR Section 6.9 provides a high-level overview of benchmarking the GOTHIC code against the CVTR integral test data. The applicant has referenced the CVTR integral tests to benchmark the GOTHIC code simulation against the CVTR test data for a steam pipe break with slightly superheated steam injection into a closed containment. LTR Figure 6-22 illustrates the CVTR Test Facility geometry, and the corresponding three-dimensional GOTHIC model used for the qualification. The applicant used Test Case #3 as the most applicable to the BWRX-300 containment [[ ]]. The staff found the selection of CVTR containment geometry and Test Case #3 for BWRX-300 application acceptable because [[

]]. The staff confirmed the corresponding descriptions of the test facility and qualification of the GOTHIC model in the respective references.

LTR Figures 6-23, 6-24, and 6-25 show the CVTR test data benchmarking for the containment pressure, airspace temperature (thermal stratification), and structure temperature, respectively. In the CVTR assessment, a condensation heat transfer sensitivity study was performed to investigate the pressurization effect, which showed that [[

]]. The three-dimensional GOTHIC model using the DLM-FM model with condensation heat transfer enhancement due to film roughening predicts the measured pressure, thermal stratification, and structure temperatures closely. During the audit, the applicant confirmed [[

]] in LTR Figure 6-23. LTR Figure 6-23 demonstrates that the application of the conservative DLM option available in GOTHIC (DLM condensation option without the film enhancement feature), along with the condensation/convection heat transfer biases described in Section 6.8.2, leads to a bounding prediction of the CVTR test data. The staff confirmed through the audit that the red curve in LTR Figure 6-23 (DLM, Conservative) was generated by the applicant using an appropriate GOTHIC model developed for the CVTR facility.

Applying the same CVTR GOTHIC model, the applicant also generated curves for the corresponding case using the Uchida correlation, which is a well-supported condensation correlation in the literature. The comparisons in LTR Figures 6-23, 6-24, and 6-25 demonstrate that the containment pressure, airspace temperature, and structure temperature predicted using the conservative DLM option with biases bound the values predicted by the best-estimate DLM option, Uchida correlation, as well as the CVTR test data. Code limitations prevented the applicant from generating the Uchida correlation curves using all conservative biases from LTR Section 6.8.2, however, this does not affect the essential conclusion of this benchmarking study, that the conservative DLM option selected for the CEM bounds the test data.

LTR Figures 6-24 and 6-25 compare the CVTR GOTHIC model predictions against the test data for the airspace and structure surface temperatures, respectively. The calculations were performed for the test data at two airspace and structure elevations, using conservative DLM, Uchida, and best-estimate heat transfer models. The staff noted that the predicted airspace and structure surface temperatures are higher than the measured temperatures and capture the temperature stratification trends observed in the CVTR test data well before and after the steam flow stops. However, the staff confirmed that the predicted airspace and structure surface temperature differentials for the biological shield elevation in LTR Figures 6-24 and 6-25 are close to the measured CVTR temperature differentials. Furthermore, the differences in the calculated temperatures in LTR Figures 6-24 and 6-25 at higher and lower elevations are close to the differences in the measured temperatures. Therefore, even though the CVTR GOTHIC model predictions are biased toward a higher airspace temperature, they would not result in a higher condensation rate due to an equally biased higher surface temperature. The staff also noted that the conservatism inherent in the GOTHIC conservative DLM model is manifested by the fact that it typically bounds the Uchida and best-estimate models.

Based on the information provided in the LTR about the CVTR benchmarking, the staff agreed that the conservative DLM condensation option when used with additional condensation/convection heat transfer biases appropriately bounds the CVTR test data for pressure and temperature stratification trends. Therefore, this modeling approach is acceptable for use in the BWRX-300 CEM that resolves three-dimensional effects via GOTHIC nodalization.

6.10 Demonstration of the Method for Large and Small Breaks, Conservative Cases

LTR Sections 6.10.1 and 6.10.2 provide information to demonstrate the conservatism in the evaluation method for containment response to the large and small steam pipe breaks. For that purpose, the LTR presents the containment response results for the conservative cases for the limiting large and small steam pipe breaks, as discussed below.

6.10.1 Containment Response to Large Steam Pipe Break, Conservative Case

LTR Figures 6-26 and 6-27 compare the containment pressure and temperature responses for a large steam pipe break LBLOCA case, calculated using the conservative case assumptions and the base case assumptions. LTR Figure 6-26 shows the calculated PCP to be [[

]]. LTR Figure 6-26 also shows that containment gauge pressure decreases to [[ ]], continuing to follow a decreasing trend for both the base and conservative cases. The staff evaluated these assumptions and concludes that the biases used in the CEM add a significant conservatism to the peak pressure values, which the staff finds to be sufficient to address the uncertainties in the method.

For the final BWRX-300 design, the applicant would need to demonstrate that the acceptance criteria in SRP Section 6.2.1.1.A, “PWR Dry Containments, Including Subatmospheric Containments,” Revision 3, issued March 2007 (ADAMS Accession No. ML063600402) are met for the limiting design-basis accidents: (1) the containment design pressure should provide at least a 10-percent margin above the calculated conservative PCP, and (2) the containment pressure should be reduced to less than 50 percent of the peak calculated pressure within 24 hours after the postulated accident.

LTR Figure 6-27 shows the calculated maximum shell temperature to be [[ ]] for the conservative LBLOCA case. The NRC staff found that the trends in this figure correlate to those in the break flow and enthalpy from TRACG, as well as the biases included in the conservative case. The staff determined that they are also consistent with the trends demonstrated by the staff confirmatory analysis.

LTR Figures 6-28, 6-29, and 6-30 compare the containment pressures, heat transfer rates, and containment temperatures results predicted by the biased DLM and Uchida condensation correlations. All comparisons were made between the biased DLM and Uchida condensation correlation predictions for the conservative large steam pipe break case, with all other inputs and assumptions the same. LTR Figure 6-28 shows that the difference in the predicted PCPs is negligible. The staff agrees that the biased DLM correlation predicts higher shell temperatures in LTR Figure 6-30 due to its ability to account for the impact of break velocities on condensation heat transfer. As the Uchida correlation does not account for the flow field, it underpredicts the shell temperature in the presence of break flow in the near wall region. The staff concludes that after the initial break flow impact subsides, the Uchida correlation calculates a higher condensation rate on the shell and PCCS and, thus, leads to less conservative long-term containment pressure and temperature responses, (i.e., a faster reduction in containment pressure). The staff finds that the applicant has demonstrated a sufficient level of conservatism in the biased DLM correlation used in the CEM and its ability to account for the flow field effect on condensation heat transfer compared to the Uchida correlation, as also demonstrated in the CVTR benchmarking discussed in Section 6.9 of this SE.

LTR Figure 6-11 presents the vertical and horizontal cross-sectional views of the three-dimensional GOTHIC grids used for the BWRX-300 containment model. It shows that [[

]]. The analyses presented in the LTR [[

]]. To address this possibility, the applicant performed a break location sensitivity study in its response to RAI 06.02.01-03 dated September 17, 2021, and further clarified in RAI response dated October 29, 2021, for the conservative case of large steam pipe break LBLOCA, and presented the description and results for the following three break locations, with the break flow directed toward the containment wall:

(1) placed near the containment wall [[ ]], which is the same break location and orientation as presented in LTR Section 6.10.1

(2) placed near the RPV [[ ]], which is at the same horizontal level as (1) but is located radially inward closer to the RPV

(3) placed near the RPV [[ ]], which would be [[ ]] below (1) and (2)

The applicant provided figures comparing the containment pressure and temperature responses for the initial four hours, for the three large break location cases. [[

]]. The staff finds this treatment of the limiting break locations for calculating the PCP and maximum shell temperature to be acceptable because it maximizes the conservatisms for the two FOM under DBA conditions.

6.10.2 Containment Response to Small Steam Pipe Break, Conservative Case

Limiting Small-Break Loss-of-Coolant Accident

The applicant provided conservative case GOTHIC analysis results for a small steam pipe break and a small liquid pipe break. A comparison showed that the results for the steam and liquid SBLOCA are similar, and [[

]]. The conservative case containment response for small pipe breaks is shown in LTR Figures 6-31 through 6-34 for steam SBLOCA and in LTR Figures 6-39 through 6-41 for liquid SBLOCA. Based on the LTR description, the staff understands that, for the BWRX-300 licensing basis, both steam and liquid SBLOCA scenarios will be evaluated for the PCP and maximum shell temperature at the respective limiting location and break flow orientation.

The applicant also performed a break location and flow orientation sensitivity case for a steam SBLOCA in its response to RAI 06.02.01-03 dated September 17, 2021, and further clarified in RAI Question 06.02.01-01 response dated October 29, 2021, at the limiting PCP and maximum shell temperature break locations discussed for the LBLOCA in SE Section 6.10.1. The results provided in the response for 72-hours show that [[
]]. Based on the results, the limiting SBLOCA [[
]]. The maximum containment pressures for SBLOCA [[ ]] are significantly lower than the LBLOCA PCP [[ ]], while the maximum shell temperatures are somewhat comparable for SBLOCA]] and the limiting LBLOCA [[ ]].

Small-Break Loss-of-Coolant Accident Nodalization Study and Containment Backpressure

The applicant performed a SBLOCA nodalization study to show that the default base case nodalization [[ ]] would be acceptable to predict the SBLOCA FOM for the BWRX-300 containment. LTR Figures 6-31 and 6-39 show that the containment pressure responses for the default [[ ]] containment grid with conservative inputs and model biases are similar for the steam and liquid SBLOCAs. The TRACG model in the BWRX-300 CEM does not credit the containment back pressure in calculating the small break M&E into the containment for its response calculations. This is a conservative assumption because, if containment back pressure was realistically considered, the break flow would become unchoked and start decreasing when the pressure differential between the RPV and the containment becomes low enough. Not crediting containment back pressure in break flow calculations also has the convenience of avoiding iteration and convergence between the TRACG and GOTHIC solutions.

The applicant also states that the RPV and containment pressures would eventually equalize, after which there is essentially no more mass discharged to the containment unless the containment pressure decreases at a faster rate than the RPV pressure. LTR Figure 6-31 shows a simplified analysis of the pressure equalization. Assuming a constant atmospheric pressure boundary condition in the BWRX-300 CEM until the RPV-containment pressure equalization point in LTR Figure 6-31 maximizes the M&E into the containment and hence, its pressure. The blue-dashed RPV curve in LTR Figure 6-31 represents the highest possible RPV pressure [[
]]. The applicant used the limiting [[ ]] RPV pressure as the upper bound for the containment pressure for break cases, as shown by the red dashed extension of the blue-dashed curve in LTR Figure 6-31. The staff finds the [[ ]] RPV pressure as the upper bound on containment pressure for equalization to be reasonable, as it would be higher than the lower RPV pressure bound [[ ]], as shown by the solid blue curve in LTR Figure 6-38.

The lower containment pressure bound shown by the red dotted curve in LTR Figure 6-31 is calculated by assuming no more break flow in the SBLOCA after the time the RPV and containment pressures equalize. This approach to establishing the upper and lower bounds means that the upper containment pressure bound is dictated by the ICS heat removal capacity, while the lower containment pressure bound is dictated by the PCCS heat removal capacity. A conservative prediction for the containment pressure is the solid red curve calculated using atmospheric pressure as the containment backpressure for the M&E release until the point of

pressure equalization, followed by a value that would be between the upper and lower bounds. In response to RAI 06.02.01-01, dated December 17, 2021, the applicant provided an expanded LTR Figure 6-31 which includes all four nodalization schemes discussed in LTR Section 6.7.1, as well as a lower bound on the RPV pressure with SBLOCA break flow accounted for, while the upper bound is still established by the RPV pressure [[ ]]. The staff recognizes that the lower and upper bounds of containment and RPV pressures are introduced mainly to illustrate that the general containment pressure response and pressure reduction trend are not safety-significant for all four containment nodalizations.

LTR Figure 6-32 shows the PCCS exit temperature and the RCP temperature. The staff concludes that the [[

]]. LTR Figure 6-33 shows the maximum and average steam volume fractions in the main containment. LTR Figures 6-31, 6-32, 6-33, and 6-38 reflect that [[ ]]. The LTR states that the calculations conservatively assume no heat loss from the RCP to the surroundings through the walls, but they do account for the heat loss due to surface evaporation from the pool. LTR Figure 6-34 shows that the peak shell temperature trends are similar for SBLOCA and LBLOCA with the expected time lag.

As discussed earlier, the break flow is maximized by assuming the containment to be at atmospheric pressure until the pressure equalization point. However, if the ICS can depressurize the RPV faster than the PCCS can depressurize the containment, NCGs, such as nitrogen may get ingested into the RPV and accumulate in the ICS heat exchangers. This may degrade the heat removal rate of ICS, causing the system to repressurize again. The applicant investigated the NCGs ingestion into the RPV by performing a coupled TRACG-GOTHIC calculation for a steam SBLOCA by accounting for the effect of containment back pressure on unchoked break flow using TRACG-GOTHIC iterations. LTR Figures 6-36, 6-37, and 6-38 show the results of the coupled TRACG-GOTHIC calculations. LTR Figure 6-36 shows that the RPV and containment pressures do not equalize, and the pressure differential between the RPV and containment becomes smaller with time, [[ ]]. LTR Figure 6-37 confirms a positive break flow and, thus, no break flow reversal. LTR Figure 6-38 is very similar to LTR Figure 6-31 as discussed above, but it also shows the coupled TRACG-GOTHIC calculation results from iteratively using the containment pressure calculated by GOTHIC as back pressure in calculating the break flow by TRACG. [[ ]] in LTR Figure 6-38, [[ ]]. The red dashed line in LTR Figure 6-38 also shows the containment pressure resulting from the break flow calculated based on a constant atmospheric pressure boundary condition for the TRACG M&E release calculations.

The staff evaluated the results presented in LTR Figure 6-38 and concludes that ignoring the back pressure in TRACG M&E release calculations introduces conservatism in the long-term GOTHIC containment response for the small break cases. LTR Figures 6-39 through 6-42 show the containment responses for the small liquid pipe breaks until the RPV and containment pressures equalize, [[ ]]. The staff agrees that the containment response trends for the small liquid and small steam pipe breaks are similar. The staff agrees that [[ ]], the liquid SBLOCA behaves like a steam SBLOCA.

Based on the above discussions, the staff concludes that the LBLOCA and SBLOCA nodalization studies provided by the applicant have demonstrated that the nodalization selection does not significantly impact the results for the FOM, (i.e., the PCP resulting from LBLOCA and the containment depressurization to less than 50 percent of the limiting PCP value within 24 hours). Therefore, the default base case nodalization [[ ]] using the CEM is an acceptable representation of the BWRX-300 for containment safety analyses.

The staff did not review the coupled TRACG-GOTHIC calculations as a part of the process by which the PCP and maximum shell temperature are determined, since the LTR clearly states that no containment back pressure is credited in the calculation of the FOM. The staff finds the qualitative trends predicted by the coupled calculations by crediting the back pressure for the example case to be realistic and considers this to be a reasonable approach to demonstrating that flow reversal does not occur through the first 72-hours of a SBLOCA. The staff cannot generically extend the conclusion from the study to the future final design for BWRX-300; therefore, the staff has formulated L&C # 3 as documented in Section 7.0 of this SE that would require a demonstration at the licensing stage of no safety-significant break flow reversal during the first 72-hours of the event.

TRACG/GOTHIC Model Changes

The applicant submitted updated information supporting the LTR review that included the original and updated sets of TRACG and GOTHIC models for the LBLOCA and small steam break LOCA base and conservative cases. The results presented in LTR Section 6.10 were generated using the last updated models from December 14, 2021, with some additional changes resulting from RAI responses, but the sensitivity studies were performed using the original models and were not repeated with the latest models. The applicant stated that the results in LTR Section 6.10 showed small differences relative to those in LTR Revision 0 due to modeling differences and use of a different code version. The staff compared the LTR Section 6.10 results from LTR Revision 0 against those from LTR Revision 2 and agrees that the updated results demonstrate that no new or additional phenomena were introduced by the model/code changes. As these differences affect all base and conservative cases in the same manner, they do not affect any of the uncertainty discussions. Therefore, the staff confirmed that no major CEM conclusions based on the original models regarding the limiting transients, rapid cooling requirements, nodalizations, and modeling uncertainties have been adversely affected by the updated models.

6.10.3 Containment Mixing for Combustible Gases

LTR Section 5.2.4 presents the discussion and calculations for the radiolytic hydrogen and oxygen generation in BWRX-300 DBAs. Oxygen and hydrogen are generated from radiolysis in a stoichiometric ratio of 0.5. As the radiolytic gases are well mixed in steam or liquid water, the volumetric ratio of radiolytic oxygen to hydrogen remains 0.5 as they migrate in the RPV, from the RPV to the containment, and within the containment. The radiolytic gases mixed in steam and liquid are discharged into the containment along with the break flow, and there is also a small amount of oxygen is also present initially in the containment. Radiolytic hydrogen and oxygen distributions in the containment are not a concern for large breaks [[

]]. However, radiolytic gases may build up in the containment following unisolated small breaks over time even though the rate of release is very small. LTR Figure 6-43 shows the radiolytic gas generation and release from the RPV for the limiting

conservative case of a small steam pipe break with two ICS trains. It shows that the total amount of radiolytic hydrogen and oxygen produced in the RPV during the first 72-hours is [[ ]].

The radiolytic gas volume fractions are specified in the break flow boundary condition as calculated in LTR Section 5.2.4, and the radiolytic gas volume fraction distribution in the containment and the dome region was calculated for the limiting conservative case of a small steam pipe break with 2 ICS trains. LTR Figure 6-44 shows the average and maximum hydrogen volume fractions in the main containment volume and the dome region. [[

]].

Although the volume fraction of radiolytic gases in the steam is small, it may accumulate in the dome region over time. The applicant clarified that the deflagration and detonation limits for the combustible gases depend not only on the hydrogen and oxygen volume fractions, but also on other parameters, such as pressure, temperature, steam volume fraction, potential flame propagation directions, and geometry. The flammability limit for hydrogen in dry air is 4 percent, and the minimum oxygen required for combustion to take place is 5 percent. The autoignition temperature, whether it is the gas temperature or the surface temperature, is in the range of 580–800°C. The flammability limits of hydrogen documented in two referenced cases of different conditions in containment are 7.3-7.9 percent, and 8 percent respectively. When the steam fraction is 40 percent, the required hydrogen fraction in the mixture increases to as much as 15 to 40 percent. Combustion is inhibited at even higher steam concentrations. In all the referenced cases described in the response, the flammable limits are well above 4 percent. The deflagration and detonation limits are above the flammable limit.

The results in LTR Figure 6-44 show that the hydrogen volume fraction in the dome region is higher than the main containment volume as expected, but the difference is not large. The figure also shows that the differences in maximum and average combustible gases in the main containment and containment dome are very small. It indicates that sufficient mixing of combustible gases has been demonstrated. In addition, the LTR Section 1.2 states that the BWRX-300 containment subcompartments are well mixed due to the open connections between containment and the volume below the RPV and containment and the space between the RPV and the biological shield. Sufficient mixing in containment subcompartments eliminates the concern for deflagration in the containment subcompartments. In the response to RAI 06.02.05-01 dated September 17, 2021, GEH clarified that the hydrogen volume fractions in the containment dome shown in LTR Figure 6-44 for BWRX-300 are far below the deflagration limits by 2 orders of magnitude even if there is sufficient oxygen. Based on the additional information, the staff concludes that the calculated combustible gases concentrations inside the containment following unisolated small breaks are far below the deflagration limits.

Based on above, the NRC staff confirms that gases generated by radiolysis are not likely a concern for deflagration in the containment and the identified containment subcompartments could have sufficient mixing, contingent on the final design. The NRC staff will review the specific features of the containment design during future licensing activities for the BWRX-300 SMR.

6.11 Summary of the Assumptions and Inputs Used in the BWRX-300 GOTHIC Method Conservative Cases

LTR Section 6.11 summarizes the assumptions and inputs to be used for the conservative BWRX-300 GOTHIC containment analyses as part of the NEDC-33922P CEM.

Both the base and conservative cases for containment analyses use the following modeling parameters:

- The initial containment pressure is at the maximum technical specification containment pressure.
- The initial bulk containment temperature and the structures are at a reasonably low value that would occur during normal operation.
- The initial humidity of the containment airspace is 20 percent.
- The initial RCP temperature is at the technical specification limit. For the purpose of demonstration calculations, [[ ]].
- Bounding values are used for form loss coefficients in the containment and in the PCCS units.
- The free space volume in the containment is conservatively calculated.
- The containment is modeled using a [[ ]] nodalization, as presented in the base cases in the LTR.
- The initial airspace temperature above the RCP is assumed to be the same as the pool water temperature.
- The initial relative humidity of the RCP airspace is assumed to be 100 percent.

The conservative cases for containment analyses use the following biased modeling parameters and conservative modeling assumptions:

- [[ ]]
- The condensation and convection heat transfer correlations are biased as described in Section 6.8.2. The resulting heat transfer coefficients on the containment shell, PCCS and containment dome are appropriately reduced.
- [[

  ]]
- [[

  ]]

- No credit is taken for heat transfer from the outer surface of the metal containment shell to the concrete or surroundings, except for heat transfer from the submerged section of the containment dome to the RCP above the dome.

- The RCP is modeled as a lumped parameter volume, whose air space is connected the ambient atmosphere through a constant pressure boundary condition, such that the airspace pressure remains nearly constant.

- There is no heat loss from the RCP to the walls. Surface evaporation from the pool is accounted for.

The applicant also provided additional information in LTR Table 6-2 regarding the following PIRT phenomena that are pertinent to the RCP for the first 24 hours of a LBLOCA and first 72-hours of a SBLOCA.

- [[

-]]

Based on the information provided by the applicant, the staff found that modeling the airspace above the RCP at an initial temperature equal to the uniform pool water temperature, and an initial relative humidity of 100 percent, is conservative. The staff found the RCP liquid modeling at a uniform temperature with no stratification, to be conservative as PCCS intake location in the pool is near the bottom of the pool, and the PCCS return pipe discharge elevation is at least [[ ]] the PCCS intake elevation. The remainder of the assumptions listed above are consistent with the information discussed and found to be acceptable earlier in this SE. The staff also found the information to be consistent with the submitted GOTHIC models, and thus, these assumptions capture the staff findings based on the sensitivity studies, demonstration calculations, and confirmatory analyses.

The applicant additionally clarified that the applicability of the BWRX-300 CEM is not based on a time limit, such that as the first 72-hours of the DBE, but on the modeled phenomena and biases. The PCCS heat removal capacity will decrease as the RCP heats up, but the PCCS heat transfer modeling does not have any specific limitation until boiling starts in the PCCS tubes. The applicant recognized that the capability of the GOTHIC model has not been demonstrated for specific phenomena such as the release into the containment of significant amounts of hydrogen or superheated steam from the RPV. The staff finds this justification to be acceptable as these phenomena do not occur within 72-hours during a DBE
the scope of this LTR does not include approval for the quantification of their uncertainties.

The conservatism in the BWRX-300 CEM evaluation model is achieved by simultaneously biasing the individual inputs and key modeling parameters to bound the uncertainties in the conservative cases, rather than performing a statistical sampling of the uncertainties and adding margin to the base case results. The staff agrees that compounding conservatisms through individual biases greatly reduces the number of sensitivity runs needed for statistical sampling, and gives reasonable assurance that the overall analysis results bound the uncertainties.

7.0 LIMITATIONS AND CONDITIONS

If an applicant chooses to incorporate the LTR by reference as part of an application for approval of a reactor design, or a construction or operating license, it must abide by the following L&Cs or provide additional justification for any deviations.

7.1 L&C #1 - Isolation Condenser Radiolytic Gas Removal

The use of this CEM is limited to a BWRX-300 design that limits the total volumetric fraction of radiolytic gases in the IC lower drum to a sufficiently low level throughout a 72-hour period following the event such that condensation heat transfer in the ICs is not adversely affected and the hydrogen deflagration margin is maintained.

7.2 L&C #2 - Isolation Condenser Return Line Design and Further Demonstration of Transient Reactor Analysis Code General Electric Modeling Capability

The use of this CEM is limited to a BWRX-300 design that a proper isolation condenser return line layout is chosen, such as a loop seal or a water trap, to prevents reverse flow from RPV into the IC return line throughout a 72-hour period following the event or where an applicant or licensee referencing this report demonstrates that the TRACG code is capable of conservatively modeling the overall ICs heat removal capacity when reverse flow occurs in the IC discharge lines.

7.3 L&C #3 – Demonstration of No Safety-Significant Break Flow Reversal During the First 72-Hours into the Event

The use of this CEM is limited to a BWRX-300 design in which the PCCS is sized sufficiently large such that a reverse flow from containment back to RPV does not occur during the first 72-hours into the event. The applicant or licensee referencing this report needs to demonstrate that no reverse flow could occur, or any reverse flow that occurs under the most bounding flow reversal conditions resulting in the degradation of IC heat transfer is not safety-significant with respect to the acceptance criteria for the BWRX-300 CEM.

7.4 L&C #4 – Demonstration of the Applicability of the BWRX-300 Containment Evaluation Method to the Final Passive Containment Cooling System Licensing-Basis Analysis

The use of this CEM was demonstrated for a BWRX-300 design with the [[
]] and placement described in this LTR. For any alternate PCCS design configuration and placement, the applicability of this method and the PCCS modeling approach must be reviewed and found to be acceptable by the NRC for BWRX-300 licensing-basis analyses.

8.0 CONCLUSIONS

The GEH LTR provides sufficient information to justify the method to evaluate the BWRX-300 containment response for the acceptance criteria documented in LTR Section 1.3, using a novel application of the GOTHIC code. The staff found the TRACG M&E method acceptable based on it being consistent with the guidance in SRP Section 6.2.1.3 and found the method appropriately conservative for determining the M&E release, subject to the L&Cs noted in SE Section 7.0. The staff reviewed the PIRT developed for DBE evaluations with the BWRX-300

containment, the validation of the selected GOTHIC modeling to capture the relevant thermal-hydraulic phenomena, the sensitivity studies performed to assess the modeling choices in the LTR, and the uncertainty quantification. As a result of this review, the NRC staff found the proposed BWRX-300 analytical approach and GOTHIC modeling described in the LTR to be acceptable for their intended purpose, with the appropriate conservative biases and modeling inputs to address the model uncertainties.

Based on the above discussion, the NRC staff concludes that the analysis method presented in the LTR is acceptable for reference in future licensing activities to demonstrate that the BWRX-300 containment design can meet the acceptance criteria listed in LTR NEDC-33911P-A, Revision 3. This method is acceptable for use, consistent with the conditions and limitations noted in SE Section 7.0, in containment analysis of AOOs, station blackout, ATWS, LBLOCAs, and SBLOCAs.

As previously discussed in Section 1 of the SE, the NRC staff will evaluate the regulatory compliance of the final design of the containment and the final CEM for the BWRX-300 SMR during future licensing activities, in accordance with 10 CFR Part 50 or 10 CFR Part 52, as applicable.

TABLE OF CONTENTS

LIST OF TABLES

LIST OF FIGURES

REVISION SUMMARY

Revision Number	Description of Change
0	Initial Submittal
1	Revised to incorporate the following responses to NRC Requests for Additional Information (eRAIs): • NRC eRAI 9829 Question 06.02.04-01 revised Section 1.3. • NRC eRAI 9831 Question 06.02.01-02 revised Section 6.11. • NRC eRAI 9862 Question 06.02.01-01 added a new Section 1.4 and Table 6-6 and revised Sections 6.0, 6.10.1 and 6.10.2. • NRC eRAI 9862 Question 06.02.01-02 revised Section 6.10.2 and added Figures 6-39 to 6-41. • NRC eRAI 9862 Question 06.02.01-03 revised Sections 6.5, 6.6.1, 6.6.2, 6.10, 6.10.2 and 6.11 and revised Figures 6-26, 6-28, and 6-31. • NRC eRAI 9862 Question 06.02.01-05 revised Sections 6.10.2 and 6.11. • NRC eRAI 9862 Question 06.02.01-07 revised several figures. • NRC eRAI 9862 Question 06.02.01-08 revised Sections 6.5 and 6.8.2. Revised in response to the following Audit Issues: • Audit Issue 2 revised Figures 6-31 through 6-34. • Audit Issue 26 corrected Figures 5-3 and 5-4. • Audit Issue 30 revised Section 6.9 and clarified the legends in Figures 6-23, 6-24, and 6-25. • Audit Issue 35 corrected a broken link in Section 6.9. • Audit Issue 36 deleted all references to a design option in Sections 2.0 and 6.1 and Table 6-2. • Audit Issue 45 revised Section 6.5 and 6.8.2 to describe the steam dome biases in more detail. In general, the following figures were updated to reflect updated results: Figure 5-1, Figures 5-3 through 5-27, Figures 6-1, 6-4 through 6-10, 6-13, 6-16, 6-23 through 6-34, and 6-38 through 6-41. A new figure, Figure 6-42, was added. Because of the revisions noted above, the following additional revisions occurred:

Revision Number	Description of Change
	• Figures 6-39 and 6-40 were renumbered as Figures 6-43 and 6-44. • Section 6.10.3: Figure references were updated to reflect that Figures 6-39 and 6-40 were renumbered as Figures 6-43 and 6-44. The following additional editorial corrections were made: • Section 5.2.4: Added back in the missing equation for the radiolytic gas production correlation. • Corrected broken links in Sections 4.0, 6.0, 6.8, 6.8.2, 6.9, 6.10, and 6.11.
2	Revised the following tables, figures, and sections consistent with the revised response to NRC eRAI 9862 Question 06.02.01-01: • Table 6-6 • Figure 6-2 • Figures 6-4 through 6-13 • Figures 6-15 through 6-17 • Figures 6-26 through 6-44 • Sections 6.5, 6.6.1, 6.6.2, 6.7.1, 6.7.2, 6.10.1, 6.10.2, and 6.11. Section 5.2.4: Added a sentence to the first paragraph in response to Audit Issue 38. Section 6.8.2: Deleted the reference to CONAN test data. The following additional editorial corrections were made: • Figures 5-3 and 5-4: Corrected the clarity of the images. • Figures 5-5, 5-8, 5-11, 5-15, 5-18, and 5-23: In the notes below these figures, added quotations around Q IC-A and Q IC-B for clarity. • Figure 5-11: Revised the note to delete Q IC-B. • Figures 5-8, 5-15, 5-18, and 5-23: Removed proprietary markings in the notes below the figures. • Sections 5.2.4, 5.2.5, 5.3.1, 6.7.2, 6.8, 6.8.1, 6.8.3, and 6.10.1 and in Table 5-3 and Table 6-2 (Items 8, 9, 12, 13, and 14): Added the missing article “the” in several places. • Table 6-2 (Items 14 and 21): Changed “effects” to “affects”. • Section 6.10.1: Deleted the word “one”. It is redundant with the word “first” • Section 6.10.3: Changed “is” to “are”.

Revision Number	Description of Change
3	Created "-A" version by adding GEH's responses to the NRC's Requests for Additional Information (RAIs) (References 7.23 through 7.27) and the NRC's Final Safety Evaluation (Reference 7.28). Added References 7.23 through 7.28. Made the following editorial corrections: • Figure 2-4: Marked [[ ]] as proprietary in the title. • Section 6.6.1: 1st paragraph: Marked [[ ]] as proprietary. • Section 6.9: Changed Carolina to Carolinas in the section title.

Acronyms and Abbreviations

Term	Definition
ABWR	Advanced Boiling Water Reactor
AC	Alternating Current
ALARA	As Low As Reasonably Achievable
AOO	Anticipated Operational Occurrence
ASME	American Society of Mechanical Engineers
ATWS	Anticipated Transient Without Scram
B&PV	Boiler & Pressure Vessel
BDBA	Beyond Design Basis Accident
BTP	Branch Technical Position
BWR	Boiling Water Reactor
COL	Combined Operating License
CP	Construction Permit
CSAU	Code, Scaling, Applicability and Uncertainty
DCA	Design Certification Application
ECCS	Emergency Core Cooling System
EFCV	Excess Flow Check Valve
EMDAP	Evaluation Model Development and Assessment Process
ESBWR	Economic Simplified Boiling Water Reactor
GDC	General Design Criteria
GEH	GE Hitachi Nuclear Energy
GOTHIC	Generation of Thermal-Hydraulic Information for Containments
HGNE	Hitachi-GE Nuclear Energy Ltd.
HT	Heat Transfer
I&C	Instrumentation and Control
IC	Isolation Condenser
ICS	Isolation Condenser System
IE	Infrequent Event
LOCA	Loss-of-Coolant Accident
LOOP	Loss of Offsite Power

Term	Definition
LTR	Licensing Topical Report
LWR	Light Water Reactor
NBS	Nuclear Boiler System
NC	Non-Condensable
NRC	Nuclear Regulatory Commission
OL	Operating License
PCCS	Passive Containment Cooling System
PIRT	Phenomena Identification and Ranking Table
PSAR	Preliminary Safety Analysis Report
RCPB	Reactor Coolant Pressure Boundary
RCS	Reactor Coolant System
RG	Regulatory Guide
RPS	Reactor Protection System
RPV	Reactor Pressure Vessel
RWCU	Reactor Water Clean Up
SDC	Shut Down Cooling
SMR	Small Modular Reactor
SRP	Standard Review Plan
SSC	Structure, System, and Component
TAF	Top of Active Fuel
TMI	Three Mile Island
TRACG	Transient Reactor Analysis Code General Electric

1.0 INTRODUCTION

1.1 Purpose

This report presents the analysis method used for the BWRX-300 containment thermal hydraulics performance to demonstrate that the containment design satisfies the acceptance criteria listed in Section 4.0 of Licensing Topical Report (LTR) NEDC-33911P, BWRX-300 Containment Performance (Reference 7.2).

The containment analysis method is outlined in Section 3.0 of NEDC-33911P (Reference 7.2). The scope of the evaluation method are the design basis and special events that are evaluated to establish the suitability of the containment performance acceptance criteria:

- Anticipated Operational Occurrences (AOOs)
- Station Blackout as required by 10 CFR 50.63
- Anticipated Transients Without Scram (ATWS) as required by 10 CFR 50.62
- Large Break Loss of Coolant Accident (LOCA) inside containment
- Small Break LOCA inside containment

1.2 Scope of Application

This report scope includes:

- Method description
- Method qualification
- Sensitivity studies
- Application of the method to the BWRX-300 for the events identified in Section 1.1
- Demonstration cases

Because the BWRX-300 Reactor Pressure Vessel and Isolation Condensers System (ICS) are similar to those of the Economic Simplified Boiling Water Reactor (ESBWR), the TRACG method developed for the ESBWR reactor pressure vessel (RPV) thermal hydraulics and mass and energy release is also used for the BWRX-300 RPV thermal hydraulics and mass and energy release. This report provides an overview of the TRACG thermal hydraulics method for the mass and energy release and its applicability to the BWRX-300 RPV.

The containment analysis is performed by using the GOTHIC code (Reference 7.16). The development outline for the GOTHIC containment evaluation method is given in Section 3.4.2 of NEDC-33911P utilizing the applicable elements of the Code, Scaling, Applicability, and Uncertainty (CSAU) framework.

The application of TRACG and GOTHIC for the BWRX-300 containment includes a base case using nominal inputs and assumptions, and a conservative case using inputs and assumptions that are biased to bound the uncertainties.

[[

]] The

subcompartments are included in the analyses to determine the containment atmosphere remains sufficiently well mixed to preclude deflagration or detonation of combustible gases, and to demonstrate that the containment internal structures forming the boundaries of the subcompartments do not experience large pressure differentials [[ ]]. Jet loads that may be exerted on structures and equipment in containment are addressed as part of the structural loads evaluation that will be submitted in a future licensing submittal.

1.3 Acceptance Criteria

The evaluation method demonstrates that the BWRX-300 containment meets the following acceptance criteria:

- Accident pressure and temperature are less than design pressure and temperature with appropriate margin
- Containment pressure is reduced to less than 50% of the peak accident pressure for the most limiting LOCA within 24 hours
- Containment pressure responses after 24 hours for LOCAs that do not produce the peak accident pressure are maintained below 50% of the peak pressure for the most limiting LOCA
- Containment atmosphere remains sufficiently mixed such that deflagration or detonation does not occur inside containment

Containment venting or leakage shall not be credited for at least 72 hours in demonstrating that the above acceptance criteria are met during a design basis event or accident.

Regulatory Guides (RG) 1.203 (Reference 7.3) and RG 1.157 (Reference 7.4) provide guidance for acceptable evaluation methods applicable to light water reactors. RG 1.157 provides analyses guidance for demonstrating compliance to the fuel clad integrity requirements of 10 CFR 50.46 “Acceptance criteria for emergency core cooling systems in light water nuclear power reactors”. The BWRX-300 LOCA sequences do not progress into significant core uncovery and refill/reflooding. BWRX-300 LOCAs do not result in significant fuel heat-up and oxidation and are not mitigated by an active injection system. Therefore, most RG 1.157 guidance are not applicable to the BWRX-300 LOCA analyses. Only the RG 1.157 guidance relating to the general best practice elements of a rigorous method development are applicable. These best practice elements are also included in RG 1.203. RG 1.203 provides guidance for all elements and stages of developing an acceptable method and references the CSAU analysis methodology (Reference 7.12). The BWRX-300 containment analysis utilizes mature computer codes that have been widely reviewed and used. The application method presented in this LTR addresses conformance with the RG 1.203 elements that are applicable to those mature codes and the CSAU methodology.

1.4 Methodology Overview

TRACG calculates the mass and energy release from modeled breaks of various sizes and locations (Section 5.2.2). In all cases, atmospheric pressure is used for the TRACG pressure boundary condition at the break. This approach provides no credit for the back pressure from containment; consequently, the retained RPV inventory calculated by TRACG represents the minimum

condition as though the break occurred outside containment. Breaks inside containment would realistically experience back pressure from the containment which would reduce the mass and energy release calculated by TRACG once the break flow became unchoked; however, this effect is not treated explicitly because it would require two-way coupling between the TRACG calculation and the GOTHIC containment calculation. Instead, the methodology has only a one-way coupling with the mass and energy release rates conservatively calculated by TRACG supplied as inputs to the GOTHIC calculation up until the point in time when the containment and RPV pressures first match. Choked flow naturally satisfies the assumed one-way coupling because the calculated choked flow rate does not depend on the downstream pressure. Select TRACG inputs are specified (Section 5.2.5 and 5.2.6) so that mass and energy release rates will be conservatively calculated.

For large breaks, the rapid mass and energy release into the containment before the break is isolated leads to the highest containment peak pressure, which occurs at approximately the same time that the break is isolated. For large breaks, the containment shell is the dominant short term energy sink; heat transfer to the containment shell will cause the containment pressure to decrease from its peak value after isolation of the break occurs. The large steam line break determines the overall highest peak containment pressure as shown by the demonstration calculations provided in Section 6.10.

Compared to the large breaks, small unisolated breaks have a much slower mass and energy release rate from the RPV into the containment. The lowest break on the RPV that remains unisolated and occurs outside the containment will produce the most limiting scenario for minimum RPV inventory. Regardless of break location and whether the break is inside or outside containment, the break flow will slowly decrease with time because the RPV is being depressurized largely by the ICS operation with some contribution from the energy released in the break flow. The containment pressure will slowly increase and eventually equal the RPV pressure if the break is inside containment. After the point in time when the containment and RPV pressures first become equal, it is no longer realistic to use the TRACG break flow that was calculated using an atmospheric pressure boundary condition as input to the GOTHIC containment calculation. The methodology does not require the GOTHIC calculation to continue beyond the point where the containment and RPV pressures equalize because the longer-term containment pressure will be bounded by the RPV pressure calculated by assuming zero break flow provided that the PCCS is depressurizing containment faster than the ICS is depressurizing the RPV for the case of zero break flow beyond the intersection time.

2.0 OVERVIEW OF THE BWRX-300 RPV AND CONTAINMENT FEATURES PERTINENT TO THE APPLICATION METHOD

The BWRX-300 RPV and internals are shown on Figure 2-1 and described in Reference 7.1. The Isolation Condensers (IC) are also described in Reference 7.1 with illustrations included on Figure 2-2 and Figure 2-3. As described in Reference 7.1, all piping [[

]]. For an ICS train, the RPV isolation valves on both the steam and condensate pipes for that train close when a break is detected in that train. All other RPV isolation valves close on detection of high drywell pressure. Isolation condensers are initiated on [[

]]. The other isolation and initiations signals are described in References 7.1 and 7.2 and not repeated here because they are not pertinent to the containment thermal-hydraulic response analyses.

A conceptual containment design, penetrations and Passive Containment Cooling System (PCCS) are also described in Reference 7.2. As stated in NEDC-33911P, the containment structure, shape and PCCS design may be different, but the containment design would be functionally the same. The containment conceptual design has evolved subsequent to the issuance of Reference 7.2. The containment shape shown on Figure 2-4 is the configuration used in the method development because [[

]]. Regardless of the type of the vessel support, it is necessary that the support structure has large openings for personnel access and maintenance or replacement of the control blades and control rod drives.

Containment penetrations and containment isolation valves are also discussed in Reference 7.2.

The following containment design features are relevant to the purposes of this report:

- Containment is a dry enclosure, near atmospheric pressure during normal operation
- Containment design pressure and temperature are within the experience base of conventional BWRs
- Containment is inerted with nitrogen during normal operation
- There are no subcompartments containing large bore high energy lines
- The subcompartments have sufficiently large openings such that the boundaries of the subcompartments do not experience large pressure differentials resulting from pipe breaks outside the subcompartments.
- The PCCS [[

]].

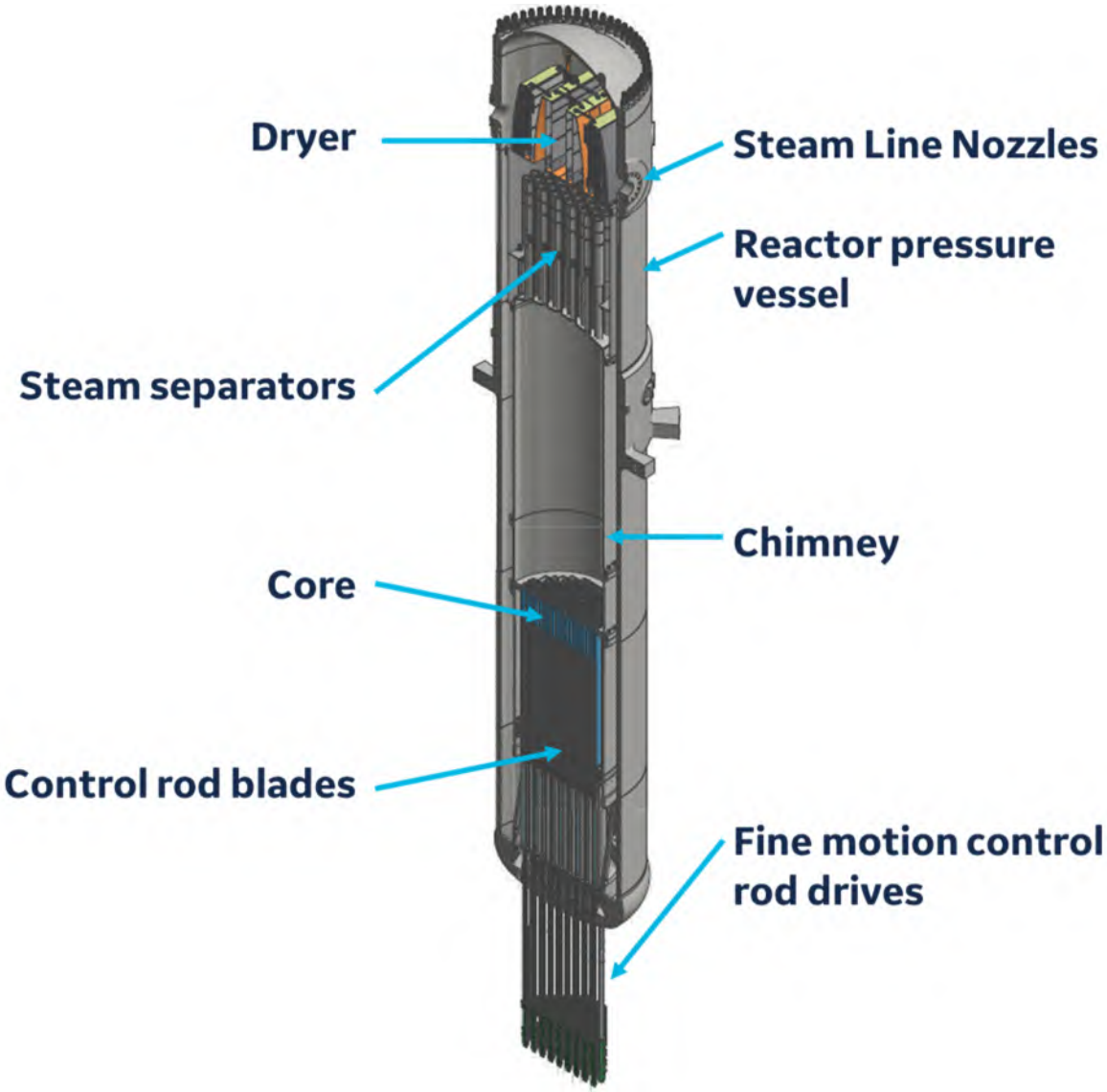

Figure 2-1: BWRX-300 RPV and Internals

[[

]]

Figure 2-2: BWRX-300 Isolation Condenser System

[[

]]

Figure 2-3: Isolation Condenser CIVs Connected to the RPV Boundary

[[

]].

[[

]]

Figure 2-4: BWRX-300 Containment with PCCS Utilizing [[ ]] (typical configuration)

3.0 LOCA Scenarios and Limiting Pipe Breaks

All large bore piping attached to the BWRX-300 RPV has two isolation valves. The RPV isolation valves, except for those on the IC piping, close on either of the following conditions:

- High drywell pressure
- Low-Low RPV water level

The containment isolation valves also close on the same signals but may have a longer delay than the RPV isolation valves. The outboard containment isolation valves are assumed to remain open for a main steam pipe break, but the turbine stop valve is closed instantaneously, concurrent with the break. Because the two steam pipes are connected to a common header upstream of the turbine stop and control, the intact loop also contributes to the break flow rate before the RPV isolation valves are closed. Using this set of assumptions maximizes the discharge of steam to containment.

The feedwater pipes have a check valve outside containment. As a result, the intact feedwater loop does not feed backwards to the break. The feedwater pump trips on a pipe break. The hot water in the feedwater piping may flash and contribute to break flow.

Both the steam supply and the condensate return pipes of an IC train are also isolated when a break is detected on either pipe in that train. The IC condensate return pipe flow area is much smaller than the feedwater pipe; therefore, a break in the condensate piping in an IC train is bounded by the feedwater pipe breaks. The IC steam supply pipe flow area is no larger than the main steam pipe flow limiter flow area. Main steam pipe flow area is at least twice as large as the flow limiter flow area. Further, pipe inventory in the main steam piping is much larger than the inventory in an IC train and its attached piping. Therefore, the initial steam discharge rate following a main steam pipe break is significantly larger than the initial discharge rate from an IC steam pipe break.

The isolation signals for ICS pipe breaks are [[ ]] and do not require a high containment pressure signal. There is no inherent reason that isolation of ICS pipe breaks would be delayed further than isolation of other pipe breaks. Although there may be differences in electronic signal delays to develop for various pipe breaks, the isolation times considered in the analysis are bounding for all large pipe breaks. Considering the pipe size, configuration and isolation signal timing assumed in the analysis, a break in the ICS piping is bounded by a break in the main steam and / or feedwater pipe as analyzed.

Reactor water cleanup (RWCU) and shutdown cooling (SDC) pipes also have RPV isolation valves. Because the RWCU and shutdown cooling pipes are smaller in diameter than the feedwater pipes, and the isolation valve closure timing is the same for all pipes, breaks in the RWCU and SDC pipes are bounded by feedwater pipe breaks.

The inside diameters of the instrument lines are [[ ]]. These pipes are not isolated and assumed to discharge steam or liquid indefinitely. Also, the leak detection system in the ICS has a lower limit on the break size that it can detect. Such a break will remain unisolated even if the containment pressure exceeds the setpoint for isolation.

All small steam pipe breaks that remain unisolated are bounded by a break in a pipe of [[ ]] attached to the RPV dome.

All small liquid pipe breaks that remain unisolated are bounded by a break in a pipe of [[

]].

An assumed single failure rendering an ICS train inoperative is the most limiting single failure for small breaks because the small breaks rely on ICS to depressurize the RPV. [[

]].

In summary, the limiting large breaks are:

- Main steam pipe
- Feedwater pipe

All design basis large breaks are rapidly isolated at the RPV nozzle.

The limiting small breaks are unisolated instrument line breaks, either in the steam or liquid space.

4.0 OVERVIEW OF THE EVALUATION MODEL

TRACG is used to evaluate the mass and energy release from the BWRX-300 RPV, and GOTHIC is used to evaluate the BWRX-300 containment response. As shown in this report, there is no adverse effect of containment backpressure on the TRACG mass and energy releases. As a result, there is no need to iterate between the two codes to obtain a best estimate solution for the mass and energy release, and the application method is not dependent on predicting back pressure. Instead, mass and energy releases calculated by TRACG are used as a boundary condition in the GOTHIC calculations, and the containment pressure and temperature response are calculated using GOTHIC.

The mass and energy release model for the BWRX-300 containment response utilizes the applicable parts of the approved LTR, TRACG Application for ESBWR (Reference 7.10), which is incorporated in the approved ESBWR Design Certification (Reference 7.11). Section 5.0 of this report details the application of the ESBWR TRACG method to the BWRX-300.

As described in NEDC-33911P, Section 2.0, the BWRX-300 containment design is much simpler than the ESBWR containment, and many of the ESBWR containment phenomena do not apply to the BWRX-300 containment. Phenomena that are of secondary importance to the ESBWR containment response may become important to the BWRX-300 containment response. Therefore, a new containment model using GOTHIC has been developed for the BWRX-300 and is presented in this LTR. GOTHIC is a continuously maintained and improved computer code. The GOTHIC code has been developed compliant with 10 CFR 50, Appendix B requirements and meets the GEH software quality requirements. The results in this report have been generated using GOTHIC Version 8.3 that is the latest released version at this time. Future BWRX-300 containment analyses may be performed using newer versions of the GOTHIC code provided the newer versions meet the same 10 CFR50 Appendix B quality requirements and changes in calculated results for our BWRX-300 containment application caused by any code changes can be successfully dispositioned.

The evaluation method for the BWRX-300 containment response to design basis events has been developed following the applicable elements of Regulatory Guide 1.203 (Reference 7.3). The application method includes base cases and conservative cases. The individual key inputs, assumptions and modeling parameters are conservatively biased simultaneously in the conservative cases, rather than sampling the uncertainties and adding margin to the base case results. While this method compounds conservatisms, it gives reasonable assurance that the overall method results bound the uncertainties, and greatly reduces the number of sensitivity calculations. This is the same approach that was taken for the ESBWR containment method in Reference 7.10. The containment response method is described in detail in Section 6.

5.0 TRACG METHOD FOR MASS AND ENERGY RELEASE

5.1 TRACG Code and Qualification

TRACG is the GE Hitachi Nuclear (GEH) proprietary version of the Transient Reactor Analysis Code (TRAC). TRACG uses realistic one-dimensional and three-dimensional (3D) models and numerical methods to simulate phenomena that are experienced in the operation of boiling water reactors (BWRs). TRACG code and models are described in detail in Reference 7.5. The TRACG qualification report, Reference 7.6, includes comparisons of TRACG calculations with data from separate effects, component performance and integral system effects tests that directly support its use for BWR LOCA analyses. References 7.7 and 7.8 present TRACG qualification specifically for natural circulation plants with IC systems similar to the BWRX-300.

TRACG ECCS-LOCA analysis method for BWR/2–6 (Reference 7.9) and for ESBWR (Reference 7.10) have been approved previously. The uncertainties in the TRACG ECCS-LOCA analysis methods are quantified for the BWR/2-6 application method in Reference 7.9, and for ESBWR in Reference 7.10. It should be noted that only the uncertainties relating to RPV inventory and break flow would be accounted for in the BWRX-300 application because like the ESBWR application, the core always remains well cooled.

5.2 Application of the ESBWR TRACG LOCA Method to BWRX-300 Mass and Energy Release Calculations

The BWRX-300 RPV is an evolution of the ESBWR RPV. The main differences between the BWRX-300 RPV and ESBWR RPV are the RPV dimensions, connected piping, and the RPV isolation functions. These differences affect the modeling inputs but are still within the same qualified application range as the ESBWR. The BWRX-300 operating accident pressure and temperature ranges are similar to the ESBWR operating pressure and temperature ranges.

As discussed in this LTR, significant fuel heat-up does not occur in the BWRX-300 as is the case for the ESBWR. The phenomena that affect the mass and energy release from the BWRX-300 RPV case also apply to the ESBWR mass and energy release. The modeling, experimental and scaling uncertainties identified for ESBWR are also relevant to the BWRX-300 design. Therefore, the TRACG qualification for the ESBWR application equally applies to the BWRX-300 application. Furthermore, the BWRX-300 mass and energy release analysis is much less challenging than the ESBWR analysis for mass and energy release from a large break because the BWRX-300 large breaks are isolated. Small breaks are slow evolving events where the modeling and phenomenological uncertainties are significantly diminished.

In the BWRX-300, the RPV is isolated following a large break LOCA. After the isolation valves closure, the energy generated by decay heat must be removed directly from the RPV. Therefore, it is not appropriate to make the same assumptions as were made for the ESBWR where the PCCS is credited as the primary heat removal for ECCS-LOCA and containment analyses, while the ICS is credited for transients, but not for ECCS-LOCA or containment analyses. The BWRX-300 ICS is credited in accordance with its purpose, specification, and safety classification. The BWRX-300 ICs modeling and TRACG qualification are discussed in detail in Section 5.2.4.

The ESBWR TRACG LOCA method in Reference 7.10 includes ECCS-LOCA analysis and containment analysis. The TRACG models used for these analyses have some differences. The TRACG RPV model used for the ECCS-LOCA analysis (Figure 2.7-1 of Reference 7.10) is more

detailed with respect to the nodalization than the TRACG RPV model used for the ESBWR LOCA/Containment analysis (Section 3.7-1 of Reference 7.10). The axial detail in the RPV model is essentially equivalent for the BWRX 300 and ESBWR.

5.2.1 TRACG RPV Nodalization for BWRX-300

The TRACG RPV radial nodalization for the ESBWR ECCS LOCA analysis, shown on Figure 2.7-1 of Reference 7.10, is more detailed than the TRACG RPV radial nodalization used for the ESBWR analysis, shown on Figure 3.7-1 of Reference 7.10. Although either nodalization would be adequate for the BWRX 300 mass and energy release calculations, the demonstration cases presented in this LTR use a finer nodalization as shown on Figure 5-2. This refinement allows the use of the same RPV model both in transient and LOCA analyses.

Although the IC model developed for ESBWR is adequate for the BWRX-300 LOCA analyses, the IC model used in the BWRX-300 demonstration cases (Figure 5-4) is more detailed than the one used in the ESBWR analyses. This refinement was made for transient and ATWS analyses that are not in the scope of this report. The model on Figure 5-4 also reproduces the ESBWR IC specification heat removal rate for a single IC train. Only train A is shown on Figure 5-4, the other trains are modeled similarly.

5.2.2 Large and Small Pipe Breaks

The steam and feedwater piping attached to the RPV are shown on Figure 5-3. The large breaks are represented by [[

]].

5.2.3 Channel Grouping, Decay Heat and Power Shape

Containment analyses are not sensitive to the power shape and [[ ]]. These inputs are more relevant to the fuel heat-up calculations and transient analyses. [[

]].

5.2.4 Isolation Condenser Modeling and Radiolytic Gases

The IC capacity is assured to be at least 33.75 MW as stated in Supplement 2 of Reference 7.10. Although the ICS is credited for the AOOs in the ESBWR (Section 4.7 and Supplement 2 of Reference 7.10), but not for LOCA analyses, any potential adverse effects and parallel unit effects have been addressed in Reference 7.10. [[

]] The ESBWR containment analyses credit the PCCS attached to the containment, but do not credit the ICS. However, the ESBWR PCCS heat

exchanger is identical to one of the two heat exchangers in an IC train. Both the ICS and the PCCS use the same qualification base and testing that were originally performed for the Simplified Boiling Water Reactor (SBWR) design and supplemented for ESBWR design.

TRACG qualification for the ICS is based on two sets of PANDA tests as described in Reference 7.7: the M-series tests, which are used in the TRACG qualification for SBWR, and the later complimentary P-series tests for ESBWR configuration, including the effects of the non-condensable gases. TRACG04 is qualified based on both sets of tests, and for both water and steam, and steam containing air or helium (Reference 7.8).

Because there is no significant oxidation in the BWRX-300, the only non-condensable gases that may migrate into the IC tubes are the radiolysis products following a design basis LOCA. [[

]] The build-up of hydrogen and oxygen in steam following a one-inch liquid break is shown on Figure 5-1.

Unlike hydrogen generated from cladding oxidation, hydrogen and oxygen liberate from radiolysis at a slow rate and distributes over a relatively large region. The gases become mixed in water both in steam and liquid phases. The well-mixed hydrogen and oxygen in steam also migrates into the ICs when the ICs are put in service. The hydrogen and oxygen concentration in steam may increase as the steam condenses in the IC tubes. It should be noted that because hydrogen and oxygen are mixed in water when they are formed near the core region, they do not separate from water or steam again until the steam condenses.

The effect of the radiolytic gases on the ICs has been determined using TRACG. [[

]] Nevertheless, a bias was applied to the IC performance to account for degradation due to the potential of radiolytic gas build-up.

[[

]]

Figure 5-1: Volume Fraction of Radiolytic Gases ($H_2 + O_2$) in Steam in the RPV Following a 1-Inch Liquid Break

5.2.5 Modeling Biases (PIRTs)

TRACG has a feature to bias various modeling parameters, which are called PIRTs. A TRACG PIRT is a coefficient which multiplies an internally calculated nominal value over a specified range of the solution domain. The PIRTs used in the ESBWR TRACG application (Reference 7.10) for conservative cases are listed in Table 5-1. [[

]].

In addition to the parameters listed in Table 5-1, a 2σ uncertainty is also added to the decay heat in the conservative cases. This is accomplished through the decay heat input rather than a TRACG PIRT parameter; hence, this is not included in the PIRT. The delayed neutron effect is also included in the decay heat.

Table 5-1: TRACG PIRT Parameters Used in Mass and Energy Release Calculations

TRACG PIRT Parameter	Modeling Parameter	Standard deviation (σ)	ESBWR ECCS-LOCA	ESBWR Containment Mass and Energy Release	BWRX-300 Containment Mass and Energy Release
[[					
					]]

5.2.6 Initial Conditions for Base and Conservative Cases, Trips

The initial values used in the base and conservative cases are listed in Table 5-2. The trips and isolation signals used in pipe break cases are listed in Table 5-3.

Table 5-2: Initial Conditions Used in TRACG Mass and Energy Calculations

Parameter	Base Case Input	Conservative Case Input
Reactor power before shutdown	100% of rated power	102% of rated power
Feedwater temperature	Normal feedwater temperature	Reduced feedwater temperature for liquid break, normal feedwater temperature for steam break
Steam and feedwater flow rates	From heat balance at 100% of rated power	From heat balance at 102% of rated power
Dome pressure	Rated dome pressure	[[ ]] higher than rated dome pressure
Hot channel power shape	Obtained from core loading of a typical core design	Top peaked [[
Initial water level	Normal water level	]]

Table 5-3: Trips and Isolations Used in Both Base and Conservative Cases

Event or isolation	Trip	Notes
Shutdown	Load rejection (loss of offsite power)	Delay in generating the scram signal + time required for prompt neutron fission power to diminish because of the control rod insertion. Note that delayed neutron effect is accounted for in the decay heat separately.
Isolation of large pipes except IC piping	High drywell pressure or Low-Low level (Level 2)	These are the only RPV isolation signals credited in pipe break analyses.
Isolation of IC piping	[[	]]
Containment isolation	Same as RPV isolation valves	Containment isolation for main steam pipe break is conservatively ignored (see Section 3.0).
ICS Initiation	Low-low level (Level 2) or high drywell pressure	These are the only initiation signals for the ICS credited in the pipe break analyses.

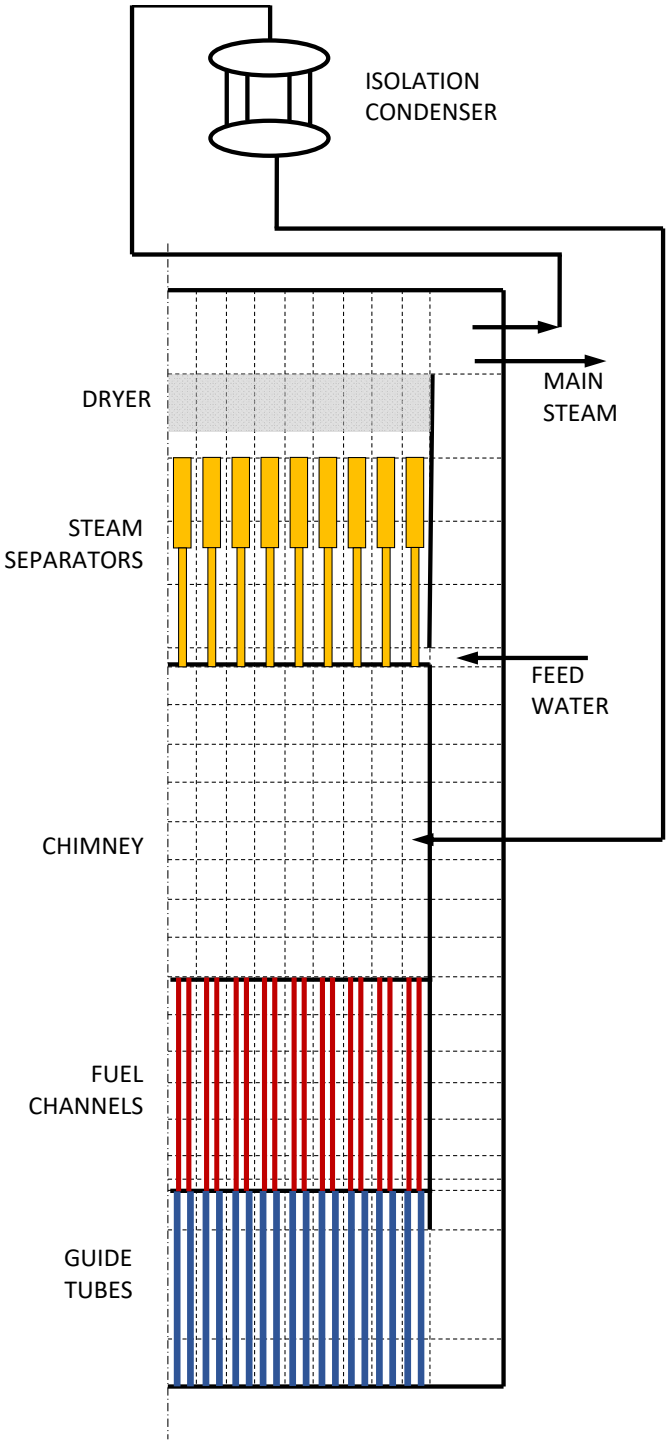

Figure 5-2: TRACG RPV Nodalization

[[

]]

Figure 5-3: Main Steam, Feedwater and Instrument Piping Attached to the RPV

[[

]]

Figure 5-4: TRACG IC Modeling for BWRX-300

5.3 Demonstration Cases for Large Breaks

The worst assumed single failure for a large break is the loss of an ICS train. [[

]]. For all other breaks, two ICS trains are available to remove the decay heat and depressurize the RPV after the loss of one ICS train due to a single failure. [[

]].

The demonstration cases for large steam and feedwater pipe breaks were performed for two sets of assumptions discussed below.

Base Case: Using nominal initial conditions and nominal modeling parameters. The nominal modeling parameters are used when all the PIRT multipliers described in Section 5.2.5 are set to 1.0. It should be noted that the base cases also include some conservatism due to the scenario and various input parameters. For example, [[

]].

Conservative Case: The initial conditions listed in Table 5-2 are biased and the modeling parameters listed in Table 5-1 are biased in the conservative direction.

The key input parameters used in the demonstration cases for base and conservative cases are collected in Table 5-4.

The scenario assumptions for main steam pipe break are as follows:

- Main steam pipe break inside the containment concurrent with loss of offsite power
- Feedwater pump trip [[ ]]
- Reactor trip [[

]].

- Drywell pressure increases to the high drywell pressure setpoint. [[

]].

- The ICS valves for one IC train begin opening [[
]].

Table 5-4: Key RPV Input Parameters Used in Demonstration Cases

Parameter	Base Case	Conservative Case
Initial power (MW)	870	887.4
Decay heat	ANS 5.1-1979 nominal	ANS 5.1-1979 + 2σ
Number of fuel bundles	240	240
Initial dome pressure (kPa)	[[	
Initial feedwater temperature (°C)		
Initial downcomer level (m above TAF)		
Main steam pipe inside diameter (m)		
Main steam flow limiter diameter (m)		
Feedwater pipe inside diameter (m)		
Low-low setpoint (m above TAF)		
High drywell pressure setpoint (kPa-g)		]]

5.3.1 Base Case for Large Feedwater and Steam Breaks

The large steam pipe breaks results are shown on Figure 5-5 through Figure 5-7. As discussed in Section 5.2.3, reactor power is obtained from decay heat tables.

The reactor power shown on Figure 5-5 is [[

]].

Only one ICS train is assumed to be put in service for large steam breaks. As the ICS condensate return valve starts opening at [[ ]], the cold condensate that has accumulated in the heat exchanger tubes and the condensate return lines starts flowing into the RPV, and a rush of steam to the ICS occurs. [[

]]. After this initial transient, the ICS heat removal rate starts approaching the 33.75 MW quasi steady state design value

As shown on Figure 5-6, the reactor pressure decreases for [[ ]] due to the break. [[ ]] the ICS starts depressurizing the RPV because the heat removal by one IC train exceeds the decay heat after approximately 20 seconds. [[

]].

The break flow rates from the broken loop and the intact loop sides of the break are shown on Figure 5-7. [[

]].

The large feedwater pipe break cases consider reduced feedwater temperature [[

]]. The results of the large feedwater pipe breaks are shown on Figure 5-8 through Figure 5-10.

In the steam pipe break cases, scram signal is inserted due to [[

]].

5.3.2 Conservative Case for Large Feedwater and Steam Breaks

The results of the large steam pipe breaks are shown on Figure 5-11 through Figure 5-13. The discussions in Section 5.3.1 for the base case also apply to the conservative case.

[[

]].

The results for the large feedwater pipe breaks are shown in Figure 5-15 through Figure 5-17. [[

]].

5.4 Demonstration Cases for Small Breaks

Base and conservative cases were run for the small steam and liquid pipe break cases. The small break events are slowly evolving events; therefore, the trends for the base and conservative steam and liquid breaks are very similar to each other. The results of the conservative small steam and liquid break cases are shown and discussed in this section.

The results of the conservative case for small break are shown on Figure 5-18 through Figure 5-22. As shown on Figure 5-18 and Figure 5-19, the ICS heat removal rate decreases as the RPV pressure decreases. The difference between the heat removed by the ICS and the power generated by decay heat is what is discharged from the break. The pressure boundary condition used in the TRACG calculation remains at atmospheric pressure to maximize the break flow rate. [[

]].

Even without crediting any inventory makeup, the downcomer level shown on Figure 5-20 remains above TAF out through 72 hours when the calculation ends for the conservative small steam break. As shown on Figure 5-21, the Peak Cladding Temperature (PCT) always remains only slightly above the fluid saturation temperature, [[

]]

As shown on Figure 5-22, at 72 hours after initiation of the small steam break, the break flow rate from the conservative case has reduced to well below the flow rate that can be made up with CRD flow.

Results from the conservative case for the small liquid breaks are shown on Figure 5-23 through Figure 5-27. There are differences from small steam break results in the break flow rate and RPV level while the break location is in the liquid space. Break uncovery starts to occur at [[ ]]. Because of the higher flow rate prior to the break uncovery and higher RPV inventory depletion as a result, downcomer level decreases [[ ]] as shown on Figure 5-25.

By 72 hours, downcomer [[

]].

At 72 hours after initiation of the small liquid break, the break flow rate from the conservative case has reduced [[ ]] as shown on Figure 5-27. This break flow at 72 hours corresponds roughly to the total steaming rate from decay heat minus the ICS steam condensation rate. The break flow at 72 hours is essentially the same as for the small steam break because the small liquid break became a small steam break when the break elevation uncovered [[ ]]. The break flow rate is well below the rate that can be made up with CRD flow.

5.5 Summary of the Application Method for Large and Small Break LOCA Analyses

The BWRX-300 TRACG nodalization for the RPV and ICS modeling is more detailed than the nodalization used in the ESBWR application discussed in Section 5.2.1.

The main steam piping of both loops up to the turbine stop valves are included in the model, and a large steam pipe break flow includes the flow from both ends of the break conservatively assuming instantaneous separation of the pipes.

Conservative biases listed in Table 5-1 are used to bound uncertainties in key TRACG models. For the conservative cases, the initial operating conditions are also conservatively biased as listed in Table 5-4.

Initiation of valve actuation timing used in the analysis bounds the time required to reach the analytical setpoint, signal development time, and the time required for valve stem travel until the area restriction starts to occur.

Reactor trip occurs due to load rejection in the small pipe break cases. RPV isolation valves are closed when the containment pressure exceeds the high containment pressure trip setpoint. The delay in this trip can be estimated conservatively.

[[

]]

[[

]]

Figure 5-5: Reactor Power, Main Steam Pipe Break, Base Case

Note: Decay Heat curve represents fission power as well as decay heat. "Q IC-A" is the heat removal rate by ICS Train A.

[[

]]

Figure 5-6: RPV Pressure, Main Steam Pipe Break, Base Case

[[

]]

Figure 5-7: Break Flow Rate and Enthalpy, Main Steam Pipe Break, Base Case

[[

]]

Figure 5-8: Reactor Power, Feedwater Pipe Break, Base Case

Note: Decay Heat curve represents fission power as well as decay heat. "Q IC-A" and "Q IC-B" are heat removal rates by ICS Trains A and B.

[[

]]

Figure 5-9: RPV Pressure, Feedwater Pipe Break, Base Case

[[

]]

Figure 5-10: Break Flow Rate and Enthalpy, Feedwater Pipe Break, Base Case

[[

]]

Figure 5-11: Reactor Power, Main Steam Pipe Break, Conservative Case

Note: Decay Heat curve represents fission power as well as decay heat. "Q IC-A" is the heat removal rate by ICS Train A.

[[

]]

Figure 5-12: RPV Pressure, Main Steam Pipe Break, Conservative Case

[[

]]

Figure 5-13: Break Flow Rate and Enthalpy, Main Steam Pipe Break, Conservative Case

[[

]]

Figure 5-14: RPV Level, Main Steam Pipe Break, Base and Conservative Cases

[[

]]

Figure 5-15: Reactor Power, Feedwater Pipe Break, Conservative Case

Note: Decay Heat curve represents fission power as well as decay heat. "Q IC-A" and "Q IC-B" are the heat removal rates by ICS Train A and ICS Train B.

[[

]]

Figure 5-16: RPV Pressure, Feedwater Pipe Break, Conservative Case

[[

]]

Figure 5-17: Break Flow Rate and Enthalpy, Feedwater Pipe Break, Conservative Case

[[

]]

Figure 5-18: Power, Small Steam Break, 2 ICS Trains, Conservative Case

Note: Decay Heat curve represents fission power as well as decay heat. "Q IC-A" and "Q IC-B" are heat removal rates by ICS Trains A and B.

[[

]]

Figure 5-19: RPV Pressure, Small Steam Break, 2 ICS Trains, Conservative Case

[[

]]

Figure 5-20: RPV Level, Small Steam Break, 2 ICS Trains, Conservative Case

[[

]]

Figure 5-21: PCT, Small Steam Break, 2 ICS Trains, Conservative Case

[[

]]

Figure 5-22: Break Flow Rate and Enthalpy, Small Steam Break, 2 ICS Trains, Conservative Case

Note: The initial break flow rate is off-scale. [[
]]

[[

]]

Figure 5-23: Power, Small Liquid Break, 2 ICS Trains, Conservative Case

Note: Decay Heat curve represents fission power as well as decay heat. "Q IC-A" and "Q IC-B" are heat removal rates by ICS Trains A and B.

[[

]]

Figure 5-24: RPV Pressure, Small Liquid Break, 2 ICS Trains, Conservative Case

[[

]]

Figure 5-25: RPV Level, Small Liquid Break, 2 ICS Trains, Conservative Case

[[

]]

Figure 5-26: PCT, Small Liquid Break, 2 ICS Trains, Conservative Case

[[

]]

Figure 5-27: Break Flow Rate and Enthalpy, Small Liquid Break, 2 ICS Trains, Conservative Case

6.0 CONTAINMENT ANALYSIS METHOD USING GOTHIC

The GOTHIC application methodology includes base cases and conservative cases. For the base cases, nominal inputs, assumptions, and correlations are used. The individual key inputs, assumptions and modeling parameters are conservatively biased simultaneously in the conservative cases, rather than sampling the uncertainties and adding margin to the base case results. While this method compounds conservatisms, it gives reasonable assurance that the overall method results bound the uncertainties, and greatly reduces the number of sensitivity runs. This is the same approach that was taken for the ESBWR containment method in Reference 7.10.

Sections 6.1 through 6.4 describe the identification of the relevant inputs and phenomena relevant to the BWRX-300 containment response and the selection of the models and correlations used to develop the base GOTHIC containment model. Section 6.5 describes the GOTHIC input model for the BWRX-300 containment. Section 6.6 describes the base cases and the results obtained from those base cases. Section 6.7 shows how nodalization impacts the calculated results. Sections 6.5 through 6.7 help to establish what model uncertainties and biases of the GOTHIC methodology are most important for application of the GOTHIC model for analyses of the BWRX-300 containment; that is why Sections 6.5 through 6.7 are presented before the discussion of the model biases and uncertainties in Section 6.8. Section 6.8 reviews the key model uncertainties and biases used in developing the conservative GOTHIC containment model. Section 6.9 provides benchmark predictions of test data. Demonstration analyses showing the BWRX-300 containment response for various break sizes and locations using the conservative GOTHIC containment model are provided in Section 6.10.

The large steam line break result described in Section 6.10.1 produces the highest calculated containment pressure. Containment pressure and temperature responses calculated using the conservative case assumptions are compared to the base case results to quantify the amount of conservatism provided by the methodology.

The small steam or liquid breaks described in Section 6.10.2 demonstrate that the peak containment pressures from unisolated small breaks are well below the peak pressure resulting from the large steam break. The small break calculations are primarily useful for demonstrating the capability of the PCCS to reduce the containment pressure in the longer term. The methodology assumes a one-way coupling between the TRACG and GOTHIC calculations whereby atmospheric pressure is always used for the break boundary condition used to calculate conservative TRACG mass and energy release rates that are input to the GOTHIC containment calculation. This methodology is demonstrated in Section 6.10.2 to result in peak containment pressures from the small breaks that are greater or more conservative than what would be obtained if a more complex two-way coupled methodology that credits how increased containment pressure were used. After the containment pressure increases to the RPV pressure, the RPV pressure calculated without a break bounds the containment pressure.

6.1 GOTHIC Phenomenon Identification and Ranking Table (PIRT)

The PIRT purpose is to identify phenomena important to the analysis of the BWRX-300 containment response for design basis events. The phenomena is then used to assess the ability of the model to calculate the effect of the phenomena on containment pressure and temperature, and the qualification of the evaluation model for calculating the phenomena, including the available

tests and determining any additional testing, scaling or analysis needed to qualify GOTHIC for the BWRX-300.

The initial phenomena list relevant to BWRX-300 containment analysis has been obtained by reviewing the following sources:

- NEDC-33083P-A Revision 1, TRACG Application for ESBWR (Reference 7.10)
- NEA/CSNI/R3(2014), Containment Code Validation Matrix (Reference 7.13)
- SMSAB-02-02, An Assessment of CONTAIN 2.0: A Focus on Containment Thermal Hydraulics (Including Hydrogen Distributions) (Reference 7.14)

Table 3.2-1 of Reference 7.10 was reviewed for phenomena that are applicable to the BWRX-300 containment pressure and temperature analysis, including phenomena that would have an equivalent phenomena in BWRX-300, even if the component was of a different design (for example, the secondary side heat transfer to the ultimate sink pools was evaluated because the phenomena are equivalent for the [[ ]]).

Two additional references (References 7.13 and 7.14) were used for additional important phenomena that might apply to the BWRX-300, but not to the ESBWR. This provides a complete check that covers phenomena that were not determined important for ESBWR but might be important for the BWRX-300. Table 3-1, *Containment Thermal Hydraulics Phenomena*, and Table 3-6, *Systems Phenomena*, of Reference 7.13 were reviewed. Note that the phenomena applicable only to the beyond design basis events and severe accidents are not included in the review. Reference 7.13 report classifies the significance of phenomena as Major/Minor. Phenomena evaluated as having major significance were reviewed for BWRX-300 applicability. The phenomena were then correlated with the ESBWR PIRT to eliminate duplication.

The third reference (Reference 7.14) contains Table 2.3, *Illustrative Phenomena Identification and Ranking Table for Containment Thermal Hydraulics*, during the Rapid Pressurization Phase of a Design Basis Accident in a Large Dry Pressurized Water Reactor Containment. This Table repeats the same phenomenon in different structures/components of the containment, but if the phenomenon was ranked H, M or L-M for either Pressure or Temperature, it was evaluated for correlation with the phenomenon in the previous two sources. Note that fan dynamics, spray dynamics and spray mass and energy exchange are not applicable to BWRX-300 and are not evaluated. All the buoyancy phenomena in Reference 7.14 are combined into one buoyancy phenomena, and the convection/advection phenomena are combined. The phenomena in Reference 7.14 report phenomena are then correlated with the ESBWR PIRT to eliminate duplication.

The names of phenomena are different in the reports cited above, although they refer to the same phenomena. For the BWRX-300 containment PIRT, the phenomena names and descriptions provided in Reference 7.10 were generally used.

6.2 PIRT Survey

The initial list of PIRTs was distributed in a survey to six Subject Matter Experts who reviewed the PIRT list, ranked them in importance to the GOTHIC BWRX-300 containment pressure and temperature analysis, and solicited any missing significant phenomena. The experts were provided with the BWRX-300 design description, including the information in Section 3.0 discussed previously. Phenomena ranking was requested according to the criteria in Table 6-1.

Table 6-1: Phenomena Ranking Criteria

Importance	Definition
High (H)	Phenomenon has controlling effect on GOTHIC DBA LOCA Containment Pressure and Temperature
Medium (M)	Phenomenon has moderate effect on GOTHIC DBA LOCA Containment Pressure and Temperature
Low (L)	Phenomenon has low effect on GOTHIC DBA LOCA Containment Pressure and Temperature
Not Applicable / Not Relevant (N/A)	Phenomenon has no, or insignificant effect on GOTHIC DBA LOCA Containment Pressure and Temperature for the design basis events described in Section 1.2. This category also applies to phenomena that are only significant to TRACG DBA LOCA mass and energy release

To facilitate downstream application to the GOTHIC methodology qualification, the rankings were broken down into two phases:

1. Short-term is the period during which the momentum and inertia effects resulting from the break flow have a significant contribution to the circulation, stratification and heat tranfer in the containment. [[

]]

2. Long-term is the period during which the momentum and inertia effects are diminished, and the buoyancy is the major contributor to the circulation, stratification and heat transfer. This phase may be as long as 30 days, but the calculations are continued only until conditions are considered stable.

The experts were asked to evaluate the Systems Structures and Components (SSCs) involved in GOTHIC modeling of the BWRX-300 containment in their ranking and provide a single highest importance rank for the phenomena. Similarly, if the phenomena might have different rankings between a liquid pipe break and a steam pipe break, they were asked to provide the higher/bounding rank, to make the presentation of the ranking simpler and the ranking/consensus building process more efficient.

The surveys were provided for expert's comments and additional input on the applicable SSCs. They were encouraged to: "Use the comments column if meaning of the phenomena are unclear." Blank fields were provided to add any missing phenomena thought to be significant.

Before the survey was completed, a "Pre-job brief" meeting was held to explain the process and answer general questions.

In consolidating the survey results, comments on the description/definition of the phenomena were identified. A few additional phenomena were identified by the experts during the survey. Additional input was obtained with clarified definitions and with ranking of the added phenomena.

After the initial survey was received and compiled, multiple meetings were held to discuss the results and develop a consensus ranking. These discussions focused on phenomena with the highest variance in the ranking. Explanation of the rationale for an individual's ranking usually resulted in changes to the ranking and built a consensus ranking.

The High/Medium/Low/N/A ranking was assigned a numerical score of 3/2/1/0, respectively. The rank was then averaged and rounded up (if the average is 2.5 or greater it is assigned a H/High importance, and if it is less than that and above 1.5 it is assigned a M/Medium importance).

It should be noted that the ranking was completed before performing sensitivity studies and before the preliminary best estimate calculations were progressed. Therefore, the rankings reflect phenomena that may potentially be applicable. In this context, the rankings can be viewed as a conservative estimate such that a phenomenon will be included in the uncertainty evaluations if there is a potential for it to affect the calculations. A phenomenon ranked medium or high may turn out to be not applicable or of low effect when the calculations are performed. But the opposite would not be the case (i.e., phenomena ranked low following the consensus ranking process were not revisited).

The summary of the PIRT is provided in Table 6-2. A description of each phenomena is given below the Table corresponding to the item number in Table 6-2.

Table 6-2: Phenomena Identification and Ranking Table for Containment (Excluding RPV)

[[

]]

6.3 Overview of the Development of Assessment Base

Development of the assessment base follows the applicable sections of RG 1.203 guidance. It should be noted that most Elements 2 and 3 in RG 1.203 have been completed as part of the GOTHIC code development and documented in the GOTHIC technical and qualification reports. The remaining items of RG 1.203 Elements 2 and 3 include:

- Determining uncertainty in the correlations relating to the phenomena ranked high and medium based upon the existing experimental base for these correlations
- Establishing suitably conservative biases in the above correlations
- Establishing suitably conservative input parameters
- Benchmarking the method against the integral tests representative of the BWRX-300 containment to demonstrate the conservatism in the method

6.4 Knowledge Level for the Phenomena Pertinent to Containment Analysis

The phenomena that are ranked High or Medium for either short or long-term are included in the uncertainty evaluation. The first step in this process is to assess the knowledge level for each of these phenomena. The same expert panel that formed the PIRT in Table 6-2, with one substitute due to the departure of one member from GEH, also voted on the knowledge level in Table 6-3. The knowledge level is ranked from 1 to 4 for each phenomenon, 1 representing the least confidence and 4 representing the most confidence. The consolidated rationale for the knowledge level is also listed in Table 6-3.

In general, a phenomenon ranked high in Table 6-2 for importance and low in Table 6-3 for knowledge level requires additional research. However, some of the phenomena ranked High or Medium importance may not be applicable or the effect may turn out to be small for the type of modeling and the analysis of the events that are in the scope of this report as mentioned in Section 6.3. It is for this reason that the base GOTHIC model and the base case results will be introduced in the next section before discussing the uncertainties in the inputs and correlations.

Table 6-3: Knowledge Level for the Phenomena Ranked High or Medium

[[

]]

6.5 GOTHIC Containment Model

A schematic of the GOTHIC model used for the BWRX-300 containment analysis is shown on Figure 6-1. Volume 1s represents the main section of the containment, Volume 2s represents the containment dome region above the refueling bellows, Volume 3s is the PCCS, and Volume 4 is the reactor cavity pool.

The containment dome is connected to the main section of the containment through two flow paths, 1 and 2, representing the manholes in the refueling bellows.

Flow paths 4 through 13 are the exit of the hot channels of the [[ ]] PCCS units connected to the reactor cavity. Flow paths 14 through 23 are the intake openings of the PCCS units connected to the reactor cavity pool. Flow paths 25 through 34 are openings between the cold tubes and heated tubes of the PCCS units at the bottom.

Three dimensional volumes, so-called subdivided volumes in GOTHIC terminology, are used to model the main section of containment. Nodalization of the main section (Volume 1s) and the containment dome (Volume 2s) used in the base model are shown on Figure 6-2.

The RPV is modeled by using a blockage corresponding to the outer dimensions of the RPV insulation as shown on Figure 6-2. Approximately [[ ]] of the remaining volume is assumed to be obstructed by various support structures, piping, catwalks, etc. Thermal conductors are distributed over cells on the RPV surfaces and where the piping is routed. The thermal conductor properties are set to the mirror insulation properties using conservative inputs to maximize the heat loads from the RPV and piping. The fluid temperature in the piping is assumed to be the same as the RPV fluid temperature and is specified as a function of time as obtained from the TRACG mass and energy release calculations.

The flow path representing the break flow is placed [[ ]], next to the containment shell and the break flow is directed toward the shell when calculating the peak shell temperature. [[

]] The break mass flow rate and enthalpy are specified as a function of time as obtained from the TRACG mass and energy release calculation.

The figures based on the GOTHIC runs with break location maximizing the pressure are identified with “[MaxP]”, and the figures based on the GOTHIC runs with break location maximizing the shell temperature are identified with “[MaxT]” in the figure captions.

Nodalization for the small containment dome region is shown in the upper right part of Figure 6-2. [[

]]

The PCCS is represented by subdivided volumes as shown on Figure 6-3. [[

]]

The following is a list of the key modeling parameters used in the base cases. The reasoning for the choice of the models and their uncertainties is discussed in Section 6.8.

- Mass and energy release are obtained from the TRACG base case results in Section 5.3.1 for large breaks.
- The form loss coefficients in the PCCS are set to conservatively high values, accounting for the flow losses due to the typical spacers, as well as entrance and exit losses and [[ ]].
- Wall friction is calculated from the Colebrook relationship for smooth wall.
- The heat transfer coefficient in containment is the sum of two parts as follows:
    - The Nusselt number for heat transfer due to sensible heat can be calculated from the forced convection or natural convection. The forced flow convection correlation is the Dittus-Boelter correlation given by:

      $$Nu_{FC} = 0.023\,\mathrm{Re}^{0.8}\,\mathrm{Pr}^{0.3}$$

      where Nu is the Nusselt number, Re is the Reynolds number, and Pr is the Prandtl number. Reynolds number is calculated based on the velocity and properties in the node next to the wall and the user-specified characteristic length. The exponent of the Prandtl number is 0.4 for the heated walls (RPV and hot piping).

      The Nu for heat transfer in natural convection is calculated from the [[

]]

The following relationship is used in GOTHIC to select which mode of heat transfer applies:

[[ ]]

- Heat transfer due to latent heat in condensation is calculated using the Diffusion Layer Model (DLM) (Section 9.1.6 of Reference 7.16).

- The characteristic length for the forced convection is set to the [[ ]].
- Radiation heat transfer to the shell and the PCCS is conservatively ignored.
- [[

]]

[[

]]

Figure 6-1: Schematic of the GOTHIC Model of BWRX-300 Containment

[[

]]

Figure 6-2: Nodalization of Containment Main Volume, Volume 1s (left), Containment Dome, Volume 2s, (upper right) and the Break Flow Path in Volume 1s at Vertical Node 14 (lower right) [MaxT]

[[

]]

Figure 6-3: Volumes Representing PCCS Units

6.6 Base Cases and Results

This section presents the containment response for the mass and energy releases calculated in Section 5.3.1 for large steam and feedwater breaks using the base model described in Section 6.5. The key containment inputs are listed in Table 6-4. The containment nodalization and modeling parameters are described in Section 6.5.

Table 6-4: Containment Inputs Used in Base Cases

Parameter	Value
Containment height	[[
Containment diameter	
Free containment volume (excluding dome)	
Containment dome height	
Containment dome diameter	
Containment shell thickness	
Containment head thickness	
Number of manholes on the refueling bellows	
Diameter of the manholes	
Number of PCCS units	
PCCS type	
PCCS outer diameter	
PCCS outer pipe thickness	
PCCS cold tube outer diameter	
PCCS cold tube thickness	
PCCS height inside the containment	]]
Initial containment temperature	43.33 °C
Initial containment relative humidity	20%
Initial containment pressure	101.325 kPa
Initial reactor cavity pool temperature	43.33 °C

6.6.1 Containment Response to Large Steam Break, Base Case

The containment pressure response to a large break in a steam line is shown on Figure 6-4. The peak pressure [[ ]] is reached at approximately the time the RPV isolation valves fully close [[ ]]. After the closure of the RPV isolation valves, the only heat input to the containment is due to convection from the RPV wall and hot pipe walls through the insulation. With the break flow isolated, the containment pressure starts decreasing. [[

]]

The airspace and containment shell temperature responses are shown on Figure 6-5. The maximum air temperature is the maximum of all nodal temperatures in the containment; the bulk temperature is the average air temperature throughout the containment. These temperatures are higher than the temperature resulting from the isenthalpic expansion of steam from the RPV conditions to the containment pressure. The additional temperature increase is due to the compression of nitrogen in containment. Following the break, there is a rigorous circulation of

the air in containment. Prior to isolation, the [[

]]. The peak temperature moves around in containment as the hot steam / nitrogen mixture circulates. After the break flow stops, the location of the maximum temperature continues to vary with the changing flow patterns, but most of the time remains in locations near the RPV wall.

Although the containment air temperature is high [[ ]], the containment shell remains at a much lower temperature. [[

]]

The PCCS exit temperature is also shown on Figure 6-5. [[

]] A sensitivity analysis for the PCCS is presented in Section 6.6.1.

The decay heat rate and the heat removal rates by the various heat removal mechanisms are plotted on Figure 6-6. As shown on the plot, the containment shell initially absorbs a large amount of energy for a short duration before the heat removal diminishes as the shell warms up [[ ]]. The isolation condensers are the primary mechanism for removing decay heat from the isolated RPV. [[

]] No credit is taken in these cases for the heat transfer from the containment shell to the concrete supporting structures.

The subcompartment formed by the containment head and refueling bellows is the limiting location with respect to differential pressures acting across subcompartment boundaries because of the relatively small flow areas provided by the access manholes in the bellows. The other subcompartments inside the containment (e.g., [[ ]]) have much larger openings. The pressure differential across the refueling bellows is shown on Figure 6-8. In this variation of the base case, the flow loss coefficient across the manholes is set to an extremely high value [[ ]] in order to maximize the differential pressure during the event. The GOTHIC model captures the pressure waves travelling through the containment immediately following the break, and the peaks and valleys in the pressure trend correspond to physical phenomena. The time

difference between the first peaks of the red and blue curves is consistent with the pressure wave travelling at nearly the speed of sound. [[ ]]. This is a small pressure differential across the boundary of a subcompartment. The pressure drop across the other subcompartment boundaries were not calculated because they have much larger flow area-to-volume ratios and are located farther away from the break, [[ ]].

If the pipe routing is designed such that a potential pipe break may occur in close proximity of the biological shield wall or vessel support, the same method used here can be used to assess the differential pressure loads to be considered in the detailed structural designs. However, if a significant pressure differential occurs across the biological shield due to the close proximity of the break, it is likely that the jet impingement loads would be the more limiting concern. The determination of the jet impingement loads acting on the containment structures is outside the scope of this LTR.

6.6.2 Containment Response to Large Feedwater Pipe Break, Base Case

The containment pressure response to a large break in the feedwater pipe is shown on Figure 6-9. The peak pressure [[ ]] is reached at the time the RPV isolation valves fully close [[ ]]. Similar to the large steam break, after the closure of the RPV isolation valves the only heat input to the containment is from the RPV wall and hot pipe walls through the insulation. [[ ]] The peak containment pressure for a feedwater pipe break is bounded by the peak containment pressure for a large steam pipe break.

The airspace and containment shell temperature responses in the containment are shown on Figure 6-10. The containment temperature discussion in Section 6.6.1 also apply to the response to feedwater pipe breaks. It can be seen on Figure 6-10 that the maximum shell temperature is well below the containment atmosphere temperature, [[ ]].

6.7 Nodalization Studies

6.7.1 Nodalization Study for Containment

A nodalization study was performed using the base case for the large main steam pipe break presented in Section 6.6.1.

The nodalization study for the main containment section included the following cases, also shown on Figure 6-11:

- Base case: [[ ]]
- Coarser grid. Twice the node size of the base case in each direction: [[ ]]
- Finer grid in the horizonal plane. Half the node size of the base case in each direction in the horizontal plane: [[ ]]. Same node size in the vertical direction
- Finer grid in the vertical direction: Half the node size of the base case in the vertical direction: [[ ]]. Same node size as in the base case in the horizontal plane

The PCCS unit placement is accurate in the [[ ]] cases. [[ ]].

The large steam break base case was rerun using different nodalization schemes described above. As shown on Figure 6-12, the effect of nodalization on the containment pressure response is very small. The curve for [[ ]] case is not visible because it is overlapped by the results of the [[ ]] nodalization case. There is an insignificant difference, [[ ]], in the peak pressure between the base case and finer nodalization cases. The nodalization trend also shows that the coarser nodalization slightly overpredicts the peak pressure. As shown on this figure, reducing the node size [[ ]] does not make a significant difference in the pressure response.

The temperature trends shown on Figure 6-13 also display similar behaviors. The air/steam mixture temperatures are similar in all cases. The temperature trend differences between the cases are consistent with the differences shown between the pressure trends. There are some differences in the air/steam temperatures in the longer term, but the shell temperatures remain close to each other in all nodalization schemes. [[ ]].

Based on the above results, it is concluded that the containment nodalization [[ ]] is adequate for containment pressure, air/steam temperature and the shell temperature predictions.

6.7.2 Nodalization Study for PCCS

The effect of nodalization on the PCCS has been studied for a single PCCS unit placed in a large containment volume. The containment volume is kept at the prescribed temperature and steam concentration. The base case nodalization in the vertical direction is the same as the BWRX-300 containment model, [[

]]

The second case used in the nodalization study doubles the number of nodes both in the PCCS and the containment, and the third case doubles the number of nodes again.

The effect of nodalization on the heat removal rate is shown on Figure 6-14 at three containment temperatures. [[

]] A [[ ]] reduction is applied to the heat transfer on the outer surface of the PCCS unit. [[ ]] The results show negligible effect of nodalization on the PCCS heat removal rate.

[[

]]

Figure 6-4: Containment Pressure Following Large Main Steam Pipe Break, Base Case [MaxP]

[[

]]

Figure 6-5: Temperatures in the Containment Following a Large Main Steam Pipe Break, Base Case [MaxT]

[[

]]

Figure 6-6: Heat Removal Rates by Various Mechanisms Following Large Main Steam Pipe Break, Base Case [MaxP]

[[

]]

Figure 6-7: Longer Term Heat Removal Rates by Various Mechanisms Following Large Main Steam Pipe Break, Base Case [MaxP]

[[

]]

Figure 6-8: Pressures Next to Refueling Bellows Following Large Main Steam Pipe Break, Base Case [MaxT]

[[

]]

Figure 6-9: Containment Pressure Following Large Feedwater Pipe Break, Base Case [MaxP]

[[

]]

Figure 6-10: Temperatures in the Containment Following a Large Feedwater Pipe Break, Base Case [MaxT]

[[

]]

Figure 6-11: Grid Used in Nodalization Studies [MaxP]

Note: Orange circles in the plan view and orange bars in the vertical view represent the PCCS units. Blue arrows represent the break locations. In the vertical view, the break location arrows indicate only the vertical node number. The break location is shown for the cases maximizing temperature. In the cases maximizing pressure, the break flow is directed upwards, in cell IX=12, IY=6, IZ=10 in the 16x16x16 case, and in the corresponding cells in the other cases.

[[

]]

Figure 6-12: Effect of Nodalization on the Containment Pressure Response to Large Steam Pipe Break, Base Case [MaxP]

[[

]]

Figure 6-13: Effect of Nodalization on the Containment Temperature Response to Large Steam Pipe Break, Base Case [MaxT]

[[

]]

Figure 6-14: Effect of Nodalization on the PCCS Heat Removal Rate

6.8 Model Uncertainties and Biases

The source of uncertainties in the phenomena important to the containment pressure and temperature response are identified in Section 6.2. The knowledge level for these phenomena is discussed in Section 6.4 and summarized in Table 6-3. The following is the grouping of phenomena and their assessment based on the observations from the results of the base case containment analysis discussed in Section 6.6.

- [[

]]

- Items 2, 5, 6, 11, 12 are inputs. [[

]].

- The natural and forced circulation and stratification are affected by the friction factors, turbulence modeling, and the model nodalization. A nodalization study is presented in Section 6.7 for the containment and the PCCS. A sensitivity study for the friction factors and turbulence modeling is presented in Section 6.8.1 [[ ]]. This addresses Items 9, 10, 13, and 14.
- Uncertainties in the convection and condensation heat transfer coefficients, Items 3 and 7, are discussed in Section 6.8.2 where bounding values have been developed.
- In the RPV the production of hydrogen and oxygen by radiolysis is modeled by the bounding correlation given in Section 5.2.4. There are no other mechanisms for producing significant amounts of NC gases in either the RPV or the containment. [[ ]]. This addresses Items 19 and 20.
- Multi-component gas properties are calculated using the most accurate models available in the GOTHIC code as described in Reference 7.16.

6.8.1 Effect of the Friction Factors and Turbulence Parameters on the Containment Response

The importance of friction factors and turbulence on containment pressure and temperature response has been investigated by sensitivity studies for the containment and the PCCS separately.

The nominal cases use Colbrook's friction factors for a smooth surface. To determine the sensitivity of the pressure and temperature to the friction factor, the relative roughness was increased [[ ]]. Given the large hydraulic diameter, this relative roughness corresponds to an unreasonably high absolute value of surface roughness [[ ]]. The increased surface roughness case is identified as the "High C_f" case in the comparisons.

[[

]]

The results obtained by the above sensitivity cases are compared on Figure 6-15 through Figure 6-17 for the large steam pipe break. [[

]]

[[

]]

Figure 6-15: Effect of Friction and Turbulence on Containment Pressure, Large Steam Pipe Break [MaxP]

[[

]]

Figure 6-16: Effect of Friction and Turbulence on Containment Temperatures, Large Steam Pipe Break [MaxT]

[[

]]

Figure 6-17: Effect of Friction and Turbulence on Steam Volume Fraction, Large Steam Pipe Break [MaxT]

6.8.2 Uncertainties in the Convection and Condensation Heat Transfer Coefficient and the Bounding Values

The BWRX-300 containment model uses the DLM option for condensation built into GOTHIC (Reference 7.16) to calculate the condensation rate. The DLM correlation is based on a mechanistic model which recognizes the similarity between the heat and mass transfer. The benchmarking of both the convection and condensation correlations to the data is also provided in Reference 7.18. DLM is selected over the other options available in the code due to its mechanistic nature representing the underlying phenomena as opposed to curve fit to data. Recently, Heat and Mass Transfer Analogy Method (HMTAM) has been developed and compared to the CONAN and COPAIN test data (References 7.19 and 7.20). HMTAM is also based on the analogy between heat and mass transfer and is similar to DLM. As will be shown, the DLM method is more conservative than the HMTAM method for the BWRX-300 containment application. The uncertainties in the convection and condensation correlations with respect to the data will be evaluated based on the COPAIN test data in Reference 7.19. The uncertainties will be first presented for the HMTAM method.

The total heat transfer to a condensing surface has two parts: convection heat transfer from bulk to liquid film and the heat transfer by condensation. [[

]]

COPAIN data is collected over a range of 1 to 6.7 bars, non-condensable gas mass fraction range of 0.1 to 1.0, velocity range of 0.1 to 3.0 m/s and steam superheating up to 40 °C. The range of parameters in the BWRX-300 containment response is within the COPAIN data range. The COPAIN data also includes pure convection measurements. More information on the COPAIN data can be found in Reference 7.19.

A comparison of the forced and natural convection correlations to the data is shown on Figure 6-18. The black markers are the ratio of forced convection measured Nusselt number divided by the Nu number predicted by the Schlichting forced convection correlation. The points larger than 1.0 indicate that correlation underpredicts the forced convection Nusselt number. The x-axis in the plot is the Richardson number, Ri. Theoretically, inertia forces are dominant when the Richardson number is less than 1, and buoyancy forces are dominant when the Richardson number is greater than 1. As expected, the black markers corresponding to the Richardson numbers greater than about 5 show that the data is grossly underpredicted if the forced convection correlation is used where buoyancy forces are important. Conversely, the red markers, which show the ratio of the measured Nusselt number to the Nusselt number predicted by the McAdams natural convection correlation show that the data is grossly underpredicted if the natural convection heat transfer coefficient is used where the buoyancy forces are overwhelmed by the inertia forces due to the free stream velocity, i.e., where forced convection correlation should be used. There is a transition region between the high and low Richardson number ranges that is reviewed in more detail below.

The heat transfer is enhanced by the turbulence near the wall. As the free stream velocity is increased from zero in the same direction as in flow driven by buoyancy near the wall, it suppresses the turbulence and reduces the heat transfer until the free stream velocity is increased large enough that the inertial forces overwhelm the buoyancy forces. This phenomenon may occur in the transition region from natural convection to forced convection and is called re-laminarization. [[

]] Re-laminarization does not occur if the free stream flow is in upward direction near a cold wall as explained in Reference 7.21 and shown on Figure 6-19.

The analogy between the condensation and convection has been shown to be a valid basis to predict condensation in the more recent research and supported by data (see References 7.18 and 7.19). In condensation, the correlation forms and coefficients for forced and natural convection remain the same as in convection, but the Prandtl (Pr) number is replaced by the Schmidt (Sc) number, and the Nusselt (Nu) number is replaced by the Sherwood (Sh) number. The definitions of the dimensionless numbers are found in Reference 7.19.

[[
]] The uncertainty bands are shown on Figure 6-20 for forced and natural convection as compared to the data. [[

]] This is discussed further in the following application to BWRX-300 containment.

The discussion above is presented as it pertains to the HMTAM model of condensation, using Schlichting correlation for forced convection and McAdams correlation for natural convection.

The BWRX-300 containment model uses the DLM condensation model, [[
]].

The ratio of the condensation heat transfer predicted by DLM to that of HMTAM is shown on Figure 6-21 for various wall temperatures, flow rates and mass fractions. [[

]]

Based on the above observations, the following are the minimum biases applied to the DLM and convection correlations used in the GOTHIC model of the BWRX-300 containment to ensure the calculated results are conservative.

Convection correlation bias:

- [[

]]

Condensation correlation bias:

- [[

]]

[[

]]

As will be shown in Section 6.9, the above biases bound the integral test data and also add conservatism to the BWRX-300 containment response results that is comparable to the conservatism that would be introduced by using the Uchida correlation. Comparisons of the BWRX-300 containment response predicted by the Uchida correlation and the biased DLM correlation will be presented in Section 6.10.1.

[[

]]

[[

]]

Figure 6-18: Comparison of Data and Convection Correlations

[[

]]

Figure 6-19: Non-Dimensional Heat Transfer Coefficient Obtained With a Heated Tube in Upward Flow Conditions (from Reference 7.21)

[[

]]

Figure 6-20: Non-Dimensional Sherwood Number Obtained in the COPAIN Facility (Reference 7.19) With the Proposed Uncertainty Bands Added

[[

]]

Figure 6-21: Ratio of Condensation Mass Flow Rate Obtained by DLM to that of HMTAM

6.8.3 Sensitivity Analyses for PCCS Performance

Sensitivity analyses have been performed for the PCCS performance to determine the effect of:

- PCCS loss coefficients
- PCCS liquid-side heat transfer coefficient
- Fouling

Sensitivity cases also include the potential for the onset of boiling.

To determine the effect of each parameter without interference from other phenomena, a single PCCS unit was placed in a large volume representing a section of the containment. The containment pressure, temperature and steam volume fraction were kept constant at various values and each of the sensitivity parameters were varied to determine the effect on PCCS performance. The PCCS nodalization and geometry are the same as those used in the BWRX-300 containment model described in Section 6.5. The volume representing the containment was also nodalized in the vertical direction that is the same as the containment nodalization described in Section 6.5, with the exception of using one node in the horizontal direction.

The sensitivity study was performed for the following conditions. The PCCS heat removal rate at each condition was obtained after a steady state was reached.

Containment pressure: [[ ]]

Containment temperature: [[ ]]

Steam volume fraction: [[ ]]

PCCS inlet temperature: [[ ]]

PCCS total loss coefficient: [[ ]]

[[

]] The base case has no fouling or no paint.

The sensitivity cases for paint and crud assume thermal resistance of the paint on the outer surface of the PCCS is [[ ]] and the thermal resistance of the crud on the inner surface is [[ ]].

The results of the sensitivity cases are summarized in Table 6-5. [[

]]

Table 6-5: Summary of the Sensitivity Study Results for PCCS

Containment pressure (kPa)	[[					
Containment temperature (°C)						
Heat removal rate (kW)						
Loss coefficient x 1.5						
Loss coefficient x 2.0						
Fouling + paint						
Heat transfer coefficient inside the PCCS is reduced by [[ ]]						]]

6.9 Benchmarking to the Carolinas Virginia Tube Reactor (CVTR) Integral Tests

The CVTR tests simulate a steam pipe break by injecting slightly superheated steam into a closed containment (Reference 7.22). CVTR has a dry containment, with a free volume of 6428 m^3 (227,000 ft^3), [[ ]]. The

walls are concrete with a 6.35 millimeter (1/4 inch) thick steel liner, [[
]].

The CVTR test has several cases [[ ]]. Test case #3 is relevant to the BWRX-300 containment benchmarking [[

]] The GOTHIC model for CVTR is shown on Figure 6-22.

As discussed in Reference 7.17, the three-dimensional GOTHIC model using the best estimate DLM, including the Film Enhancement condensation heat transfer, predicts the measured pressure and thermal stratification closely. In the "biased DLM" cases presented here, the DLM method is used without the Film Enhancement feature and the biases in Section 6.8.2 are applied to the heat transfer surfaces. The comparisons also include the pressure and temperature predicted by the Uchida correlation. Uchida condensation correlation does not include a bias. However, the same bias described in Section 6.8.2 is also applied to the convection heat transfer in the Uchida correlation cases.

Figure 6-23 shows the containment pressure benchmarking to test data. The peak pressure calculated by the biased DLM heat transfer coefficient is approximately [[ ]] higher than the data. The biased DLM case also bounds the pressure predicted by the Uchida correlation.

Figure 6-24 shows the airspace temperature and Figure 6-25 shows the structure surface temperatures. The calculated temperatures are higher than the measured temperatures. The differences in the calculated temperatures on Figure 6-24 and Figure 6-25 at higher and lower elevations are close to the differences in the measured temperatures. These results indicate that GOTHIC predicts stratification well while there is steam flow and after the steam flow stops. The predicted surface temperatures are higher than the data.

[[

]]

Figure 6-22: CVTR Facility (Reference 7.22) and the GOTHIC Model (Reference 7.17)

[[

]]

Figure 6-23: GOTHIC Benchmarking to CVTR Test Data, Containment Pressure

[[

]]

Figure 6-24: GOTHIC Benchmarking to CVTR Test Data, Airspace Temperature

[[

]]

Figure 6-25: GOTHIC Benchmarking to CVTR Test Data, Structure Temperature

6.10 Demonstration of the Method for Large and Small Breaks, Conservative Cases

The large and small steam pipe breaks presented in this section demonstrate the conservatism in the method. The [[

]] correlations are biased as described in Section 6.8.2.

6.10.1 Containment Response to Large Steam Pipe Break, Conservative Case

Containment pressure and temperature responses calculated by using the conservative case assumptions are compared to the results of the base case assumptions for a large steam pipe break shown on Figure 6-26 and Figure 6-27. The biases in the inputs and assumptions cause adding approximately [[ ]] to the peak pressure as shown on Figure 6-26. This difference decreases to approximately [[ ]] in four hours.

The peak containment pressure and temperatures are listed in Table 6-6.

The differences between the temperatures using base case and conservative case assumptions are not as large as the differences in the pressure. [[

]]

It can be concluded from the above observations that the biases used in the conservative cases add a significant margin to the peak pressure values. However, there is not a significant difference in the peak shell temperatures. The cooldown of the shell is slower in the conservative case as compared to the base case.

Containment gauge pressure decreases [[ ]] and shows a decreasing trend in the conservative case. In the base case, containment gauge pressure decreases [[ ]], and also shows a decreasing trend. [[

]] The heat load in the containment becomes small. In the absence of break flow, containment pressure continues to decrease [[ ]].

On Figure 6-28 through Figure 6-30, the conservative case results are compared to those obtained by using the Uchida correlation for condensation keeping all other inputs and assumptions the same. The difference in the peak pressure is negligible. [[

]] Because the PCCS surface temperature remains below the saturation temperature in the long term, condensation heat transfer to the PCCS continues. Because of the conservatism in the biased DLM correlation as compared to the Uchida correlation after the peak, the containment pressure decreases faster in the long term

in the BWRX-300 GOTHIC conservative case than it would if the Uchida correlation were also used.

Containment temperatures predicted by using the biased DLM correlation and Uchida correlation are compared on Figure 6-30. There is not a significant difference in the air temperatures. However, the shell temperatures show some differences in the very short-term. It should be noted that the shell inner and outer surfaces shown on Figure 6-30 are the maximum shell temperatures; they are not the average shell temperatures. Because the Uchida correlation does not include any information about the velocities near the wall, it cannot predict the high condensation heat transfer that occurs locally. As a result, Uchida correlation underpredicts the shell temperature while high velocities exist and misses the initial peak that occur in the shell temperature. However, shell temperatures predicted by the Uchida and the modified DLM correlations approach each other after the velocities subside.

The comparisons above show that the condensation model used in the BWRX-300 containment method represents the trends accurately, it applies a sufficient level of conservatism comparable to that predicted by the Uchida condensation heat transfer correlation that has been found to be acceptable by the NRC staff previously.

[[

]]

Figure 6-26: Containment Pressure Following a Large Steam Pipe Break, Comparison of Conservative and Base Cases [MaxP]

[[

]]

Figure 6-27: Containment Temperatures Following a Large Steam Pipe Break, Comparison of Conservative and Base Cases [MaxT]

[[

]]

Figure 6-28: Comparison of Containment Pressures Predicted by the Biased DLM and Uchida Correlations [MaxP]

[[

]]

Figure 6-29: Comparison of Heat Transfer Rates Predicted by Biased DLM and Uchida Correlations [MaxP]

[[

]]

Figure 6-30: Comparison of Containment Temperatures Predicted by the Biased DLM and Uchida Correlations [MaxT]

6.10.2 Containment Response to Small Pipe Breaks, Conservative Cases

The containment response predicted by using the conservative case assumptions for small pipe breaks is shown on Figures 6-31 through 6-34 for small steam pipe breaks and on Figures 6-39 through 6-41 for small liquid pipe breaks. [[

]]. The peak containment pressure and temperatures are listed in Table 6-6.

The maximum pressure on Figure 6-31 for the small steam break is well below the peak pressure resulting from a large steam break shown previously on Figure 6-26 and discussed in Section 6.10.1. The mass and energy release rate calculated by assuming no back pressure in Section 5.4 is used in the GOTHIC model to calculate the containment pressure. In reality, the break flow will start decreasing after it becomes unchoked as the containment pressure approaches the RPV pressure and will become very small when the RPV and containment pressures are nearly the same. After this time, mass discharge to the containment becomes small enough to maintain containment pressure slightly below the RPV pressure. If the mass discharge rate were to increase momentarily, containment pressure would increase above the RPV pressure and the mass discharge would stop again until the containment pressure returns to a value below the RPV pressure. Therefore, after the time that the RPV and containment pressures equalize, the upper bound for the containment pressure is the RPV pressure corresponding to the no-break case. The lower bound of the containment pressure is the containment pressure calculated by assuming no break flow after the time the RPV and containment pressures equalize. It should be noted that the lower bound for the containment pressure is discussed here to illustrate the trends but does not have any associated acceptance criteria. In reality, there may be other favorable conditions that may make the containment pressure lower than the values calculated here.

[[

]]

The PCCS exit temperature and the reactor cavity pool temperature are shown on Figure 6-32. PCCS #1 is the PCCS unit closest to the break location, PCCS #6 is the farthest. The steam volume fraction in the containment (excluding the dome region) is shown on Figure 6-33. The maximum steam volume fraction, which occurs in the higher sections of the containment, [[ ]], decreases slowly in the long term. Note that the calculations conservatively assume no heat loss from the reactor cavity pool to the surroundings through the walls. However, heat loss due to surface evaporation from the pool is taken into account.

The peak shell temperature shown on Figure 6-34 resulting from a small steam pipe break is comparable to the peak shell temperature resulting from a large steam pipe break shown on Figure 6-30, although the timing of the peak is much different.

As discussed in Section 5.4, containment pressure is assumed to be at atmospheric pressure to maximize the break flow rate. However, if the ICS can depressurize the RPV faster than the PCCS can depressurize the containment, it is conceivable that non-condensable gases in the containment will be ingested into the RPV and into the ICS heat exchangers. For all cases, the effect of nitrogen ingestion, if it does occur, is modeled for all components of the TRACG model (e.g., RPV, ICS, piping). As discussed in Section 5.2.4, TRACG is well qualified to predict the effects of non-condensable gases that may be ingested into the ICS. Build-up of non-condensable gases in the ICS heat exchangers may degrade the heat removal rate of the ICS, causing the system to re-pressurize again. This potential was investigated by performing an iteration between the TRACG calculations for a small steam pipe break accounting for the containment back pressure, and GOTHIC calculations for the containment using the modified break flow from TRACG. Note that the containment back pressure has no effect on the break flow rate until the break flow becomes unchoked. Therefore, the results of the cases with and without back pressure are identical while the break flow is choked. [[

]]

The RPV pressure, the containment pressure specified as back pressure in the break flow calculations, and the containment pressure calculated by GOTHIC are plotted on Figure 6-36. The difference between the RPV and containment pressures becomes progressively smaller with time, but the containment pressure always remains below the RPV pressure [[

]] As shown on Figure 6-37, there are no reversals in the break flow. As shown in the results without back pressure, the PCCS is capable of reducing the containment pressure well below the RPV pressure in the absence of break flow. Therefore, if the back pressure were to increase slightly above the RPV pressure, the break flow would stop, and containment pressure would decrease again. The total amount of nitrogen ingested into the RPV would be insignificant. The ICS heat exchangers are capable of removing decay heat in the presence of much higher levels of non-condensable gases as discussed in Section 5.2.4.

The effect of using the containment back pressure in calculating the break flow on the containment pressure is shown on Figure 6-38. [[

]]

The calculated peak containment pressure is not affected by the assumption made for containment pressure used to calculate the break flow because the break flow remains choked well past the time of the peak containment pressure for either assumption. Any impact on containment pressure occurs only in the long-term and is in the conservative direction when the containment back

pressure is not considered in the break flow calculation. The sensitivity case presented here shows that ignoring the back pressure increases the conservatism in the analysis.

Containment responses were calculated for small liquid pipe breaks until the RPV and containment pressures equalize. [[
]] The results are shown on Figures 6-39 through 6-42. The containment response trends for the liquid pipe breaks are similar to the small steam pipe breaks. After the RPV level falls below the break location, the break flow is fed from the steam space in the RPV and displays the characteristics of a small steam pipe break. Therefore, the trends observed in Figures 6-39 through 6-42 are consistent with the trends in steam pipe break shown in Figures 6-31 through 6-34.

[[

]]

Figure 6-31: Containment Pressure Following a Small Steam Pipe Break [MaxP]

[[

]]

Figure 6-32: PCCS Exit and Reactor Cavity Pool Temperatures Following a Small Steam Pipe Break, Conservative Case [MaxT]

[[

]]

Figure 6-33: Steam Volume Fraction in the Containment Following a Small Steam Pipe Break, Conservative Case [MaxP]

[[

]]

Figure 6-34: Containment Temperatures Following a Small Steam Pipe Break [MaxT]

[[

]]

Figure 6-35: Power, Small Steam Break, 2 ICS Trains, Conservative Case, with Containment Back Pressure Obtained from the MaxP Case

[[

]]

Figure 6-36: Pressure, Small Steam Break, 2 ICS Trains, Conservative Case, with Containment Back Pressure [MaxP]

[[

]]

Figure 6-37: Break Flow, Small Steam Break, 2 ICS Trains, Conservative Case, with Containment Back Pressure

[[

]]

Figure 6-38: Containment Pressure Using Break Flow With and Without Back Pressure [MaxP]

[[

]]

Figure 6-39: Containment Pressure Following a Small Liquid Pipe Break [MaxP]

[[

]]

Figure 6-40: PCCS Exit and Reactor Cavity Pool Temperatures Following a Small Liquid Pipe Break, Conservative Case [MaxT]

[[

]]

Figure 6-41: Containment Temperatures Following a Small Liquid Pipe Break [MaxT]

[[

]]

Figure 6-42: Steam Volume Fraction in the Containment Following a Small Liquid Pipe Break, Conservative Case [MaxP]

Table 6-6: Summary of the Peak Containment Pressure and Temperatures Calculated by Using the Conservative Assumptions

[[		
		]]

6.10.3 Containment Mixing for Combustible Gases

Hydrogen and oxygen generation results from radiolysis in BWRX-300 design basis accidents are discussed in Section 5.2.4. The radiolytic gases mixed in steam and liquid are discharged from the break along with the break flow. The volumetric fractions are calculated in Section 5.2.4. Hydrogen and oxygen distributions in the containment are not a concern for large breaks [[

]]. Radiolytic gases may build up in the containment following unisolated small breaks over time even though the rate of release is very small.

Total mass fraction of hydrogen and oxygen produced by radiolysis, remaining in the RPV and released to the containment are shown on Figure 6-43. [[

]]

Radiolytic gases mixed in steam enter into the dome region and condense on the containment dome, liberating the radiolytic gases mixed within. Although the volume fraction of radiolytic gases in the steam is small, it may accumulate in the dome region over time.

The radiolytic gas volume fractions are specified in the break flow boundary condition as calculated in Section 5.2.4, and radiolytic gas volume fraction distribution in the containment and the dome region was calculated for small steam pipe break case presented in Section 6.10.2.

Hydrogen volume fraction in the containment is shown on Figure 6-44. Hydrogen volume fraction in the dome region is higher than the main containment volume as expected, but the difference is not large. [[

]] The hydrogen volume fractions shown on Figure 6-44 are far below the deflagration limits even if there is sufficient oxygen.

Hydrogen and oxygen are generated at stoichiometric ratio from radiolysis; the molecular (or volume) ratio of radiolytic oxygen to hydrogen is 0.5. Because the radiolytic gases are well mixed in steam or liquid water where they are generated, the molecular or volume ratio of radiolytic oxygen to hydrogen remains 0.5 as they migrate in the RPV, from RPV to containment and within the containment. Therefore, radiolytic oxygen volume fraction in the containment is exactly half of the hydrogen volume fraction shown on Figure 6-44. There is also some small amount of oxygen initially present in the containment. [[

]]

The results presented here show that gases generated by radiolysis do not create a concern for deflagration in the containment and that the containment subcompartments remain sufficiently mixed.

[[

]]

Figure 6-43: Radiolytic Gas Generation and Release from RPV, Small Steam Pipe Break, 2 ICS Trains, Conservative Case

[[

]]

Figure 6-44: Hydrogen Volume Fraction in the Containment Main Volume and in the Dome Region, Small Steam Pipe Break, 2 ICS Trains, Conservative Case

6.11 Summary of the Assumptions and Inputs Used in the BWRX-300 GOTHIC Method Conservative Cases

The conservative containment response cases use the following inputs:

- Initial containment pressure is at the Technical Specification limit.
- Initial bulk containment temperature and the structures are at a reasonably low value that would occur during normal operation.
- Initial humidity in the containment is 20%.
- Reactor cavity pool temperature is at the Technical Specification limit.
- Bounding values are used for form loss coefficients in containment and in the PCCS units.
- Free space volume in the containment is conservatively calculated.
- The containment nodalization uses node sizes as presented in the base cases in this report.
- The initial airspace temperature above the reactor cavity pool is assumed to be the same as the pool water temperature.
- The initial relative humidity of the airspace is assumed to be 100%.

The conservative containment response cases use the following modeling parameters:

- [[ ]]
- Condensation and convection heat transfer correlations are biased as described in Section 6.8.2.
- [[

]]
- No credit is taken for heat transfer from the outer surface of the metal containment shell to the concrete or surroundings, except for heat transfer from the submerged section of the containment dome to the reactor cavity pool above the dome.
- The reactor cavity pool is modeled as a lumped parameter volume. The air space is connected to a constant pressure boundary condition such that the airspace pressure is nearly constant at atmospheric pressure.
- There is no heat loss from the pool to the walls. Surface evaporation from the pool is accounted for.
- Heat transfer coefficients on the containment shell, PCCS and containment dome are biased as described in Section 6.8.2.

7.0 REFERENCES

7.1 NEDC-33910P, BWRX-300 Reactor Pressure Vessel Isolation and Overpressure Protection

7.2 NEDC-33911P, BWRX-300 Containment Performance

7.3 Regulatory Guide 1.203, Revision 0, "Transient and Accident Analysis Methods," December 2005

7.4 Regulatory Guide 1.157, Revision 0, "Best-Estimate Calculations of Emergency Core Cooling System Performance," May 1989

7.5 NEDE-32176P, Revision 4, "TRACG Model Description," January 2008

7.6 NEDE-32177P, Revision 3, "TRACG Qualification," August 2007

7.7 NEDC-32725P, Revision 1, Volumes 1 and 2, "TRACG Qualification for SBWR," September 1997

7.8 NEDC-33080P, Revision 1, "TRACG Qualification for ESBWR," May 2005

7.9 NEDC-33005P-A, Revision 2, "TRACG Application for Emergency Core Cooling Systems / Loss-of-Coolant-Accident Analyses for BWR/2-6," May 2018

7.10 NEDC-33083P-A, Revision 1, "TRACG Application for ESBWR," September 2010

7.11 26A6642AT, Revision 10, "ESBWR Design Control Document, Tier 2, Chapter 6 Engineered Safety Features," GE Hitachi Nuclear Energy, April 2014

7.12 NUREG/CR-5249, Revision 4, "Quantifying Reactor Safety Margins: Application of Code Scaling, Applicability, and Uncertainty Evaluation Methodology to a Large-Break, Loss-of-Coolant Accident," October 1989

7.13 NEA/CSNI/R3(2014), "Containment Code Validation Matrix," May 2014

7.14 SMSAB-02-02, "An Assessment of CONTAIN 2.0: A Focus on Containment Thermal Hydraulics (Including Hydrogen Distributions)," July 2002

7.15 NEDC-33004P-A, Revision 4, "Constant Pressure Power Uprate," July 2003

7.16 GOTHIC Thermal Analysis Package Technical Manual, Version 8.3(QA), November 2018

7.17 GOTHIC Thermal Analysis Package Qualification Report, Version 8.3(QA), November 2018

7.18 Peterson, P.F., V.E. Schrock and T. Kageyama, "Diffusion Layer Theory for Turbulent Vapor Condensation with Noncondensable Gases," Transaction of ASME, Vol. 115, pp. 998-1003, November 1993

7.19 Bucci, Matteo, "Experimental and Computational Analysis of Condensation Phenomena for the Thermal-Hydraulic Analysis of LWRs Containments," PhD Thesis, University of Pisa, Italy, 2009

7.20 Bucci, Matteo, Walter Ambrosini and Nicola Forgione, "Experimental and Computational Analysis of Steam Condensation in The Presence of Air and Helium," Nuclear Technology, Volume 181, pp. 115-132, January 2013

7.21 Cotton, M.A. and Jackson, J.D. "Vertical tube air flows in the turbulent mixed convection regime calculated using a low-Reynolds-number k~ ϵ model," International Journal of Heat and Mass Transfer, Volume 33, Issue 2, pp. 275-286, February 1990

7.22 Idaho Nuclear Corporation Report IN-1403, "Simulated Design Basis Accident Tests of the Carolinas Virginia Tube Reactor Containment Final Report," December 1970. NRC Adams Accession Number: ML12009A104

7.23 GEH Letter M210050, "Responses to Requests for Additional Information (eRAIs) 9817, 9826, 9829, and 9831 for Licensing Topical Report NEDC 33922P, Revision 0 BWRX-300 Containment Evaluation Method," May 19, 2021.

7.24 GEH Letter M210099, "Response to Requests for Additional Information (eRAIs) 9854, 9856, and 9862 and Supplemental Response to eRAI 9817 for Licensing Topical Report NEDC 33922P, Revision 0, BWRX-300 Containment Evaluation Method," September 17, 2021.

7.25 GEH Letter M210116, "Response to Requests for Additional Information (eRAIs) 9857 and 9862 for Licensing Topical Report NEDC 33922P, Revision 0, BWRX-300 Containment Evaluation Method," October 8, 2021.

7.26 GEH Letter M210132, "Response to Request for Additional Information (eRAI) 9862 for Licensing Topical Report NEDC 33922P, Revision 0, BWRX-300 Containment Evaluation Method," October 29, 2021.

7.27 GEH Letter M210152, "Revised Response to Request for Additional Information (eRAI) 9862 Question 06.02.01-01 for Licensing Topical Report NEDC-33922P, Revision 0, BWRX-300 Containment Evaluation Method and Submittal of Revision 2 of NEDC-33922P, BWRX-300 Containment Evaluation Method Licensing Topical Report," December 17, 2021.

7.28 NRC Letter, "Final Safety Evaluation for GE-Hitachi Licensing Topical Report NEDC 33922P, Revision 2, "BWRX-300 Containment Evaluation Method" (Docket No. 99900003)," April 27, 2022.

Appendix A
GEH Responses to NRC RAIs on NEDC-33922P, Revisions 0 and 1

SRP-Review Section: 06.02.01 - Containment Functional Design Application Section:

06.02.01-01 (eRAI 9817)
Date of eRAI Issue: 04/08/2021

Requirement

General Design Criterion 50 – Containment design basis, requires the reactor containment structure, including access openings, penetrations, and the containment heat removal system be designed so that the containment structure and its internal compartments can accommodate, without exceeding the design leakage rate and with sufficient margin, the calculated pressure and temperature conditions resulting from any loss-of-coolant accident (LOCA).

Issue

In order to determine the conservative mass and energy discharge to the containment, a computer code and the associated evaluation model needs to have the capability to model relevant physical phenomenon during a LOCA with a conservative treatment of uncertainties. Standard Review Plan (NUREG-0800) Section 6.2.1.3, "Mass and Energy Release Analysis for Postulated Loss-of-Coolant Accidents (LOCAs)," notes that "calculations of the mass and energy release rates for a LOCA should be performed in a manner that conservatively establishes the containment internal design pressure (i.e., maximizes the post-accident containment pressure and the containment subcompartment response)."

GEH states in Section 5.2.4 of licensing topical report "BWRX-300 Containment Evaluation Method (NEDC-33922P, Revision 0)," that the only non-condensable gases that may migrate into the isolation condenser system (ICS) tube bundles are the radiolysis products following a design basis LOCA. This is based on the design not experiencing any significant fuel cladding oxidation during a LOCA.

However, based on the BWRX-300 ICS design, [[

]]

Request

Therefore, the staff is requesting additional information regarding [[
]] the associated modeling uncertainties, and the subsequent consequences for both large break and small break LOCA limiting cases.

GEH Response to NRC Question 06.02.01-01

It should be noted that the radiolytic gas concentration in the reactor pressure vessel (RPV) is very small even over the long term; therefore, the radiolytic gas concentration at the inlet of the isolation condensers (ICs) is far below the test conditions, such as those used in the PANTHERS tests (see Section 4.2 of Reference R9817-1.).

TRACG has been shown to be in good agreement with the test data as discussed in Section 5.2.4 of NEDC-33922P Revision 0. TRACG accounts for how non-condensable gases (NCGs) degrade the condensation rate as described in Section 6.6.11.2 of Reference R9817-2. The same modeling as approved for the ESBWR PCCS is being used. [[

]] The containment response to large pipe breaks is not affected by any reduction in the IC performance because the RPV isolation valves close long before any buildup of radiolytic gas accumulation could occur. The heat removal rate of the ICs is more than sufficient to maintain the RPV at low pressure after it is isolated, even with severely degraded IC performance. The fuel heat up for small liquid pipe break cases may be affected by degraded IC performance if there is no water injection for three days. In this situation, a reduced IC heat removal rate might result in a higher RPV pressure and faster discharge of RPV inventory. Therefore, the small liquid break case was selected for the sensitivity study.

The comparisons to the small liquid break cases in NEDC-33922P Revision 0 are shown in Figures 9817-1 through 9817-3, below. The red curves are for the expected concentrations of radiolytic oxygen and hydrogen for the conservative case presented in NEDC-33922P Revision 0 whereas the blue curves are for the same conservative case with the concentrations of radiolytic oxygen and hydrogen increased [[ ]]. As shown in Figure 9817-1, there is a small effect on the downcomer level, but the peak cladding temperature still meets the acceptance criteria as shown in Figure 9817-2. The small difference in the liquid level results from [[

]]

As discussed above, the radiolytic gas build up in the IC does not cause a significant degradation in the IC performance because any potential buildup occurs [[

]] Furthermore, the sensitivity calculations demonstrate that the effects of the potential degradation in the IC performance resulting from the presence of radiolytic gases are small even for much higher than reasonably expected radiolytic gas concentrations. The design goal is to limit the radiolytic gas volume fraction in the IC [[ ]]

[[

]]

Figure 9817-1. RPV Level, Small, Unisolated Liquid Break Sensitivity Study, Conservative Case.

[[

]]

Figure 9817-2. Peak Cladding Temperature, Small, Unisolated Liquid Break Sensitivity Study, Conservative Case.

[[

]]

Figure 9817-3. RPV Pressure and Isolation Condenser Efficiency, Small, Unisolated Liquid Break Sensitivity Study, Conservative Case.

References

R9817-1. NEDC-32725P, "TRACG Qualification for SBWR," Revision 1, August 2002.

R9817-2. NEDE-32176P, "TRACG Model Description," Revision 4, January 2008.

Proposed Changes to NEDC-33922P Revision 0

None

06.02.01-02 (eRAI 9831)
Date of eRAI Issue: 04/08/2021

BWRX-300 Containment External Surface Thermal Boundary Condition & Shell Modeling

Requirement

Guided by the Standard Review Plan (SRP) Section 6.2.1 and the General Design Criteria (GDCs) 16, 38, and 50 of Appendix A to 10 CFR Part 50 relevant to the containment design basis, the staff is reviewing the applicant's analytical model and assumptions used in the GEH LTR NEDC-33922P, Revision 0, BWRX-300 Containment Evaluation Method. The staff needs to assess the conservatism of the presented model, constitutive/closure relations, model input parameters, and initial/boundary conditions used for the design basis event (DBE) containment response analyses, in order to determine whether the methodology would be acceptably conservative over the applicable range of DBE conditions.

Issue

LTR NEDC-33922P, Section 2.0 states that [[

]]. However, the LTR does not describe the thermal boundary condition assumed for the containment outer surface, except for the PCCS pipes and the containment dome. The LTR is also not clear about whether [[

]] is intended to be a standard assumption within the proposed containment evaluation (CE) methodology, or it is just a convenient assumption made for the LTR demonstration analyses. As containment external surface thermal boundary condition and [[

]] are key assumptions in meeting several acceptance criteria identified in Section 1.3 of the LTR, the NRC staff would consider them as part of their safety finding about the conservatism.

Request

Therefore, the staff requests a detailed description of the containment outer surface thermal boundary condition as well as [[ ]] assumed as a part of the CE methodology. The applicant is also requested to update the LTR, accordingly.

GEH Response to NRC Question 06.02.01-02

The BWRX-300 containment boundary includes a metal shell. This shell may be free-standing (metal containment type), in loose contact with concrete (reinforced concrete containment vessel type), or in tight contact with concrete (steel concrete composite structure type). Regardless of the eventual containment type, no credit is taken for heat loss from the outer surface of the metal shell to air or concrete (i.e., the containment shell is adiabatic on the outer surface). This is not only an

assumption used in demonstration calculations but is a boundary condition to be used in the application method. This will be clarified in the licensing topical report (LTR).

There are also structures in the containment. The geometry and heat capacity of these structures are currently in development. The demonstration calculations did not credit the energy absorbed in these structures. Neither the composition of the containment shell nor the modeling of internal structures is a limitation on the application method.

Proposed Changes to NEDC-33922P Revision 0

A bullet item will be added to the first set of bullets in Section 6.11 of NEDC-33922P as follows.

- No credit is taken for heat transfer from the outer surface of the metal containment shell to concrete or surroundings, except for heat transfer from the submerged section of the containment dome to the reactor cavity pool above the dome.

SRP-Review Section: 06.02.01.03 - Mass and Energy Release Analysis for Postulated Loss-of-Coolant Accidents (LOCAs) Application Section:

06.02.01.03-01 (eRAI 9826)
Date of eRAI Issue: 04/08/2021

Requirement

General Design Criterion 50 – Containment design basis, requires the reactor containment structure, including access openings, penetrations, and the containment heat removal system be designed so that the containment structure and its internal compartments can accommodate, without exceeding the design leakage rate and with sufficient margin, the calculated pressure and temperature conditions resulting from any loss-of-coolant accident.

Standard Review Plan (NUREG-0800) Section 6.2.1.3, "Mass and Energy Release Analysis for Postulated Loss-of-Coolant Accidents (LOCAs)," identifies 10 CFR Part 50 Appendix K, "ECCS Evaluation Models," as providing the appropriate analysis assumptions and requirements related to sources of energy during the LOCA. SRP 6.2.1.3 further states that calculations of the energy available for release "should be done in general accordance with the requirements of 10 CFR Part 50, Appendix K, paragraph I.A" and that additional conservatism should be included to maximize the energy release to the containment.

Issue

In this licensing topical report, "BWRX-300 Containment Evaluation Method (NEDC-33922P, Revision 0)," GEH developed a [[

]] considering the specific BWRX-300 dry containment design features.

In contrast to the ESBWR, the BWRX-300 [[

]] Therefore, the staff is requesting additional information from GEH to justify the overall conservatism of the proposed BWRX-300 mass and energy evaluation model.

Request

In particular, additional justification is needed for the following aspects:

1. Isolation Condenser Performance due to accumulating non-condensable radiolytic gas;
2. Core decay heat model using ANS 1979 standard with 2 sigma uncertainty instead of ANS 1971 standard with 1.2 multiplier following the requirement of Appendix K to 10 CFR Part 50;
3. [[

]]

GEH Response to NRC Question 06.02.01.03-01

The responses to each item are presented below:

1. Accumulation of the non-condensable gases generated from radiolysis is discussed in the response to Question 06.02.01-01 (eRAI 9817). The volume fraction of radiolytic gases in the isolation condensers will be determined after the system requirements for the radiolytic gas removal mechanisms are developed. The method includes a method for calculating radiolytic gas generation and use of a multiplier for the degradation of the isolation condenser heat removal rate as a function of the radiolytic gas volume fraction in the isolation condenser. This method is described in Section 5.2.4 of NEDC-33922P Revision 0. When the method is applied to the eventual isolation condenser design with the radiolytic gas removal mechanisms, the multiplier for the heat removal rate will be set corresponding to the maximum non-condensable gas volume fraction in the isolation condensers.

2. The modeling features in 10 CFR 50 Appendix K provide an acceptable method for demonstrating that the 10 CFR 50.46 acceptance criteria are met for the emergency core cooling systems (ECCS) to maintain fuel integrity. The modeling features in 10 CFR 50.46 do not apply to the BWRX-300 containment analyses because there is no effect of containment performance on the ECCS performance or fuel integrity in the BWRX-300. Section D.2 of Appendix K is not applicable because the containment backpressure is not credited in the BWRX-300 reactor pressure vessel (RPV) mass and energy release calculations and there are no ECCS taking suction from the containment.

   Section 5.3.3 of the NRC final safety evaluation report in Reference R9826-1 acknowledges that the mass and energy release rates used in the BWRX-300 containment analyses will be calculated accounting for all applicable sources of energy required for consideration in 10 CFR 50 Appendix K using the assumptions and correlations similar to those used in Reference R9826-2. The energy sources in 10 CFR 50 Appendix K are listed below along with their applicability to BWRX-300.

   a. Initial stored energy in the fuel: Explicitly accounted for in the TRACG model for each node in the core.

b. Fission heat: A bounding fission power is used as described in Section 5.3.1 of NEDC-33922P Revision 0. Fission power resulting from delayed neutrons is included as part of the decay heat.

c. Decay of actinides: Bounding values are used in the American Nuclear Society (ANS) 5.1-1979 decay heat implementation.

d. Fission product decay: This correlation is obtained from ANS 5.1-1979 + 2 sigma uncertainty, which is the same as in Section 3.2.4 of Reference R9826-2 as stated above.

e. Metal-water reaction rate: Metal-water reaction is precluded in BWRX-300 design basis accidents by requiring that the fuel cladding temperature remain below normal operating temperature.

f. Reactor internals heat transfer: This is explicitly calculated as part of the TRACG method.

g. Pressurized water reactor primary-to-secondary heat transfer: Not applicable to BWRX-300.

Section 5.2.5 of NEDC-33922P Revision 0 uses the decay heat and the decay heat uncertainty used in the previously approved Reference R9826-2 (Reference 7.10 of NEDC-33922P Revision 0). The bounding cases in Reference R9826-2 also use nominal + 2 sigma uncertainty values by compounding the conservatisms rather than combining them using a statistical method, which is the same as in NEDC-33922P Revision 0. The applicability of Reference R9826-2 to BWRX-300 is discussed in Sections 5.1 and 5.2 of NEDC-33922P Revision 0.

3. The base cases use nominal feedwater temperature, but the conservative cases use either the nominal or reduced feedwater temperature as shown in Table 5-2 of NEDC-33922P Revision 0. The uncertainty in the feedwater temperature is very small (see Section 6.2.2 of Reference R9826-3). However, plants may operate with a reduced feedwater temperature as an equipment out-of-service condition. The flow rate from a liquid pipe break increases with reduced feedwater temperature. At BWRX-300 operating conditions, this increase in flow rate has a larger effect on the total energy release to the containment than the reduction in the enthalpy. Therefore, both the mass release and the energy release from a feedwater pipe break is higher if the feedwater temperature is decreased. As shown in Table 5-2 in the NEDC-33922P Revision 0, reduced feedwater temperature is used for the liquid pipe break conservative cases.

   Reduced feedwater temperatures do not have an adverse effect on the steam pipe break mass and energy release. The liquid at the top of the downcomer above the feedwater spargers flashes when the pressure decreases because this fluid is saturated regardless of the feedwater temperature. With reduced feedwater temperature, flashing and level swell become less pronounced. [[

   ]] As a result, the normal feedwater temperature case is the more limiting case although the difference from the reduced feedwater temperature case is insignificant for steam pipe breaks.

4. As shown in Section 8 of Reference R9826-3, the effect of the steam dome pressure is small on the overall RPV response to a pipe break. The BWRX-300 technical specifications do not yet exist, and therefore the allowable values have not yet been established. A dome pressure of 20 psi higher than the normal pressure is a bounding value for the pressure controller uncertainties and is a typical value for the difference between the normal operating pressure and the technical specification allowable value for conventional plants. If a limit is established in the BWRX-300 technical specifications for the allowable dome pressure similar to the conventional plants, the application methodology will use the dome pressure in the limiting conditions for operation in Modes 1 and 2 in the BWRX-300 technical specifications. Otherwise, the upper limit of the pressure controller uncertainty band will be used for the initial pressure.
5. As shown in Section 8.1 of Reference R9826-3 and also as stated in its safety evaluation, the initial water level does not have a significant effect on the LOCA analyses. Large break cases, which are rapidly isolated, use normal water level. However, the initial RPV water inventory may be important in the small unisolated break cases in BWRX-300 because there is a coping period of three days without injection. In order to bound the potential variations in the initial RPV inventory, the low end of the normal operating range is used for small breaks as shown in Table 5-2 of NEDC-33922P Revision 0.
6. In the conservative cases, a two-sigma uncertainty bias is applied to the critical flow rate. The bias applied to the critical flow rate was shown to adequately bound the scatter in the data in Section 3.4.1 of Reference R9826-2. The critical flow model and the bias applied to it are the same as those in the previously approved Reference R9826-2 for ESBWR LOCA and containment analyses.
7. It was not necessary to construct a new phenomena identification and ranking table (PIRT) and identify the biases and uncertainties for BWRX-300 RPV phenomena, because the ESBWR PIRT and uncertainties are directly applicable to BWRX-300 as discussed in Sections 5.1 and 5.2 of NEDC-33922P Revision 0. The correlations used for the phenomena in the BWRX-300 RPV are the same as those in the ESBWR that have been previously reviewed and approved in Reference R9826-2. In the conservative case, the biases for these parameters are all applied in the conservative direction simultaneously rather than combining them using a statistical method.

References

R9826-1. NEDC-33911P-A, “BWRX-300 Containment Performance,” Revision 2, April 2021.

R9826-2. NEDC-33083P-A, “TRACG Application for ESBWR,” Revision 1, September 2010.

R9826-3. NEDE-33005P-A, “TRACG Application for Emergency Core Cooling Systems / Loss-of-Coolant-Accident Analyses for BWR/2-6,” Revision 2, May 2018.

Proposed Changes to NEDC-33922P Revision 0

None

SRP-Review Section: 06.02.04 - Containment Isolation System Application Section: 1.3

06.02.04-01 (eRAI 9829)
Date of eRAI Issue: 04/08/2021

Requirement

General Design Criterion 50 – Containment design basis, requires the reactor containment structure, including access openings, penetrations, and the containment heat removal system be designed so that the containment structure and its internal compartments can accommodate, without exceeding the design leakage rate and with sufficient margin, the calculated pressure and temperature conditions resulting from any loss-of-coolant accident.

Issue

LTR NEDC-33922P, Section 1.3, "Acceptance Criteria," states in one of the criteria that "containment remains isolated for 72 hours during a design basis event or accident." The staff found that this statement might not be valid in some accidents such as isolation condenser system LOCA outside containment. It is understood that the subjects of containment isolation and pipe failures outside containment are not in the scope of this LTR.

Request

The applicant is requested to clarify the statement by specifying the applicability of the statement within the LTR and applicable conditions.

GEH Response to NRC Question 06.02.04-01

The purpose of the last acceptance criterion listed in Section 1.3, which is the subject of this eRAI, is to specify that the other acceptance criteria should be met without venting the containment for at least 72 hours. This is not a requirement for the containment operation but a requirement for the acceptable demonstration of containment performance.

Proposed Changes to NEDC-33922P Revision 0

To clarify the purpose of this statement, the last bulleted item in Section 1.3 will be made a paragraph and modified as follows:

"Containment venting or leakage shall not be credited for at least 72 hours in demonstrating that the above acceptance criteria are met during a design basis event or accident."

SRP-Review Section: 06.02.01 - Containment Functional Design Application Section:

06.02.01-02 (eRAI 9862) [Audit Issue 2]
Date of eRAI Issue: 08/05/2021

Requirement

General Design Criterion 50 – *Containment design basis*. Requires the reactor containment structure, including access openings, penetrations, and the containment heat removal system be designed so that the containment structure and its internal compartments can accommodate, without exceeding the design leakage rate and with sufficient margin, the calculated pressure and temperature conditions resulting from any loss-of-coolant accident (LOCA).

General Design Criterion 38 -- *Containment heat removal*. A system to remove heat from the reactor containment shall be provided. The system safety function shall be to reduce rapidly, consistent with the functioning of other associated systems, the containment pressure and temperature following any loss-of-coolant accident and maintain them at acceptably low levels.

General Design Criterion 16 -- *Containment design*. Reactor containment and associated systems shall be provided to establish an essentially leak-tight barrier against the uncontrolled release of radioactivity to the environment and to assure that the containment design conditions important to safety are not exceeded for as long as postulated accident conditions require.

Issue

GEH LTR NEDC-33922P, Revision 0, BWRX-300 Containment Evaluation (CE) Method, presents TRACG and GOTHIC results for the conservative case of the small steam pipe break design basis event (DBE), as the limiting small break LOCA (SBLOCA) for BWRX-300. According to the LTR, this break in a pipe of [[
]] attached to the RPV dome bounds all small steam pipe breaks that remain unisolated. Figure 5-18 through Figure 5-22 show various in-vessel TRACG results for the post-accident 72 hours, including power, RPV pressure, RPV level, PCT, break flow rate and enthalpy. The LTR also includes the necessary GOTHIC results for the same DBE in Figure 6-31 through 6-40 to demonstrate the resulting containment thermal hydraulic response, steam stratification, radiolytic gas accumulation inside the containment/dome, and PCCS/reactor cavity pool environment characteristics.

However, GEH LTR NEDC-33922P presents only TRACG results for the conservative case of the small liquid pipe break DBE. Figure 5-23 through Figure 5-27 show similar in-vessel TRACG calculation results for the small liquid pipe break DBE, as the aforementioned Figure 5-18 through Figure 5-22 for the small steam pipe break DBE. However, no related GOTHIC results are presented for the small liquid pipe break DBE in the LTR similar to Figure 6-31 through 6-40 for the small steam pipe break DBE. Therefore, the results presented in the LTR for the small liquid pipe break DBE are an incomplete set of the similar results presented in the LTR for the small

steam pipe break DBE. In the absence of this information, the staff is unable to make a reasonable assurance finding for the bounding nature of the conservative case for the small steam pipe break.

Request

The applicant is requested to provide the GOTHIC results for the BWRX-300 containment for the conservative case of the small liquid pipe break similar to those provided for the small steam pipe break, and justify how the limiting small steam pipe break with the conservative case assumptions also bounds the most limiting small liquid pipe break.

GEH Response to NRC Question 06.02.01-02

The base case results in the licensing topical report (LTR) show the steam pipe breaks are bounding for containment response. However, the conservative case multipliers affect the small liquid pipe breaks [[ ]], and as a result, conservative case results for the liquid and steam pipe break cases are similar to each other. Therefore, the small liquid break conservative cases will also be analyzed explicitly in the evaluation method. The results for these conservative case containment responses to the small liquid pipe break are presented in Figures 9862-1 through 9862-3. The statement that small steam breaks are the more limiting of the steam and liquid small pipe breaks will be removed from Section 6.10.2 of the LTR and the figures shown below will be added. All discussions in Section 6.10.2 are equally applicable to the small liquid breaks.

[[

]]

Figure 9862-1. Containment Pressure Following a Small Liquid Pipe Break

[[

]]

Figure 9862-2. PCCS Exit and Reactor Cavity Pool Temperatures Following a Small Liquid Pipe Break, Conservative Case

[[

]]

Figure 9862-3. Containment Temperatures Following a Small Liquid Pipe Break

---

Proposed Changes to NEDC-33922P Revision 0

The title of Section 6.10.2 will be changed to:

Containment Response to Small ~~Steam~~ Pipe Breaks, Conservative Cases

The first paragraph of Section 6.10.2 will be changed as follows:

The containment response predicted by using the conservative case assumptions for the small ~~steam~~ pipe breaks ~~which are the more limiting of the steam and liquid small pipe breaks,~~ is shown ~~on~~ in Figure 6-31 through Figure 6-34 for small steam pipe breaks and in Figure 6-39 through 6-41 for small liquid pipe breaks.

One paragraph will be added to Section 6.10.2 to discuss the containment response to small liquid pipe breaks. This paragraph will be provided to the NRC staff in a future submittal.

The following figures will be added to the end of Section 6.10.2:

[[

]]

Figure 6-39. Containment Pressure Following a Small Liquid Pipe Break

[[

]]

Figure 6-40. PCCS Exit and Reactor Cavity Pool Temperatures Following a Small Liquid Pipe Break, Conservative Case

[[

]]

Figure 6-41. Containment Temperatures Following a Small Liquid Pipe Break

06.02.01-03 (eRAI 9862) [Audit Issue 5]
Date of eRAI Issue: 08/05/2021

Requirement

General Design Criterion 50 – *Containment design basis*. Requires the reactor containment structure, including access openings, penetrations, and the containment heat removal system be designed so that the containment structure and its internal compartments can accommodate, without exceeding the design leakage rate and with sufficient margin, the calculated pressure and temperature conditions resulting from any loss-of-coolant accident (LOCA).

General Design Criterion 38 -- *Containment heat removal*. A system to remove heat from the reactor containment shall be provided. The system safety function shall be to reduce rapidly, consistent with the functioning of other associated systems, the containment pressure and temperature following any loss-of-coolant accident and maintain them at acceptably low levels.

General Design Criterion 16 -- *Containment design*. Reactor containment and associated systems shall be provided to establish an essentially leak-tight barrier against the uncontrolled release of radioactivity to the environment and to assure that the containment design conditions important to safety are not exceeded for as long as postulated accident conditions require.

Issue

Figure 6-11 in GEH LTR NEDC-33922P, Revision 0, BWRX-300 Containment Evaluation Method, presents the vertical and horizontal cross-sectional views of various 3-D GOTHIC grids used in the BWRX-300 containment nodalization studies. The LTR Figure 6-11 [[

]]. The LTR Figure 6-11 [[

]].

As recognized in LTR Section 6.6.1, [[

]]. The staff is concerned that the increased velocity and higher steam concentration near [[ ]] that increase the condensation heat transfer, would enhance the heat removal to the [[ ]]. While this has the desired effect of maximizing the shell temperature, it would have an adverse impact on the peak containment pressure. Therefore, the staff considers the current break location to be a non-conservative assumption embedded in the BWRX-300 GOTHIC model for the purpose of predicting the peak containment pressure.

The staff also needs to evaluate that, as based on the COPAIN test data presented in the LTR, the convection and condensation heat transfer coefficients [[

]]. So, GOTHIC's qualifications need to be justified for using the flow-direction/convection-mode dependent conservatisms used in the BWRX-300 CE methodology.

Request

1. The applicant is requested to provide the results for a break location sensitivity study for the BWRX-300 containment main steam pipe break (LBLOCA) using the conservative GOTHIC containment model to justify that the chosen break location is bounding for all break locations, or identify the most limiting break locations with respect to peak containment pressure and maximum wall temperature. Please perform the sensitivity study for the default [[ ]] for 24 hours, along the radial, axial, and azimuthal directions, or justify why some or all of the sensitivity cases are not needed.
2. The applicant is also requested to perform a 180 degree break flow orientation sensitivity study for the limiting location, i.e., the break flow coming out of the pipe upward, horizontal toward the containment wall, and downward directions, for the most limiting break location, as identified in Part 1, for the default [[ ]] conservative cases of the large steam break LBLOCA as well as the small steam break SBLOCA. The requested break orientation sensitivity study results for 24 hours for LBLOCA and 72 hours for SBLOCA, along with the information requested in Part 3, will help the staff make a reasonable assurance finding regarding the conservative biases used in modeling convection and condensation to cover the uncertainties in the COPAIN test data, as documented in the LTR. The staff needs to evaluate the [[ ]] biases used for the convection and condensation heat transfer correlations.
3. [[

]], the applicant is requested to provide justification for GOTHIC's qualification to predict the flow direction in the near wall region in a subdivided volume, or provide evidence that in the limiting cases GOTHIC's prediction of flow direction is in the conservative direction in the near wall region of the subdivided containment. Otherwise, present the limiting LBLOCA and SBLOCA results using [[

]].

Please update the LTR if the responses to the above questions result in a change to the methodology as described in the LTR.

GEH Response to NRC Question 06.02.01-03

The responses to each item are presented below:

1. Break location sensitivity for a large steam pipe break was evaluated by changing the break location as listed in Table 9862-1. The case, [[ ]] is the same case that is presented in Section 6.10.1 of the licensing topical report (LTR) for a large steam pipe break, conservative case.

   The break locations are shown in Figure 9862-4. The large break cases are run up to four (4) hours. Because the break is isolated in [[
   ]]. Because the differences in the results are due to the differences in break location and the break flow was terminated [[ ]], the trends will continue to converge over time. Therefore, it was determined that no further relevant information would be gained by extending the analyses to 24 hours.

Table 9862-1. Break Location Cases for a Large Steam Pipe Break

Case Identifier	Description
[[ ]]	Break is at [[ ]], placed near a wall and directed towards the wall. This is the same break location and orientation as in NEDC-33922P Revision 0.
[[ ]]	Break is at [[ ]], placed near the reactor pressure vessel (RPV), directed towards the wall.
[[ ]]	Break is at [[ ]], placed near the RPV, directed towards the wall.

   The containment pressure and temperature are shown in Figures 9862-5 and 9862-6. The containment pressure shown in Figure 9862-5 [[
   ]]. The reason for this can be seen in Figure 9862-6.
   [[

   ]]

   A sensitivity case in the azimuthal direction was not performed because the containment is circular and [[
   ]].

2. The sensitivity to the break orientation for the most limiting break location case above [[ ]] was evaluated for a large steam pipe break, as listed in Table 9862-2. The

results are plotted in Figure 9862-7. [[

]] Therefore, a small break orientation sensitivity study was not performed.

However, a break location sensitivity case was performed for a small steam pipe break as listed in Table 9862-3. The results are compared in Figure 9862-8. [[

]] The peak containment pressure resulting from small breaks is far below the peak containment pressure resulting from large breaks. The only concern with respect to the containment response for small breaks is the elevated pressure over the long-term (i.e., one day or longer). There is also a large margin in the long-term results as discussed below.

The containment back pressure is not credited in calculating the small break mass and energy release so as to bound potential scenarios where the containment may leak, normal containment cooling may be running during the event, or the break may be outside the containment. Therefore, it may not be justifiable to credit containment back pressure in all cases for the core cooling response. [[

]] However, the results presented in LTR Figure 6-38 show that [[

]]

Table 9862-2. Break Flow Orientation Sensitivity Cases for a Large Steam Pipe Break

Case Identifier	Description
[[ ]]	Break is at [[ ]], placed near the RPV, oriented towards the shell.
[[ ]]	Break is at [[ ]], placed near the RPV, oriented upwards.
[[ ]]	Break is at [[ ]], placed near the RPV, oriented downwards.

Table 9862-3. Break Flow Location Sensitivity Cases for a Small Steam Pipe Break

Case Identifier	Description
[[ ]]	Break is at [[ ]], placed near the shell, oriented towards the shell. This is the same break location and orientation as in LTR Section 6.10.2.
[[ ]]	Break is at [[ ]], placed near the RPV, oriented upwards.

3. The GOTHIC validation includes several comparisons with experimental test data for situations that involve multidimensional flows where buoyancy forces are significant, as described below. Examples 1 and 5 include direct comparison of the measured and calculated velocity. For the other tests, reasonable agreement with the test velocities can be inferred from the comparisons of the measured local temperature with the GOTHIC calculated temperatures. These tests are documented in Reference R9862-1. Taken together they show that GOTHIC has the fundamental capability to calculate the velocity field in a vessel due to local jets and buoyancy.

    1. GOTHIC provides good agreement for the steady velocity profile in a thermally driven cavity as presented in Section 5.5.1 of Reference R9862-1. The test from Reference R9862-2 is for two-dimensional flow in an air-filled cavity (2.5m high x 0.5 m wide). The top and bottom of the cavity were insulated, and the sides were maintained at 72.9°C and 27.1°C. Based on the peak velocity and the wall spacing, the Reynolds (Re) number for this test is ~10,000 and the Grashof (Gr) number is ~$8x10^8$. The velocity comparison is shown in Figure 5.14 in Reference R9862-1.

    2. Comparisons to a two-dimensional natural convection from a horizontal cylinder in a rectangular cavity is presented in Section 5.6 of Reference R9862-1. This case is two-dimensional natural convection from a heated horizontal cylinder in a rectangular cavity with cooled side walls, an insulated bottom and convective heat loss from the top. The GOTHIC predicted Nusselt number for the overall heat transfer from the cylinder agrees with the measured data to within 10% over a Rayleigh (Ra) range of 1300 to 3400. The discrepancy is within the uncertainty of the experiment.

    3. GOTHIC was used to model a mixed convection test in three different test facilities that made up International Standard Problem 47 in References R9862-3 and R9862-4 as presented in Section 15 of Reference R9862-1. The TOSQAN test (Volume (V)=7 m^3, Height (H)=5 m) and the MISTRA test (V=100 m^3, H=7.4 m) were axisymmetric with an upward vertical steam or steam and helium jet at the vessel center and cooled vessel wall. The THAI test (V=60 m^3, H=9.2 m) was three-dimensional with upward vertical and horizontal steam and helium injection and a cooled vessel wall. Local Re and Gr numbers varied widely throughout the vessel for these tests, covering forced, mixed and free

convection regimes. GOTHIC generally compares well with the local temperature and concentration measurements indicating that the velocity field is reasonably predicted.

4. GOTHIC was used to simulate the HEDL experiments for hydrogen mixing in a scaled ice condenser containment as presented in Section 9 of Reference R9862-1. The tests included vertical upward and horizontal hydrogen jets that evolved to buoyant plumes, with and without mixing fans. Generally good agreement was obtained with the measured local hydrogen concentration indicating that the velocity field was reasonably well predicted.
5. GOTHIC benchmarking to the velocity profiles for a two-dimensional turbulent jet (slot jet) is presented in Section 5.9 of Reference R9862-1. The GOTHIC comparison with the centerline velocity versus distance from the slot for a selected test is shown in Figure 5.33 of Reference R9862-1 and shows good agreement.

The test cases above demonstrate GOTHIC's capability to calculate the velocity field resulting from jets and buoyancy.

For the small steam break case, [[ ]], in Figure 9862-5 the velocities at each PCCS location along the entire height of the containment are shown in Figures 9862-9a and 9862-9b at approximately the time of the peak pressure [[ ]], and at one (1) day. [[

]]

[[

]] Relaminarization simply does not occur if the flow direction is counter to the direction of the buoyancy forces as discussed in Section 6.8.2 of the LTR. The containment evaluation method presented in the LTR also superimposes each source of conservatism, compounding the effects of the biases. Furthermore, the assumption that the break mass flow rate is not affected by the containment back pressure alone adds more than [[ ]]. When added together, any variations resulting from [[ ]] are much smaller than the overall conservatism in the method for containment response to small breaks.

[[

]]

Figure 9862-4. Break Location Sensitivity Study, Break Locations for Steam Pipe Breaks.

[[

]]

Figure 9862-5. Containment Pressure Sensitivity to Break Location for Large Steam Pipe Break. (See Figure 9862-4 for Legend).

[[

]]

Figure 9862-6. Containment Temperature Sensitivity to Break Location for Large Steam Pipe Break. (See Figure 9862-4 for Legend).

[[

]]

Figure 9862-7. Containment Pressure Sensitivity to Break Orientation for Large Steam Pipe Break. (See Figure 9862-4 for Legend).

[[

]]

Figure 9862-8. Containment Pressure Sensitivity to Break Location for a Small Steam Pipe Break. (See Figure 9862-4 for Legend).

[[

]]

Figure 9862-9a. Velocities at the PCCS Locations from Containment Bottom to Top at 7200 seconds. Maximum Velocity: [[ ]]**. Small Steam Pipe Break** [[ ]] **in Figure 9862-8.**

[[

]]

Figure 9862-9b. Velocities at the PCCS Locations from Containment Bottom to Top at 86400 seconds. Maximum Velocity: [[ ]]**. Small Steam Pipe Break Case,** [[ ]] **in Figure 9862-8.**

References

R9862-1. GOTHIC Thermal Hydraulic Analysis Package, Version 8.3(QA), Qualification Report, EPRI, Palo Alto, CA: 2018.

R9862-2. R Cheesewright, KJ King, and S Ziai. Experimental Data for the Validation of Computer Codes for the Prediction of Two-Dimensional Buoyant Cavity Flows, in Significant Questions in Buoyancy Affected Enclosure or Cavity Flows. Technical report, ASME Winter Annual Meeting, Anaheim, CA, December 1986. HTD Vol. 60.

R9862-3. P Cornet, J Malet, E Porcheron, J Vendel, E Studer, and M Caron-Charles. ISP-47 Specification of International standard problem on containment thermal hydraulics,

Step 1: TOSQAN-MISTRA. Technical report, Institut de Radioprotection et de Surete Nucleaire, Saclay, France, July 2002. Revision 1, DPEA/SERAC/LPMAC/02-44.

R9862-4. K Fischer et al. International Standard Problem ISP-47 on Containment Thermal-Hydraulics, Step 2: ThAI, Comparison Report of Blind Phases I-IV. Technical report, Becker Technologies GmbH, Eschborn, January 2005. BF-R 70031-2.

Proposed Changes to NEDC-33922P Revision 0

The pressures for the conservative case in Figure 6-26, and all cases in Figures 6-28 and 6-31 will be based on the break location near the RPV and at [[ ]]. This updated information will be provided to the NRC staff in a future submittal.

A statement will be added to Sections 6.10.1 and 6.10.2 to explain that break location near the RPV is used to maximize the containment pressure, and break location near the shell is used to maximize the shell temperature. This text will be provided to the NRC staff in a future submittal.

In Section 6.11, the following bullets will be added under the “conservative containment cases”:

- [[

  ]]
- [[

  ]]

06.02.01-04 (eRAI 9862) [Audit Issue 36]
Date of eRAI Issue: 08/05/2021

Requirement

General Design Criterion 38 -- *Containment heat removal*. A system to remove heat from the reactor containment shall be provided. The system safety function shall be to reduce rapidly, consistent with the functioning of other associated systems, the containment pressure and temperature following any loss-of-coolant accident and maintain them at acceptably low levels.

General Design Criterion 16 -- *Containment design*. Reactor containment and associated systems shall be provided to establish an essentially leak-tight barrier against the uncontrolled release of radioactivity to the environment and to assure that the containment design conditions important to safety are not exceeded for as long as postulated accident conditions require.

Issue

Section 2.0 of the GEH LTR NEDC-33922P, Revision 0, BWRX-300 Containment Evaluation (CE) Method, states that [[

]]. The GOTHIC models submitted with this application, the sensitivity studies, results, and descriptions documented in the LTR, the correlations the BWRX-300 CE methodology relies on, as well as the staff review and confirmatory analyses are all based on [[

]]. The study presented in the LTR for the effect of nodalization on a single PCCS unit's performance is also based on [[

]].

However, the LTR also mentions a [[ ]] design option, and LTR Section 6.1 states [[

]]) to establish the applicability of the BWRX-300 PCCS phenomenology independent of the PCCS design configuration. The staff is concerned that without a supplementary review of any new PCCS design configuration, the associated model for secondary side heat transfer to the reactor cavity pool, and supporting containment/PCCS results, the staff may not be able make a reasonable assurance finding about the applicability of the BWRX-300 CE methodology to the new PCCS design.

Request

The applicant is requested to provide justification to extend the BWRX-300 CE methodology that was reviewed for the [[

]] without a supplementary NRC review. Otherwise, please remove all LTR references to the [[

]]

GEH Response to NRC Question 06.02.01-04

The water jacket configuration had been a potential option earlier in the development of the BWRX-300 containment design. However, the water jacket design presented challenges to the [[ ]] and has been abandoned. The water jacket is no longer a design option.

Currently, two variations of the pipe configuration are being considered. The GOTHIC methodology is capable of analyzing either configuration. In the concentric pipe configuration shown in Figure 2-4 of NEDC-33922P, the cold pipe is enclosed inside the hot channel. This configuration requires that each unit has a different penetration. [[

]] Heat transfer occurs on the vertical PCCS pipes, the same geometry as in the concentric pipe configuration. [[ ]]

Proposed Changes to NEDC-33922P Revision 0

None.

06.02.01-05 (eRAI 9862) [Audit Issue 37]
Date of eRAI Issue: 08/05/2021

Requirement

General Design Criterion 38 -- *Containment heat removal*. A system to remove heat from the reactor containment shall be provided. The system safety function shall be to reduce rapidly, consistent with the functioning of other associated systems, the containment pressure and temperature following any loss-of-coolant accident and maintain them at acceptably low levels.

General Design Criterion 16 -- *Containment design*. Reactor containment and associated systems shall be provided to establish an essentially leak-tight barrier against the uncontrolled release of radioactivity to the environment and to assure that the containment design conditions important to safety are not exceeded for as long as postulated accident conditions require.

Issue

Table 6-2 of the GEH LTR NEDC-33922P, Revision 0, BWRX-300 Containment Evaluation (CE) Method, presents the Phenomena Identification and Ranking Table for BWRX-300 containment. The table recognizes [[

]]

These phenomena are pertinent to the first 24 hours of LBLOCA and first 72 hours of SBLOCA. However, the staff found a lack of information in the LTR about the safety-related assumptions and modeling details about [[ ]]. Therefore, the applicant is requested to address the following questions about [[ ]] modeling.

Request

1. Section 6.10.2 of the GEH LTR NEDC-33922P, Revision 0, BWRX-300 Containment Evaluation (CE) Method, states "the calculations conservatively assume no heat loss from the reactor cavity pool to the surroundings." In addition, the LTR on Page 59 refers to [[ ]]. However, LTR Figure 6-1 shows [[ ]] So, the LTR does not recognize [[ ]] The applicant is requested to provide a clarification regarding [[ ]] and document the reactor cavity pool's exposure to the ambient atmosphere as a part of the CE methodology described in the LTR.
2. Please provide and justify the assumptions made in the BWRX-300 CE methodology about modeling the above-mentioned [[ ]] PIRT phenomena as identified in the

LTR Table 6-2, and describe how they were addressed in the model. A review of the GOTHIC model submitted with the application shows [[

]] The LTR does not include these CE methodology details and justifications, lacks information on the ambient temperature and initial humidity conditions, and is unclear as to whether [[ ]] is a part of the model. The applicant is requested to document the modeling details as part of the BWRX- 300 CE methodology description.

3. Even though the LTR does not explicitly state as such, the staff infers that the BWRX-300 CE methodology review scope is limited to the first 72 hours after the initiation of the postulated design basis events (DBEs). [[

]]. Therefore, the staff requests the applicant to clarify the staff's understanding regarding the LTR review scope being limited to the first 72 hours of the postulated DBEs. Otherwise, provide additional information to justify that the BWRX-300 containment design would remain safe with sufficient cooling mechanisms beyond 72 hours.

GEH Response to NRC Question 06.02.01-05

1. Heat loss from the pool to the surroundings through the walls are not included. However, there is some heat loss by evaporation at the surface of the pool.

   Using the small steam pipe break results, the following data are obtained from the GOTHIC output, where Volume 4 in the model is comprised of the reactor cavity pool and the reactor building airspace volume above the refuel floor. This volume is initially filled with water in the pool and air at atmospheric pressure in the airspace.

[[		

]]

The pool mass, M_{pool}, is calculated from the GOTHIC results as,

$$M_{pool} = V\left(1-\alpha\right)\rho_{\ell}$$

where [[ ]] is the volume of the pool and the airspace in the refueling floor, α is the volume fraction of steam/air and ρ_ℓ is the density of liquid.

At the initial and final conditions, the mass of the pool is calculated as

[[

]]

The amount of energy lost to evaporation is approximately [[ ]] of the energy deposited in the pool. The majority of the energy lost to evaporation is not released to the environment but remains in the refueling floor atmosphere. Although the energy lost to evaporation is a small fraction, the statement in the licensing topical report (LTR) will be revised by stating that the energy loss from the pool due to surface evaporation is accounted for.

2. The passive containment cooling system (PCCS) intake location in the pool is near the bottom of the pool. The PCCS return pipe discharge elevation is at least [[ ]] the PCCS intake elevation. Hot water rising from the discharge of the PCCS return pipe may cause some stratification in the pool. If the stratification is significant, the water temperature at the intake location of the PCCS would be lower than the bulk pool temperature. It is not plausible that stratification would occur in such a manner that hot water would collect at the bottom of the pool. Ignoring this temperature difference and using a lumped parameter model for the pool is more conservative than resolving the temperature gradients in the pool.

   The initial humidity in the pool area was assumed to be [[ ]] in the demonstration calculations. This has little effect on the calculations. The LTR will include the following requirements for the application method:

   - The initial airspace temperature above the reactor cavity pool is assumed to be the same as the pool water temperature.
   - The initial relative humidity of the airspace is assumed to be 100%.
   - The reactor cavity pool is modeled as a lumped parameter volume. The air space is connected to a constant pressure boundary condition such that the airspace pressure is nearly constant at atmospheric pressure.

3. The applicability of the LTR is not based on a time limit, but rather on the phenomena that are modeled and the applicability of the biases. The heat removal capacity of the PCCS will

decrease as the pool heats up, but the model does not have a particular limitation on the heat transfer modeling up to the point where [[ ]]. Also, the capability of the model has not been demonstrated for degraded event analyses where the steam released from the reactor pressure vessel (RPV) may be significantly superheated or may contain significant amounts of hydrogen. Significant superheating or significant hydrogen generation does not occur within 72 hours during a design basis accident.

Although GOTHIC is fundamentally capable of modeling the phenomena if significant hydrogen generation and/or significant superheat occurs, the LTR does not attempt to quantify the additional uncertainties, if any, resulting in such progression of an accident, and GEH does not seek approval for this quantification of additional uncertainties in this LTR.

Proposed Changes to NEDC-33922P Revision 0

The last sentence in the 2nd paragraph of Section 6.10.2 will be revised as follows:

Note that the calculations conservatively assume no heat loss from the reactor cavity pool to the surroundings through the walls. However, heat loss due to surface evaporation is accounted for.

The following bullets will be added to Section 6.11:

- The initial airspace temperature above the reactor cavity pool is assumed to be the same as the pool water temperature.
- The initial relative humidity of the airspace is assumed to be 100%.
- The reactor cavity pool is modeled as a lumped parameter volume. The air space is connected to a constant pressure boundary condition such that the airspace pressure is nearly constant at atmospheric pressure.

06.02.01-09 (eRAI 9856) [Audit Issue 21]
Date of eRAI Issue: 08/05/2021

Requirement

General Design Criterion 50 – Containment design basis, requires the reactor containment structure, including access openings, penetrations, and the containment heat removal system be designed so that the containment structure and its internal compartments can accommodate, without exceeding the design leakage rate and with sufficient margin, the calculated pressure and temperature conditions resulting from any loss-of-coolant accident (LOCA).

Issue

In order to determine the conservative mass and energy discharge to the containment, a computer code and the associated evaluation model needs to have the capability to model relevant physical phenomenon during a LOCA with a conservative treatment of uncertainties. Standard Review Plan (NUREG-0800) Section 6.2.1.3, "Mass and Energy Release Analysis for Postulated Loss-of-Coolant Accidents (LOCAs)," notes that "calculations of the mass and energy release rates for a LOCA should be performed in a manner that conservatively establishes the containment internal design pressure (i.e., maximizes the post-accident containment pressure and the containment sub-compartment response)."

In response to staff RAI #9817, GEH proposed a conceptual design change to limit the non-condensable gas volume concentration [[ ]] below a safe threshold value. Possible conceptual changes include [[ ]], the combustible gas recombining could generate heat upon the actuation of Isolation Condensers. The current SBLOCA and LBLOCA TRACG model including the Isolation Condenser model [[

]].

Request

Therefore, the staff is requesting additional information regarding the potential heat addition [[ ]] and the potential impact on the ICs heat removal capacity when the non-condensable gas concentration in the lower drum is maintained up to the safe threshold value.

GEH Response to NRC Question 06.02.01-09

The radiolytic gas control design is currently in process, and the amount of energy that will be added to the steam [[ ]], if any, has yet to be determined. Therefore, a bounding estimate is presented herein assuming all of the energy that can theoretically

be released from the recombination of hydrogen and oxygen at the stoichiometric ratio will be added to the ICS for the cases presented in the GEH response to RAI 9817.

[[

]]

The cases presented in the GEH response to RAI 9817 were re-run to account for the energy addition described above. The ratio of the energy release rate from recombination of radiolytic gases to the ICS heat removal rate is shown in Figure 9856-1 for the two cases presented in the GEH response to RAI 9817. [[

]] Therefore, the radiolytic gas fraction at the inlet of the isolation condenser is not diluted in this calculation and increases continuously. Despite this added conservatism, the energy addition [[ ]] is still a small fraction of the heat removal rate of the isolation condenser.

The ICS heat removal rates are compared with and without energy addition in Figure 9856-2. The heat removal rates are indistinguishable from each other, indicating that [[
]] has practically no effect on the heat removal rate as discussed above.

[[

]]

Figure 9856-1. Ratio of the Energy Release Rate from Recombination of Radiolytic Gases to the Heat Removal Rate of Isolation Condenser.

[[

]]

Figure 9856-2. Isolation Condenser Heat Removal Rate With and Without Recombination Energy

Reference

R2856-1. Kenneth K. Kuo, "Principles of Combustion," 2nd Edition, John Wiley & Sons, 2005.

Proposed Changes to NEDC-33922P Revision 0

None.

SRP-Review Section: 06.02.05 - Combustible Gas Control in Containment

---

06.02.05-01 (eRAI 9854) [Audit Issue 14]
Date of eRAI Issue: 08/05/2021

Requirement

The NRC regulations in 10 CFR 50.44(c) set forth combustible gas control requirements for future water-cooled nuclear power reactor designs. In accordance with SRP Section 6.2.5, the NRC staff reviewed the BWRX-300 containment design for consistency with 10 CFR 50.44 (c).

Issue

To meet 10 CFR 50.44 (c), Section 6.10.3 of the LTR (NEDC-33922P, Revision 0) states that the calculated hydrogen and oxygen volume fractions are far below the "deflagration limits." In addition, the BWRX-300 is designed to have an inert containment such that the oxygen concentration must be limited. GEH indicated in electronic reading room (eRR) [[

]] to meet the definition of inerted atmosphere in 10 CFR 50.44(c).
[[ ]]

Request

Since these quantitative limits are necessary for the combustible gas control in containment and the audit files in the eRR are not on docket nor are referenced in the LTR, the applicant is requested to confirm or specify the quantitative hydrogen and oxygen concentration limits being used to ensure the compliance of 10 CFR 50.44(c) for combustible gas control in containment on docket.

GEH Response to NRC Question 06.02.05-01

The licensing topical report (LTR) does not try to set and does not assume combustible gas fraction limits or deflagration limits. Note also that 10 CFR 50.44(c) only requires that the initial oxygen volume fraction be kept below 4% for an inerted containment. There is no regulatory requirement for a hydrogen volume fraction.

The statement in Section 6.10.3 of the LTR with respect to the radiolytic gas fractions being well below deflagration limits refers to the order of magnitude of the volume fractions that may cause deflagration rather than the precise values.

Deflagration and detonation limits for the combustible gases depend not only on the hydrogen and oxygen volume fractions, but also on other parameters, such as pressure, temperature, steam volume fraction, potential flame propagation directions, and geometry.

Hydrogen deflagration limits are discussed in References R9854-1, R9854-2 and R9854-3.

Reference R9854-3 states that the flammability limit for hydrogen in dry air is 4%. Combustion is inhibited above 75% hydrogen concentration. The minimum oxygen required for combustion to take place is 5%. The autoignition temperature, whether it is the gas temperature or the surface temperature, is in the range of 580 – 800°C. Figure 1.2.3-1 of Reference R9854-2 shows the flammability limits for upward propagation and downward propagation at two different pressures and various temperatures. As shown in this figure, the downward propagation limit for the flammability of hydrogen in dry air is at least 8%, which would be representative of hydrogen collecting at the top of the containment if the containment were filled with dry air.

The hydrogen burn in the Three Mile Island (TMI) containment was estimated to result from a hydrogen accumulation of 7.3 – 7.9% in the containment (Appendix S of Reference R9854-1). The TMI containment is not inerted. Table S.3-2 of Reference R9854-1 shows that the minimum hydrogen concentration required for combustion increases significantly when the steam fraction in dry air increases. When the steam fraction is 40%, the required hydrogen fraction in the mixture increases to as much as 15 to 40%. Combustion is inhibited at even higher steam concentrations (Table S.3-1 of Reference R9854-1). At high steam concentrations, combustion is incomplete even if it could occur.

The LTR asserts that the radiolytic gas volume fractions in the BWRX-300 containment are far below any of the values quoted above but are not compared to a specific limit.

References

R9854-1. EPRI Final Report, 1025295, “Severe Accident Management Guidance Technical Basis Report, Volume 2: The Physics of Accident Progression,” October 2012.

R9854-2. NEA/CSNI/R(2014)8, “Status Report on Hydrogen Management and Related Computer Codes,” June 2014.

R9854-3. NEA/CSNI/R(2000)10, “Carbon Monoxide – Hydrogen Combustion Characteristics in Severe Accident Containment Conditions,” March 2000.

Proposed Changes to NEDC-33922P Revision 0

None

SRP-Review Section: 06.02.01 - Containment Functional Design Application Section:

06.02.01-01 (eRAI 9817)
Date of eRAI Issue: 04/08/2021

Requirement

General Design Criterion 50 – Containment design basis, requires the reactor containment structure, including access openings, penetrations, and the containment heat removal system be designed so that the containment structure and its internal compartments can accommodate, without exceeding the design leakage rate and with sufficient margin, the calculated pressure and temperature conditions resulting from any loss-of-coolant accident (LOCA).

Issue

In order to determine the conservative mass and energy discharge to the containment, a computer code and the associated evaluation model needs to have the capability to model relevant physical phenomenon during a LOCA with a conservative treatment of uncertainties. Standard Review Plan (NUREG-0800) Section 6.2.1.3, "Mass and Energy Release Analysis for Postulated Loss-of-Coolant Accidents (LOCAs)," notes that "calculations of the mass and energy release rates for a LOCA should be performed in a manner that conservatively establishes the containment internal design pressure (i.e., maximizes the post-accident containment pressure and the containment subcompartment response)."

GEH states in Section 5.2.4 of licensing topical report "BWRX-300 Containment Evaluation Method (NEDC-33922P, Revision 0)," that the only non-condensable gases that may migrate into the isolation condenser system (ICS) tube bundles are the radiolysis products following a design basis LOCA. This is based on the design not experiencing any significant fuel cladding oxidation during a LOCA.

However, based on the BWRX-300 ICS design, [[

]]

Request

Therefore, the staff is requesting additional information regarding [[
]] the associated modeling uncertainties, and the subsequent consequences for both large break and small break LOCA limiting cases.

GEH Supplemental Response to NRC Question 06.02.01-01

The isolation condenser heat removal rate is calculated using a stand-alone isolation condenser model with the boundary conditions obtained from the conservative small break case shown in Figures 5-18 through 5-22 of the licensing topical report (LTR). The stand-alone isolation condenser model used for this purpose is shown in Figure 9817-4 below to simulate a recombiner to control the volumetric fraction of radiolytic gases [[

]]

The boundary conditions used in the stand-alone isolation condenser are shown in Figure 9817-5. The reactor pressure vessel (RPV) dome pressure is obtained from the conservative small break results. The pressure of the chimney boundary condition is set sufficiently higher than the pressure at the dome boundary condition such that liquid does not clear from the condensate return line trapping all radiolytic gases in the isolation condenser. The radiolytic gas volume fraction at the boundary conditions representing the RPV is also obtained from the conservative small steam break case.

It is assumed that a recombiner maintains [[
]]. The heat removal rates calculated for the two cases are compared to the clean isolation condenser case in which the radiolytic gas volume fraction is set to zero at the boundary conditions representing the RPV. The comparisons are plotted in Figure 9817-6. The heat removal rates are indistinguishable from each other, indicating practically no effect of the radiolytic gas build up on the isolation condenser heat removal rate.

The reason that there is practically no effect of radiolytic gases on the heat removal rate can be deduced from Figures 9817-7 and 9817-8. Although the radiolytic gas volume fraction is allowed to build up to [[

]].

The above results show that there is practically no effect of radiolytic gases on the isolation condenser performance as long as the radiolytic gas volume fraction is maintained below a sufficiently low value.

The results presented above are also applicable to the large break cases. The difference between the large and small break cases is the radiolytic gas volume fraction at the boundary condition of the stand-alone isolation condenser model. The radiolytic gas volume fraction at the boundary condition would be somewhat higher in the large break cases as calculated in this analysis. [[

]] Because of this assumption, the method already has a substantial conservatism built in and, therefore, the results presented for a small break case bounds the large break cases. It should also be noted that some degradation in the isolation condenser heat removal capacity for large breaks does not have an adverse effect in the long term response. It has only a minor effect on the final value of the long-term RPV pressure.

[[

]]

Figure 9817-4. Stand-Alone Isolation Condenser Model Used to Demonstrate Isolation Condenser Performance with Radiolytic Gas Control

[[

]]

Figure 9817-5. Boundary Conditions Obtained from NEDC-33922P Conservative Small Steam Break Case, and the Increased Chimney Pressure to Maintain a Liquid Plug in Condensate Return Pipe

[[

]]

Figure 9817-6. Isolation Condenser Heat Removal Rate Comparisons

[[

]]

Figure 9817-7. Radiolytic Gas Volume Fraction in the Isolation Condenser. [[
]]

[[

]]

Figure 9817-8. Radiolytic Gas Volume Fraction in the Isolation Condenser. [[
]]

SRP-Review Section: 06.02.01 - Containment Functional Design Application Section:

06.02.01-06 (eRAI 9857) [Audit Issue 38]
Date of eRAI Issue: 08/05/2021

Requirement

General Design Criterion 50 – Containment design basis, requires the reactor containment structure, including access openings, penetrations, and the containment heat removal system be designed so that the containment structure and its internal compartments can accommodate, without exceeding the design leakage rate and with sufficient margin, the calculated pressure and temperature conditions resulting from any loss-of-coolant accident (LOCA).

Issue

In order to determine the conservative mass and energy discharge to the containment, a computer code and the associated evaluation model needs to have the capability to model relevant physical phenomenon during a LOCA with a conservative treatment of uncertainties. Standard Review Plan (NUREG-0800) Section 6.2.1.3, "Mass and Energy Release Analysis for Postulated Loss-of-Coolant Accidents (LOCAs)," notes that "calculations of the mass and energy release rates for a LOCA should be performed in a manner that conservatively establishes the containment internal design pressure (i.e., maximizes the post-accident containment pressure and the containment sub-compartment response)."

The pipe lay out of BWRX-300 Isolation Condensers (ICs) return line is different from that of GE ESBWR design. [[

]].

Request

Therefore, the staff is requesting additional information regarding the modeling capability of TRACG to simulate the ICS return line clearing, in particular, the conservatism of the existing TRACG SBLOCA model regarding the impact of clearing on the overall ICS heat removal capacity.

GEH Response to NRC Question 06.02.01-06

The piping layout for condensate return from the ICs has not been finalized. Earlier calculations had shown that flushing of Non-Condensable Gases (NCGs) from the ICs back into the Reactor Pressure Vessel (RPV) was possible if the water loop seal was not present. This flushing phenomenon relies on the interfacial drag between the liquid condensate and the gases which include varying concentrations of steam with NCGs. The interfacial drag force depends on the relative velocities between the liquid and gases which will vary substantially during the time when the ICs are in service. The TRACG modeling of two-phase flow has been validated and qualified for vertical geometries for co-current upward and downward flows and countercurrent flow with gas(es) moving upward and liquid moving downward. [[

]]

Any possibility for complete flushing of NCGs from the ICs should not be relied upon as a means for limiting the buildup of NCGs in the ICs. When the geometry is vertical, the downward transport of NCGs is reliably calculated by TRACG when the liquid velocity is large enough to drag gases down. [[

]] GEH concurs with the NRC staff's assessment that countercurrent flow could be possible in these inclined or nearly horizontal sections of piping which would allow steam to backflow into the ICs *if the loop seal was not present to prevent it*. Therefore, there is no advantage for *not* having a water seal in the condensate return lines. The loop seal will be retained in the final design. With the loop seal present, the reverse flow of steam into the IC loop will be prevented. The calculations previously performed remain valid because reverse steam flow had been prevented by applying a directionally dependent artificially large loss coefficient at the pipe discharge into the chimney. Also, when the loop seal is present, the ability to flush NCGs will be limited or even prevented entirely. As shown by calculations presented in the GEH Supplemental Response to NRC Question 06.02.01-01 (eRAI 9817) (Reference R9857-1), when NCG accumulation is maintained below a certain amount in the lower regions of the ICs and the condensate lines, then there is no significant degradation in the heat removal capabilities of the ICs. The final IC design will provide a means to limit the NCG buildup so that modeling of the heat removal capability will remain valid and conservative based on the tested IC configuration with little to no NCGs present.

Reference

R9857-1. GEH Letter M210099, "Response to Requests for Additional Information (eRAIs) 9854, 9856, and 9862 and Supplemental Response to eRAI 9817 for Licensing Topical

Report NEDC-33922P, Revision 0, BWRX-300 Containment Evaluation Method," September 17, 2021.

Proposed Changes to NEDC-33922P Revision 0

None.

06.02.01-07 (eRAI 9862) [Audit Issue 40]
Date of eRAI Issue: 08/05/2021

Requirement

General Design Criterion 50 – *Containment design basis*. Requires the reactor containment structure, including access openings, penetrations, and the containment heat removal system be designed so that the containment structure and its internal compartments can accommodate, without exceeding the design leakage rate and with sufficient margin, the calculated pressure and temperature conditions resulting from any loss-of-coolant accident (LOCA).

General Design Criterion 38 -- *Containment heat removal*. A system to remove heat from the reactor containment shall be provided. The system safety function shall be to reduce rapidly, consistent with the functioning of other associated systems, the containment pressure and temperature following any loss-of-coolant accident and maintain them at acceptably low levels.

General Design Criterion 16 -- *Containment design*. Reactor containment and associated systems shall be provided to establish an essentially leak-tight barrier against the uncontrolled release of radioactivity to the environment and to assure that the containment design conditions important to safety are not exceeded for as long as postulated accident conditions require.

Issue

In the course of the staff's review of the GEH LTR NEDC-33922P, Revision 0, BWRX-300 Containment Evaluation (CE), GEH submitted a deliverable package on the docket, dated December 8, 2020. The package included original (NEDC-33922P-R0) and updated (UPDATE) sets of TRACG and GOTHIC models, along with some parameter comparisons between the original and updated models for the large break and small steam break LOCA conservative cases. However, no calculation results were included in the package to demonstrate the impact of changes made to the original TRACG/GOTHIC models to update them. The results presented and discussed in LTR NEDC-33922P, Revision 0, pertain to the original TRACG/GOTHIC models. According to GEH, the future LTR revision will be based on the calculation results from the updated TRACG/GOTHIC models.

During the course of confirmatory analyses, the staff also executed the submitted updated TRACG model and compared the resulting mass and energy release with the original TRACG model results presented in LTR Revision 0, and found significant differences in the break flow of the conservative large steam break LOCA. Without a complete review of the updated TRACG/GOTHIC model results, the staff cannot determine whether the updated models introduce any additional phenomena that were not captured in the original models, and thereby potentially adversely impact the major CE methodology conclusions based on the original models.

Request

1. Present and explain the prediction differences between the original and updated models in terms of the magnitude and sequence of events during the transient due to the changes in the updated models. Provide justification that no new phenomena were caused by the model/code

changes in the updated models. This would involve the key CE methodology parameters, e.g., RPV pressure, downcomer level, fuel temperature, mass and energy release, containment pressure, shell temperature, and PCCS exit and reactor cavity pool temperatures. Address the above requests for both the limiting large break and small break LOCA.

2. Justify that the updated TRACG/GOTHIC models remain bounding, and no major CE methodology conclusions regarding the limiting transients, rapid cooling requirements, nodalizations, and modeling uncertainties are adversely impacted compared to the original models.

3. Confirm that the LTR will be updated to reflect calculation results based on verified updated TRACG/GOTHIC models for all the demonstration transients.

GEH Response to NRC Question 06.02.01-07

1. The updated steady state and transient TRACG results were obtained from version 76.01 whereas the original results were obtained from version 75.00. Differences in code versions (provided during the audit) do not explain the differences in calculated results because none of the code differences would produce any differences in calculated break flow. Similarly, no effect on calculated results would be caused by cosmetic and trivial differences observed in the transient input files because the bulk of transient inputs are obtained via the dump/restart file from the end of the steady state cases. Differences in calculated transient results are attributed to input changes made in the steady state where the loss coefficients for radial steam flow in the dryer were increased. This change results in a minor difference in the void fraction for steam entering the steam line when the break occurs. This is not a new phenomenon. In both the UPDATED and LTR cases, the void fraction decreased momentarily in the reactor pressure vessel (RPV) at the entry point to the steam line because of the rapid RPV pressure reduction. There was only a slight difference in the amount that the void fraction decreased.

   Figure 9862-10 compares the break flows and enthalpies at the two separated ends of the guillotine break for both the LTR and UPDATED inputs. The effect of these differences is small in terms of total integrated energy released via the break from the RPV to the containment shown in Figure 9862-11. As expected, the containment pressure is slightly higher for the UPDATED case shown in Figure 9862-12 because the integrated energy into the containment was higher. The tailoff in the containment pressure [[ ]] is addressed in the response to Part 2 of this RAI question. The break flow and enthalpy can only have an effect on the RPV pressure before the RPV isolation valves are fully closed; therefore, the RPV pressure response is not shown in Figure 9862-13 after the break flow from the isolated steam line has stopped. Also as expected, the RPV pressure for the UPDATED case is slightly lower because the integrated energy release from the RPV to containment was slightly greater. Because of the additional energy and mass release from the RPV, the RPV level is lower for the updated case as shown in Figure 9862-14. The slight plateau in RPV level [[ ]] in the figure corresponds to when the isolated steam line pressure and containment pressure equalize. In this time frame [[ ]] the UPDATED

RPV level response tracks parallel to the RPV level response reported in the LTR. In the longer term, the RPV level responses become similar because the level in the downcomer and inside the chimney will approximately equalize to the level in the downcomer. This equilibrium level is sensitive to two-phase conditions inside the core barrel, especially in the core. The core averaged void fraction for the UPDATED case is higher than the LTR case in this time frame which reflects the integral effect of lower recirculation flow caused by the earlier lower downcomer level [[ ]]. There are no significant differences in the progression or timing of events for the large steam break.

The updated results demonstrate that no new or additional phenomena were introduced by the model/code changes. The effects of code and input changes are not shown for the liquid large breaks and the small liquid and steam breaks because they are negligible.

[[

]]

Figure 9862-10. Break Flows and Enthalpies for Conservative LB Steam Break

[[

]]

Figure 9862-11. Total Break Integrated Energy for Conservative LB Steam Break

[[

]]

Figure 9862-12. Containment Pressure for Conservative for LB Steam Break

[[

]]

Figure 9862-13. RPV Pressure for Conservative for LB Steam Break

[[

]]

Figure 9862-14. RPV Level for Conservative for LB Steam Break

2. There were minor unintentional differences between the model described in the LTR and the model that produced the figures in the LTR. The effect of these differences was not noticeable in most cases. In two instances the results were noticeable. These are (a) the tail end of the containment pressure should have decreased faster in both the base and conservative cases shown in LTR Figure 6-26; and (b) the shell temperatures shown in Figures 6-27, 6-30, and 6-34 should have been about 8°C lower for all cases because of a unit conversion error. The transmittal of the files in the UPDATE folder also included the comparisons showing the differences for the limiting cases. These differences affect all curves, base and conservative, in the same manner. These differences do not affect any of the uncertainty discussions. Therefore, no major CE methodology conclusions based on the original models regarding the limiting transients, rapid cooling requirements, nodalizations, and modeling uncertainties have been adversely affected by the updated models.
3. The final LTR figures will be produced using the corrected model provided in the UPDATE folder after making the additional changes resulting from the RAI responses.

Proposed Changes to NEDC-33922P Revision 0

The LTR figures will be updated as stated in the RAI response to Item 3.

06.02.01-08 (eRAI 9862) [Audit Issue 43]
Date of eRAI Issue: 08/05/2021

Requirement

General Design Criterion 38 -- *Containment heat removal*. A system to remove heat from the reactor containment shall be provided. The system safety function shall be to reduce rapidly, consistent with the functioning of other associated systems, the containment pressure and temperature following any loss-of-coolant accident and maintain them at acceptably low levels.

General Design Criterion 16 -- *Containment design*. Reactor containment and associated systems shall be provided to establish an essentially leak-tight barrier against the uncontrolled release of radioactivity to the environment and to assure that the containment design conditions important to safety are not exceeded for as long as postulated accident conditions require.

Issue

Table 6-2 of the GEH LTR NEDC-33922P, Revision 0, BWRX-300 Containment Evaluation (CE) Method, presents the Phenomena Identification and Ranking Table for BWRX-300 containment. The table recognizes [[

]]

These phenomena are pertinent to [[

]], during the first 24 hours of LBLOCA and first 72 hours of SBLOCA. As presented in the LTR, the BWRX-300 CE methodology uses a [[

]]. The staff has two primary concerns in this regard.

- Several correlations are being used in a manner that may not accurately capture the PCCS geometry and flow conditions, and
- As the same [[ ]], the applicable flow and heat transfer regimes may not be accurately captured by the model. The staff needs to make a reasonable assurance finding regarding the single-phase heat transfer modeling inside the PCCS tubes. No test data were presented for the PCCS channels thermal performance either as a separate effect or an integral experiment, so the modeling is dependent on use

of appropriate theoretical models to capture the phenomena within the PCCS tubes. Therefore, the applicant is requested to address the following questions about the PCCS tube-side heat transfer and flow-rate modeling and the related assumptions.

Request

1. Section 6.5 of the GEH LTR NEDC-33922P, Revision 0, BWRX-300 Containment Evaluation (CE) Method, presents a PCCS tube-side heat transfer model, as captured by the following three equations on the LTR Page 65.

$$Nu_{FC} = 0.023Re^{0.8}Pr^{0.3} \quad (1)$$

[[ ]] (2)

[[ ]] (3)

Equation 3 [[

]].

Even though, "alternate calculation.docx" file GEH submitted as a part of Package-3 in the DBR-0055078-R0 folder, does provide additional thermosyphon modeling details, the staff was not able to find a reference for using the three equations for modeling natural convection flow and heat transfer [[

]]. The applicant is requested to provide a citation for this modeling approach and its separate-effect validation basis [[

]] used in BWRX-300. The staff has following specific concerns about the potential non-conservatisms in the three-equation [[ ]] formulation that need to be addressed.

a. [[

]]. The applicant is requested to justify the applicability of the [[

]]. Also justify why [[

]].

b. This model does not appear to appropriately and consistently model all expected flow conditions that would occur during the postulated events, including [[

]]. Unlike the [[

]] (Figures 6-18 & 6-20), no such criteria are used to identify the applicable natural, forced, or mixed convection mode inside the PCCS tubes.

Please justify the three-equation based model's presumption of [[

]] even during conditions that are expected to be laminar, which is expected to be non-conservative. In this backdrop, also justify the use of Dittus-Boelter correlation (Equation 1) for turbulent forced-convection that is expected to be non-conservative in the initial phase until the Reynolds number exceeds a certain threshold.

2. There is almost no information provided in the LTR on how the resulting density-driven single-phase flow recirculation gets imposed [[

]], except the statement that "Wall friction is calculated from the Colebrook relationship for smooth wall." The staff requests a summary of the flow modeling details be included in the LTR describing the related BWRX-300 CE methodology.

3. The applicant is requested to provide the LBLOCA and SBLOCA short-term and long-term plots for PCCS flowrate, total heat transfer, and temperatures [[

]] to demonstrate that the PCCS model predicts the physically consistent trends in overcoming the initial thermal inertia of the single-phase thermosyphon, as well as the long-term PCCS thermal performance characteristics. Also provide representative plots of the applicable non-dimensional numbers (e.g. Reynolds, Rayleigh) to support the choice of heat transfer correlations and convection regimes, or show that the [[ ]] will yield the same or more conservative results compared to a generally accepted correlation that is more directly applicable. For this study, use the limiting break location [[ ]] that was identified in response to RAI (06.02.01-03). The results would help the staff make a reasonable assurance finding regarding the modeling of PCCS single-phase heat transfer modeling in general and understand the Figure 6-32 trends better.

Please update the LTR with any information needed to clarify modeling details necessary to perform the containment evaluation analyses.

GEH Response to NRC Question 06.02.01-08

1. The Nu number can be calculated as the higher of the Nu numbers in the laminar and turbulent natural convection regimes instead of determining whether the flow is in the laminar or turbulent flow regimes and calculating the Nu number from the respective correlation for natural convection. [[

   a.

   ]]

   b. Equation (1) is applicable to the turbulent regime. Equation (2) is applicable to both the laminar and turbulent flow regimes. [[

]]

The above discussion shows that the equation set used for convection inside the PCCS tubes correctly selects the mode of the heat transfer during the period that the PCCS is removing heat from the containment by heating up the liquid.

2. [[

]] The input parameters required for this calculation are derived from the PCCS design and will be finalized when the design is finalized.

[[

]]

3. The plots provided in the response to Part 1.b and the discussion above convey the information requested in this RAI question. [[

]]

Therefore, overcoming the initial thermal inertia and the short-term PCCS performance characteristics are not important in determining the key containment response characteristics.

Table 9862-1. Re, Gr, Pr and Nu numbers at Node #4 of PCCS Units 1 and 5

		PCCS Unit 1	PCCS Unit 5	PCCS Unit 1	PCCS Unit 5
		Node #4	Node #4	Node #4	Node #4
		[[			
Pressure	kPa				
Wall temperature	°C				
Liquid temperature	°C				
Velocity	m/s				
Film temperature	°C				
Density	kg/m^3				
Dynamic viscosity	kg/m-s				
Specific heat	kJ/kg-K				
Thermal conductivity	W/m-K				
Vol. expansion coefficient	1/K				
Re					
Gr					
Pr					
Ra					
Ri					
Nu, Forced Convection					
Nu, Natural Convection					
Nu Mixed Convection					]]

[[

]]

Figure 9862-15. Comparison of McAdams Correlation to Churchill and Chu Correlation

[[

]]

Figure 9862-16. Containment, Wall and Liquid Temperatures at Node #4 of PCCS Unit 1, Closest to the Break Location, Small Steam Pipe Break

[[

]]

Figure 9862-17. Containment, Wall and Liquid Temperatures at Node #4 of PCCS Unit 5, Farthest to the Break Location, Small Steam Pipe Break

[[

]]

Figure 9862-18. Velocities in the Annuli of PCCS Unit 1 (Closest to the Break Location) and PCCS Unit 5 (Farthest from the Break Location), Small Steam Pipe Break

References

R9862-5. W.H. McAdams, "Heat Transmission," McGraw-Hill, Third Edition, New York, 1954.

R9862-6, S.W. Churchill and H.H.S. Chu, "Correlating Equations for Laminar and Turbulent Free Convection From a Vertical Plate," Int. J. Heat and Mass Transfer, Vol. 18, pp. 1323-1329, (1975).

Proposed Changes to NEDC-33922P Revision 0

A summary of the discussion provided in this RAI response will be added to the LTR to describe the heat transfer and fluid flow in the cold and hot channels of the PCCS units.

SRP-Review Section: 06.02.01 - Containment Functional Design Application Section:

06.02.01-01 (eRAI 9862) [Audit Issue 1]
Date of eRAI Issue: 08/05/2021

Requirement

General Design Criterion 50 – *Containment design basis*. Requires the reactor containment structure, including access openings, penetrations, and the containment heat removal system be designed so that the containment structure and its internal compartments can accommodate, without exceeding the design leakage rate and with sufficient margin, the calculated pressure and temperature conditions resulting from any loss-of-coolant accident (LOCA).

General Design Criterion 38 -- *Containment heat removal*. A system to remove heat from the reactor containment shall be provided. The system safety function shall be to reduce rapidly, consistent with the functioning of other associated systems, the containment pressure and temperature following any loss-of-coolant accident and maintain them at acceptably low levels.

General Design Criterion 16 -- *Containment design*. Reactor containment and associated systems shall be provided to establish an essentially leak-tight barrier against the uncontrolled release of radioactivity to the environment and to assure that the containment design conditions important to safety are not exceeded for as long as postulated accident conditions require.

Issue

Guided by the Standard Review Plan (SRP) Section 6.2.1 and the General Design Criteria (GDCs) 50, 38, and 16 of Appendix A to 10 CFR Part 50 relevant to the containment design basis, the staff is reviewing the applicant's analytical model and assumptions used in the GEH LTR NEDC-33922P, Revision 0, BWRX-300 Containment Evaluation (CE) Method. An important objective of this LTR review is to assess the conservativisms and non-conservatisms associated with the presented GOTHIC model, in order to determine whether the CE methodology would be acceptably conservative and physically meaningful with respect to the containment thermal-hydraulic response. The staff needs to ensure that the BWRX-300 CE methodology incorporates sufficient conservatism to analyze the short-term and long-term containment thermal hydraulics response to the limiting design basis events (DBEs) to offset the inherent methodology uncertainties. In this regard, the applicant is requested to provide the following additional information regarding the precedent-setting BWRX-300 containment nodalization approach used in the GOTHIC code.

Request

1. In the GEH LTR NEDC-33922P, a containment nodalization study is presented for the large steam line break (LBLOCA) event. [[

   ]]. However, LTR Figure 6-12 shows that a [[

]] for the LBLOCA base case. This demonstrates that [[ ]] result in more conservative results. In this backdrop, the applicant is requested to justify that the default [[ ]] choice is sufficiently conservative to bound the uncertainties in the LBLOCA containment analysis, or provide an upper bound on the non-conservatism inherent in finer nodalizations for conservative LBLOCA case.

The plots in Figures 6-26 and 6-27 show the [[ ]] for the conservative LBLOCA case, though they are not documented in the LTR as such. As they are among the most important parameters predicted by the CE methodology, the staff requests documenting the limiting PCP and maximum shell temperature values for the conservative case in the LTR as updated by the break location and break flow direction sensitivity studies requested in RAI 06.02.01-03. This information is needed by the staff to establish the overall conservatism in the containment evaluation (CE) methodology for LBLOCA.

2. The small break LOCA (SBLOCA) and LBLOCA are different DBEs that involve different phenomenological concerns. However, the staff noted that no containment nodalization study is presented in the LTR for the SBLOCA. As the break flow is [[ ]]. As shown by Figure 6-17, [[ ]]. LTR Figures 6-12 and 6-13 show [[ ]]. These phenomena are equally applicable to SBLOCA. With the complex SBLOCA phenomenology involving the novel PCCS design and Reactor Cavity pool heat-up in the later stage of transient, [[ ]].

   Therefore, the applicant is requested to provide information to confirm that the nodalization is adequate for SBLOCA, consistent with the information provided for LBLOCA. For this purpose, the staff requests GEH to provide similar justification for nodalization used in the limiting SBLOCA analysis up to 72 hours to demonstrate that the predicted limiting containment pressure and temperature responses remain conservative and insensitive to nodalization changes, and to quantify the conservatisms in the [[ ]]. The associated PCCS temperature plots (similar to LTR Figure 6-32), PCCS heat removal rate plots, and the containment steam volume fraction plots (similar to Figure 6-17) in the SBLOCA nodalization study should be included and discussed.

GEH Response to NRC Question 06.02.01-01

1. The nodalization study is performed to demonstrate that the results are sufficiently converged as the node size is decreased. The purpose of nodalization is not to introduce additional conservatism, but to increase the accuracy by ensuring that the spatial gradients of the phenomena controlling the containment response are adequately resolved. Increasing the node size (i.e., coarser nodalization) will provide less accurate results but does not necessarily assure that those results will be conservative for all cases. The differences between the base case and the finer nodalization cases are approximately [[ ]] in Figure 6-12 of the Licensing Topical Report (LTR). This can be compared to the difference between the base case and the conservative case shown in Figure 6-26 of the LTR. The difference between the peak pressures for the base and conservative cases is approximately [[ ]]. This result shows that the additional resolution resulting from finer nodalization beyond the base case is much smaller than the conservatism introduced by biasing the inputs and modeling parameters, and the results using the base case nodalization are in the conservative direction.

2. A nodalization study was performed for the small breaks. The results of the study are presented below.

   The purpose of the small break cases is to show that the containment pressure resulting from small breaks is bounded by the containment pressure resulting from the large break cases. The small break cases also demonstrate that the containment does not stay at the peak pressure in the long term and the pressure decreases. The target for the containment depressurization rate is to reduce the containment pressure to half of the peak accident pressure of the most limiting case within 24 hours. For the BWRX-300, the decrease in the containment pressure in the long term is primarily accomplished by the isolation condensers as shown below.

   A small break case was performed to maximize the containment pressure as presented in the GEH response to NRC Question 06.02.01-03 (eRAI 9862) (Reference R9862-1) using the base case [[ ]] nodes (the first number is the number of nodes in x-direction, the second number is the number of nodes in y-direction, and the last number is the number of nodes in the axial direction). This case uses the conservative inputs and model biases. In the nodalization study presented here, the same case was run using [[
   ]] nodes. The comparisons are shown in Figure 9862-19.

   The nodalization study cases were run until the Reactor Pressure Vessel (RPV) pressure falls below the containment pressure. Once the RPV and containment pressures equalize, the containment pressure will not exceed the RPV pressure. There are two RPV pressures plotted in Figure 9862-19. The solid line is the RPV pressure with a small steam pipe break. This line is applicable until the break flow becomes unchoked. As discussed in the LTR, the break flow is calculated assuming no containment back pressure (i.e., the break flow is calculated assuming the containment remains at atmospheric pressure). When containment back pressure is not considered, the RPV pressure remains sufficiently above atmospheric pressure, and the

break flow remains choked for 72 hours. The solid line is consistent with the cases presented in Chapter 5 of the LTR.

As the event progresses, the RPV pressure decreases and the containment pressure increases. Realistically, when containment back pressure is considered, the break flow becomes unchoked when the pressure differential between the RPV and the containment becomes low enough. The RPV and containment pressures eventually equalize, after which there is essentially no more mass discharged to the containment unless the containment pressure decreases at a faster rate than the RPV pressure. Instead of resolving exactly when the break flow becomes unchoked and when it stops, the upper and lower bounds for the RPV pressure are plotted in Figure 9862-19. The small break case is the lower bound (solid red line) and the no break case is the upper bound (dashed red line) for RPV pressure. The actual RPV pressure would be between these two lines. The fact that the upper and lower bounds for the RPV pressure are close to each other indicates that the primary mechanism for the RPV depressurization is the heat removal by the isolation condensers, not the energy discharged by the break flow. As expected, with time, the RPV pressures calculated with and without break flow converge and continue to decrease together because the decreasing break flow with time becomes less important in determining the RPV pressure.

The containment pressure is calculated assuming no reduction in the break flow rate due to the containment back pressure. There are several containment pressures shown in Figure 9862-19 corresponding to the different nodalization cases. As an example, the containment pressure calculated for [[ ]] nodes is shown by the solid black line in Figure 9862-19. The containment and RPV pressures equalize at approximately [[ ]] in this case. Because the break flow to the containment is practically zero after this point for the remainder of the transient, the Passive Containment Cooling System (PCCS) and containment dome are removing more energy from the containment than the energy being added from the RPV, so the RPV and the containment pressure start to decrease. This is shown with the dashed black line in Figure 9862-19. When the containment pressure starts falling below the RPV pressure, there will be a small break flow again which prevents the containment pressure from falling much below the RPV pressure. However, the containment pressure will not exceed the RPV pressure in any case. It follows that the actual containment pressure is between the red dashed line and the black dashed line in Figure 9862-19. The plotted lines in Figure 9862-19 show that the long term containment pressures for all SBLOCA cases are reduced to less than 50% of the peak pressure from the LBLOCA in less than 24 hours (86,400 seconds).

The nodalization study was performed up to the point where the containment and RPV pressures equalize. The cases include [[ ]], in addition to the base case of [[ ]] nodes. [[
]]

The nodalization of the PCCS units in the axial direction is the same as the containment axial nodalization in all cases. In the base case, which has [[ ]] total axial nodes in the containment, the PCCS model has [[ ]] heated nodes in the axial direction and one (1) unheated node at the top representing the section of the PCCS above the containment, as shown

in Figure 6-3 of LTR. The heated PCCS nodes are aligned with containment nodes [[ ]]. In the [[ ]] case, the PCCS has [[ ]] heated axial nodes aligned with the containment axial nodes [[ ]] and one (1) unheated top node. In the [[ ]] case, the PCCS has [[ ]] heated nodes aligned with axial containment nodes [[ ]], and one (1) unheated top node.

The PCCS units are placed in one cell in the horizontal direction that is closest to their actual location.

The coarse nodalization case ([[ ]]), shown by the blue curve in Figure 9862-19, results in [[ ]]. As compared to the finer nodalization cases, this case [[ ]] the containment pressure and appears to have inadequate fidelity. All other nodalization cases converge to roughly the same containment pressure. Although the base case has a somewhat [[ ]] pressure than the finest nodalization case, the results are not far from each other as more nodes are added to the base case. The peak pressure for the bounding accident, a large steam pipe break, is shown with a dotted-dashed line at about [[ ]] in Figure 9862-19. As shown, the containment pressure resulting from a small break is well below that of the large break case. In addition, the containment pressure in the long term is limited by the RPV pressure, and any calculated differences resulting from the nodalization scheme used in the containment small break analyses do not have an effect on the bounding long term containment pressure.

The steam volume fraction distributions in the containment are plotted in Figure 9862-20. The color palette is set to exaggerate any stratification effects. This figure shows that the [[ ]] nodalization lacks the needed spatial resolution, which results in a higher condensation rate, and consequently, lower steam fractions as compared to the steam fractions calculated using the finer nodalizations. The other nodalization schemes ([[ ]]) provide reasonably close results. The steam volume fraction distributions shown in Figure 9862-20 are consistent with the trends in pressure displayed in Figure 9862-19. The PCCS heat removal rate and temperatures are shown in Figures 9862-21 and 9862-22. As shown by the trends in Figure 9862-21, all the nodalizations indicate that the PCCS heat removal rates are, in the long term, approaching a similar asymptotic value that is sufficient to cause the containment to continue to depressurize as shown in Figure 9862-19. The reactor cavity pool is not being actively cooled so it will continue to heat up; however, the temperature difference between the pool and the PCCS exit temperature which is indicative of the heat removal rate remains approximately the same. Because decay heat is being removed by the isolation condenser system, there is very little energy being deposited into the containment from the RPV after about [[ ]] when the RPV and containment pressures equalize. Even as the reactor cavity pool slowly heats up, the PCCS will continue to cool and depressurize the containment to a sufficiently low value long term by moving energy that is already in the containment to the reactor cavity pool until the containment and reactor cavity pool temperatures approach within a few degrees of each other. Although there are some variations with nodalization, the variations do not have a significant effect on the containment pressure with nodalizations [[ ]] and finer as shown in Figure 9862-19.

Based on the conclusions of the large break nodalization study and the results of the small break nodalization study discussed above, the use of the base case [[ ]] nodalization for the small break containment analyses is adequate and further refinement of the containment node size does not increase confidence in the results with respect to the purpose of the small break analyses.

[[

]]

Figure 9862-19. Nodalization Study for Small Steam Pipe Breaks

[[

]]

[[

]]

Figure 9862-20. Steam Volume Fraction Distribution in the Containment

[[

]]

Figure 9862-21. Heat Removal Rates by the PCCS and the Steam Dome

Note: Negative values indicate heat removal from the containment.

[[

]]

Figure 9862-22. PCCS Exit and Reactor Cavity Pool Temperatures

Reference

R9862-1 GEH Letter M210099, "Response to Requests for Additional Information (eRAIs) 9854, 9856, and 9862 and Supplemental Response to eRAI 9817 for Licensing Topical Report NEDC 33922P, Revision 0, BWRX 300 Containment Evaluation Method," September 17, 2021.

Proposed Changes to NEDC-33922P Revision 0

The LTR will be updated with the limiting peak containment pressure and maximum shell temperature values for the conservative case in the LTR as updated by the break location and break flow direction sensitivity studies requested in NRC Question 06.02.01-03 (eRAI 9862).

06.02.01-03 (eRAI 9862) [Audit Issue 5]
Date of eRAI Issue: 08/05/2021

Requirement

General Design Criterion 50 – *Containment design basis*. Requires the reactor containment structure, including access openings, penetrations, and the containment heat removal system be designed so that the containment structure and its internal compartments can accommodate, without exceeding the design leakage rate and with sufficient margin, the calculated pressure and temperature conditions resulting from any loss-of-coolant accident (LOCA).

General Design Criterion 38 -- *Containment heat removal*. A system to remove heat from the reactor containment shall be provided. The system safety function shall be to reduce rapidly, consistent with the functioning of other associated systems, the containment pressure and temperature following any loss-of-coolant accident and maintain them at acceptably low levels.

General Design Criterion 16 -- *Containment design*. Reactor containment and associated systems shall be provided to establish an essentially leak-tight barrier against the uncontrolled release of radioactivity to the environment and to assure that the containment design conditions important to safety are not exceeded for as long as postulated accident conditions require.

Issue

Figure 6-11 in GEH LTR NEDC-33922P, Revision 0, BWRX-300 Containment Evaluation Method, presents the vertical and horizontal cross-sectional views of various 3-D GOTHIC grids used in the BWRX-300 containment nodalization studies. The LTR Figure 6-11 [[

]]. The LTR Figure 6-11 [[

]].

As recognized in LTR Section 6.6.1, [[

]]. The staff is concerned that the increased velocity and higher steam concentration near [[ ]] that increase the condensation heat transfer, would enhance the heat removal to the [[ ]]. While this has the desired effect of maximizing the shell temperature, it would have an adverse impact on the peak containment pressure. Therefore, the staff considers the current break location to be a non-conservative assumption embedded in the BWRX-300 GOTHIC model for the purpose of predicting the peak containment pressure.

The staff also needs to evaluate that, as based on the COPAIN test data presented in the LTR, the convection and condensation heat transfer coefficients [[

]]. So, GOTHIC's qualifications need to be justified for using the flow-direction/convection-mode dependent conservatisms used in the BWRX-300 CE methodology.

Request

1. The applicant is requested to provide the results for a break location sensitivity study for the BWRX-300 containment main steam pipe break (LBLOCA) using the conservative GOTHIC containment model to justify that the chosen break location is bounding for all break locations, or identify the most limiting break locations with respect to peak containment pressure and maximum wall temperature. Please perform the sensitivity study for the default [[ ]] for 24 hours, along the radial, axial, and azimuthal directions, or justify why some or all of the sensitivity cases are not needed.
2. The applicant is also requested to perform a 180 degree break flow orientation sensitivity study for the limiting location, i.e., the break flow coming out of the pipe upward, horizontal toward the containment wall, and downward directions, for the most limiting break location, as identified in Part 1, for the default [[ ]] conservative cases of the large steam break LBLOCA as well as the small steam break SBLOCA. The requested break orientation sensitivity study results for 24 hours for LBLOCA and 72 hours for SBLOCA, along with the information requested in Part 3, will help the staff make a reasonable assurance finding regarding the conservative biases used in modeling convection and condensation to cover the uncertainties in the COPAIN test data, as documented in the LTR. The staff needs to evaluate the [[ ]] biases used for the convection and condensation heat transfer correlations.
3. [[

]], the applicant is requested to provide justification for GOTHIC's qualification to predict the flow direction in the near wall region in a subdivided volume, or provide evidence that in the limiting cases GOTHIC's prediction of flow direction is in the conservative direction in the near wall region of the subdivided containment. Otherwise, present the limiting LBLOCA and SBLOCA results using [[

]].

Please update the LTR if the responses to the above questions result in a change to the methodology as described in the LTR.

Supplemental GEH Response to NRC Question 06.02.01-03

In response to a request from the NRC audit staff during a call on October 7, 2021, the language provided by GEH in the response to NRC Question 06.02.01-03 (eRAI 9862) [Audit Issue 5] Item 1 (Reference R9862-2) has been revised.

The 2nd paragraph below Table 9862-1 in the GEH response to NRC Question 06.02.01-03 (eRAI 9862) [Audit Issue 5] Item 1 (Reference R9862-2) has been revised from:

[[

]]

to

[[

]]

Reference

R9862-2 GEH Letter M210099, "Response to Requests for Additional Information (eRAIs) 9854, 9856, and 9862 and Supplemental Response to eRAI 9817 for Licensing Topical Report NEDC 33922P, Revision 0, BWRX 300 Containment Evaluation Method," September 17, 2021.

Proposed Changes to NEDC-33922P Revision 0

None

SRP-Review Section: 06.02.01 - Containment Functional Design Application Section:

06.02.01-01 (eRAI 9862) [Audit Issue 1]
Date of eRAI Issue: 08/05/2021

Requirement

General Design Criterion 50 – *Containment design basis*. Requires the reactor containment structure, including access openings, penetrations, and the containment heat removal system be designed so that the containment structure and its internal compartments can accommodate, without exceeding the design leakage rate and with sufficient margin, the calculated pressure and temperature conditions resulting from any loss-of-coolant accident (LOCA).

General Design Criterion 38 -- *Containment heat removal*. A system to remove heat from the reactor containment shall be provided. The system safety function shall be to reduce rapidly, consistent with the functioning of other associated systems, the containment pressure and temperature following any loss-of-coolant accident and maintain them at acceptably low levels.

General Design Criterion 16 -- *Containment design*. Reactor containment and associated systems shall be provided to establish an essentially leak-tight barrier against the uncontrolled release of radioactivity to the environment and to assure that the containment design conditions important to safety are not exceeded for as long as postulated accident conditions require.

Issue

Guided by the Standard Review Plan (SRP) Section 6.2.1 and the General Design Criteria (GDCs) 50, 38, and 16 of Appendix A to 10 CFR Part 50 relevant to the containment design basis, the staff is reviewing the applicant's analytical model and assumptions used in the GEH LTR NEDC-33922P, Revision 0, BWRX-300 Containment Evaluation (CE) Method. An important objective of this LTR review is to assess the conservativisms and non-conservatisms associated with the presented GOTHIC model, in order to determine whether the CE methodology would be acceptably conservative and physically meaningful with respect to the containment thermal-hydraulic response. The staff needs to ensure that the BWRX-300 CE methodology incorporates sufficient conservatism to analyze the short-term and long-term containment thermal hydraulics response to the limiting design basis events (DBEs) to offset the inherent methodology uncertainties. In this regard, the applicant is requested to provide the following additional information regarding the precedent-setting BWRX-300 containment nodalization approach used in the GOTHIC code.

Request

1. In the GEH LTR NEDC-33922P, a containment nodalization study is presented for the large steam line break (LBLOCA) event. [[

   ]]. However, LTR Figure 6-12 shows that a [[

]] for the LBLOCA base case. This demonstrates that [[ ]] result in more conservative results. In this backdrop, the applicant is requested to justify that the default [[ ]] choice is sufficiently conservative to bound the uncertainties in the LBLOCA containment analysis, or provide an upper bound on the non-conservatism inherent in finer nodalizations for conservative LBLOCA case.

The plots in Figures 6-26 and 6-27 show the [[ ]] for the conservative LBLOCA case, though they are not documented in the LTR as such. As they are among the most important parameters predicted by the CE methodology, the staff requests documenting the limiting PCP and maximum shell temperature values for the conservative case in the LTR as updated by the break location and break flow direction sensitivity studies requested in RAI 06.02.01-03. This information is needed by the staff to establish the overall conservatism in the containment evaluation (CE) methodology for LBLOCA.

2. The small break LOCA (SBLOCA) and LBLOCA are different DBEs that involve different phenomenological concerns. However, the staff noted that no containment nodalization study is presented in the LTR for the SBLOCA. As the break flow is [[ ]]. As shown by Figure 6-17, [[ ]]. LTR Figures 6-12 and 6-13 show [[ ]]. These phenomena are equally applicable to SBLOCA. With the complex SBLOCA phenomenology involving the novel PCCS design and Reactor Cavity pool heat-up in the later stage of transient, [[ ]].

   Therefore, the applicant is requested to provide information to confirm that the nodalization is adequate for SBLOCA, consistent with the information provided for LBLOCA. For this purpose, the staff requests GEH to provide similar justification for nodalization used in the limiting SBLOCA analysis up to 72 hours to demonstrate that the predicted limiting containment pressure and temperature responses remain conservative and insensitive to nodalization changes, and to quantify the conservatisms in the [[ ]]. The associated PCCS temperature plots (similar to LTR Figure 6-32), PCCS heat removal rate plots, and the containment steam volume fraction plots (similar to Figure 6-17) in the SBLOCA nodalization study should be included and discussed.

Revised GEH Response to NRC Question 06.02.01-01

1. The nodalization study is performed to demonstrate that the results are sufficiently converged as the node size is decreased. The purpose of nodalization is not to introduce additional conservatism, but to increase the accuracy by ensuring that the spatial gradients of the phenomena controlling the containment response are adequately resolved. Increasing the node size (i.e., coarser nodalization) will provide less accurate results but does not necessarily assure that those results will be conservative for all cases. The differences between the base case and the finer nodalization cases are approximately [[ ]], as shown in Figure 6-12 of the Licensing Topical Report (LTR). This can be compared to the difference between the base case and the conservative case shown in Figure 6-26 in Revision 1 of the LTR. The difference between the peak pressures for the base and conservative cases is approximately [[ ]]. This result shows that the additional resolution resulting from finer nodalization beyond the base case is much smaller than the conservatism introduced by biasing the inputs and modeling parameters, and the results using the base case nodalization are in the conservative direction.

2. A nodalization study was performed for the small breaks. The results of the study are presented below.

   The purpose of the small break cases is to show that the containment pressure resulting from small breaks is bounded by the containment pressure resulting from the large break cases. The small break cases also demonstrate that the containment does not stay at the peak pressure in the long term and that the pressure decreases. The target for the containment depressurization rate is to reduce the containment pressure to half of the peak accident pressure of the most limiting case within 24 hours. For the BWRX-300, the decrease in the containment pressure in the long term is primarily accomplished by the isolation condensers as demonstrated below.

   A small break case was performed to maximize the containment pressure as presented in the GEH response to NRC Question 06.02.01-03 (eRAI 9862) (Reference R9862-1) using the base case [[ ]] nodes (the first number is the number of nodes in the x-direction, the second number is the number of nodes in the y-direction, and the last number is the number of nodes in the axial direction). This case uses the conservative inputs and model biases. In the nodalization study presented here, the same case was run using [[ ]] nodes. The results presented in the original GEH response to this NRC question (Reference R9862-2) contained a large conservatism in the containment response to small break cases, which was not intended. In this revised response, the condensation film thickness calculation was corrected to calculate the heat removal rate of the Passive Containment Cooling System (PCCS) units consistent with the method described in Section 6 of the LTR.

   [[

]]

The comparisons for the small break nodalization study are shown in Figure 9862-19.

The nodalization study cases were run until the Reactor Pressure Vessel (RPV) pressure falls below the containment pressure. Once the RPV and containment pressures equalize, the

containment pressure will not exceed the RPV pressure. There are two RPV pressures plotted in Figure 9862-19. The solid line is the RPV pressure with a small steam pipe break. This line is applicable until the break flow becomes unchoked. As discussed in the LTR, the break flow is calculated assuming no containment back pressure (i.e., the break flow is calculated assuming the containment remains at atmospheric pressure). When containment back pressure is not considered, the RPV pressure remains sufficiently above atmospheric pressure, and the break flow remains choked for 72 hours. The solid line is consistent with the cases presented in Chapter 5 of the LTR.

As the event progresses, the RPV pressure decreases and the containment pressure increases. Realistically, when containment back pressure is considered, the break flow becomes unchoked when the pressure differential between the RPV and the containment becomes low enough. The RPV and containment pressures eventually equalize, after which there is essentially no more mass discharged to the containment unless the containment pressure decreases at a faster rate than the RPV pressure. Instead of resolving exactly when the break flow becomes unchoked and when it stops, the upper and lower bounds for the RPV pressure are plotted in Figure 9862-19. The small break case is the lower bound (solid red line) and the no break case is the upper bound (dashed red line) for the RPV pressure. The actual RPV pressure would be between these two lines. The fact that the upper and lower bounds for the RPV pressure are close to each other indicates that the primary mechanism for the RPV depressurization is the heat removal by the isolation condensers, not the energy discharged by the break flow. As expected, with time, the RPV pressures calculated with and without break flow converge and continue to decrease together because the decreasing break flow with time becomes less important in determining the RPV pressure.

The containment pressure is calculated assuming no reduction in the break flow rate due to the containment back pressure. There are several containment pressures shown in Figure 9862-19 corresponding to the different nodalization cases. As an example, the containment pressure calculated for [[ ]] nodes is shown by the solid black line in Figure 9862-19. The containment and RPV pressures equalize at approximately [[ ]] in this case. Because the break flow to the containment is practically zero after this point for the remainder of the transient, the PCCS and containment dome are removing more energy from the containment than the energy being added from the RPV. As a result, the RPV and the containment pressure start to decrease. This is shown with the dashed black line in Figure 9862-19. When the containment pressure starts falling below the RPV pressure, there will be a small break flow again which prevents the containment pressure from falling much below the RPV pressure. However, the containment pressure will not exceed the RPV pressure in any case. It follows that the actual containment pressure is between the red dashed line and the black dashed line in Figure 9862-19. The plotted lines in Figure 9862-19 show that the long term containment pressures for all SBLOCA cases are reduced to less than 50% of the peak pressure from the LBLOCA in less than 24 hours (86,400 seconds).

The nodalization study was performed up to the point where the containment and RPV pressures equalize. The cases include [[ ]], in addition to the

base case of [[ ]] nodes. [[
]]

The nodalization of the PCCS units in the axial direction is the same as the containment axial nodalization in all cases. In the base case, which has [[ ]] total axial nodes in the containment, the PCCS model has [[ ]] heated nodes in the axial direction and one (1) unheated node at the top representing the section of the PCCS above the containment, as shown in Figure 6-3 of LTR. The heated PCCS nodes are aligned with containment nodes [[ ]]. In the [[ ]] case, the PCCS has [[ ]] heated axial nodes aligned with containment axial nodes [[ ]] and one (1) unheated top node. In the [[ ]] case, the PCCS has [[ ]] heated nodes aligned with containment axial nodes [[ ]], and one (1) unheated top node.

The PCCS units are placed in one cell in the horizontal direction that is closest to their actual location.

The coarse nodalization case ([[ ]]), shown by the blue curve in Figure 9862-19, results in [[ ]]. As compared to the finer nodalization cases, this case [[ ]] the containment pressure. It can be concluded by comparing the results of the [[ ]] and [[ ]] cases that refinement of nodalization in the radial direction does not change the results. There is a small effect due to the nodalization in the axial direction. All cases display a similar pressure trend and magnitude. The peak pressure for the bounding accident, a large steam pipe break, is shown with a dotted-dashed line at approximately [[ ]] in Figure 9862-19. As shown, the containment pressure resulting from a small break is well below that of the large break case. In addition, the containment pressure in the long term is limited by the RPV pressure, and any calculated differences resulting from the nodalization scheme used in the containment small break analyses do not have an effect on the bounding long term containment pressure.

The steam volume fraction distributions in the containment are plotted in Figure 9862-20. The color palette is set to exaggerate any stratification effects. This figure shows that the [[ ]] nodalization underestimates the stratification, and consequently predicts lower steam fractions at the PCCS locations as compared to the steam fractions calculated using the finer nodalizations. As a result, the condensation rate is smaller and the containment pressure is higher than the other cases. The other nodalization schemes ([[ ]]) provide reasonably close results. The steam volume fraction distributions shown in Figure 9862-20 are consistent with the trends in pressure displayed in Figure 9862-19. The PCCS heat removal rate and temperatures are shown in Figures 9862-21 and 9862-22. As shown by the trends in Figure 9862-21, all the nodalizations indicate that the PCCS heat removal rates are, in the long term, approaching a similar asymptotic value that is sufficient to cause the containment to continue to depressurize as shown in Figure 9862-19. The reactor cavity pool is not being actively cooled so it will continue to heat up; however, the temperature difference between the pool and the PCCS exit temperature which is indicative of the heat removal rate remains approximately the same. Because decay heat is being removed by the

isolation condenser system, there is very little energy being deposited into the containment from the RPV after about [[ ]]. Even as the reactor cavity pool slowly heats up, the PCCS will continue to cool and depressurize the containment to an even lower value long term after the break flow becomes practically zero by moving energy that is already in the containment to the reactor cavity pool until the containment and reactor cavity pool temperatures approach within a few degrees of each other. Although there are some variations with nodalization, they do not have a significant effect on the containment pressure with nodalizations of [[ ]] and finer as shown in Figure 9862-19. The [[ ]] nodalization case overpredicts the containment pressure due to lack of resolution in steam stratification.

Based on the conclusions of the large break nodalization study and the results of the small break nodalization study discussed above, the use of the base case [[ ]] nodalization for the small break containment analyses is adequate and further refinement of the containment node size does not increase confidence in the results with respect to the purpose of the small break analyses.

[[

]]

Figure 9862-19. Nodalization Study for Small Steam Pipe Breaks

[[

]]

[[

]]

Figure 9862-20. Steam Volume Fraction Distribution in the Containment

[[

]]

Figure 9862-21. Heat Removal Rates by the PCCS and the Steam Dome

Note: Negative values indicate heat removal from the containment.

[[

]]

Figure 9862-22. PCCS Exit and Reactor Cavity Pool Temperatures

References

R9862-1 GEH Letter M210099, "Response to Requests for Additional Information (eRAIs) 9854, 9856, and 9862 and Supplemental Response to eRAI 9817 for Licensing Topical Report NEDC 33922P, Revision 0, BWRX 300 Containment Evaluation Method," September 17, 2021.

R9862-2 GEH Letter M210132, "Response to Request for Additional Information (eRAI) 9862 for Licensing Topical Report NEDC-33922P, Revision 0, BWRX-300 Containment Evaluation Method," October 29, 2021.

Proposed Changes to NEDC-33922P Revision 1

The following figures have been updated in Revision 2 of the LTR:

- Figure 6-2
- Figures 6-4 through 6-13
- Figures 6-15 through 6-17
- Figures 6-26 through 6-44

Table 6-6 and any text in the LTR affected by the modified figures have been updated in Revision 2 of the LTR.

Appendix B
Replaced Pages from NEDC-33922P, Revision 1

REVISION SUMMARY

Revision Number	Description of Change
0	Initial Submittal
1	Revised to incorporate the following responses to NRC Requests for Additional Information (eRAIs): • NRC eRAI 9829 Question 06.02.04-01 revised Section 1.3. • NRC eRAI 9831 Question 06.02.01-02 revised Section 6.11. • NRC eRAI 9862 Question 06.02.01-01 added a new Section 1.4 and Table 6-6 and revised Sections 6.0, 6.10.1 and 6.10.2. • NRC eRAI 9862 Question 06.02.01-02 revised Section 6.10.2 and added Figures 6-39 to 6-41. • NRC eRAI 9862 Question 06.02.01-03 revised Sections 6.5, 6.6.1, 6.6.2, 6.10, 6.10.2 and 6.11 and revised Figures 6-26, 6-28, and 6-31. • NRC eRAI 9862 Question 06.02.01-05 revised Sections 6.10.2 and 6.11. • NRC eRAI 9862 Question 06.02.01-07 revised several figures. • NRC eRAI 9862 Question 06.02.01-08 revised Sections 6.5 and 6.8.2. Revised in response to the following Audit Issues: • Audit Issue 2 revised Figures 6-31 through 6-34. • Audit Issue 26 corrected Figures 5-3 and 5-4. • Audit Issue 30 revised Section 6.9 and clarified the legends in Figures 6-23, 6-24, and 6-25. • Audit Issue 35 corrected a broken link in Section 6.9. • Audit Issue 36 deleted all references to a design option in Sections 2.0 and 6.1 and Table 6-2. • Audit Issue 45 revised Section 6.5 and 6.8.2 to describe the steam dome biases in more detail. In general, the following figures were updated to reflect updated results: Figure 5-1, Figures 5-3 through 5-27, Figures 6-1, 6-4 through 6-10, 6-13, 6-16, 6-23 through 6-34, and 6-38 through 6-41. A new figure, Figure 6-42, was added. Because of the revisions noted above, the following additional revisions occurred:

Revision Number	Description of Change
	• Figures 6-39 and 6-40 were renumbered as Figures 6-43 and 6-44. • Section 6.10.3: Figure references were updated to reflect that Figures 6-39 and 6-40 were renumbered as Figures 6-43 and 6-44. The following additional editorial corrections were made: • Section 5.2.4: Added back in the missing equation for the radiolytic gas production correlation. • Corrected broken links in Sections 4.0, 6.0, 6.8, 6.8.2, 6.9, 6.10, and 6.11.

subcompartments are included in the analyses to determine the containment atmosphere remains sufficiently well mixed to preclude deflagration or detonation of combustible gases, and to demonstrate that the containment internal structures forming the boundaries of the subcompartments do not experience large pressure differentials [[ ]]. Jet loads that may be exerted on structures and equipment in containment are addressed as part of the structural loads evaluation that will be submitted in a future licensing submittal.

1.3 Acceptance Criteria

The evaluation method demonstrates that the BWRX-300 containment meets the following acceptance criteria:

- Accident pressure and temperature are less than design pressure and temperature with appropriate margin
- Containment pressure is reduced to less than 50% of the peak accident pressure for the most limiting LOCA within 24 hours
- Containment pressure responses after 24 hours for LOCAs that do not produce the peak accident pressure are maintained below 50% of the peak pressure for the most limiting LOCA
- Containment atmosphere remains sufficiently mixed such that deflagration or detonation does not occur inside containment

Containment venting or leakage shall not be credited for at least 72 hours in demonstrating that the above acceptance criteria are met during a design basis event or accident.

Regulatory Guides (RG) 1.203 (Reference 7.3) and RG 1.157 (Reference 7.4) provide guidance for acceptable evaluation methods applicable to light water reactors. RG 1.157 provides analyses guidance for demonstrating compliance to the fuel clad integrity requirements of 10 CFR 50.46 “Acceptance criteria for emergency core cooling systems in light water nuclear power reactors”. The BWRX-300 LOCA sequences do not progress into significant core uncovery and refill/reflooding. BWRX-300 LOCAs do not result in significant fuel heat-up and oxidation and are not mitigated by an active injection system. Therefore, most RG 1.157 guidance are not applicable to the BWRX-300 LOCA analyses. Only the RG 1.157 guidance relating to the general best practice elements of a rigorous method development are applicable. These best practice elements are also included in RG 1.203. RG 1.203 provides guidance for all elements and stages of developing an acceptable method and references the CSAU analysis methodology (Reference 7.12). The BWRX-300 containment analysis utilizes mature computer codes that have been widely reviewed and used. The application method presented in this LTR addresses conformance with the RG 1.203 elements that are applicable to those mature codes and the CSAU methodology.

1.4 Methodology Overview

TRACG calculates the mass and energy release from modeled breaks of various sizes and locations (Section 5.2.2). In all cases, atmospheric pressure is used for the TRACG pressure boundary condition at the break. This approach provides no credit for the back pressure from containment; consequently, the retained RPV inventory calculated by TRACG represents the minimum

condition as though the break occurred outside containment. Breaks inside containment would realistically experience back pressure from the containment which would reduce the mass and energy release calculated by TRACG once the break flow became unchoked; however, this effect is not treated explicitly because it would require two-way coupling between the TRACG calculation and the GOTHIC containment calculation. Instead, the methodology has only a one-way coupling with the mass and energy release rates conservatively calculated by TRACG supplied as inputs to the GOTHIC calculation up until the point in time when the containment and RPV pressures first match. Choked flow naturally satisfies the assumed one-way coupling because the calculated choked flow rate does not depend on the downstream pressure. Select TRACG inputs are specified (Section 5.2.5 and 5.2.6) so that mass and energy release rates will be conservatively calculated.

For large breaks, the rapid mass and energy release into the containment before the break is isolated leads to the highest containment peak pressure, which occurs at approximately the same time that the break is isolated. For large breaks, the containment shell is the dominant short term energy sink; heat transfer to the containment shell will cause the containment pressure to decrease from its peak value after isolation of the break occurs. The large steam line break determines the overall highest peak containment pressure as shown by the demonstration calculations provided in Section 6.10.

Compared to the large breaks, small unisolated breaks have a much slower mass and energy release rate from the RPV into the containment. The lowest break on the RPV that remains unisolated and occurs outside the containment will produce the most limiting scenario for minimum RPV inventory. Regardless of break location and whether the break is inside or outside containment, the break flow will slowly decrease with time because the RPV is being depressurized largely by the ICS operation with some contribution from the energy released in the break flow. The containment pressure will slowly increase and eventually equal the RPV pressure if the break is inside containment. After the point in time when the containment and RPV pressures first become equal, it is no longer realistic to use the TRACG break flow that was calculated using an atmospheric pressure boundary condition as input to the GOTHIC containment calculation. The methodology does not require the GOTHIC calculation to continue beyond the point where the containment and RPV pressures equalize because the longer-term containment pressure will be bounded by the RPV pressure calculated by assuming zero break flow provided that the PCCS is depressurizing containment faster than the ICS is depressurizing the RPV for the case of zero break flow beyond the intersection time.

2.0 OVERVIEW OF THE BWRX-300 RPV AND CONTAINMENT FEATURES PERTINENT TO THE APPLICATION METHOD

The BWRX-300 RPV and internals are shown on Figure 2-1 and described in Reference 7.1. The Isolation Condensers (IC) are also described in Reference 7.1 with illustrations included on Figure 2-2 and Figure 2-3. As described in Reference 7.1, all piping [[

]]. For an ICS train, the RPV isolation valves on both the steam and condensate pipes for that train close when a break is detected in that train. All other RPV isolation valves close on detection of high drywell pressure. Isolation condensers are initiated on [[

]]. The other isolation and initiations signals are described in References 7.1 and 7.2 and not repeated here because they are not pertinent to the containment thermal-hydraulic response analyses.

A conceptual containment design, penetrations and Passive Containment Cooling System (PCCS) are also described in Reference 7.2. As stated in NEDC-33911P, the containment structure, shape and PCCS design may be different, but the containment design would be functionally the same. The containment conceptual design has evolved subsequent to the issuance of Reference 7.2. The containment shape shown on Figure 2-4 is the configuration used in the method development because [[

]]. Regardless of the type of the vessel support, it is necessary that the support structure has large openings for personnel access and maintenance or replacement of the control blades and control rod drives.

Containment penetrations and containment isolation valves are also discussed in Reference 7.2.

The following containment design features are relevant to the purposes of this report:

- Containment is a dry enclosure, near atmospheric pressure during normal operation
- Containment design pressure and temperature are within the experience base of conventional BWRs
- Containment is inerted with nitrogen during normal operation
- There are no subcompartments containing large bore high energy lines
- The subcompartments have sufficiently large openings such that the boundaries of the subcompartments do not experience large pressure differentials resulting from pipe breaks outside the subcompartments.
- The PCCS [[

]].

4.0 OVERVIEW OF THE EVALUATION MODEL

TRACG is used to evaluate the mass and energy release from the BWRX-300 RPV, and GOTHIC is used to evaluate the BWRX-300 containment response. As shown in this report, there is no adverse effect of containment backpressure on the TRACG mass and energy releases. As a result, there is no need to iterate between the two codes to obtain a best estimate solution for the mass and energy release, and the application method is not dependent on predicting back pressure. Instead, mass and energy releases calculated by TRACG are used as a boundary condition in the GOTHIC calculations, and the containment pressure and temperature response are calculated using GOTHIC.

The mass and energy release model for the BWRX-300 containment response utilizes the applicable parts of the approved LTR, TRACG Application for ESBWR (Reference 7.10), which is incorporated in the approved ESBWR Design Certification (Reference 7.11). Section 5.0 of this report details the application of the ESBWR TRACG method to the BWRX-300.

As described in NEDC-33911P, Section 2.0, the BWRX-300 containment design is much simpler than the ESBWR containment, and many of the ESBWR containment phenomena do not apply to the BWRX-300 containment. Phenomena that are of secondary importance to the ESBWR containment response may become important to the BWRX-300 containment response. Therefore, a new containment model using GOTHIC has been developed for the BWRX-300 and is presented in this LTR. GOTHIC is a continuously maintained and improved computer code. The GOTHIC code has been developed compliant with 10 CFR 50, Appendix B requirements and meets the GEH software quality requirements. The results in this report have been generated using GOTHIC Version 8.3 that is the latest released version at this time. Future BWRX-300 containment analyses may be performed using newer versions of the GOTHIC code provided the newer versions meet the same 10 CFR50 Appendix B quality requirements and changes in calculated results for our BWRX-300 containment application caused by any code changes can be successfully dispositioned.

The evaluation method for the BWRX-300 containment response to design basis events has been developed following the applicable elements of Regulatory Guide 1.203 (Reference 7.3). The application method includes base cases and conservative cases. The individual key inputs, assumptions and modeling parameters are conservatively biased simultaneously in the conservative cases, rather than sampling the uncertainties and adding margin to the base case results. While this method compounds conservatisms, it gives reasonable assurance that the overall method results bound the uncertainties, and greatly reduces the number of sensitivity calculations. This is the same approach that was taken for the ESBWR containment method in Reference 7.10. The containment response method is described in detail in Section 6.

5.0 TRACG METHOD FOR MASS AND ENERGY RELEASE

5.1 TRACG Code and Qualification

TRACG is the GE Hitachi Nuclear (GEH) proprietary version of the Transient Reactor Analysis Code (TRAC). TRACG uses realistic one-dimensional and three-dimensional (3D) models and numerical methods to simulate phenomena that are experienced in the operation of boiling water reactors (BWRs). TRACG code and models are described in detail in Reference 7.5. The TRACG qualification report, Reference 7.6, includes comparisons of TRACG calculations with data from separate effects, component performance and integral system effects tests that directly support its use for BWR LOCA analyses. References 7.7 and 7.8 present TRACG qualification specifically for natural circulation plants with IC systems similar to the BWRX-300.

TRACG ECCS-LOCA analysis method for BWR/2–6 (Reference 7.9) and for ESBWR (Reference 7.10) have been approved previously. The uncertainties in the TRACG ECCS-LOCA analysis methods are quantified for the BWR/2-6 application method in Reference 7.9, and for ESBWR in Reference 7.10. It should be noted that only the uncertainties relating to RPV inventory and break flow would be accounted for in the BWRX-300 application because like the ESBWR application, the core always remains well cooled.

5.2 Application of the ESBWR TRACG LOCA Method to BWRX-300 Mass and Energy Release Calculations

The BWRX-300 RPV is an evolution of the ESBWR RPV. The main differences between the BWRX-300 RPV and ESBWR RPV are the RPV dimensions, connected piping, and the RPV isolation functions. These differences affect the modeling inputs but are still within the same qualified application range as the ESBWR. The BWRX-300 operating accident pressure and temperature ranges are similar to the ESBWR operating pressure and temperature ranges.

As discussed in this LTR, significant fuel heat-up does not occur in the BWRX-300 as is the case for the ESBWR. The phenomena that affect the mass and energy release from the BWRX-300 RPV case also apply to the ESBWR mass and energy release. The modeling, experimental and scaling uncertainties identified for ESBWR are also relevant to the BWRX-300 design. Therefore, the TRACG qualification for the ESBWR application equally applies to the BWRX-300 application. Furthermore, the BWRX-300 mass and energy release analysis is much less challenging than the ESBWR analysis for mass and energy release from a large break because the BWRX-300 large breaks are isolated. Small breaks are slow evolving events where the modeling and phenomenological uncertainties are significantly diminished.

In the BWRX-300, the RPV is isolated following a large break LOCA. After the isolation valves closure, the energy generated by decay heat must be removed directly from the RPV. Therefore, it is not appropriate to make the same assumptions as were made for the ESBWR where the PCCS is credited as the primary heat removal for ECCS-LOCA and containment analyses, while the ICS is credited for transients, but not for ECCS-LOCA or containment analyses. The BWRX-300 ICS is credited in accordance with its purpose, specification, and safety classification. The BWRX-300 ICs modeling and TRACG qualification are discussed in detail in Section 5.2.4.

The ESBWR TRACG LOCA method in Reference 7.10 includes ECCS-LOCA analysis and containment analysis. The TRACG models used for these analyses have some differences. The TRACG RPV model used for the ECCS-LOCA analysis (Figure 2.7-1 of Reference 7.10) is more

performed for the Simplified Boiling Water Reactor (SBWR) design and supplemented for ESBWR design.

TRACG qualification for ICS is based on two sets of PANDA tests as described in Reference 7.7: the M-series tests, which are used in the TRACG qualification for SBWR, and the later complimentary P-series tests for ESBWR configuration, including the effects of the non-condensable gases. TRACG04 is qualified based on both sets of tests, and for both water and steam, and steam containing air or helium (Reference 7.8).

Because there is no significant oxidation in the BWRX-300, the only non-condensable gases that may migrate into the IC tubes are the radiolysis products following a design basis LOCA. [[

]] The build-up of hydrogen and oxygen in steam following a one-inch liquid break is shown on Figure 5-1.

Unlike hydrogen generated from cladding oxidation, hydrogen and oxygen liberate from radiolysis at a slow rate and distributes over a relatively large region. The gases become mixed in water both in steam and liquid phases. The well-mixed hydrogen and oxygen in steam also migrates into the ICs when the ICs are put in service. The hydrogen and oxygen concentration in steam may increase as the steam condenses in the IC tubes. It should be noted that because hydrogen and oxygen are mixed in water when they are formed near the core region, they do not separate from water or steam again until the steam condenses.

The effect of the radiolytic gases on the ICs has been determined using TRACG. [[

]] Nevertheless, a bias was applied to the IC performance to account for degradation due to the potential of radiolytic gas build-up.

[[

]]

Figure 5-1: Volume Fraction of Radiolytic Gases ($H_2 + O_2$) in Steam in the RPV Following a 1-Inch Liquid Break

5.2.5 Modeling Biases (PIRTs)

TRACG has a feature to bias various modeling parameters, which are called PIRTs. A TRACG PIRT is a coefficient which multiplies an internally calculated nominal value over a specified range of the solution domain. The PIRTs used in the ESBWR TRACG application (Reference 7.10) for conservative cases are listed in Table 5-1. [[

[[

]]

Figure 5-3: Main Steam, Feedwater and Instrument Piping Attached to the RPV

[[

]]

Figure 5-4: TRACG IC Modeling for BWRX-300

5.3 Demonstration Cases for Large Breaks

The worst assumed single failure for a large break is the loss of an ICS train. [[

]]. For all other breaks, two ICS trains are available to remove the decay heat and depressurize the RPV after the loss of one ICS train due to a single failure. [[

]].

The large feedwater pipe break cases consider reduced feedwater temperature [[

]]. The results of the large feedwater pipe breaks are shown on Figure 5-8 through Figure 5-10.

In the steam pipe break cases, scram signal is inserted due to [[

]].

5.3.2 Conservative Case for Large Feedwater and Steam Breaks

The results of the large steam pipe breaks are shown on Figure 5-11 through Figure 5-13. The discussions in Section 5.3.1 for the base case also apply to the conservative case.

[[

]].

The results for the large feedwater pipe breaks are shown in Figure 5-15 through Figure 5-17. [[

]].

5.4 Demonstration Cases for Small Breaks

Base and conservative cases were run for the small steam and liquid pipe break cases. The small break events are slowly evolving events; therefore, the trends for the base and conservative steam and liquid breaks are very similar to each other. The results of the conservative small steam and liquid break cases are shown and discussed in this section.

The results of the conservative case for small break are shown on Figure 5-18 through Figure 5-22. As shown on Figure 5-18 and Figure 5-19, the ICS heat removal rate decreases as the RPV pressure decreases. The difference between the heat removed by the ICS and the power generated by decay heat is what is discharged from the break. The pressure boundary condition used in the TRACG calculation remains at atmospheric pressure to maximize the break flow rate. [[

]].

Reactor trip occurs due to load rejection in the small pipe break cases. RPV isolation valves are closed when the containment pressure exceeds the high containment pressure trip setpoint. The delay in this trip can be estimated conservatively.

[[

]]

[[

]]

Figure 5-5: Reactor Power, Main Steam Pipe Break, Base Case

Note: Decay Heat curve represents fission power as well as decay heat. Q IC-A is the heat removal rate by ICS Train A.

[[

]]

Figure 5-6: RPV Pressure, Main Steam Pipe Break, Base Case

[[

]]

Figure 5-7: Break Flow Rate and Enthalpy, Main Steam Pipe Break, Base Case

[[

]]

Figure 5-8: Reactor Power, Feedwater Pipe Break, Base Case

Note: Decay Heat curve represents fission power as well as decay heat. [[
]]

[[

]]

Figure 5-9: RPV Pressure, Feedwater Pipe Break, Base Case

[[

]]

Figure 5-10: Break Flow Rate and Enthalpy, Feedwater Pipe Break, Base Case

[[

]]

Figure 5-11: Reactor Power, Main Steam Pipe Break, Conservative Case

Note: Decay Heat curve represents fission power as well as decay heat. [[
]]

[[

]]

Figure 5-12: RPV Pressure, Main Steam Pipe Break, Conservative Case

[[

]]

Figure 5-13: Break Flow Rate and Enthalpy, Main Steam Pipe Break, Conservative Case

[[

]]

Figure 5-14: RPV Level, Main Steam Pipe Break, Base and Conservative Cases

[[

]]

Figure 5-15: Reactor Power, Feedwater Pipe Break, Conservative Case

Note: Decay Heat curve represents fission power as well as decay heat. [[
]]

[[

]]

Figure 5-16: RPV Pressure, Feedwater Pipe Break, Conservative Case

[[

]]

Figure 5-17: Break Flow Rate and Enthalpy, Feedwater Pipe Break, Conservative Case

[[

]]

Figure 5-18: Power, Small Steam Break, 2 ICS Trains, Conservative Case

Note: Decay Heat curve represents fission power as well as decay heat. [[
]]

[[

]]

Figure 5-19: RPV Pressure, Small Steam Break, 2 ICS Trains, Conservative Case

[[

]]

Figure 5-20: RPV Level, Small Steam Break, 2 ICS Trains, Conservative Case

[[

]]

Figure 5-21: PCT, Small Steam Break, 2 ICS Trains, Conservative Case

[[

]]

Figure 5-22: Break Flow Rate and Enthalpy, Small Steam Break, 2 ICS Trains, Conservative Case

Note: The initial break flow rate is off-scale. [[
]]

[[

]]

Figure 5-23: Power, Small Liquid Break, 2 ICS Trains, Conservative Case

Note: Decay Heat curve represents fission power as well as decay heat. [[
]]

[[

]]

Figure 5-24: RPV Pressure, Small Liquid Break, 2 ICS Trains, Conservative Case

[[

]]

Figure 5-25: RPV Level, Small Liquid Break, 2 ICS Trains, Conservative Case

[[

]]

Figure 5-26: PCT, Small Liquid Break, 2 ICS Trains, Conservative Case

[[

]]

Figure 5-27: Break Flow Rate and Enthalpy, Small Liquid Break, 2 ICS Trains, Conservative Case

6.0 CONTAINMENT ANALYSIS METHOD USING GOTHIC

The GOTHIC application methodology includes base cases and conservative cases. For the base cases, nominal inputs, assumptions, and correlations are used. The individual key inputs, assumptions and modeling parameters are conservatively biased simultaneously in the conservative cases, rather than sampling the uncertainties and adding margin to the base case results. While this method compounds conservatisms, it gives reasonable assurance that the overall method results bound the uncertainties, and greatly reduces the number of sensitivity runs. This is the same approach that was taken for the ESBWR containment method in Reference 7.10.

Sections 6.1 through 6.4 describe the identification of the relevant inputs and phenomena relevant to the BWRX-300 containment response and the selection of the models and correlations used to develop the base GOTHIC containment model. Section 6.5 describes the GOTHIC input model for the BWRX-300 containment. Section 6.6 describes the base cases and the results obtained from those base cases. Section 6.7 shows how nodalization impacts the calculated results. Sections 6.5 through 6.7 help to establish what model uncertainties and biases of the GOTHIC methodology are most important for application of the GOTHIC model for analyses of the BWRX-300 containment; that is why Sections 6.5 through 6.7 are presented before the discussion of the model biases and uncertainties in Section 6.8. Section 6.8 reviews the key model uncertainties and biases used in developing the conservative GOTHIC containment model. Section 6.9 provides benchmark predictions of test data. Demonstration analyses showing the BWRX-300 containment response for various break sizes and locations using the conservative GOTHIC containment model are provided in Section 6.10.

The large steam line break result described in Section 6.10.1 produces the highest calculated containment pressure. Containment pressure and temperature responses calculated using the conservative case assumptions are compared to the base case results to quantify the amount of conservatism provided by the methodology.

The small steam or liquid breaks described in Section 6.10.2 demonstrate that the peak containment pressures from unisolated small breaks are well below the peak pressure resulting from the large steam break. The small break calculations are primarily useful for demonstrating the capability of the PCCS to reduce the containment pressure in the longer term. The methodology assumes a one-way coupling between the TRACG and GOTHIC calculations whereby atmospheric pressure is always used for the break boundary condition used to calculate conservative TRACG mass and energy release rates that are input to the GOTHIC containment calculation. This methodology is demonstrated in Section 6.10.2 to result in peak containment pressures from the small breaks that are greater or more conservative than what would be obtained if a more complex two-way coupled methodology that credits how increased containment pressure were used. After the containment pressure increases to the RPV pressure, the RPV pressure calculated without a break bounds the containment pressure.

6.1 GOTHIC Phenomenon Identification and Ranking Table (PIRT)

The PIRT purpose is to identify phenomena important to the analysis of the BWRX-300 containment response for design basis events. The phenomena is then used to assess the ability of the model to calculate the effect of the phenomena on containment pressure and temperature, and the qualification of the evaluation model for calculating the phenomena, including the available

tests and determining any additional testing, scaling or analysis needed to qualify GOTHIC for the BWRX-300.

The initial phenomena list relevant to BWRX-300 containment analysis has been obtained by reviewing the following sources:

- NEDC-33083P-A Revision 1, TRACG Application for ESBWR (Reference 7.10)
- NEA/CSNI/R3(2014), Containment Code Validation Matrix (Reference 7.13)
- SMSAB-02-02, An Assessment of CONTAIN 2.0: A Focus on Containment Thermal Hydraulics (Including Hydrogen Distributions) (Reference 7.14)

Table 3.2-1 of Reference 7.10 was reviewed for phenomena that are applicable to the BWRX-300 containment pressure and temperature analysis, including phenomena that would have an equivalent phenomena in BWRX-300, even if the component was of a different design (for example, the secondary side heat transfer to the ultimate sink pools was evaluated because the phenomena are equivalent for the [[ ]]).

Two additional references (References 7.13 and 7.14) were used for additional important phenomena that might apply to the BWRX-300, but not to the ESBWR. This provides a complete check that covers phenomena that were not determined important for ESBWR but might be important for the BWRX-300. Table 3-1, *Containment Thermal Hydraulics Phenomena*, and Table 3-6, *Systems Phenomena*, of Reference 7.13 were reviewed. Note that the phenomena applicable only to the beyond design basis events and severe accidents are not included in the review. Reference 7.13 report classifies the significance of phenomena as Major/Minor. Phenomena evaluated as having major significance were reviewed for BWRX-300 applicability. The phenomena were then correlated with the ESBWR PIRT to eliminate duplication.

The third reference (Reference 7.14) contains Table 2.3, *Illustrative Phenomena Identification and Ranking Table for Containment Thermal Hydraulics*, during the Rapid Pressurization Phase of a Design Basis Accident in a Large Dry Pressurized Water Reactor Containment. This Table repeats the same phenomenon in different structures/components of the containment, but if the phenomenon was ranked H, M or L-M for either Pressure or Temperature, it was evaluated for correlation with the phenomenon in the previous two sources. Note that fan dynamics, spray dynamics and spray mass and energy exchange are not applicable to BWRX-300 and are not evaluated. All the buoyancy phenomena in Reference 7.14 are combined into one buoyancy phenomena, and the convection/advection phenomena are combined. The phenomena in Reference 7.14 report phenomena are then correlated with the ESBWR PIRT to eliminate duplication.

The names of phenomena are different in the reports cited above, although they refer to the same phenomena. For the BWRX-300 containment PIRT, the phenomena names and descriptions provided in Reference 7.10 were generally used.

6.2 PIRT Survey

The initial list of PIRTs was distributed in a survey to six Subject Matter Experts who reviewed the PIRT list, ranked them in importance to the GOTHIC BWRX-300 containment pressure and temperature analysis, and solicited any missing significant phenomena. The experts were provided with the BWRX-300 design description, including the information in Section 3.0 discussed previously. Phenomena ranking was requested according to the criteria in Table 6-1.

]]

6.5 GOTHIC Containment Model

A schematic of the GOTHIC model used for the BWRX-300 containment analysis is shown on Figure 6-1. Volume 1s represents the main section of the containment, Volume 2s represents the containment dome region above the refueling bellows, Volume 3s is the PCCS, and Volume 4 is the reactor cavity pool.

The containment dome is connected to the main section of the containment through two flow paths, 1 and 2, representing the manholes in the refueling bellows.

Flow paths 4 through 13 are the exit of the hot channels of the [[ ]] PCCS units connected to the reactor cavity. Flow paths 14 through 23 are the intake openings of the PCCS units connected to the reactor cavity pool. Flow paths 25 through 34 are openings between the cold tubes and heated tubes of the PCCS units at the bottom.

Three dimensional volumes, so-called subdivided volumes in GOTHIC terminology, are used to model the main section of containment. Nodalization of the main section (Volume 1s) and the containment dome (Volume 2s) used in the base model are shown on Figure 6-2.

The RPV is modeled by using a blockage corresponding to the outer dimensions of the RPV insulation as shown on Figure 6-2. Approximately [[ ]] of the remaining volume is assumed to be obstructed by various support structures, piping, catwalks, etc. Thermal conductors are distributed over cells on the RPV surfaces and where the piping is routed. The thermal conductor properties are set to the mirror insulation properties using conservative inputs to maximize the heat loads from the RPV and piping. The fluid temperature in the piping is assumed to be the same as the RPV fluid temperature and is specified as a function of time as obtained from the TRACG mass and energy release calculations.

The flow path representing the break flow is placed [[ ]], next to the containment shell and the break flow is directed toward the shell when calculating the peak shell temperature. [[

]] The break mass flow rate and enthalpy are specified as a function of time as obtained from the TRACG mass and energy release calculation.

Nodalization for the small containment dome region is shown in the upper right part of Figure 6-2. [[

]]

The PCCS is represented by subdivided volumes as shown on Figure 6-3. [[

]]

The following is a list of the key modeling parameters used in the base cases. The reasoning for the choice of the models and their uncertainties is discussed in Section 6.8.

- Mass and energy release are obtained from the TRACG base case results in Section 5.3.1 for large breaks.
- The form loss coefficients in the PCCS are set to conservatively high values, accounting for the flow losses due to the typical spacers, as well as entrance and exit losses and [[ ]].
- Wall friction is calculated from the Colebrook relationship for smooth wall.
- The heat transfer coefficient in containment is the sum of two parts as follows:
    - The Nusselt number for heat transfer due to sensible heat can be calculated from the forced convection or natural convection. The forced flow convection correlation is the Dittus-Boelter correlation given by:

      $$Nu_{FC} = 0.023\,\mathrm{Re}^{0.8}\,\mathrm{Pr}^{0.3}$$

      where Nu is the Nusselt number, Re is the Reynolds number, and Pr is the Prandtl number. Reynolds number is calculated based on the velocity and properties in the node next to the wall and the user-specified characteristic length. The exponent of the Prandtl number is 0.4 for the heated walls (RPV and hot piping).

      The Nu for heat transfer in natural convection is calculated from the [[

]]

The following relationship is used in GOTHIC to select which mode of heat transfer applies:

[[ ]]

- Heat transfer due to latent heat in condensation is calculated using the Diffusion Layer Model (DLM) (Section 9.1.6 of Reference 7.16).

- The characteristic length for the forced convection is set to the [[ ]].
- Radiation heat transfer to the shell and the PCCS is conservatively ignored.
- [[

]]

[[

]]

Figure 6-1: Schematic of the GOTHIC Model of BWRX-300 Containment

6.6 Base Cases and Results

This section presents the containment response for the mass and energy releases calculated in Section 5.3.1 for large steam and feedwater breaks using the base model described in Section 6.5. The key containment inputs are listed in Table 6-4. The containment nodalization and modeling parameters are described in Section 6.5.

Table 6-4: Containment Inputs Used in Base Cases

Parameter	Value
Containment height	[[
Containment diameter	
Free containment volume (excluding dome)	
Containment dome height	
Containment dome diameter	
Containment shell thickness	
Containment head thickness	
Number of manholes on the refueling bellows	
Diameter of the manholes	
Number of PCCS units	
PCCS type	
PCCS outer diameter	
PCCS outer pipe thickness	
PCCS cold tube outer diameter	
PCCS cold tube thickness	
PCCS height inside the containment	]]
Initial containment temperature	43.33 °C
Initial containment relative humidity	20%
Initial containment pressure	101.325 kPa
Initial reactor cavity pool temperature	43.33 °C

6.6.1 Containment Response to Large Steam Break, Base Case

The containment pressure response to a large break in a steam line is shown on Figure 6-4. The peak pressure [[ ]] is reached at the time the RPV isolation valves fully close at ten seconds. After the closure of the RPV isolation valves, the only heat input to the containment is due to convection from the RPV wall and hot pipe walls through the insulation. With the break flow isolated, the containment pressure starts decreasing. [[

]]

The airspace and containment shell temperature responses are shown on Figure 6-5. The maximum air temperature is the maximum of all nodal temperatures in the containment; the bulk temperature is the average air temperature throughout the containment. These temperatures are higher than the temperature resulting from the isenthalpic expansion of steam from the RPV conditions to the containment pressure. The additional temperature increase is due to the compression of nitrogen in containment. Following the break, there is a rigorous circulation of

the air in containment. Prior to isolation, the [[

]]. The peak temperature moves around in containment as the hot steam / nitrogen mixture circulates. After the break flow stops, the location of the maximum temperature continues to vary with the changing flow patterns, but most of the time remains in locations near the RPV wall.

Although the containment air temperature is high [[ ]], the containment shell remains at a much lower temperature. [[

]]

The PCCS exit temperature is also shown on Figure 6-5. [[

]] A sensitivity analysis for the PCCS is presented in Section 6.6.1.

The decay heat rate and the heat removal rates by the various heat removal mechanisms are plotted on Figure 6-6. As shown on the plot, the containment shell initially absorbs a large amount of energy for a short duration before the heat removal diminishes as the shell warms up [[ ]]. The isolation condensers are the primary mechanism for removing decay heat from the isolated RPV. [[

]] No credit is taken in these cases for the heat transfer from the containment shell to the concrete supporting structures.

The subcompartment formed by the containment head and refueling bellows is the limiting location with respect to differential pressures acting across subcompartment boundaries because of the relatively small flow areas provided by the access manholes in the bellows. The other subcompartments inside the containment (e.g., [[ ]]) have much larger openings. The pressure differential across the refueling bellows is shown on Figure 6-8. In this variation of the base case, the flow loss coefficient across the manholes is set to an extremely high value [[ ]] in order to maximize the differential pressure during the event. The GOTHIC model captures the pressure waves travelling through the containment immediately following the break, and the peaks and valleys in the pressure trend correspond to physical phenomena. The time

difference between the first peaks of the red and blue curves is consistent with the pressure wave travelling at nearly the speed of sound. [[ ]]. This is a small pressure differential across the boundary of a subcompartment. The pressure drop across the other subcompartment boundaries were not calculated because they have much larger flow area-to-volume ratios and are located farther away from the break, [[ ]].

If the pipe routing is designed such that a potential pipe break may occur in close proximity of the biological shield wall or vessel support, the same method used here can be used to assess the differential pressure loads to be considered in the detailed structural designs. However, if a significant pressure differential occurs across the biological shield due to the close proximity of the break, it is likely that the jet impingement loads would be the more limiting concern. The determination of the jet impingement loads acting on the containment structures is outside the scope of this LTR.

6.6.2 Containment Response to Large Feedwater Pipe Break

The containment pressure response to a large break in the feedwater pipe is shown on Figure 6-9. The peak pressure [[ ]] is reached at the time the RPV isolation valves fully close [[ ]]. Similar to the large steam break, after the closure of the RPV isolation valves the only heat input to the containment is from the RPV wall and hot pipe walls through the insulation. [[ ]] The peak containment pressure for a feedwater pipe break is bounded by the peak containment pressure for a large steam pipe break.

The airspace and containment shell temperature responses in the containment are shown on Figure 6-10. The containment temperature discussion in Section 6.6.1 also apply to the response to feedwater pipe breaks. It can be seen on Figure 6-10 that the shell temperature is well below the containment atmosphere temperature, [[ ]].

6.7 Nodalization Studies

6.7.1 Nodalization Study for Containment

A nodalization study was performed using the base case for the large main steam pipe break presented in Section 6.6.1.

The nodalization study for the main containment section included the following cases, also shown on Figure 6-11:

- Base case: [[ ]]
- Coarser grid. Twice the node size of the base case in each direction: [[ ]]
- Finer grid in the horizonal plane. Half the node size of the base case in each direction in the horizontal plane: [[ ]]. Same node size in the vertical direction
- Finer grid in the vertical direction: Half the node size of the base case in the vertical direction: [[ ]]. Same node size as in the base case in the horizontal plane

[[

]]

Figure 6-4: Containment Pressure Following Large Main Steam Pipe Break, Base Case

[[

]]

Figure 6-5: Temperatures in the Containment Following a Large Main Steam Pipe Break, Base Case

[[

]]

Figure 6-6: Heat Removal Rates by Various Mechanisms Following Large Main Steam Pipe Break, Base Case

[[

]]

Figure 6-7: Longer Term Heat Removal Rates by Various Mechanisms Following Large Main Steam Pipe Break, Base Case

[[

]]

Figure 6-8: Pressures Next to Refueling Bellows Following Large Main Steam Pipe Break, Base Case

[[

]]

Figure 6-9: Containment Pressure Following Large Feedwater Pipe Break, Base Case

[[

]]

Figure 6-10: Temperatures in the Containment Following a Large Feedwater Pipe Break, Base Case

[[

]]

Figure 6-13: Effect of Nodalization on the Containment Temperature Response to Large Steam Pipe Break, Base Case

[[

]]

Figure 6-14: Effect of Nodalization on the PCCS Heat Removal Rate

6.8 Model Uncertainties and Biases

The source of uncertainties in the phenomena important to the containment pressure and temperature response are identified in Section 6.2. The knowledge level for these phenomena is discussed in Section 6.4 and summarized in Table 6-3. The following is the grouping of phenomena and their assessment based on the observations from the results of the base case containment analysis discussed in Section 6.6.

- [[

]]

- Items 2, 5, 6, 11, 12 are inputs. [[

]].

- The natural and forced circulation and stratification are affected by the friction factors, turbulence modeling, and the model nodalization. A nodalization study is presented in Section 6.7 for the containment and PCCS. A sensitivity study for the friction factors and turbulence modeling is presented in Section 6.8.1 [[ ]]. This addresses Items 9, 10, 13, and 14.
- Uncertainties in the convection and condensation heat transfer coefficients, Items 3 and 7, are discussed in Section 6.8.2 where bounding values have been developed.
- In the RPV the production of hydrogen and oxygen by radiolysis is modeled by the bounding correlation given in Section 5.2.4. There are no other mechanisms for producing significant amounts of NC gases in either the RPV or the containment. [[ ]]. This addresses Items 19 and 20.
- Multi-component gas properties are calculated using the most accurate models available in the GOTHIC code as described in Reference 7.16.

6.8.1 Effect of the Friction Factors and Turbulence Parameters on the Containment Response

The importance of friction factors and turbulence on containment pressure and temperature response has been investigated by sensitivity studies for the containment and PCCS separately.

The nominal cases use Colbrook's friction factors for a smooth surface. To determine the sensitivity of the pressure and temperature to the friction factor, the relative roughness was increased [[ ]]. Given the large hydraulic diameter, this relative roughness corresponds to an unreasonably high absolute value of surface roughness [[ ]]. The increased surface roughness case is identified as the "High C_f" case in the comparisons.

[[

]]

The results obtained by the above sensitivity cases are compared on Figure 6-15 through Figure 6-17 for the large steam pipe break. [[

[[

]]

Figure 6-16: Effect of Friction and Turbulence on Containment Temperatures, Large Steam Pipe Break

Based on the above observations, the following are the minimum biases applied to the DLM and convection correlations used in the GOTHIC model of the BWRX-300 containment to ensure the calculated results are conservative.

Convection correlation bias:

- [[

]]

Condensation correlation bias:

- [[

]]

[[

]]

As will be shown in Section 6.9, the above biases bound the integral test data and also add conservatism to the BWRX-300 containment response results that is comparable to the conservatism that would be introduced by using the Uchida correlation. Comparisons of the BWRX-300 containment response predicted by the Uchida correlation and the biased DLM correlation will be presented in Section 6.10.1.

[[

]]

walls are concrete with a 6.35 millimeter (1/4 inch) thick steel liner, [[
]].

The CVTR test has several cases [[ ]]. Test case #3 is relevant to the BWRX-300 containment benchmarking [[

]] The GOTHIC model for CVTR is shown on Figure 6-22.

As discussed in Reference 7.17, the three-dimensional GOTHIC model using the best estimate DLM, including the Film Enhancement condensation heat transfer, predicts the measured pressure and thermal stratification closely. In the "biased DLM" cases presented here, the DLM method is used without the Film Enhancement feature and the biases in Section 6.8.2 are applied to the heat transfer surfaces. The comparisons also include the pressure and temperature predicted by the Uchida correlation. Uchida condensation correlation does not include a bias. However, the same bias described in Section 6.8.2 is also applied to the convection heat transfer in the Uchida correlation cases.

Figure 6-23 shows the containment pressure benchmarking to test data. The peak pressure calculated by the biased DLM heat transfer coefficient is approximately [[ ]] higher than the data. The biased DLM case also bounds the pressure predicted by the Uchida correlation.

Figure 6-24 shows the airspace temperature and Figure 6-25 shows the structure surface temperatures. The calculated temperatures are higher than the measured temperatures. The differences in the calculated temperatures on Figure 6-24 and Figure 6-25 at higher and lower elevations are close to the differences in the measured temperatures. These results indicate that GOTHIC predicts stratification well while there is steam flow and after the steam flow stops. The predicted surface temperatures are higher than the data.

[[

]]

Figure 6-23: GOTHIC Benchmarking to CVTR Test Data, Containment Pressure

[[

]]

Figure 6-24: GOTHIC Benchmarking to CVTR Test Data, Airspace Temperature

[[

]]

Figure 6-25: GOTHIC Benchmarking to CVTR Test Data, Structure Temperature

6.10 Demonstration of the Method for Large and Small Breaks, Conservative Cases

The large and small steam pipe breaks presented in this section demonstrate the conservatism in the method. The [[

]] correlations are biased as described in Section 6.8.2.

6.10.1 Containment Response to Large Steam Pipe Break, Conservative Case

Containment pressure and temperature responses calculated by using the conservative case assumptions are compared to the results of the base case assumptions for a large steam pipe break shown on Figure 6-26 and Figure 6-27. The biases in the inputs and assumptions cause adding approximately [[ ]] to the peak pressure as shown on Figure 6-26. This difference decreases to approximately [[ ]] in four hours.

The peak containment pressure and temperatures are listed in Table 6-6.

The differences between the temperatures using base case and conservative case assumptions are not as large as the differences in the pressure. [[

]]

It can be concluded from the above observations that the biases used in the conservative cases add a significant margin to the peak pressure values. However, there is not a significant difference in the peak shell temperatures. The cooldown of the shell is slower in the conservative case as compared to the base case.

Containment gauge pressure decreases [[ ]] and shows a decreasing trend in the conservative case. In the base case, containment gauge pressure decreases [[ ]], and also shows a decreasing trend. [[

]] The heat load in the containment becomes small. In the absence of break flow, containment pressure continues to decrease [[ ]].

On Figure 6-28 through Figure 6-30, the conservative case results are compared to those obtained by using the Uchida correlation for condensation keeping all other inputs and assumptions the same. The difference in the peak pressure is negligible. However, pressure decrease after the peak predicted by using the Uchida correlation is faster than that predicted by the biased DLM correlation used in the BWRX-300 conservative containment case above. The reason for the difference in the pressure trend can be explained by comparing the heat transfer rates to the shell and PCCS as shown on Figure 6-29. [[

]] Because PCCS surface temperature remains below the saturation temperature in the long term, condensation heat transfer to PCCS continues. There is a large difference between the condensation heat transfer rates predicted by the biased DLM and Uchida correlations as shown on Figure 6-29. Because of the conservatism in the biased DLM correlation as compared to the Uchida correlation after the peak, containment pressure decreases faster in the BWRX-300 GOTHIC conservative case than it would be if Uchida correlation were to be used.

Containment temperatures predicted by using the biased DLM correlation and Uchida correlation are compared on Figure 6-30. There is not a significant difference in the air temperatures. However, the shell temperatures show some differences in the very short-term. It should be noted that the shell inner and outer surfaces shown on Figure 6-30 are the maximum shell temperatures; they are not the average shell temperatures. Because the Uchida correlation does not include any information about the velocities near the wall, it cannot predict the high condensation heat transfer that occurs locally. As a result, Uchida correlation underpredicts the shell temperature while high velocities exist and misses the initial peak that occur in the shell temperature. However, shell temperatures predicted by the Uchida and the modified DLM correlations approach each other after the velocities subside.

The comparisons above show that the condensation model used in the BWRX-300 containment method represents the trends accurately, it applies a sufficient level of conservatism comparable to that predicted by the Uchida condensation heat transfer correlation that has been found to be acceptable by the NRC staff previously.

[[

]]

Figure 6-26: Containment Pressure Following a Large Steam Pipe Break, Comparison of Conservative and Base Cases

[[

]]

Figure 6-27: Containment Temperatures Following a Large Steam Pipe Break, Comparison of Conservative and Base Cases

[[

]]

Figure 6-28: Comparison of Containment Pressures Predicted by the Biased DLM and Uchida Correlations

[[

]]

Figure 6-29: Comparison of Heat Transfer Rates Predicted by Biased DLM and Uchida Correlations

[[

]]

Figure 6-30: Comparison of Containment Temperatures Predicted by the Biased DLM and Uchida Correlations

6.10.2 Containment Response to Small Pipe Breaks, Conservative Cases

The containment response predicted by using the conservative case assumptions for small pipe breaks is shown on Figures 6-31 through 6-34 for small steam pipe breaks and on Figures 6-39 through 6-41 for small liquid pipe breaks. [[

]]. The peak containment pressure and temperatures are listed in Table 6-6.

The maximum pressure on Figure 6-31 for the small steam break is well below the peak pressure resulting from a large steam break shown previously on Figure 6-26 and discussed in Section 6.10.1. The mass and energy release rate calculated by assuming no back pressure in Section 5.4 is used in the GOTHIC model to calculate the containment pressure. In reality, the break flow will start decreasing after it becomes unchoked as the containment pressure approaches the RPV pressure and will become very small when the RPV and containment pressures are nearly the same. After this time, mass discharge to the containment becomes small enough to maintain containment pressure slightly below the RPV pressure. If the mass discharge rate were to increase momentarily, containment pressure would increase above the RPV pressure and the mass discharge would stop again until the containment pressure returns to a value below the RPV pressure. Therefore, after the time that the RPV and containment pressures equalize, the upper bound for the containment pressure is the RPV pressure corresponding to the no-break case. The lower bound of the containment pressure is the containment pressure calculated by assuming no break flow after the time the RPV and containment pressures equalize. It should be noted that the lower bound for the containment pressure is discussed here to illustrate the trends but does not have any associated acceptance criteria. In reality, there may be other favorable conditions that may make the containment pressure lower than the values calculated here.

[[

]]

The PCCS exit temperature and the reactor cavity pool temperature are shown on Figure 6-32. PCCS #1 is the PCCS unit closest to the break location, PCCS #6 is the farthest. The trend in the PCCS exit temperatures follows the trend in the reactor cavity pool temperature. The steam volume fraction in the containment (excluding the dome region) is shown on Figure 6-33. The maximum steam volume fraction, which occurs in the higher sections of the containment, [[

]], decreases slowly in the long term. [[

]] Note that the calculations conservatively assume no heat loss from the

reactor cavity pool to the surroundings through the walls. However, heat loss due to surface evaporation from the pool is taken into account.

The peak shell temperature shown on Figure 6-34 resulting from a small steam pipe break is comparable to the peak shell temperature resulting from a large steam pipe break shown on Figure 6-30, although the timing of the peak is much different.

As discussed in Section 5.4, containment pressure is assumed to be at atmospheric pressure to maximize the break flow rate. However, if ICS can depressurize the RPV faster than PCCS can depressurize the containment, it is conceivable that non-condensable gases are ingested into the RPV and into the ICS heat exchangers. Build-up of non-condensable gases in the ICS heat exchangers may degrade the heat removal rate of ICS causing the system to re-pressurize again. This potential was investigated by performing an iteration between the TRACG calculations for a small steam pipe break accounting for the containment back pressure, and GOTHIC calculations for the containment using the modified break flow from TRACG. [[

]]

The RPV pressure and the containment pressure used as back pressure in the break flow calculations are plotted on Figure 6-36. [[

]] As shown on Figure 6-37, break flow reversals start to occur [[ ]] and the flow rate fluctuates within a very small band about zero. The total amount of nitrogen ingested into the RPV is insignificant. This small amount of nitrogen ingestion does not cause an appreciable degradation in the ICS performance, as shown on Figure 6-35. ICS heat exchangers are capable of removing decay heat in the presence of much higher levels of non-condensable gases as discussed in Section 5.2.4.

The effect of using the containment back pressure in calculating the break flow on the containment pressure is shown on Figure 6-38. [[

]]

The calculated peak containment pressure is not affected by the assumption made for containment pressure used to calculate the break flow because the break flow remains choked well past the time of the peak containment pressure for either assumption. Any impact on containment pressure occurs only in the long-term and is in the conservative direction when the containment back pressure is not considered in the break flow calculation. [[

]] The sensitivity case presented here shows that ignoring the back pressure increases the conservatism in the analysis.

Containment responses were calculated for small liquid pipe breaks until the RPV and containment pressures equalize. [[

]] The results are shown on Figures 6-39 through 6-42. The containment response trends for the liquid pipe breaks are similar to the small steam pipe breaks. After the RPV level falls below the break location, the break flow is fed from the steam space in the RPV and displays the characteristics of a small steam pipe break. Therefore, the trends observed in Figures 6-39 through 6-42 are consistent with the trends in steam pipe break shown in Figures 6-31 through 6-34.

[[

]]

Figure 6-31: Containment Pressure Following a Small Steam Pipe Break

[[

]]

Figure 6-32: PCCS Exit and Reactor Cavity Pool Temperatures Following a Small Steam Pipe Break, Conservative Case

[[

]]

Figure 6-33: Steam Volume Fraction in the Containment Following a Small Steam Pipe Break, Conservative Case

[[

]]

Figure 6-34: Containment Temperatures Following a Small Steam Pipe Break

[[

]]

Figure 6-38: Containment Pressure Using Break Flow With and Without Back Pressure

[[

]]

Figure 6-39: Containment Pressure Following a Small Liquid Pipe Break

[[

]]

Figure 6-40: PCCS Exit and Reactor Cavity Pool Temperatures Following a Small Liquid Pipe Break, Conservative Case

[[

]]

Figure 6-41: Containment Temperatures Following a Small Liquid Pipe Break

[[

]]

Figure 6-42: Steam Volume Fraction in the Containment Following a Small Liquid Pipe Break, Conservative Case

Table 6-6: Summary of the Peak Containment Pressure and Temperatures Calculated by Using the Conservative Assumptions

[[		
		]]

6.10.3 Containment Mixing for Combustible Gases

Hydrogen and oxygen generation results from radiolysis in BWRX-300 design basis accidents is discussed in Section 5.2.4. The radiolytic gases mixed in steam and liquid are discharged from the break along with the break flow. The volumetric fractions are calculated in Section 5.2.4. Hydrogen and oxygen distributions in the containment are not a concern for large breaks [[

]]. Radiolytic gases may build up in the containment following unisolated small breaks over time even though the rate of release is very small.

Total mass fraction of hydrogen and oxygen produced by radiolysis, remaining in the RPV and released to the containment are shown on Figure 6-43. [[

]]

[[

]]

Radiolytic gases mixed in steam enter into the dome region and condense on the containment dome, liberating the radiolytic gases mixed within. Although the volume fraction of radiolytic gases in the steam is small, it may accumulate in the dome region over time.

The radiolytic gas volume fractions are specified in the break flow boundary condition as calculated in Section 5.2.4, and radiolytic gas volume fraction distribution in the containment and the dome region was calculated for small steam pipe break case presented in Section 6.10.2.

Hydrogen volume fraction in the containment is shown on Figure 6-44. Hydrogen volume fraction in the dome region is higher than the main containment volume as expected, but the difference is not large. [[

]] The hydrogen volume fractions shown on Figure 6-44 are far below the deflagration limits even if there is sufficient oxygen.

Hydrogen and oxygen are generated at stoichiometric ratio from radiolysis; the molecular (or volume) ratio of radiolytic oxygen to hydrogen is 0.5. Because the radiolytic gases are well mixed in steam or liquid water where they are generated, the molecular or volume ratio of radiolytic oxygen to hydrogen remains 0.5 as they migrate in the RPV, from RPV to containment and within the containment. Therefore, radiolytic oxygen volume fraction in the containment is exactly half of the hydrogen volume fraction shown on Figure 6-44. There is also some small amount of oxygen initially present in the containment. [[

]]

The results presented here show that gases generated by radiolysis do not create a concern for deflagration in the containment and that the containment subcompartments remain sufficiently mixed.

[[

]]

Figure 6-43: Radiolytic Gas Generation and Release from RPV, Small Steam Pipe Break, 2 ICS Trains, Conservative Case

[[

]]

Figure 6-44: Hydrogen Volume Fraction in the Containment Main Volume and in the Dome Region, Small Steam Pipe Break, 2 ICS Trains, Conservative Case

6.11 Summary of the Assumptions and Inputs Used in the BWRX-300 GOTHIC Method Conservative Cases

The conservative containment response cases use the following inputs:

- Initial containment pressure is at the maximum Technical Specification containment pressure
- Initial bulk containment temperature and the structures are at a reasonably low value that would occur during normal operation
- Initial humidity in the containment is 20%
- Reactor cavity pool temperature is at the Technical Specification limit
- Bounding values are used for form loss coefficients in containment and in the PCCS units
- Free space volume in the containment is conservatively calculated
- The containment nodalization uses node sizes as presented in the base cases in this report
- The initial airspace temperature above the reactor cavity pool is assumed to be the same as the pool water temperature.
- The initial relative humidity of the airspace is assumed to be 20%.

The conservative containment response cases use the following modeling parameters:

- [[ ]]
- Condensation and convection heat transfer correlations are biased as described in Section 6.8.2.
- [[

]]
- No credit is taken for heat transfer from the outer surface of the metal containment shell to the concrete or surroundings, except for heat transfer from the submerged section of the containment dome to the reactor cavity pool above the dome.
- The reactor cavity pool is modeled as a lumped parameter volume. The air space is connected to a constant pressure boundary condition such that the airspace pressure is nearly constant at atmospheric pressure.
- There is no heat loss from the pool to the walls. Surface evaporation from the pool is accounted for.
- Heat transfer coefficients on the containment shell, PCCS and containment dome are biased as described in Section 6.8.2.

Appendix C
Replaced Pages from NEDC-33922P, Revision 2

Revision Number	Description of Change
	• Figures 6-39 and 6-40 were renumbered as Figures 6-43 and 6-44. • Section 6.10.3: Figure references were updated to reflect that Figures 6-39 and 6-40 were renumbered as Figures 6-43 and 6-44. The following additional editorial corrections were made: • Section 5.2.4: Added back in the missing equation for the radiolytic gas production correlation. • Corrected broken links in Sections 4.0, 6.0, 6.8, 6.8.2, 6.9, 6.10, and 6.11.
2	Revised the following tables, figures, and sections consistent with the revised response to NRC eRAI 9862 Question 06.02.01-01: • Table 6-6 • Figure 6-2 • Figures 6-4 through 6-13 • Figures 6-15 through 6-17 • Figures 6-26 through 6-44 • Sections 6.5, 6.6.1, 6.6.2, 6.7.1, 6.7.2, 6.10.1, 6.10.2, and 6.11. Section 5.2.4: Added a sentence to the first paragraph in response to Audit Issue 38. Section 6.8.2: Deleted the reference to CONAN test data. The following additional editorial corrections were made: • Figures 5-3 and 5-4: Corrected the clarity of the images. • Figures 5-5, 5-8, 5-11, 5-15, 5-18, and 5-23: In the notes below these figures, added quotations around Q IC-A and Q IC-B for clarity. • Figure 5-11: Revised the note to delete Q IC-B. • Figures 5-8, 5-15, 5-18, and 5-23: Removed proprietary markings in the notes below the figures. • Sections 5.2.4, 5.2.5, 5.3.1, 6.7.2, 6.8, 6.8.1, 6.8.3, and 6.10.1 and in Table 5-3 and Table 6-2 (Items 8, 9, 12, 13, and 14): Added the missing article “the” in several places. • Table 6-2 (Items 14 and 21): Changed “effects” to “affects”. • Section 6.10.1: Deleted the word “one”. It is redundant with the word “first” • Section 6.10.3: Changed “is” to “are”.

]].

5.2.4 Isolation Condenser Modeling and Radiolytic Gases

The IC capacity is assured to be at least 33.75 MW as stated in Supplement 2 of Reference 7.10. Although the ICS is credited for the AOOs in the ESBWR (Section 4.7 and Supplement 2 of Reference 7.10), but not for LOCA analyses, any potential adverse effects and parallel unit effects have been addressed in Reference 7.10. [[

]] The ESBWR containment analyses credit the PCCS attached to the containment, but do not credit the ICS. However, the ESBWR PCCS heat

exchanger is identical to one of the two heat exchangers in an IC train. Both the ICS and the PCCS use the same qualification base and testing that were originally performed for the Simplified Boiling Water Reactor (SBWR) design and supplemented for ESBWR design.

TRACG qualification for the ICS is based on two sets of PANDA tests as described in Reference 7.7: the M-series tests, which are used in the TRACG qualification for SBWR, and the later complimentary P-series tests for ESBWR configuration, including the effects of the non-condensable gases. TRACG04 is qualified based on both sets of tests, and for both water and steam, and steam containing air or helium (Reference 7.8).

Because there is no significant oxidation in the BWRX-300, the only non-condensable gases that may migrate into the IC tubes are the radiolysis products following a design basis LOCA. [[

]] The build-up of hydrogen and oxygen in steam following a one-inch liquid break is shown on Figure 5-1.

Unlike hydrogen generated from cladding oxidation, hydrogen and oxygen liberate from radiolysis at a slow rate and distributes over a relatively large region. The gases become mixed in water both in steam and liquid phases. The well-mixed hydrogen and oxygen in steam also migrates into the ICs when the ICs are put in service. The hydrogen and oxygen concentration in steam may increase as the steam condenses in the IC tubes. It should be noted that because hydrogen and oxygen are mixed in water when they are formed near the core region, they do not separate from water or steam again until the steam condenses.

The effect of the radiolytic gases on the ICs has been determined using TRACG. [[

]] Nevertheless, a bias was applied to the IC performance to account for degradation due to the potential of radiolytic gas build-up.

[[

]]

Figure 5-1: Volume Fraction of Radiolytic Gases ($H_2 + O_2$) in Steam in the RPV Following a 1-Inch Liquid Break

5.2.5 Modeling Biases (PIRTs)

TRACG has a feature to bias various modeling parameters, which are called PIRTs. A TRACG PIRT is a coefficient which multiplies an internally calculated nominal value over a specified range of the solution domain. The PIRTs used in the ESBWR TRACG application (Reference 7.10) for conservative cases are listed in Table 5-1. [[

Table 5-3: Trips and Isolations Used in Both Base and Conservative Cases

Event or isolation	Trip	Notes
Shutdown	Load rejection (loss of offsite power)	Delay in generating the scram signal + time required for prompt neutron fission power to diminish because of the control rod insertion. Note that delayed neutron effect is accounted for in the decay heat separately.
Isolation of large pipes except IC piping	High drywell pressure or Low-Low level (Level 2)	These are the only RPV isolation signals credited in pipe break analyses.
Isolation of IC piping	[[	]]
Containment isolation	Same as RPV isolation valves	Containment isolation for main steam pipe break is conservatively ignored (see Section 3.0).
ICS Initiation	Low-low level (Level 2) or high drywell pressure	These are the only initiation signals for the ICS credited in the pipe break analyses.

[[

]]

Figure 5-3: Main Steam, Feedwater and Instrument Piping Attached to the RPV

[[

]]

Figure 5-4: TRACG IC Modeling for BWRX-300

5.3 Demonstration Cases for Large Breaks

The worst assumed single failure for a large break is the loss of an ICS train. [[

]]. For all other breaks, two ICS trains are available to remove the decay heat and depressurize the RPV after the loss of one ICS train due to a single failure. [[

]].

The large feedwater pipe break cases consider reduced feedwater temperature [[

]]. The results of the large feedwater pipe breaks are shown on Figure 5-8 through Figure 5-10.

In the steam pipe break cases, scram signal is inserted due to [[

]].

5.3.2 Conservative Case for Large Feedwater and Steam Breaks

The results of the large steam pipe breaks are shown on Figure 5-11 through Figure 5-13. The discussions in Section 5.3.1 for the base case also apply to the conservative case.

[[

]].

The results for the large feedwater pipe breaks are shown in Figure 5-15 through Figure 5-17. [[

]].

5.4 Demonstration Cases for Small Breaks

Base and conservative cases were run for the small steam and liquid pipe break cases. The small break events are slowly evolving events; therefore, the trends for the base and conservative steam and liquid breaks are very similar to each other. The results of the conservative small steam and liquid break cases are shown and discussed in this section.

The results of the conservative case for small break are shown on Figure 5-18 through Figure 5-22. As shown on Figure 5-18 and Figure 5-19, the ICS heat removal rate decreases as the RPV pressure decreases. The difference between the heat removed by the ICS and the power generated by decay heat is what is discharged from the break. The pressure boundary condition used in the TRACG calculation remains at atmospheric pressure to maximize the break flow rate. [[

]].

Reactor trip occurs due to load rejection in the small pipe break cases. RPV isolation valves are closed when the containment pressure exceeds the high containment pressure trip setpoint. The delay in this trip can be estimated conservatively.

[[

]]

[[

]]

Figure 5-5: Reactor Power, Main Steam Pipe Break, Base Case

Note: Decay Heat curve represents fission power as well as decay heat. "Q IC-A" is the heat removal rate by ICS Train A.

[[

]]

Figure 5-8: Reactor Power, Feedwater Pipe Break, Base Case

Note: Decay Heat curve represents fission power as well as decay heat. "Q IC-A" and "Q IC-B" are heat removal rates by ICS Trains A and B.

[[

]]

Figure 5-11: Reactor Power, Main Steam Pipe Break, Conservative Case

Note: Decay Heat curve represents fission power as well as decay heat. "Q IC-A" is the heat removal rate by ICS Train A.

[[

]]

Figure 5-15: Reactor Power, Feedwater Pipe Break, Conservative Case

Note: Decay Heat curve represents fission power as well as decay heat. "Q IC-A" and "Q IC-B" are the heat removal rates by ICS Train A and ICS Train B.

[[

]]

Figure 5-18: Power, Small Steam Break, 2 ICS Trains, Conservative Case

Note: Decay Heat curve represents fission power as well as decay heat. "Q IC-A" and "Q IC-B" are heat removal rates by ICS Trains A and B.

[[

]]

Figure 5-23: Power, Small Liquid Break, 2 ICS Trains, Conservative Case

Note: Decay Heat curve represents fission power as well as decay heat. "Q IC-A" and "Q IC-B" are heat removal rates by ICS Trains A and B.

]]

6.5 GOTHIC Containment Model

A schematic of the GOTHIC model used for the BWRX-300 containment analysis is shown on Figure 6-1. Volume 1s represents the main section of the containment, Volume 2s represents the containment dome region above the refueling bellows, Volume 3s is the PCCS, and Volume 4 is the reactor cavity pool.

The containment dome is connected to the main section of the containment through two flow paths, 1 and 2, representing the manholes in the refueling bellows.

Flow paths 4 through 13 are the exit of the hot channels of the [[ ]] PCCS units connected to the reactor cavity. Flow paths 14 through 23 are the intake openings of the PCCS units connected to the reactor cavity pool. Flow paths 25 through 34 are openings between the cold tubes and heated tubes of the PCCS units at the bottom.

Three dimensional volumes, so-called subdivided volumes in GOTHIC terminology, are used to model the main section of containment. Nodalization of the main section (Volume 1s) and the containment dome (Volume 2s) used in the base model are shown on Figure 6-2.

The RPV is modeled by using a blockage corresponding to the outer dimensions of the RPV insulation as shown on Figure 6-2. Approximately [[ ]] of the remaining volume is assumed to be obstructed by various support structures, piping, catwalks, etc. Thermal conductors are distributed over cells on the RPV surfaces and where the piping is routed. The thermal conductor properties are set to the mirror insulation properties using conservative inputs to maximize the heat loads from the RPV and piping. The fluid temperature in the piping is assumed to be the same as the RPV fluid temperature and is specified as a function of time as obtained from the TRACG mass and energy release calculations.

The flow path representing the break flow is placed [[ ]], next to the containment shell and the break flow is directed toward the shell when calculating the peak shell temperature. [[

]] The break mass flow rate and enthalpy are specified as a function of time as obtained from the TRACG mass and energy release calculation.

The figures based on the GOTHIC runs with break location maximizing the pressure are identified with “[MaxP]”, and the figures based on the GOTHIC runs with break location maximizing the shell temperature are identified with “[MaxT]” in the figure captions.

Nodalization for the small containment dome region is shown in the upper right part of Figure 6-2. [[

]]

The PCCS is represented by subdivided volumes as shown on Figure 6-3. [[

]]

The following is a list of the key modeling parameters used in the base cases. The reasoning for the choice of the models and their uncertainties is discussed in Section 6.8.

- Mass and energy release are obtained from the TRACG base case results in Section 5.3.1 for large breaks.
- The form loss coefficients in the PCCS are set to conservatively high values, accounting for the flow losses due to the typical spacers, as well as entrance and exit losses and [[ ]].
- Wall friction is calculated from the Colebrook relationship for smooth wall.
- The heat transfer coefficient in containment is the sum of two parts as follows:
    - The Nusselt number for heat transfer due to sensible heat can be calculated from the forced convection or natural convection. The forced flow convection correlation is the Dittus-Boelter correlation given by:

      $$Nu_{FC} = 0.023\,\mathrm{Re}^{0.8}\,\mathrm{Pr}^{0.3}$$

      where Nu is the Nusselt number, Re is the Reynolds number, and Pr is the Prandtl number. Reynolds number is calculated based on the velocity and properties in the node next to the wall and the user-specified characteristic length. The exponent of the Prandtl number is 0.4 for the heated walls (RPV and hot piping).

      The Nu for heat transfer in natural convection is calculated from the [[

[[

]]

Figure 6-2: Nodalization of Containment Main Volume, Volume 1s (left), Containment Dome, Volume 2s, (upper right) and the Break Flow Path in Volume 1s at Vertical Node 14 (lower right) [MaxT]

6.6 Base Cases and Results

This section presents the containment response for the mass and energy releases calculated in Section 5.3.1 for large steam and feedwater breaks using the base model described in Section 6.5. The key containment inputs are listed in Table 6-4. The containment nodalization and modeling parameters are described in Section 6.5.

Table 6-4: Containment Inputs Used in Base Cases

Parameter	Value
Containment height	[[
Containment diameter	
Free containment volume (excluding dome)	
Containment dome height	
Containment dome diameter	
Containment shell thickness	
Containment head thickness	
Number of manholes on the refueling bellows	
Diameter of the manholes	
Number of PCCS units	
PCCS type	
PCCS outer diameter	
PCCS outer pipe thickness	
PCCS cold tube outer diameter	
PCCS cold tube thickness	
PCCS height inside the containment	]]
Initial containment temperature	43.33 °C
Initial containment relative humidity	20%
Initial containment pressure	101.325 kPa
Initial reactor cavity pool temperature	43.33 °C

6.6.1 Containment Response to Large Steam Break, Base Case

The containment pressure response to a large break in a steam line is shown on Figure 6-4. The peak pressure [[ ]] is reached at approximately the time the RPV isolation valves fully close at ten seconds. After the closure of the RPV isolation valves, the only heat input to the containment is due to convection from the RPV wall and hot pipe walls through the insulation. With the break flow isolated, the containment pressure starts decreasing. [[

]]

The airspace and containment shell temperature responses are shown on Figure 6-5. The maximum air temperature is the maximum of all nodal temperatures in the containment; the bulk temperature is the average air temperature throughout the containment. These temperatures are higher than the temperature resulting from the isenthalpic expansion of steam from the RPV conditions to the containment pressure. The additional temperature increase is due to the compression of nitrogen in containment. Following the break, there is a rigorous circulation of

the air in containment. Prior to isolation, the [[

]]. The peak temperature moves around in containment as the hot steam / nitrogen mixture circulates. After the break flow stops, the location of the maximum temperature continues to vary with the changing flow patterns, but most of the time remains in locations near the RPV wall.

Although the containment air temperature is high [[ ]], the containment shell remains at a much lower temperature. [[

]]

The PCCS exit temperature is also shown on Figure 6-5. [[

]] A sensitivity analysis for the PCCS is presented in Section 6.6.1.

The decay heat rate and the heat removal rates by the various heat removal mechanisms are plotted on Figure 6-6. As shown on the plot, the containment shell initially absorbs a large amount of energy for a short duration before the heat removal diminishes as the shell warms up [[ ]]. The isolation condensers are the primary mechanism for removing decay heat from the isolated RPV. [[

]] No credit is taken in these cases for the heat transfer from the containment shell to the concrete supporting structures.

The subcompartment formed by the containment head and refueling bellows is the limiting location with respect to differential pressures acting across subcompartment boundaries because of the relatively small flow areas provided by the access manholes in the bellows. The other subcompartments inside the containment (e.g., [[ ]]) have much larger openings. The pressure differential across the refueling bellows is shown on Figure 6-8. In this variation of the base case, the flow loss coefficient across the manholes is set to an extremely high value [[ ]] in order to maximize the differential pressure during the event. The GOTHIC model captures the pressure waves travelling through the containment immediately following the break, and the peaks and valleys in the pressure trend correspond to physical phenomena. The time

difference between the first peaks of the red and blue curves is consistent with the pressure wave travelling at nearly the speed of sound. [[
]]. This is a small pressure differential across the boundary of a subcompartment. The pressure drop across the other subcompartment boundaries were not calculated because they have much larger flow area-to-volume ratios and are located farther away from the break, [[
]].

If the pipe routing is designed such that a potential pipe break may occur in close proximity of the biological shield wall or vessel support, the same method used here can be used to assess the differential pressure loads to be considered in the detailed structural designs. However, if a significant pressure differential occurs across the biological shield due to the close proximity of the break, it is likely that the jet impingement loads would be the more limiting concern. The determination of the jet impingement loads acting on the containment structures is outside the scope of this LTR.

6.6.2 Containment Response to Large Feedwater Pipe Break, Base Case

The containment pressure response to a large break in the feedwater pipe is shown on Figure 6-9. The peak pressure [[ ]] is reached at the time the RPV isolation valves fully close [[ ]]. Similar to the large steam break, after the closure of the RPV isolation valves the only heat input to the containment is from the RPV wall and hot pipe walls through the insulation. [[ ]] The peak containment pressure for a feedwater pipe break is bounded by the peak containment pressure for a large steam pipe break.

The airspace and containment shell temperature responses in the containment are shown on Figure 6-10. The containment temperature discussion in Section 6.6.1 also apply to the response to feedwater pipe breaks. It can be seen on Figure 6-10 that the maximum shell temperature is well below the containment atmosphere temperature, [[
]].

6.7 Nodalization Studies

6.7.1 Nodalization Study for Containment

A nodalization study was performed using the base case for the large main steam pipe break presented in Section 6.6.1.

The nodalization study for the main containment section included the following cases, also shown on Figure 6-11:

- Base case: [[ ]]
- Coarser grid. Twice the node size of the base case in each direction: [[ ]]
- Finer grid in the horizonal plane. Half the node size of the base case in each direction in the horizontal plane: [[ ]]. Same node size in the vertical direction
- Finer grid in the vertical direction: Half the node size of the base case in the vertical direction: [[ ]]. Same node size as in the base case in the horizontal plane

The PCCS unit placement is accurate in the [[ ]] cases. [[ ]].

The large steam break base case was rerun using different nodalization schemes described above. As shown on Figure 6-12, the effect of nodalization on the containment pressure response is very small. The curve for [[ ]] case is not visible because it is overlapped by the results of the [[ ]] nodalization case. There is an insignificant difference, [[ ]], in the peak pressure between the base case and finer nodalization cases. The nodalization trend also shows that the coarser nodalization slightly overpredicts the peak pressure. As shown on this figure, reducing the node size [[ ]] does not make a significant difference in the pressure response.

The temperature trends shown on Figure 6-13 also display similar behaviors. The air/steam mixture temperatures are similar in all cases. The temperature trend differences between the cases are consistent with the differences shown between the pressure trends. There are some differences in the air/steam temperatures in the longer term, but the shell temperatures remain close to each other in all nodalization schemes. [[ ]].

Based on the above results, it is concluded that the containment nodalization [[ ]] is adequate for containment pressure, air/steam temperature and the shell temperature predictions.

6.7.2 Nodalization Study for PCCS

The effect of nodalization on the PCCS has been studied for a single PCCS unit placed in a large containment volume. The containment volume is kept at the prescribed temperature and steam concentration. The base case nodalization in the vertical direction is the same as the BWRX-300 containment model, [[

]]

The second case used in the nodalization study doubles the number of nodes both in the PCCS and the containment, and the third case doubles the number of nodes again.

The effect of nodalization on the heat removal rate is shown on Figure 6-14 at three containment temperatures. [[

]] A [[ ]] reduction is applied to the heat transfer on the outer surface of the PCCS unit. [[ ]] The results show negligible effect of nodalization on the PCCS heat removal rate.

[[

]]

Figure 6-4: Containment Pressure Following Large Main Steam Pipe Break, Base Case [MaxP]

[[

]]

Figure 6-5: Temperatures in the Containment Following a Large Main Steam Pipe Break, Base Case [MaxT]

[[

]]

Figure 6-6: Heat Removal Rates by Various Mechanisms Following Large Main Steam Pipe Break, Base Case [MaxP]

[[

]]

Figure 6-7: Longer Term Heat Removal Rates by Various Mechanisms Following Large Main Steam Pipe Break, Base Case [MaxP]

[[

]]

Figure 6-8: Pressures Next to Refueling Bellows Following Large Main Steam Pipe Break, Base Case [MaxT]

[[

]]

Figure 6-9: Containment Pressure Following Large Feedwater Pipe Break, Base Case [MaxP]

[[

]]

Figure 6-10: Temperatures in the Containment Following a Large Feedwater Pipe Break, Base Case [MaxT]

[[

]]

Figure 6-11: Grid Used in Nodalization Studies [MaxP]

Note: Orange circles in the plan view and orange bars in the vertical view represent the PCCS units. Blue arrows represent the break locations. In the vertical view, the break location arrows indicate only the vertical node number. The break location is shown for the cases maximizing temperature. In the cases maximizing pressure, the break flow is directed upwards, in cell IX=12, IY=6, IZ=10 in the 16x16x16 case, and in the corresponding cells in the other cases.

[[

]]

Figure 6-12: Effect of Nodalization on the Containment Pressure Response to Large Steam Pipe Break, Base Case [MaxP]

[[

]]

Figure 6-13: Effect of Nodalization on the Containment Temperature Response to Large Steam Pipe Break, Base Case [MaxT]

- The natural and forced circulation and stratification are affected by the friction factors, turbulence modeling, and the model nodalization. A nodalization study is presented in Section 6.7 for the containment and the PCCS. A sensitivity study for the friction factors and turbulence modeling is presented in Section 6.8.1 [[ ]]. This addresses Items 9, 10, 13, and 14.
- Uncertainties in the convection and condensation heat transfer coefficients, Items 3 and 7, are discussed in Section 6.8.2 where bounding values have been developed.
- In the RPV the production of hydrogen and oxygen by radiolysis is modeled by the bounding correlation given in Section 5.2.4. There are no other mechanisms for producing significant amounts of NC gases in either the RPV or the containment. [[ ]]. This addresses Items 19 and 20.
- Multi-component gas properties are calculated using the most accurate models available in the GOTHIC code as described in Reference 7.16.

6.8.1 Effect of the Friction Factors and Turbulence Parameters on the Containment Response

The importance of friction factors and turbulence on containment pressure and temperature response has been investigated by sensitivity studies for the containment and the PCCS separately.

The nominal cases use Colbrook's friction factors for a smooth surface. To determine the sensitivity of the pressure and temperature to the friction factor, the relative roughness was increased [[ ]]. Given the large hydraulic diameter, this relative roughness corresponds to an unreasonably high absolute value of surface roughness [[ ]]. The increased surface roughness case is identified as the "High C_f" case in the comparisons.

[[

]]

The results obtained by the above sensitivity cases are compared on Figure 6-15 through Figure 6-17 for the large steam pipe break. [[

[[

]]

Figure 6-15: Effect of Friction and Turbulence on Containment Pressure, Large Steam Pipe Break [MaxP]

[[

]]

Figure 6-16: Effect of Friction and Turbulence on Containment Temperatures, Large Steam Pipe Break [MaxT]

[[

]]

Figure 6-17: Effect of Friction and Turbulence on Steam Volume Fraction, Large Steam Pipe Break [MaxT]

6.8.2 Uncertainties in the Convection and Condensation Heat Transfer Coefficient and the Bounding Values

The BWRX-300 containment model uses the DLM option for condensation built into GOTHIC (Reference 7.16) to calculate the condensation rate. The DLM correlation is based on a mechanistic model which recognizes the similarity between the heat and mass transfer. The benchmarking of both the convection and condensation correlations to the data is also provided in Reference 7.18. DLM is selected over the other options available in the code due to its mechanistic nature representing the underlying phenomena as opposed to curve fit to data. Recently, Heat and Mass Transfer Analogy Method (HMTAM) has been developed and compared to the CONAN and COPAIN test data (References 7.19 and 7.20). HMTAM is also based on the analogy between heat and mass transfer and is similar to DLM. As will be shown, the DLM method is more conservative than the HMTAM method for the BWRX-300 containment application. The uncertainties in the convection and condensation correlations with respect to the data will be evaluated based on the COPAIN test data in Reference 7.19. The uncertainties will be first presented for the HMTAM method.

The total heat transfer to a condensing surface has two parts: convection heat transfer from bulk to liquid film and the heat transfer by condensation. [[

]]

COPAIN data is collected over a range of 1 to 6.7 bars, non-condensable gas mass fraction range of 0.1 to 1.0, velocity range of 0.1 to 3.0 m/s and steam superheating up to 40 °C. The range of parameters in the BWRX-300 containment response is within the COPAIN data range. The COPAIN data also includes pure convection measurements. More information on the COPAIN data can be found in Reference 7.19.

A comparison of the forced and natural convection correlations to the data is shown on Figure 6-18. The black markers are the ratio of forced convection measured Nusselt number divided by the Nu number predicted by the Schlichting forced convection correlation. The points larger than 1.0 indicate that correlation underpredicts the forced convection Nusselt number. The x-axis in the plot is the Richardson number, Ri. Theoretically, inertia forces are dominant when the Richardson number is less than 1, and buoyancy forces are dominant when the Richardson number is greater than 1. As expected, the black markers corresponding to the Richardson numbers greater than about 5 show that the data is grossly underpredicted if the forced convection correlation is used where buoyancy forces are important. Conversely, the red markers, which show the ratio of the measured Nusselt number to the Nusselt number predicted by the McAdams natural convection correlation show that the data is grossly underpredicted if the natural convection heat transfer coefficient is used where the buoyancy forces are overwhelmed by the inertia forces due to the free stream velocity, i.e., where forced convection correlation should be used. There is a transition region between the high and low Richardson number ranges that is reviewed in more detail below.

The heat transfer is enhanced by the turbulence near the wall. As the free stream velocity is increased from zero in the same direction as in flow driven by buoyancy near the wall, it suppresses the turbulence and reduces the heat transfer until the free stream velocity is increased large enough that the inertial forces overwhelm the buoyancy forces. This phenomenon may occur in the transition region from natural convection to forced convection and is called re-laminarization. [[

[[

]]

Figure 6-21: Ratio of Condensation Mass Flow Rate Obtained by DLM to that of HMTAM

6.8.3 Sensitivity Analyses for PCCS Performance

Sensitivity analyses have been performed for the PCCS performance to determine the effect of:

- PCCS loss coefficients
- PCCS liquid-side heat transfer coefficient
- Fouling

Sensitivity cases also include the potential for the onset of boiling.

To determine the effect of each parameter without interference from other phenomena, a single PCCS unit was placed in a large volume representing a section of the containment. The containment pressure, temperature and steam volume fraction were kept constant at various values and each of the sensitivity parameters were varied to determine the effect on PCCS performance. The PCCS nodalization and geometry are the same as those used in the BWRX-300 containment model described in Section 6.5. The volume representing the containment was also nodalized in the vertical direction that is the same as the containment nodalization described in Section 6.5, with the exception of using one node in the horizontal direction.

The sensitivity study was performed for the following conditions. The PCCS heat removal rate at each condition was obtained after a steady state was reached.

Containment pressure: [[ ]]

Containment temperature: [[ ]]

Steam volume fraction: [[ ]]

PCCS inlet temperature: [[ ]]

PCCS total loss coefficient: [[ ]]

[[

]] The base case has no fouling or no paint.

The sensitivity cases for paint and crud assume thermal resistance of the paint on the outer surface of the PCCS is [[ ]] and the thermal resistance of the crud on the inner surface is [[ ]].

The results of the sensitivity cases are summarized in Table 6-5. [[

]]

Table 6-5: Summary of the Sensitivity Study Results for PCCS

Containment pressure (kPa)	[[					
Containment temperature (°C)						
Heat removal rate (kW)						
Loss coefficient x 1.5						
Loss coefficient x 2.0						
Fouling + paint						
Heat transfer coefficient inside the PCCS is reduced by [[ ]]						]]

6.9 Benchmarking to the Carolina Virginia Tube Reactor (CVTR) Integral Tests

The CVTR tests simulate a steam pipe break by injecting slightly superheated steam into a closed containment (Reference 7.22). CVTR has a dry containment, with a free volume of 6428 m^3 (227,000 ft^3), [[ ]]. The

6.10 Demonstration of the Method for Large and Small Breaks, Conservative Cases

The large and small steam pipe breaks presented in this section demonstrate the conservatism in the method. The [[

]] correlations are biased as described in Section 6.8.2.

6.10.1 Containment Response to Large Steam Pipe Break, Conservative Case

Containment pressure and temperature responses calculated by using the conservative case assumptions are compared to the results of the base case assumptions for a large steam pipe break shown on Figure 6-26 and Figure 6-27. The biases in the inputs and assumptions cause adding approximately [[ ]] to the peak pressure as shown on Figure 6-26. This difference decreases to approximately [[ ]] in four hours.

The peak containment pressure and temperatures are listed in Table 6-6.

The differences between the temperatures using base case and conservative case assumptions are not as large as the differences in the pressure. [[

]]

It can be concluded from the above observations that the biases used in the conservative cases add a significant margin to the peak pressure values. However, there is not a significant difference in the peak shell temperatures. The cooldown of the shell is slower in the conservative case as compared to the base case.

Containment gauge pressure decreases [[ ]] and shows a decreasing trend in the conservative case. In the base case, containment gauge pressure decreases [[ ]], and also shows a decreasing trend. [[

]] The heat load in the containment becomes small. In the absence of break flow, containment pressure continues to decrease [[ ]].

On Figure 6-28 through Figure 6-30, the conservative case results are compared to those obtained by using the Uchida correlation for condensation keeping all other inputs and assumptions the same. The difference in the peak pressure is negligible. [[

]] Because the PCCS surface temperature remains below the saturation temperature in the long term, condensation heat transfer to the PCCS continues. Because of the conservatism in the biased DLM correlation as compared to the Uchida correlation after the peak, the containment pressure decreases faster in the long term

in the BWRX-300 GOTHIC conservative case than it would if the Uchida correlation were also used.

Containment temperatures predicted by using the biased DLM correlation and Uchida correlation are compared on Figure 6-30. There is not a significant difference in the air temperatures. However, the shell temperatures show some differences in the very short-term. It should be noted that the shell inner and outer surfaces shown on Figure 6-30 are the maximum shell temperatures; they are not the average shell temperatures. Because the Uchida correlation does not include any information about the velocities near the wall, it cannot predict the high condensation heat transfer that occurs locally. As a result, Uchida correlation underpredicts the shell temperature while high velocities exist and misses the initial peak that occur in the shell temperature. However, shell temperatures predicted by the Uchida and the modified DLM correlations approach each other after the velocities subside.

The comparisons above show that the condensation model used in the BWRX-300 containment method represents the trends accurately, it applies a sufficient level of conservatism comparable to that predicted by the Uchida condensation heat transfer correlation that has been found to be acceptable by the NRC staff previously.

[[

]]

Figure 6-26: Containment Pressure Following a Large Steam Pipe Break, Comparison of Conservative and Base Cases [MaxP]

[[

]]

Figure 6-27: Containment Temperatures Following a Large Steam Pipe Break, Comparison of Conservative and Base Cases [MaxT]

[[

]]

Figure 6-28: Comparison of Containment Pressures Predicted by the Biased DLM and Uchida Correlations [MaxP]

[[

]]

Figure 6-29: Comparison of Heat Transfer Rates Predicted by Biased DLM and Uchida Correlations [MaxP]

[[

]]

Figure 6-30: Comparison of Containment Temperatures Predicted by the Biased DLM and Uchida Correlations [MaxT]

6.10.2 Containment Response to Small Pipe Breaks, Conservative Cases

The containment response predicted by using the conservative case assumptions for small pipe breaks is shown on Figures 6-31 through 6-34 for small steam pipe breaks and on Figures 6-39 through 6-41 for small liquid pipe breaks. [[

]]. The peak containment pressure and temperatures are listed in Table 6-6.

The maximum pressure on Figure 6-31 for the small steam break is well below the peak pressure resulting from a large steam break shown previously on Figure 6-26 and discussed in Section 6.10.1. The mass and energy release rate calculated by assuming no back pressure in Section 5.4 is used in the GOTHIC model to calculate the containment pressure. In reality, the break flow will start decreasing after it becomes unchoked as the containment pressure approaches the RPV pressure and will become very small when the RPV and containment pressures are nearly the same. After this time, mass discharge to the containment becomes small enough to maintain containment pressure slightly below the RPV pressure. If the mass discharge rate were to increase momentarily, containment pressure would increase above the RPV pressure and the mass discharge would stop again until the containment pressure returns to a value below the RPV pressure. Therefore, after the time that the RPV and containment pressures equalize, the upper bound for the containment pressure is the RPV pressure corresponding to the no-break case. The lower bound of the containment pressure is the containment pressure calculated by assuming no break flow after the time the RPV and containment pressures equalize. It should be noted that the lower bound for the containment pressure is discussed here to illustrate the trends but does not have any associated acceptance criteria. In reality, there may be other favorable conditions that may make the containment pressure lower than the values calculated here.

[[

]]

The PCCS exit temperature and the reactor cavity pool temperature are shown on Figure 6-32. PCCS #1 is the PCCS unit closest to the break location, PCCS #6 is the farthest. The steam volume fraction in the containment (excluding the dome region) is shown on Figure 6-33. The maximum steam volume fraction, which occurs in the higher sections of the containment, [[ ]], decreases slowly in the long term. Note that the calculations conservatively assume no heat loss from the reactor cavity pool to the surroundings through the walls. However, heat loss due to surface evaporation from the pool is taken into account.

The peak shell temperature shown on Figure 6-34 resulting from a small steam pipe break is comparable to the peak shell temperature resulting from a large steam pipe break shown on Figure 6-30, although the timing of the peak is much different.

As discussed in Section 5.4, containment pressure is assumed to be at atmospheric pressure to maximize the break flow rate. However, if the ICS can depressurize the RPV faster than the PCCS can depressurize the containment, it is conceivable that non-condensable gases in the containment will be ingested into the RPV and into the ICS heat exchangers. For all cases, the effect of nitrogen ingestion, if it does occur, is modeled for all components of the TRACG model (e.g., RPV, ICS, piping). As discussed in Section 5.2.4, TRACG is well qualified to predict the effects of non-condensable gases that may be ingested into the ICS. Build-up of non-condensable gases in the ICS heat exchangers may degrade the heat removal rate of the ICS, causing the system to re-pressurize again. This potential was investigated by performing an iteration between the TRACG calculations for a small steam pipe break accounting for the containment back pressure, and GOTHIC calculations for the containment using the modified break flow from TRACG. Note that the containment back pressure has no effect on the break flow rate until the break flow becomes unchoked. Therefore, the results of the cases with and without back pressure are identical while the break flow is choked. [[

]]

The RPV pressure, the containment pressure specified as back pressure in the break flow calculations, and the containment pressure calculated by GOTHIC are plotted on Figure 6-36. The difference between the RPV and containment pressures becomes progressively smaller with time, but the containment pressure always remains below the RPV pressure [[

]] As shown on Figure 6-37, there are no reversals in the break flow. As shown in the results without back pressure, the PCCS is capable of reducing the containment pressure well below the RPV pressure in the absence of break flow. Therefore, if the back pressure were to increase slightly above the RPV pressure, the break flow would stop, and containment pressure would decrease again. The total amount of nitrogen ingested into the RPV would be insignificant. The ICS heat exchangers are capable of removing decay heat in the presence of much higher levels of non-condensable gases as discussed in Section 5.2.4.

The effect of using the containment back pressure in calculating the break flow on the containment pressure is shown on Figure 6-38. [[

]]

The calculated peak containment pressure is not affected by the assumption made for containment pressure used to calculate the break flow because the break flow remains choked well past the time of the peak containment pressure for either assumption. Any impact on containment pressure occurs only in the long-term and is in the conservative direction when the containment back

pressure is not considered in the break flow calculation. The sensitivity case presented here shows that ignoring the back pressure increases the conservatism in the analysis.

Containment responses were calculated for small liquid pipe breaks until the RPV and containment pressures equalize. [[
]] The results are shown on Figures 6-39 through 6-42. The containment response trends for the liquid pipe breaks are similar to the small steam pipe breaks. After the RPV level falls below the break location, the break flow is fed from the steam space in the RPV and displays the characteristics of a small steam pipe break. Therefore, the trends observed in Figures 6-39 through 6-42 are consistent with the trends in steam pipe break shown in Figures 6-31 through 6-34.

[[

]]

Figure 6-31: Containment Pressure Following a Small Steam Pipe Break [MaxP]

[[

]]

Figure 6-32: PCCS Exit and Reactor Cavity Pool Temperatures Following a Small Steam Pipe Break, Conservative Case [MaxT]

[[

]]

Figure 6-33: Steam Volume Fraction in the Containment Following a Small Steam Pipe Break, Conservative Case [MaxP]

[[

]]

Figure 6-34: Containment Temperatures Following a Small Steam Pipe Break [MaxT]

[[

]]

Figure 6-35: Power, Small Steam Break, 2 ICS Trains, Conservative Case, with Containment Back Pressure Obtained from the MaxP Case

[[

]]

Figure 6-36: Pressure, Small Steam Break, 2 ICS Trains, Conservative Case, with Containment Back Pressure [MaxP]

[[

]]

Figure 6-37: Break Flow, Small Steam Break, 2 ICS Trains, Conservative Case, with Containment Back Pressure

[[

]]

Figure 6-38: Containment Pressure Using Break Flow With and Without Back Pressure [MaxP]

[[

]]

Figure 6-39: Containment Pressure Following a Small Liquid Pipe Break [MaxP]

[[

]]

Figure 6-40: PCCS Exit and Reactor Cavity Pool Temperatures Following a Small Liquid Pipe Break, Conservative Case [MaxT]

[[

]]

Figure 6-41: Containment Temperatures Following a Small Liquid Pipe Break [MaxT]

[[

]]

Figure 6-42: Steam Volume Fraction in the Containment Following a Small Liquid Pipe Break, Conservative Case [MaxP]

Table 6-6: Summary of the Peak Containment Pressure and Temperatures Calculated by Using the Conservative Assumptions

[[		
		]]

6.10.3 Containment Mixing for Combustible Gases

Hydrogen and oxygen generation results from radiolysis in BWRX-300 design basis accidents are discussed in Section 5.2.4. The radiolytic gases mixed in steam and liquid are discharged from the break along with the break flow. The volumetric fractions are calculated in Section 5.2.4. Hydrogen and oxygen distributions in the containment are not a concern for large breaks [[

]]. Radiolytic gases may build up in the containment following unisolated small breaks over time even though the rate of release is very small.

Total mass fraction of hydrogen and oxygen produced by radiolysis, remaining in the RPV and released to the containment are shown on Figure 6-43. [[

]]

Radiolytic gases mixed in steam enter into the dome region and condense on the containment dome, liberating the radiolytic gases mixed within. Although the volume fraction of radiolytic gases in the steam is small, it may accumulate in the dome region over time.

The radiolytic gas volume fractions are specified in the break flow boundary condition as calculated in Section 5.2.4, and radiolytic gas volume fraction distribution in the containment and the dome region was calculated for small steam pipe break case presented in Section 6.10.2.

Hydrogen volume fraction in the containment is shown on Figure 6-44. Hydrogen volume fraction in the dome region is higher than the main containment volume as expected, but the difference is not large. [[

]] The hydrogen volume fractions shown on Figure 6-44 are far below the deflagration limits even if there is sufficient oxygen.

Hydrogen and oxygen are generated at stoichiometric ratio from radiolysis; the molecular (or volume) ratio of radiolytic oxygen to hydrogen is 0.5. Because the radiolytic gases are well mixed in steam or liquid water where they are generated, the molecular or volume ratio of radiolytic oxygen to hydrogen remains 0.5 as they migrate in the RPV, from RPV to containment and within the containment. Therefore, radiolytic oxygen volume fraction in the containment is exactly half of the hydrogen volume fraction shown on Figure 6-44. There is also some small amount of oxygen initially present in the containment. [[

]]

The results presented here show that gases generated by radiolysis do not create a concern for deflagration in the containment and that the containment subcompartments remain sufficiently mixed.

[[

]]

Figure 6-43: Radiolytic Gas Generation and Release from RPV, Small Steam Pipe Break, 2 ICS Trains, Conservative Case

[[

]]

Figure 6-44: Hydrogen Volume Fraction in the Containment Main Volume and in the Dome Region, Small Steam Pipe Break, 2 ICS Trains, Conservative Case

6.11 Summary of the Assumptions and Inputs Used in the BWRX-300 GOTHIC Method Conservative Cases

The conservative containment response cases use the following inputs:

- Initial containment pressure is at the Technical Specification limit.
- Initial bulk containment temperature and the structures are at a reasonably low value that would occur during normal operation.
- Initial humidity in the containment is 20%.
- Reactor cavity pool temperature is at the Technical Specification limit.
- Bounding values are used for form loss coefficients in containment and in the PCCS units.
- Free space volume in the containment is conservatively calculated.
- The containment nodalization uses node sizes as presented in the base cases in this report.
- The initial airspace temperature above the reactor cavity pool is assumed to be the same as the pool water temperature.
- The initial relative humidity of the airspace is assumed to be 100%.

The conservative containment response cases use the following modeling parameters:

- [[ ]]
- Condensation and convection heat transfer correlations are biased as described in Section 6.8.2.
- [[

]]
- No credit is taken for heat transfer from the outer surface of the metal containment shell to the concrete or surroundings, except for heat transfer from the submerged section of the containment dome to the reactor cavity pool above the dome.
- The reactor cavity pool is modeled as a lumped parameter volume. The air space is connected to a constant pressure boundary condition such that the airspace pressure is nearly constant at atmospheric pressure.
- There is no heat loss from the pool to the walls. Surface evaporation from the pool is accounted for.
- Heat transfer coefficients on the containment shell, PCCS and containment dome are biased as described in Section 6.8.2.